Directed distances in bipolar-oriented triangulations: exact exponents and scaling limits

Jacopo Borga Ewain Gwynne MIT University of Chicago

Abstract

We study longest and shortest directed paths in the following natural model of directed random planar maps: the uniform infinite bipolar-oriented triangulation (UIBOT), which is the local limit of uniform bipolar-oriented triangulations around a typical edge. We construct the Busemann function which measures directed distance to ∞ along a natural interface in the UIBOT. We show that in the case of longest (resp. shortest) directed paths, this Busemann function converges in the scaling limit to a 2/3-stable Lévy process (resp. a 4/3-stable Lévy process).

We also prove up-to-constants bounds for directed distances in finite bipolar-oriented triangulations sampled from a Boltzmann distribution, and for size-n cells in the UIBOT. These bounds imply that in a typical subset of the UIBOT with n edges, longest directed path lengths are of order $n^{3/4}$ and shortest directed path lengths are of order $n^{3/8}$. These results give the scaling dimensions for discretizations of the (hypothetical) $\sqrt{4/3}$ -directed Liouville quantum gravity metrics.

The main external input in our proof is the bijection of Kenyon-Miller-Sheffield-Wilson (2015). We do not use any continuum theory. We expect that our techniques can also be applied to prove similar results for directed distances in other random planar map models and for longest increasing subsequences in pattern-avoiding permutations.

Contents

1	Intr	roduction	2
	1.1	Overview	2
	1.2	Busemann function on the UIBOT	
	1.3	Directed distances in finite bipolar-oriented triangulations	8
	1.4	Outline	11
2	Rel	ated models and future outlook	13
	2.1	Other discrete models	13
	2.2	Bipolar-oriented maps where faces have at most two right boundary edges	14
	2.3	Directed LQG metrics	15
	2.4	Parallels with directed first- and last-passage percolation	19
3	$\mathbf{K}\mathbf{M}$	ISW bijection and conditional independence property	21
	3.1	The Kenyon-Miller-Sheffield-Wilson bijection	21
	3.2	KMSW encodings of random bipolar-oriented triangulations	27
	3.3	Conditional independence for Boltzmann bipolar-oriented triangulations	29
	3.4	KMSW bijection for boundary-channeled bipolar-oriented triangulations	31

4	Cut	vertices and geodesics in the UIQBOT	32
	4.1	Definitions and results	32
	4.2	Existence of cut vertices in the UIQBOT	34
	4.3	Independence in the UIQBOT	37
5	Existence and basic properties of the Busemann function		
	5.1	Setup and outline	40
	5.2	Existence of the Busemann function	42
	5.3	Independent and stationary increments	44
	5.4	Symmetry via the UIBHBOT	47
	5.5	Proof of Proposition 5.1: Relation between the UIBOT and the UIQBOT	50
	5.6	Proof of Proposition 5.9: Symmetry for the UIBHBOT	56
6	Rec	cursive equations, tail asymptotics, and scaling exponents	61
Ū	6.1	The LDP case	
	6.2	The SDP case	
7	The	e case of finite triangulations	78
	7.1	LDP in size-n KMSW cells	78
	7.2	SDP in size-n KMSW cells	
	7.3	Boltzmann bipolar-oriented triangulations	
8	Ope	en problems	91
${f A}$	Proof of the Tauberian result		
	A.1	Proofs for the tail exponent asymptotics	93
	A.2	Proof that the imaginary part is positive for small t when $0 < \nu < 1 \ldots \ldots$	96

Acknowledgments. We thank Morris Ang, Olivier Bernardi, William Da Silva, Sayan Das, and Scott Sheffield for helpful discussions. We also thank Yuanzheng Wang for comments on an early draft of this paper. E.G. was partially supported by NSF grant DMS-2245832. J.B. was partially supported by NSF grant DMS-2441646.

1 Introduction

1.1 Overview

A planar map is a graph embedded in the complex plane \mathbb{C} , viewed modulo orientation-preserving homeomorphisms $\mathbb{C} \to \mathbb{C}$. Random planar maps have attracted an enormous amount of attention in probability and mathematical physics in recent years. One reason for this is that random planar maps are discrete analogs of **Liouville quantum gravity (LQG)**, a one-parameter family of random fractal surfaces, indexed by $\gamma \in (0,2]$, which arise in various areas of physics. Although the results of this paper are partially motivated by LQG, we will not use this theory in this paper; see [BP24, She23, Gwy20] for introductory expository articles.

There is a vast literature concerning graph distances in random planar maps which are sampled uniformly from some finite set of possibilities. A major achievement in this area is the independent proofs by Le Gall [Le 13] and Miermont [Mie13] of the following statement. If we take a uniform triangulation (or uniform p-angulations for even $p \ge 4$) with n edges and scale distances by $n^{-1/4}$, then the resulting metric space converges in law as $n \to \infty$, with respect to the Gromov-Hausdorff

topology, to a random metric space called the **Brownian map**. There are numerous extensions of the Brownian map convergence result to other models, including different local constraints on the maps and different underlying topologies; see, e.g., the survey [Le 19]. Miller and Sheffield [MS20, MS21] showed that the Brownian map is isomorphic to LQG with parameter $\gamma = \sqrt{8/3}$.

In contrast, much less is known about graph distances in **decorated random planar maps**, where instead of sampling a planar map uniformly from a set of possibilities, we sample a random pair (M, S) consisting of a planar map M and some sort of decoration S on M. Some interesting choices of decoration include, e.g., a spanning tree, a statistical physics model, or a bipolar orientation. When we sample a decorated planar map, the marginal law of M is not uniform: rather, it is sampled with probability proportional to the partition function of the decoration (which, roughly speaking, is the weighted number of possibilities for S on a given choice of M).

For most interesting choices of decoration, it is believed that M should have very different large-scale behavior as compared to uniform random planar maps. In many cases, the scaling limit of M is believed to be described by LQG with parameter $\gamma \in (0,2] \setminus \{\sqrt{8/3}\}$ depending on the particular type of decoration (see [GHS23] or [BP24, Section 4] for an overview of conjectures of this type). Moreover, for a map with n edges, the proper scaling for distances is believed to be $n^{-1/d\gamma}$, where d_{γ} is the Hausdorff dimension of the γ -LQG metric space. In some cases (including bipolar-oriented triangulations, as defined just below), this can be proven up to an $n^{o(1)}$ multiplicative error, see [GHS20,DG20]. However, the value of d_{γ} is unknown for $\gamma \neq \sqrt{8/3}$ (we have $d_{\sqrt{8/3}} = 4$), and computing it is one of the most important open problems in LQG theory.

In this paper, we study **directed distances** (lengths of shortest and longest directed paths) in a natural model of directed random planar maps, namely uniform bipolar-oriented triangulations (Definition 1.1 just below). This is the random planar map analog of studying *directed* first- or last-passage percolation (as opposed to *undirected* first-passage percolation). See Section 2.4 for further discussion of the analogy between this paper and results for directed first- and last-passage percolation.

Definition 1.1. A **directed planar map** is a planar map together with an orientation on its edges. The orientation is **acyclic** if there are no directed cycles. The orientation is **bipolar** if it is acyclic and it has at most one **source** (vertex with only outgoing edges) and at most one **sink** (vertex with only incoming edges).¹ A **bipolar-oriented triangulation** is a bipolar-oriented planar map whose faces all have degree three, except possibly the external (unbounded) face. See the left-hand side of Figure 1 for an illustration.

Whenever we speak about *left* and *right*, we always refer to left and right with respect to the orientation of the map (and not with respect to how we draw the map on the plane).

Bipolar orientations on planar graphs, often also called st-planar orientations, have been intensively studied in combinatorics. Indeed, they are related to the study of upward planar graph drawing and more general graph drawing on surfaces [Tam13], the study of the distributive lattice on the set of st-orientations of a fixed plane graph under cycle-flip moves [Pro02, Fel04], and the enumerative and bijective properties of various combinatorial structures, including Baxter permutations and non-intersecting lattice paths [FPS09,BBMF11]. Moreover, they have been used as bridges to study other structures on planar graphs, including (grand-)Schnyder woods [FFNO11, LSW24, BFL25]. Bipolar orientations enjoy the following properties: (i) given a finite bi-connected planar map and a designated source and sink pair on the outer face, there is always a way to orient the edges so that the result is a bipolar orientation [Lem67]; (ii) every bipolar-oriented map can be drawn in

¹For a finite planar map, an acyclic orientation always has at least one source and at least one sink, but for an infinite planar map the source, the sink, or both can be "at ∞ ".

the plane with every edge oriented from south-west to north-east [DBT88] (see also Figure 1); (iii) a bipolar orientation on a map induces a bipolar orientation on its dual map [DFdMR95].

A key tool in the study of bipolar-oriented random planar maps is the KMSW bijection of Kenyon, Miller, Sheffield, and Wilson [KMSW19], which, when restricted to triangulations, encodes a bipolar-oriented triangulation in terms of a walk in \mathbb{Z}^2 with increments in

$$\{(1,-1),(-1,0),(0,1)\}.$$

We review this bijection in Section 3.1. It can be seen from the KMSW bijection that uniform bipolar-oriented triangulations should be in the universality class of LQG with $\gamma = \sqrt{4/3}$ [KMSW19, Section 4].

The main results of this paper show that, in apparent contrast to undirected distances, directed distances in uniform bipolar-oriented triangulations are exactly solvable. In particular, we first establish the existence of the **Busemann function**, which measures "directed distances to ∞ " along a natural interface in the uniform infinite bipolar-oriented triangulation (UIBOT); see Theorem 1.4. We then show that the Busemann function converges in the scaling limit to a 2/3-stable Lévy process in the case of longest directed paths, and to a 4/3-stable Lévy process in the case of shortest directed paths (Theorem 1.6).

We also obtain the exact exponents for the typical lengths of shortest and longest directed paths in certain finite bipolar-oriented triangulations, with no o(1) error in the exponent (Theorems 1.11, 1.12, and 1.13). In particular, these results imply that in typical size-n submaps of the UIBOT, the lengths of longest directed paths grow like $n^{3/4}$ and the lengths of shortest directed paths grow like $n^{3/8}$. Prior to this work, almost² no non-trivial bounds were known for directed distances in any model of bipolar-oriented random planar maps.

The only inputs in our proof are the KMSW bijection and some elementary probabilistic facts. We do not use any continuum theory. See Section 1.4 for an outline.

Our results can be viewed as a substantial first step toward obtaining a full scaling limit of (shortest and longest) directed distances in uniform bipolar-oriented triangulations, analogous to the scaling limit of undirected distances in uniform planar maps to the Brownian map [Le 13,Mie13]. The limiting objects should be **directed versions of the** $\sqrt{4/3}$ -LQG **metric** (one version for longest paths and one for shortest paths), or equivalently $\sqrt{4/3}$ -LQG analogs of the **directed landscape** of [DOV22]. Our results suggest that the scaling exponents for the longest (resp. shortest) directed path version of the $\sqrt{4/3}$ -LQG metric should be 3/4 (resp. 3/8). These scaling exponents are the directed analogs of the (reciprocal of) the dimension of the undirected $\sqrt{4/3}$ -LQG metric space. We discuss this in more detail in Section 2.3.

Moreover, our proof strategy is fairly general. It can potentially be extended to obtain similar results for, e.g., (a) directed distances in other random planar map models, including bipolar-oriented maps with other face degree distributions and planar maps decorated by Schnyder woods; (b) shortest directed paths hit in order by various paths on random planar maps, such as the contour exploration of a uniform spanning tree or a percolation interface; and (c) longest increasing subsequences in various types of random permutations, such as Baxter permutations, semi-Baxter permutations, and strong Baxter permutations. We have several works in progress along these lines with various coauthors. See Section 2.1 for further discussion.

²It is possible to extract from [BGS22, Corollary 1.14] that the length of the longest directed path in a uniform bipolar-oriented map with n edges is typically of order o(n).

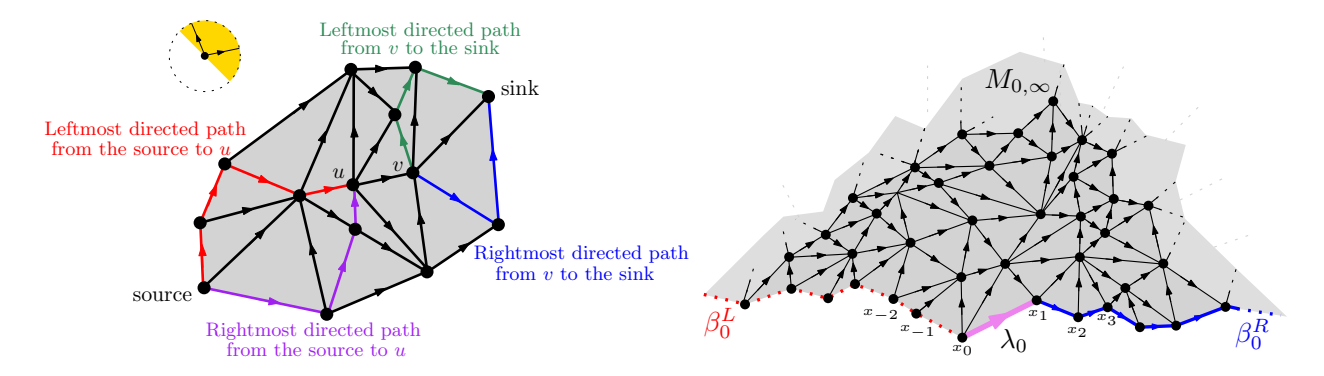


Figure 1: **Left:** A finite bipolar-oriented triangulation, drawn so that edges are directed from south-west to north-east (i.e. edges can point in the direction highlighted in yellow in the top-left circle). The four colored directed path denote the leftmost/rightmost paths introduced just before Definition 1.3. **Right:** A portion of the infinite rooted submap $(M_{0,\infty}, \lambda_0)$ of the UIBOT introduced in Definition 1.3. Edges on the boundary of $M_{0,\infty}$ lying to the west of the root edge λ_0 are not considered to be part of $M_{0,\infty}$. See Definition 3.1 for a precise definition of planar map with missing edges.

1.2 Busemann function on the UIBOT

We will henceforth assume that all of the planar maps considered in this paper are equipped with an acyclic orientation (Definition 1.1). Submaps of a map \mathfrak{m} are always assumed to be equipped with the orientation they inherit from \mathfrak{m} .

Definition 1.2. For a directed planar map \mathfrak{m} and vertices $x, y \in \mathfrak{m}$, we write $\mathrm{LDP}_{\mathfrak{m}}(x, y)$ (resp. $\mathrm{SDP}_{\mathfrak{m}}(x, y)$) for the **length of the longest** (resp. **shortest**) **directed path** in \mathfrak{m} from x to y, if at least one such path exists. If there is no directed path from x to y, we instead write $\mathrm{LDP}_{\mathfrak{m}}(x, y) = -\infty$ and $\mathrm{SDP}_{\mathfrak{m}}(x, y) = \infty$. Many of our theorem statements and proofs are the same for both longest and shortest directed paths. To express this concisely, we write $\mathrm{XDP} \in \{\mathrm{LDP}, \mathrm{SDP}\}$ to refer to either shortest or longest directed paths.

The uniform infinite bipolar-oriented triangulation is an infinite bipolar-oriented triangulation³ $(M_{-\infty,\infty}, \lambda_0)$, equipped with a directed root edge λ_0 , with no source or sink (the source is at $-\infty$ and the sink is at ∞). It arises as the (directed) Benjamini-Schramm [BS01] local limit of uniform bipolar-oriented triangulations with n edges and a fixed number of left and right boundary edges, rooted at a uniformly chosen edge [GHS20, Proposition 3.16]; see Definition 3.9.

As explained in [KMSW19, Section 1.2], for each vertex v of $M_{-\infty,\infty}$, the edges of $M_{-\infty,\infty}$ incident to v in cyclic order consist of a single group of incoming edges followed by a single group of outgoing edges. Hence, there is a unique outgoing edge from v that is leftmost in the sense that the edge immediately to its left is directed toward v. By traversing the leftmost outgoing edge from v, then the leftmost outgoing edge from the endpoint of this edge, and so forth, we obtain the **leftmost directed path** β from v to ∞ . The path β has the property that each edge traversed by β is the leftmost outgoing edge from its initial vertex. The leftmost directed path is called the "northwest path" in [KMSW19]. Since our convention is that edges go from south-west to north-east, instead of from south to north as in [KMSW19], the leftmost directed path travels

³See Definition 1.3 for the motivation for the notation $M_{-\infty,\infty}$.

in the north direction in our setting. See the green path on the left-hand side of Figure 1 for an example (in the finite setting).

Similarly, we can define the **rightmost directed path** from v to ∞ , which travels in the east direction; see the blue path on the left-hand side of Figure 1 for an example. By performing the above procedure with the orientations of the edges reversed, then reversing the resulting path, we can also define the **leftmost** and **rightmost** directed paths from $-\infty$ to v. The time reversals of these paths travel in the west and south directions, respectively. See the red and purple paths on the left-hand side of Figure 1 for an example.

Let β_0^R be the rightmost directed path from the terminal endpoint of the root edge λ_0 to ∞ . Let β_0^L be the leftmost directed path from $-\infty$ to the initial endpoint of λ_0 .

Definition 1.3. Let $(M_{0,\infty}, \lambda_0)$ be the rooted submap of $(M_{-\infty,\infty}, \lambda_0)$ consisting of the vertices, edges, and faces of $M_{-\infty,\infty}$ that lie to the left of $\beta_0^R \cup \{\lambda_0\} \cup \beta_0^L$. We consider all of the vertices lying on $\beta_0^R \cup \{\lambda_0\} \cup \beta_0^L$, the edge λ_0 , and the edges on β_0^R to be part of $M_{0,\infty}$, but not the edges on β_0^L . This means that $M_{0,\infty}$ is an infinite acyclically oriented triangulation with some missing⁴ boundary edges.

The reason for the name (and the reason why $M_{0,\infty}$ is natural) is that $M_{0,\infty}$ is exactly the submap of $M_{-\infty,\infty}$ explored by the KMSW procedure after time 0; see Lemma 3.8. See the right-hand side of Figure 1 for an illustration of $M_{0,\infty}$.

Let $\{x_k\}_{k\in\mathbb{Z}}$ be the vertices on the boundary of $M_{0,\infty}$, enumerated in directed order (i.e. from west to east) so that $\lambda_0 = (x_0, x_1)$. All vertices of $M_{0,\infty}$, including the boundary vertices, have an outgoing edge (Lemma 3.8). In particular, there is always a directed path starting from each boundary vertex. Our first theorem establishes the existence of the Busemann function for longest (and shortest) directed paths from the boundary vertices of $M_{0,\infty}$ to ∞ . Heuristically speaking, we want the Busemann function to be the function $\mathcal{X}: \mathbb{Z} \to \mathbb{Z}$ defined by

$$\mathcal{X}(k) = XDP_{M_{0,\infty}}(x_k, \infty) - XDP_{M_{0,\infty}}(x_0, \infty).$$
(1.1)

This definition does not make literal sense since $XDP_{M_{0,\infty}}(x_k,\infty) = \infty$. But we can make sense of (1.1) by, roughly speaking, taking a limit of $XDP_{M_{0,\infty}}(x_k,w) - XDP_{M_{0,\infty}}(x_0,w)$ as $w \to \infty$.

Theorem 1.4. Let XDP \in {LDP, SDP}. Let $\{x_k\}_{k\in\mathbb{Z}}$ be the boundary vertices of $M_{0,\infty}$, as above. There exists a unique function

$$\mathcal{X}: \mathbb{Z} \to \mathbb{Z}$$
,

called the **Busemann function**, such that $\mathcal{X}(0) = 0$ and the following is true. Let $k, k' \in \mathbb{Z}$ and let⁵ $\{w_j\}_{j\in\mathbb{N}}$ be a sequence⁶ of distinct vertices of $M_{0,\infty}$ such that, for each $j\in\mathbb{N}$, each of x_k and $x_{k'}$ can be joined to w_j by a directed path in $M_{0,\infty}$. Then

$$\mathcal{X}(k') - \mathcal{X}(k) = \text{XDP}_{M_{0,\infty}}(x_{k'}, w_j) - \text{XDP}_{M_{0,\infty}}(x_k, w_j), \quad \text{for each sufficiently large } j \in \mathbb{N}. \quad (1.2)$$

Remark 1.5. The term Busemann function originates from the work [Bus55]. Busemann functions are an important tool in the theory of first-passage percolation, in which setting they have been studied extensively; see [ADH17, Chapter 5] for a survey. In the context of (exponential) last-passage percolation, the existence of Busemann functions was established in [FP05] and led

⁴See Definition 3.1 for a precise definition of a planar map with missing edges.

⁵Our convention is that $\mathbb{N} = \{1, 2, \dots\}$ and $\mathbb{N}_0 = \{0, 1, 2, \dots\}$.

⁶The existence of at least one such sequence is ensured by Lemma 3.8: the rightmost directed paths in $M_{0,\infty}$ started from x_k and $x_{k'}$ coalesce into each other, so we can take $\{w_j\}$ to be a sequence of points hit by both of these rightmost directed paths.

to the construction of the stationary horizon [Bus24]. Recently, Busemann functions have also been important in the study of the directed landscape [DOV22], see [RV25, GZ22, BSS24] and the references therein. See Section 2.4 for further discussion.

To prove Theorem 1.4, we, roughly speaking, show that there are infinitely many vertices of $M_{0,\infty}$ that are each visited by every sufficiently long directed path started from x_k or $x_{k'}$ (Lemma 5.3). In particular, this implies (Lemma 5.4) that there exists a (unique) leftmost infinite XDP geodesic started from each boundary vertex x_k (Definition 4.5), and the leftmost infinite XDP geodesics from x_k and $x_{k'}$ eventually coalesce into each other, i.e. we have coalescence of geodesics. But we currently do not have any quantitative bounds on the positions of the coalescence points. Lemma 5.7 expresses the Busemann function in terms of the coalescence times of the leftmost XDP geodesics. Our next main result gives the scaling limit of the Busemann function.

Theorem 1.6. The following two scaling limit results for the Busemann function \mathcal{X} introduced in Theorem 1.4 hold with respect to the local Skorokhod topology on \mathbb{R} (here, all stable processes are strictly stable):

- In the LDP case, the re-scaled Busemann function $\{k^{-3/2}\mathcal{X}(\lfloor kt \rfloor)\}_{t \in \mathbb{R}}$ converges in law to a process $X : \mathbb{R} \to \mathbb{R}$ such that $-X|_{[0,\infty)}$ is a 2/3-stable subordinator; and $X(-\cdot)|_{[0,\infty)}$ is a symmetric 2/3-stable Lévy process independent of $X|_{[0,\infty)}$.
- In the SDP case, the re-scaled Busemann function $\{k^{-3/4}\mathcal{X}(\lfloor kt \rfloor)\}_{t \in \mathbb{R}}$ converges in law to a process $X : \mathbb{R} \to \mathbb{R}$ such that $X|_{[0,\infty)}$ is a 4/3-stable Lévy process with only upward jumps; and $X(-\cdot)|_{[0,\infty)}$ is a symmetric 4/3-stable Lévy process independent of $X|_{[0,\infty)}$.

In Theorem 1.6, the stable processes are specified only up to a positive multiplicative constant. Theorem 1.8 below shows that, in each case (LDP or SDP), the multiplicative constants for $X|_{[0,\infty)}$ and $X(-\cdot)|_{[0,\infty)}$ are the same.

Theorem 1.6 may be viewed as the $\sqrt{4/3}$ -directed LQG analog of the description of the law of the Busemann function for the directed landscape restricted to a horizontal line, as given in [BSS24]. See the end of Section 2.3 and Section 2.4 for further discussion. To prove Theorem 1.6, we will establish the following five properties of the Busemann function, then apply the heavy-tailed functional central limit theorem.

Theorem 1.7. Let XDP \in {LDP, SDP} and let \mathcal{X} be the Busemann function as in Theorem 1.4. The following properties hold:

- (i) Independent increments. The increments $\{\mathcal{X}(k) \mathcal{X}(k-1)\}_{k \in \mathbb{Z}}$ are independent.
- (ii) Stationary increments. The increments $\{\mathcal{X}(k) \mathcal{X}(k-1)\}_{k\geq 1}$ all have the same distribution, and the increments $\{\mathcal{X}(k) \mathcal{X}(k-1)\}_{k\leq 0}$ all have the same distribution.
- (iii) **Bounds on the increments for** $k \ge 1$. In the LDP case, for $k \ge 1$ we have the bound $\mathcal{X}(k) \mathcal{X}(k-1) \le -1$. In the SDP case, for $k \ge 1$, we have the bound $\mathcal{X}(k) \mathcal{X}(k-1) \ge -1$.
- (iv) Symmetry for $k \leq 0$. For $k \leq 0$, we have $\mathcal{X}(k) \mathcal{X}(k-1) \stackrel{d}{=} \mathcal{X}(k-1) \mathcal{X}(k)$.

The fifth property provides the following tail estimates for the increments of the Busemann function.

Theorem 1.8. Let XDP \in {LDP, SDP} and let \mathcal{X} be the Busemann function, as in Theorem 1.4.

(va) If XDP = LDP, then there is a constant $c_1 > 0$ such that as $x \to \infty$,

$$\mathbb{P}[\mathcal{X}(1) - \mathcal{X}(0) \le -x] = c_1 x^{-2/3} + o(x^{-2/3}),$$

$$\mathbb{P}[|\mathcal{X}(0) - \mathcal{X}(-1)| \ge x] = 2c_1 x^{-2/3} + o(x^{-2/3}).$$
(1.3)

(vb) If XDP = SDP, then there is a constant $c_2 > 0$ such that as $x \to \infty$,

$$\mathbb{P}[\mathcal{X}(1) - \mathcal{X}(0) \ge x] = c_2 x^{-4/3} + o(x^{-4/3}),$$

$$\mathbb{P}[|\mathcal{X}(0) - \mathcal{X}(-1)| \ge x] = 2c_2 x^{-4/3} + o(x^{-4/3}).$$
(1.4)

Moreover, in this case $\mathbb{E}[\mathcal{X}(k) - \mathcal{X}(k-1)] = 0$ for all $k \in \mathbb{Z}$.

The proofs of Theorems 1.7 and 1.8 constitute the bulk of the work in this paper. See Section 1.4 for a detailed outline. To briefly summarize, the independent increments property (i) of Theorem 1.7 will eventually follow from the fact that an XDP geodesic cuts a finite bipolar-oriented triangulation into two pieces that are conditionally independent given its length (Lemma 3.15). The stationary increments property (ii) will ultimately be a consequence of the stationarity of $M_{-\infty,\infty}$ under the KMSW procedure (Section 5.3). The bounds (iii) for $k \geq 1$ are immediate from the fact that the right boundary of $M_{0,\infty}$ is a directed path in $M_{0,\infty}$. The symmetry (iv) for $k \leq 0$ comes from a non-trivial "local reflection symmetry" at the edges along the left boundary of $M_{0,\infty}$ (Section 5.4). Theorem 1.8 is obtained by analyzing a recursive relation for the laws of $\mathcal{X}(1) - \mathcal{X}(0)$ and $\mathcal{X}(0) - \mathcal{X}(-1)$ which comes from applying one step of the KMSW procedure (Section 6). In principle, it may be possible to extract from this recursive relation a complete characterization of the laws of $\mathcal{X}(1) - \mathcal{X}(0)$ and $\mathcal{X}(0) - \mathcal{X}(-1)$, up to a single unknown constant. But we only need the leading-order tail asymptotics.

1.3 Directed distances in finite bipolar-oriented triangulations

From the existence and scaling limit of the Busemann function on the UIBOT, one can deduce up-to-constants estimates for directed distances in various types of finite random bipolar-oriented triangulations. We will state and prove results to this effect in two settings: Boltzmann bipolar-oriented triangulations with fixed right boundary length (Section 1.3.1) and submaps of the UIBOT explored by n steps of the KMSW procedure (Section 1.3.2). We decided to work with these models of finite bipolar orientations in order to illustrate the main ideas while keeping the exposition concise. We expect that one can also obtain analogous results for, e.g., uniform bipolar-oriented triangulations with specified left boundary length, right boundary length, and total number of edges. However, proving such results would require some technical estimates for conditioned random walks, so we do not carry it out here (the estimates we need do not seem to immediately follow from the results of [DW15a]).

1.3.1 Directed distances in Boltzmann bipolar-oriented triangulations

Definition 1.9. For $l, r \in \mathbb{N}$, a bipolar-oriented planar map with **left boundary length** l and **right boundary length** r is a finite bipolar-oriented planar map \mathfrak{m} with the following properties. The source and the sink both lie on the boundary of the external face, and the oriented path from the source to the sink on the boundary of the external face, with the external face immediately to its left (resp. right), has length l (resp. r).

For example, the bipolar-oriented triangulation on the left-hand side of Figure 1 has left boundary length 5 and right boundary length 4.

Definition 1.10.

• The Boltzmann distribution on bipolar-oriented triangulations with right boundary length $r \in \mathbb{N}$ is the law of the random bipolar-oriented triangulations M(r) such that for each bipolar-oriented triangulation \mathfrak{m} with r right boundary edges and $n \in \mathbb{N}$ total edges,

$$\mathbb{P}[M(r) = \mathfrak{m}] = \frac{3^{-n}}{C_r},\tag{1.5}$$

where $C_r > 0$ is a normalizing constant.

• The Boltzmann distribution on bipolar-oriented triangulations with right boundary length r and a marked left boundary vertex is the law of the random pair (M(r), z(r)), where M(r) is a bipolar-oriented triangulation with r right boundary edges and z(r) is a vertex on its left boundary, such that the following is true. For each bipolar-oriented triangulation \mathfrak{m} with r right boundary edges and $n \in \mathbb{N}$ total edges, and each vertex \mathfrak{z} on its left boundary,

$$\mathbb{P}[(M(r), z(r)) = (\mathfrak{m}, \mathfrak{z})] = \frac{3^{-n}}{\widetilde{C}_r}, \tag{1.6}$$

where $\tilde{C}_r > 0$ is a normalizing constant.

If (M(r), z(r)) is sampled from the Boltzmann distribution on bipolar-oriented triangulations with right boundary length r and a marked left boundary vertex, then the marginal law of M(r) is equal to the Boltzmann distribution (1.5) weighted by a constant times the number of possibilities for z(r), which is equal to the left boundary length of M(r) plus one.

It follows from the KMSW bijection that the distributions in Definition 1.10 are well-defined, in the sense that the total mass of the measure on triangulations is finite; see Lemmas 3.11 and 3.12.

The normalization factor 3^{-n} in (1.5) and (1.6) comes directly from the KMSW encoding: a bipolar-oriented triangulation with n edges is encoded by a length-n walk with three possible step types, so a uniformly sampled encoding has probability $(1/3)^n$. Thus a map with n edges naturally receives weight 3^{-n} . It should be possible to also argue that this choice is critical. Let $a_{n,r}$ be the number of bipolar-oriented triangulations with right boundary length r and n edges. Via the KMSW representation, $a_{n,r}$ is the number of length-n walks constrained to stay in a cone, and results on random walks in cones (see [DW15a, Theorem 1]) should yield $a_{n,r} = c_r 3^n n^{-\alpha} (1 + o(1))$ as $n \to \infty$, for some $\alpha > 1$ and constant $c_r > 0$. Consequently, under the Boltzmann weight 3^{-n} , we obtain $\mathbb{P}(\#\mathcal{E}(M(r)) = n) \propto a_{n,r} 3^{-n} \approx n^{-\alpha}$. So the size distribution has a power-law tail.

Our main theorem for directed distances in Boltzmann bipolar-oriented triangulations is as follows.

Theorem 1.11. For $r \in \mathbb{N}$, let (M(r), z(r)) be sampled from the Boltzmann distribution on bipolaroriented triangulations with right boundary length r and a marked left boundary vertex (Definition 1.10). Let Source(r) and Sink(r) denote the source and sink vertices of M(r). For each $\delta \in (0,1)$, there exists $A = A(\delta) > 1$ such that for each $r \in \mathbb{N}$, it holds with probability at least $1 - \delta$ that the following is true.

- $\bullet \ \ A^{-1}r^{3/2} \leq \mathrm{LDP}_{M(r)}(\mathrm{Source}(r),\mathrm{Sink}(r)) \leq Ar^{3/2}.$
- $SDP_{M(r)}(Source(r), Sink(r)) \le Ar^{3/4}$.
- There exists a vertex y on the right boundary of M(r) such that

$$SDP_{M(r)}(Source(r), y) \ge A^{-1}r^{3/4}.$$

Thanks to the result in (7.35) of Lemma 7.9, by possibly increasing A, we can arrange that with probability at least $1 - \delta$,

$$A^{-1}r^2 \le \#\mathcal{E}(M(r)) \le Ar^2$$

where $\mathcal{E}(M(r))$ is the set of edges of M(r). Therefore, Theorem 1.11 implies that LDP distances in M(r) (resp. SDP distances in M(r)) are typically comparable to $\#\mathcal{E}(M(r))^{3/4}$ (resp. $\#\mathcal{E}(M(r))^{3/8}$); see also Theorems 1.12 and 1.13 below.

We expect that also $\mathrm{SDP}_{M(r)}(\mathrm{Source}(r),\mathrm{Sink}(r)) \geq A^{-1}r^{3/4}$ with high probability when A is large, but we do not prove this here. The reason we work with the Boltzmann distribution with a marked left boundary vertex in Theorem 1.11 is for technical convenience: weighting the law of M(r) by its left boundary length allows us to relate it more directly to the uniform infinite quarter-plane bipolar-oriented triangulation of Definition 4.1. We expect that Theorem 1.11, in the case where we do not have a left marked boundary vertex, can be deduced from the current version of Theorem 1.11 together with some estimates for the KMSW encoding walk. However, for the sake of brevity, we do not carry this out here.

1.3.2 Directed distances in size-n KMSW cells

For $n \in \mathbb{N}$, let $M_{0,n}$ be the submap⁷ of the UIBOT $M_{-\infty,\infty}$ (Section 1.2) explored by the KMSW procedure between time 0 and time n. In other words, $M_{0,n}$ is the directed map obtained by applying the procedure of Definition 3.3 to the walk $\mathcal{Z}|_{[0,n]}$, where \mathcal{Z} is a walk on \mathbb{Z}^2 with i.i.d. increments sampled uniformly from $\{(1,-1),(-1,0),(0,1)\}$. The map $M_{0,n}$ is not bipolar-oriented since, for a vertex on the boundary of $M_{0,n}$, it could be that all of the incoming (or outgoing) edges for this vertex are not contained in $M_{0,n}$; see, for instance, the map \mathfrak{m}_6 in Figure 5. However, $M_{0,n}$ is believed to exhibit the same behavior in the bulk as a uniform bipolar-oriented triangulation of size n. In terms of LQG, the map $M_{0,n}$ is the discrete analog of a unit-size mated-CRT map cell.

Our results for $M_{0,n}$ are as follows.

Theorem 1.12. For each $\delta \in (0,1)$, there exists $A = A(\delta) > 1$ such that for each $n \in \mathbb{N}$, it holds with probability at least $1 - \delta$ that

$$A^{-1}n^{3/4} \le \sup \left\{ \text{LDP}_{M_{0,n}}(x,y) : x, y \in \mathcal{V}(M_{0,n}) \right\} \le An^{3/4}, \tag{1.7}$$

where here we recall that $LDP_{M_{0,n}}(x,y) = -\infty$ if there is no directed path in $M_{0,n}$ from x to y.

The map $M_{0,n}$ has a **lower boundary**, defined as its intersection with the boundary of $M_{0,\infty}$, and an **upper boundary** defined as the intersection of its boundary with the submap of $M_{-\infty,\infty}$ explored by the KMSW procedure after time n. See Definition 3.2 for an alternative definition.

Theorem 1.13. For each $\delta \in (0,1)$, there exists $A = A(\delta) > 1$ such that for each $n \in \mathbb{N}$, it holds with probability at least $1 - \delta$ that the following is true.

- For every vertex x on the lower boundary of $M_{0,n}$, there exists a vertex y on the upper boundary of $M_{0,n}$ such that $SDP_{M_{0,n}}(x,y) \leq An^{3/8}$.
- For every vertex y on the upper boundary of $M_{0,n}$, there exists a vertex x on the lower boundary of $M_{0,n}$ such that $SDP_{M_{0,n}}(x,y) \leq An^{3/8}$.
- There exists a vertex y on the lower boundary of $M_{0,n}$, lying to the right of the root edge $\lambda_0 = (x_0, x_1)$, such that $SDP_{M_{0,n}}(x_0, y) \geq A^{-1}n^{3/8}$.

⁷To be precise, this is a map with some missing edges on the boundary following our Definition 3.1. See the precise definition of the KMSW procedure in Definition 3.3 for more details.

Remark 1.14. Prior to this work, the only known non-trivial bounds for undirected graph distances in random planar maps in the γ -LQG universality class, $\gamma \neq \sqrt{8/3}$, were obtained using LQG methods (see [GHS23, Section 5.2] for an explanation of how this is done). By (crudely) upper-bounding undirected graph distance by directed graph distance, Theorem 1.11 (in the SDP case) and Theorem 1.13 provide the first non-trivial bounds for undirected distances in such maps which can be proven using only discrete arguments. However, known upper bounds for the dimension of LQG [GP19, Corollary 2.5] show that the dimension of $\sqrt{4/3}$ -LQG satisfies $0.304 \leq 1/d_{\sqrt{4/3}} \leq 0.326$. Hence the directed graph distance exponent 3/8 provides a worse bound for the undirected graph distance exponent than what one can get from LQG.

1.4 Outline

In Section 2, we discuss possible extensions to other models, relationships to directed versions of Liouville quantum gravity, and analogies to first- and last-passage percolation. This section exists only to provide additional context and is not needed for our proofs.

In Section 3, we review the KMSW bijection [KMSW19], which will be the main tool in our proofs. In particular, we explain that the UIBOT can be encoded via the KMSW bijection by a bi-infinite random walk $\mathcal{Z}: \mathbb{Z} \to \mathbb{Z}^2$ whose increments are i.i.d. uniform samples from $\{(1,-1),(-1,0),(0,1)\}$ (Proposition 3.10). We also make the following observation (Lemma 3.15). Suppose that M is a Boltzmann bipolar-oriented triangulation with specified left and right boundary lengths, and let P be the leftmost XDP geodesic in M from its source vertex to its sink vertex (Definition 3.13). Then the submaps of M lying to the left and right of P are conditionally independent given the length of P. This observation will ultimately be the source of the independent increments property of the Busemann function (Theorem 1.7). We also note that Lemma 3.15 is not true for undirected graph distance geodesics, which is one reason why our proofs do not work for undirected distances.

In Section 4, we study the uniform infinite quarter-plane bipolar-oriented triangulation (UIQBOT) (Definition 4.1), which is an infinite bipolar-oriented triangulation with infinite left and right boundary lengths, with a finite source and a sink at ∞ . We show in Proposition 4.3 that a.s. there are infinitely many cut vertices v of the UIQBOT with the property that removing v disconnects the UIQBOT. The existence of such vertices will be very useful for the proof of Theorem 1.11, since long directed paths are forced to pass through them. The proof of Proposition 4.3 is based on estimates for the KMSW encoding walk. We also show in Proposition 4.7 that the submaps of the UIQBOT lying to the left and right of its leftmost XDP geodesic from the source to ∞ are independent. This is done by applying the aforementioned conditional independence statement for finite bipolar-oriented triangulations (Lemma 3.15) and comparing such finite bipolar-oriented triangulations to the UIQBOT. However, some non-trivial work is involved to get rid in the limit of the conditioning on the length of the XDP geodesic (we use an argument based on the Hewitt-Savage zero-one law).

In Section 5, we prove Theorems 1.4 and 1.7 on the existence and basic properties of the Busemann function. To do this, we show that if $(M_{-\infty,\infty}, \lambda_0)$ is the UIBOT, then the submap $\widehat{M}_{0,\infty}$ of $M_{0,\infty}$ induced by the vertices of $M_{0,\infty}$ which are reachable by a directed path started from the initial vertex of λ_0 has the law of the UIQBOT (Proposition 5.1). This allows us to apply the result on the existence of cut vertices in the UIQBOT (Proposition 4.3) to show that infinite XDP geodesics in $M_{0,\infty}$ exist, and any two such geodesics have to have infinitely many points in common. This leads easily to the proof of Theorem 1.4.

We deduce the stationarity and independent increments properties of Theorem 1.7 using the independence property from Proposition 4.7 and the stationarity of the law of the KMSW encod-

ing walk \mathcal{Z} . In particular, we show (Lemma 5.6) that $M_{0,\infty}$ can be decomposed into countably many independent "slices" bounded by leftmost XDP geodesics started from the boundary vertices $\{x_k\}_{k\in\mathbb{Z}}$. We remark that decompositions of planar maps by geodesic slices have been used extensively in probability and combinatorics, see, e.g., [Mie21,BGM24,AB25] and the references therein. To our knowledge this is the first use of such decompositions in the setting of bipolar-oriented maps.

To prove the symmetry property $\mathcal{X}(0) - \mathcal{X}(-1) \stackrel{d}{=} \mathcal{X}(-1) - \mathcal{X}(0)$, we introduce (Definition 5.8) an infinite directed planar map with boundary, which we call the uniform infinite boundary-channeled half-plane bipolar-oriented triangulation (UIBHBOT). The UIBHBOT describes the local behavior of $M_{0,\infty}$ near a typical edge on its left boundary. We deduce the symmetry of \mathcal{X} from a non-obvious reflection symmetry of the UIBHBOT (Proposition 5.9). This reflection symmetry, in turn, follows from a symmetry of finite boundary-channeled bipolar-oriented triangulations (Lemma 3.18) and a local limit argument (Proposition 5.16).

In Section 6, we deduce Theorem 1.8 from Theorem 1.7. This is the part of the argument that leads to the exact exponents in our theorem statements. If the reader takes Theorems 1.4 and 1.7 as a black box, Section 6 can be read independently from the rest of the paper. The idea of the proof is as follows. Let $M_{1,\infty}$ be the map obtained from $M_{0,\infty}$ by applying one step of the KMSW procedure. We know that $M_{1,\infty} \stackrel{d}{=} M_{0,\infty}$, so the Busemann function \mathcal{X}^1 associated with $M_{1,\infty}$ has the same law as \mathcal{X} . Furthermore, we can explicitly express \mathcal{X} in terms of \mathcal{X}^1 (Lemmas 6.4 and 6.10). Using this and the properties in Theorem 1.7, we obtain in Propositions 6.5 and 6.11 a recursive equation satisfied by the probabilities

$$f(x) := \mathbb{P}[\mathcal{X}(0) - \mathcal{X}(-1) = x]$$
 and $g(y) := \mathbb{P}[\mathcal{X}(1) - \mathcal{X}(0) = y]$.

By multiplying by $e^{itx+isy}$ and summing over x and y, we convert this equation into a functional equation for the characteristic functions F and G of $\mathcal{X}(1) - \mathcal{X}(0)$ and $\mathcal{X}(0) - \mathcal{X}(-1)$ (see (6.21) and (6.48)). By analyzing the leading-order behavior of the terms in this equation, we can determine the asymptotic behavior of these characteristic functions as $t, s \to 0$. By a Tauberian theorem (Proposition 6.1), this leads to Theorem 1.8. Theorems 1.7 and 1.8 immediately imply Theorem 1.6 by a standard heavy-tailed functional central limit theorem (see, e.g., [JS03]).

In Section 7, we deduce our results for finite-volume planar maps from Theorems 1.6 and 1.8. The results for the KMSW cell $M_{0,n}$ (Theorems 1.12 and 1.13) follow from the results for the Busemann function and relatively straightforward geometric arguments. To prove Theorem 1.11, we find a submap $\widehat{M}(r)$ of $M_{0,\infty}$ that has the same law as the map M(r) of Theorem 1.11 (see Lemma 7.9). We then compare $\widehat{M}(r)$ to the size-n cell $M_{0,n}$, with n chosen to be comparable to r^2 .

In Section 8, we discuss some open problems. In Appendix A, we prove the Tauberian-type result for characteristic functions (Proposition 6.1) needed in Section 6.

Remark 1.15. The recent paper [ABB⁺25] obtains the exponent for longest increasing subsequences in Brownian separable permutons using a recursive equation. However, the proof strategy in [ABB⁺25] has essentially nothing in common with the proofs in this paper. In the setting of [ABB⁺25], the recursive equation arises from an encoding of the permuton in terms of a labeled tree, rather than a stationarity property as in this paper. Moreover, in [ABB⁺25], to extract the

⁸In the LDP case, the equation uniquely determines the leading order asymptotics of the characteristic functions as $t \to 0$. In the SDP case, matters are slightly more complicated. There are two possible leading order asymptotics, depending on the value of an a priori unknown parameter which we call κ . The $\kappa = 0$ case leads to the correct $x^{-4/3}$ tail in Theorem 1.8; the $\kappa > 0$ case instead leads to an $x^{-2/3}$ tail. We rule out the $\kappa > 0$ case by showing that it violates the trivial $n^{1/2}$ upper bound for SDPs in a size-n KMSW cell.

exponent from the recursive equation one has to show a priori that the distribution of the longest increasing subsequence has a regularly varying tail. In contrast, in this paper, we derive the exact tail behavior (Theorem 1.8) directly from the recursive equation, with no a priori assumptions. See Remark 2.4 for some discussion about the results of [ABB⁺25] in the context of directed LQG metrics.

2 Related models and future outlook

In Sections 2.1 and 2.2, we discuss other models to which the techniques of this paper might be applicable. In Section 2.3, we discuss conjectures related to directed versions of the LQG metric, which, in the special case when $\gamma = \sqrt{4/3}$ and $\tilde{\theta} = \pi/2$, should describe the scaling limit of the directed distances considered in this paper. In Section 2.4, we discuss some parallels between the results of this paper and the study of directed first- and last-passage percolation and the directed landscape. Nothing in this section is needed to understand the proofs of our main results.

2.1 Other discrete models

It is likely possible to extend our techniques to obtain similar results for a variety of other discrete models. One natural class of models to consider is **bipolar-oriented planar maps with more general face degree distributions** (not just triangulations), e.g., bipolar-oriented quadrangulations and bipolar-oriented maps with unconstrained face degrees. Such models can also be encoded via the KMSW bijection, and we expect that results similar to those in this paper (with the same exponents) hold in this more general setting.

A key technical difficulty in extending our results to this more general setting is as follows. If M is not a triangulation, the map $M_{0,\infty}$ considered in Section 1.2 can have vertices on its left boundary that are not incident to any non-missing edge of $M_{0,\infty}$. This makes it unclear how to properly define the Busemann function. One possible way around this is to modify the KMSW bijection and the definition of $M_{0,\infty}$. Alternatively, one could try to compare directed distances in general bipolar-oriented maps to directed distances in bipolar-oriented triangulations. A possible strategy is to use a strong coupling of the KMSW encoding walks, as was used for undirected graph distances in [GHS20] (see also Problem 8.3).

A Baxter permutation of size $n \in \mathbb{N}$ is a permutation $\sigma \in \mathcal{S}_n$ for which there do not exist indices $1 \leq i < j < k \leq n$ such that $\sigma(j+1) < \sigma(i) < \sigma(k) < \sigma(j)$ or $\sigma(j) < \sigma(k) < \sigma(i) < \sigma(j+1)$. Bipolar-oriented planar maps with general face degree distribution, with n total edges, are in bijection with Baxter permutations of size n [BBMF11]. Under this bijection, the longest increasing subsequence of the permutation corresponds to the longest directed path in the bipolar-oriented map. This leads to the following conjecture, which seems to be within reach given the results of this paper.

Conjecture 2.1. Let σ_n be a uniform Baxter permutation of size n. Then the longest increasing subsequence in σ_n grows like $n^{3/4}$ as $n \to \infty$.

It may also be possible to extend our results to biased bipolar-oriented planar maps whose face degree distributions are biased based on the number of edges on the left and right boundaries of the faces. As explained in [KMSW19, Remark 5], such maps can be in the universality class of γ -LQG for any $\gamma \in (0, \sqrt{2})$. In particular, we expect that such maps have different exponents for directed distances compared to uniform bipolar-oriented triangulations. See Section 2.2 just below for a special class of biased bipolar-oriented planar maps that seem especially amenable to our techniques.

More generally, our techniques can also potentially be applied to directed distances in other random planar map models. Indeed, the independence property for the maps to the left and right of an XDP geodesic seems to require that the orientation on our planar map is, in some sense, compatible with how the map is sampled (see, e.g., Lemma 3.15). Once we have this, the only other crucial tool in our proofs is the mating-of-trees bijection. For example, our techniques can likely be generalized to random planar maps decorated by Schnyder woods [LSW24], or more generally, grand-Schnyder woods [BFL25]. Another class of problems to which our techniques might apply is determining the minimal length of a path hit in order by some natural path on a random planar map. Some interesting examples include the contour exploration of a uniform spanning tree [Mul67,Ber07,She16] or a percolation interface (here, the peeling process would take the place of the mating-of-trees bijection [Ang03]). One could also attempt to extend our methods to determine the longest increasing subsequence exponent for other models of pattern-avoiding permutations which are related to random planar maps and LQG, such as semi-Baxter and strong-Baxter permutations [Bor22].

The authors are currently working on two papers in the above direction. One such paper (which is also joint with Yuanzheng Wang) studies shortest directed paths in spanning-tree decorated maps. Another paper (which is also joint with Leonardo Bonanno) studies longest and shortest directed paths in triangulations decorated by Schnyder woods.

2.2 Bipolar-oriented maps where faces have at most two right boundary edges

Many of our proofs work for a more general class of models of bipolar-oriented maps than just triangulations. Indeed, consider a model of bipolar-oriented maps with a face degree distribution such that each of the faces is allowed to have at most two right boundary edges, and the number of left boundary edges has finite moments of all positive orders. The infinite-volume version of such a map (analogous to the UIBOT) is the rooted map $(M_{-\infty,\infty}, \lambda_0)$ which can be constructed by applying the KMSW procedure (Definition 3.3) to a bi-infinite walk $\mathcal{Z} = (\mathcal{L}, \mathcal{R}) : \mathbb{Z} \to \mathbb{Z}^2$ with i.i.d. increments, whose increment distribution $\nu(x,y) = \mathbb{P}[\mathcal{Z}(j) - \mathcal{Z}(j-1) = (x,y)]$ satisfies the following conditions.

- The distribution ν is supported on $\{(1,-1)\} \cup \{(0,j)\}_{j\geq 1} \cup \{(-1,j)\}_{j\geq 0}$.
- The expectation of a sample from ν is (0,0).
- The second coordinate of a sample from ν has finite moments of all positive orders.

Equivalently, $(M_{-\infty,\infty}, \lambda_0)$ is the local limit (around a uniform edge) of finite bipolar-oriented maps sampled from a probability measure where each face with $i \in \{1, 2\}$ right boundary edges and $j \ge 1$ left boundary edges is assigned weight $\nu(i-1, j-1)$.

If we define $M_{-\infty,\infty}$ as above and $M_{0,\infty}$ analogously to Definition 1.3, then every face of $M_{0,\infty}$ has at most one boundary edge which is not in $M_{0,\infty}$. So, every vertex on the boundary of $M_{0,\infty}$ is the initial vertex of an infinite directed path in $M_{0,\infty}$. Moreover, \mathcal{L} has the law of a lazy random walk. Of particular interest is the case where

$$\nu(1,-1) = \frac{1}{2}, \quad \nu(-1,j) = 2^{-j-2}, \quad \forall j \ge 0,$$
 (2.1)

which is closely related to uniformly sampled triangulations decorated by a Schnyder wood (see, for instance, [FFNO11, Proposition 7.1] or [GHS20, Section 3.3.4]). Such triangulations are in the universality class of γ -LQG for $\gamma = 1$ [LSW24]. In general, by varying ν , one can get models of bipolar-oriented planar maps of the above type which belong to the γ -LQG universality class for

any $\gamma \in (0, \sqrt{4/3}]$. The value of γ is determined by the correlation ρ of the two coordinates of a sample from ν via the formula $\rho = -\cos(\pi \gamma^2/4)$, see [DMS21, Theorem 1.9].

Our proofs of Theorem 1.4 and Properties (i) through (iii) of Theorem 1.7 carry over essentially verbatim to the above setting. The moment hypothesis is needed to apply the results of [DW15b] (see Lemma 4.11). Moreover, if one assumes appropriate analogs of Theorems 1.7 and 1.8, the proofs of our results in the finite-volume setting (Theorems 1.11–1.13) also carry over without change.

However, Property (iv) of Theorem 1.4 is not true in the above more general setting. This makes it more difficult to derive tail asymptotics as in Theorem 1.8 from the recursive equation which comes from one step of the KMSW procedure. In general, we expect that the scaling limit of the Busemann function $\mathcal{X}|_{(-\infty,0]}$ could be an asymmetric stable Lévy process.

We plan to investigate bipolar-oriented planar maps of the above type further in future work.

2.3 Directed LQG metrics

Directed distances in bipolar-oriented random planar maps are believed to be discrete analogs of directed versions of the LQG metric, in the same way that undirected distances in random planar maps are discrete analogs of the undirected LQG metric (as constructed in [DDDF20, GM21]). In this subsection, we explain what we mean by this, assuming that the reader has some basic familiarity with the theory of LQG and SLE. A reader who is not familiar with these topics can skip this subsection. See Figure 2 for a visual summary of this section.

Let $\gamma \in (0,2)$, $\kappa = 16/\gamma^2 > 4$, and $\tilde{\theta} \in [0,2\pi]$. Our parameter $\tilde{\theta}$ corresponds to $\theta + \pi/2$ in the setting of [Bor23].

Let Φ be the random generalized function on $\mathbb C$ corresponding to the γ -quantum cone [DMS21, Definition 4.10]. Then Φ is a minor modification of the whole-plane Gaussian free field (GFF). When $\gamma = \sqrt{4/3}$, the LQG surface described (heuristically) by the Riemannian metric tensor $e^{\gamma \Phi} (dx^2 + dy^2)$ on $\mathbb C$ is the continuum analog of the UIBOT (see, e.g., [KMSW19, Section 4]).

Independently of Φ , let η and $\tilde{\eta}$ be a pair of whole-plane space-filling SLE_{κ} curves from ∞ to ∞ in \mathbb{C} . We assume that η and $\tilde{\eta}$ are coupled together so that they are space-filling counterflow lines of a common whole-plane GFF Ψ in the sense of Imaginary Geometry [MS17], with angles 0 and $\tilde{\theta} - \pi$, respectively. In the case when $\gamma = \sqrt{4/3}$ ($\kappa = 12$), the curve η is the continuum analog of the gold Peano path on the right-hand side of Figure 4 (see the discussion just above Definition 3.7 for a precise definition). In the case when $\gamma = \sqrt{4/3}$ and $\tilde{\theta} = \pi/2$, the curve $\tilde{\eta}$ is the continuum analog of the "dual" Peano path of the same UIBOT, defined by considering the upper-right and lower-left trees instead of the upper-left and lower-right trees [GHS16]. Directed paths in the UIBOT are visited in order by both the primal and dual Peano paths.

When $\widetilde{\theta} \in (0, \pi]$, we say that points $z, w \in \mathbb{C}$ are **ordered**, denoted $z \leq w$, if they are hit in order by both η and $\widetilde{\eta}$, i.e., there exists times $t_1 < t_2$ and $\widetilde{t}_1 < \widetilde{t}_2$ such that $\eta(t_1) = \widetilde{\eta}(\widetilde{t}_1) = z$ and $\eta(t_2) = \widetilde{\eta}(\widetilde{t}_2) = w$. When $\widetilde{\theta} \in (\pi, 2\pi]$, we instead say that $z \leq w$ if z and w are hit in order by either η_1 or η_2 , i.e., either there exists times $t_1 < t_2$ such that $\eta(t_1) = z$ and $\eta(t_2) = w$ or the same is true with $\widetilde{\eta}$ in place of η . This makes it so that the set of points $w \in \mathbb{C}$ with $0 \leq w$ is bounded by two flow lines of Ψ of angles $-\pi/2$ and $\widetilde{\theta} - \pi/2$, respectively. We note that $z \leq w$ and $z \leq w$

⁹The description of the KMSW encoding walk $\widehat{\mathcal{Z}}'$ for $\widehat{M}'_{0,\infty}$ in Lemma 5.14 is not as nice for a general choice of ν , but we still get the same description for the law of $\widehat{\mathcal{Z}}$ and the fact that $\widehat{\mathcal{Z}}$ and $\widehat{\mathcal{Z}}'$ are independent, which is all that is needed for our proofs.

¹⁰When $\widetilde{\theta} \in (0, \pi]$, such pairs of points have zero Lebesgue measure since Lebesgue-a.e. point of $\mathbb C$ is hit only once by each of η and $\widetilde{\eta}$. But, the set of such pairs does not have zero Lebesgue measure when $\theta \in (\pi, 2\pi]$.

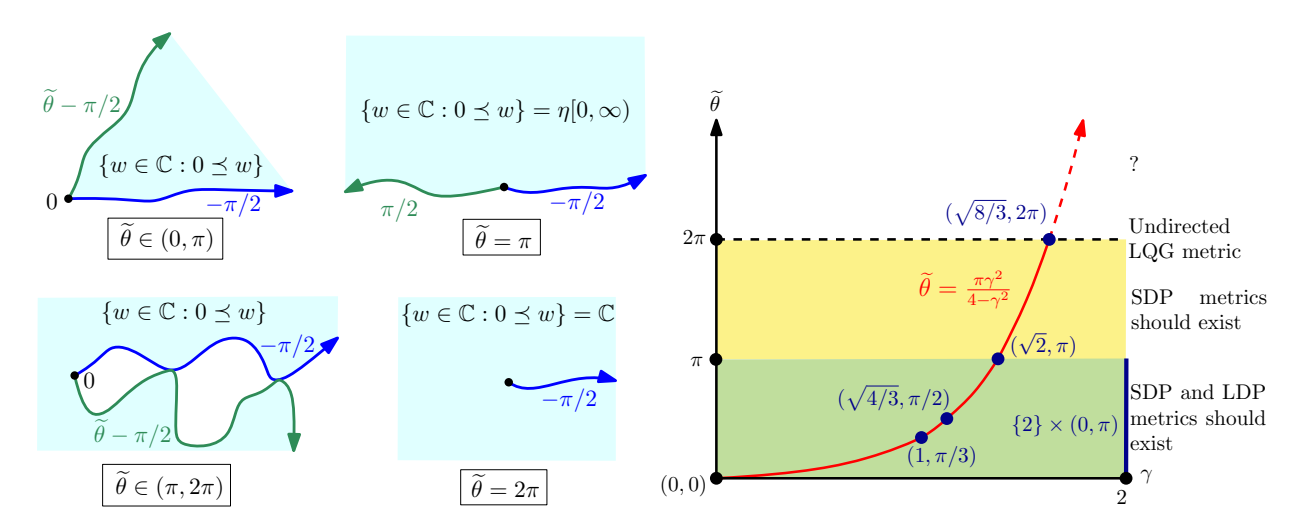


Figure 2: Left: The blue regions are the sets of points reachable by directed paths started from the origin for the hypothetical directed LQG metric in the cases when $\widetilde{\theta} \in (0, \pi)$, $\widetilde{\theta} = \pi$, $\widetilde{\theta} \in (\pi, 2\pi)$, and $\tilde{\theta} = 2\pi$. The colored curves are flow lines (in the sense of Imaginary Geometry [MS17]) of a whole plane-GFF, with angles $-\pi/2$ and $\tilde{\theta} - \pi/2$. In particular, they are each $SLE_{\gamma^2}(\gamma^2 - 2)$ curves. Right: Graph of the possible parameter values for the directed LQG metrics. The parameter value $\theta = 2\pi$ (dashed horizontal line) corresponds to the undirected LQG metric. When $\theta \in (0,\pi)$ (green region), both shortest-path and longest-path directed LQG metrics should exist. When $\theta \in [\pi, 2\pi]$ (yellow region), only the shortest-path directed LQG metric should exist. We do not know whether there is any notion of directed LQG metrics when $\theta > 2\pi$. The red curve corresponds to parameter values where we expect additional solvability. The point $(\sqrt{4/3}, \pi/2)$ corresponds to the scaling limit of directed distances in bipolar-oriented planar maps (i.e., the setting considered in this paper). The point $(\sqrt{8/3}, 2\pi)$ corresponds to the scaling limit of undirected distances on uniform planar maps (i.e., Brownian surfaces). The points $(\sqrt{2}, \pi)$ and $(1, \pi/3)$ correspond to other models which we expect can be analyzed using the techniques of this paper (spanning tree decorated maps and Schnyder-wood decorated maps, respectively); see Section 2.1. The segment $\{2\} \times (0, \pi)$ corresponds to the $\gamma \to 2$ case, which is closely related to Brownian separable permutons as studied in $[ABB^{+}25]$ (see Remark 2.4).

See the left-hand side of Figure 2 for an illustration.

We say that a path $P : [a, b] \to \mathbb{C}$ is **directed** if $P(s) \leq P(t)$ for each $s, t \in [a, b]$ with s < t.

In the case when $\gamma = \sqrt{4/3}$ and $\tilde{\theta} = \pi/2$, the relation \leq is the continuum analog of the partial ordering of the vertices of a bipolar-oriented planar map induced by the edge orientations. For general $\gamma \in (0,2)$ and $\tilde{\theta} \in (0,\pi)$, the relation \leq is closely related to the so-called **skew Brownian permutons** [Bor23]. When $\theta = \pi$, it follows from the definition of space-filling SLE_{\kappa} [MS17, Theorem 1.16] that $\eta = \tilde{\eta}$, so a path is directed if and only if it is hit in order by η . When $\theta = 2\pi$, the curves η and $\tilde{\eta}$ are time reversals of each other, so we get the trivial ordering where $z \leq w$ for every $z, w \in \mathbb{C}$. That is, the case when $\tilde{\theta} = 2\pi$ corresponds to undirected distances.

Conjecture 2.2. For each $\gamma \in (0,2)$ and $\tilde{\theta} \in (0,\pi)$, there exist two distinct random functions $\mathfrak{L}_{\Phi}^{\mathrm{LDP}}$ and $\mathfrak{L}_{\Phi}^{\mathrm{SDP}}$, called the **longest-path and shortest-path directed LQG metrics**, where for each $z, w \in \mathbb{C}$, the distance $\mathfrak{L}_{\Phi}^{\mathrm{LDP}}(z, w)$ (resp. $\mathfrak{L}_{\Phi}^{\mathrm{SDP}}(z, w)$) is a limit of regularized versions of the longest (resp. shortest) LQG length of a directed path from z to w. In the case when $\gamma = \sqrt{4/3}$ and $\tilde{\theta} = \pi/2$, these directed LQG metrics describe the scaling limits of longest and shortest directed

paths, respectively, in uniform bipolar-oriented triangulations. The shortest-path directed LQG metric $\mathfrak{L}_{\Phi}^{\mathrm{SDP}}$ also exists for $\gamma \in (0,2)$ and $\widetilde{\theta} \in [\pi, 2\pi]$ (and it coincides with the undirected γ -LQG metric when $\widetilde{\theta} = 2\pi$).

The reason why there is not an interesting longest-path directed LQG metric for $\widetilde{\theta} \in [\pi, 2\pi]$ is that in this case, the space-filling SLE_κ curves η and $\widetilde{\eta}$ are themselves directed paths. Although the directed LQG metrics $\mathfrak{L}_\Phi^{\mathrm{LDP}}$ and $\mathfrak{L}_\Phi^{\mathrm{SDP}}$ have not been constructed, our results

Although the directed LQG metrics $\mathfrak{L}_{\Phi}^{\text{LDP}}$ and $\mathfrak{L}_{\Phi}^{\text{SDP}}$ have not been constructed, our results give information about how these directed metrics should behave when $\gamma = \sqrt{4/3}$ and $\tilde{\theta} = \pi/2$. By Theorems 1.12 and 1.13, for $\gamma = \sqrt{4/3}$ and $\tilde{\theta} = \pi/2$, the scaling exponents for $\mathfrak{L}_{\Phi}^{\text{LDP}}$ and $\mathfrak{L}_{\Phi}^{\text{SDP}}$ should be 3/4 and 3/8, respectively, in the sense that scaling LQG areas by C corresponds to scaling $\mathfrak{L}_{\Phi}^{\text{LDP}}$ -distances by $C^{3/4}$ and $\mathfrak{L}_{\Phi}^{\text{SDP}}$ -distances by $C^{3/8}$. These scaling exponents are the directed analogs of $1/d_{\sqrt{4/3}}$, where $d_{\sqrt{4/3}}$ is the Hausdorff dimension of the undirected $\sqrt{4/3}$ -LQG metric space. We do not have predictions for the scaling exponents for directed LQG distances for other values of γ and θ , but we obtain some bounds in the forthcoming work [BDG25] (joint with Sayan Das).

Assume that the whole-plane space-filling SLE_{κ} curve η is parametrized so that the γ -LQG area of $\eta[a,b]$ is b-a for each $-\infty < a < b < \infty$. Theorem 1.6 suggests that for $\gamma = \sqrt{4/3}$ and $\widetilde{\theta} = \pi/2$, for each $t \in \mathbb{R}$, the Busemann function for $\mathfrak{L}_{\Phi}^{\mathrm{LDP}}$ (resp. $\mathfrak{L}_{\Phi}^{\mathrm{SDP}}$) along the boundary of $\eta(-\infty,t]$ should be a 2/3- (resp. 4/3-) stable Lévy process. It is an interesting open question to determine the joint law of such processes for different values of t; see Problem 8.2.

Directed LQG metric should have additional "solvability" properties in the special case when

$$\widetilde{\theta} = \widetilde{\theta}_*(\gamma) := \frac{\pi \gamma^2}{4 - \gamma^2}.$$
 (2.2)

Note that by [DMS21, Theorems 1.2 and 1.5], (2.2) is equivalent to the condition that the LQG surface obtained by restricting Φ to $\{w \in \mathbb{C} : 0 \leq w\}$ is an LQG wedge of weight $\gamma^2/2$ (log singularity $2/\gamma + \gamma/2$). In the forthcoming work [BDG25], we will prove several special symmetry and solvability properties for the ordering \leq when $\tilde{\theta} = \tilde{\theta}_*(\gamma)$, working exclusively in the continuum.

At least in the case when $\gamma \in (0, \sqrt{2}]$, i.e. $\tilde{\theta}_*(\gamma) \in (0, \pi]$, we expect that when $\tilde{\theta} = \tilde{\theta}_*(\gamma)$, the Busemann functions for $\mathfrak{L}_{\Phi}^{\text{LDP}}$ and $\mathfrak{L}_{\Phi}^{\text{SDP}}$ along the interface $\partial \eta(-\infty, t]$ should be a stable Lévy process (with index and skewness parameters depending on γ and the choice of LDP or SDP). See Remark 2.3 just below for a heuristic justification of this. We do not have any reason to believe that the laws of the Busemann functions for the directed LQG metrics have a nice description when $\tilde{\theta} \neq \tilde{\theta}_*(\gamma)$.

We have $\tilde{\theta}_*(\sqrt{4/3}) = \pi/2$, which corresponds to the conjectural scaling limit of directed distances in bipolar-oriented triangulations. Moreover, $\tilde{\theta}_*(\sqrt{8/3}) = 2\pi$, which corresponds to the fact that undirected distances in uniform planar maps are solvable. Additional special cases include $\tilde{\theta}_*(\sqrt{2}) = \pi$ (corresponding to paths hit in order by the contour exploration on a spanning-tree decorated map) and $\tilde{\theta}_*(1) = \pi/3$ (corresponding to directed distances in planar maps decorated by Schnyder woods). We plan to investigate these latter two cases in future work, see Section 2.1. When $\gamma > \sqrt{8/3}$, we have $\tilde{\theta}_*(\gamma) > 2\pi$. We do not know whether it is possible to make sense of a directed variant of the LQG metric with $\tilde{\theta} > 2\pi$.

Remark 2.3. Here is a heuristic justification of why $\tilde{\theta} = \tilde{\theta}_*(\gamma)$ is special, at least in the case when $\gamma \in (0, \sqrt{4/3}]$ (a similar but slightly more involved justification also works for $\gamma \in (\sqrt{4/3}, \sqrt{2}]$). The argument uses results from Sections 4 and 5, so the reader may want to return to this remark after reading those sections. Consider an infinite bipolar-oriented map $M^{\nu}_{-\infty,\infty}$ with a biased face degree distribution, encoded by a bi-infinite walk with increment distribution ν as in Section 2.2.

By varying ν , we can get walks whose coordinates have any correlation in (-1, -1/2], and hence maps in the universality class of γ -LQG for any $\gamma \in (0, \sqrt{4/3}]$.

As explained in Section 2.2, the proofs of the independent and stationary increments properties for the Busemann function in Theorem 1.7 carry over essentially verbatim to $M^{\nu}_{-\infty,\infty}$. Hence, if XDP distances on $M^{\nu}_{-\infty,\infty}$ converge to a directed LQG metric $\mathfrak{L}^{\mathrm{XDP}}_{\Phi}$, it should hold for each $t \in \mathbb{R}$ that the Busemann function of $\mathfrak{L}^{\mathrm{XDP}}_{\Phi}$ on $\partial \eta((-\infty,t])$ is a stable Lévy process. We will argue that the scaling limit of XDP distances on $M^{\nu}_{-\infty,\infty}$ should in fact correspond to $\widetilde{\theta} = \widetilde{\theta}_*(\gamma)$. In fact, we suspect that one gets $\widetilde{\theta} = \widetilde{\theta}_*(\gamma)$ for the scaling limit of directed distances in bipolar-oriented planar maps encoded by the KMSW bijection for any face degree distribution with a sufficiently light tail (such planar maps can be in the universality class of γ -LQG for any $\gamma \in (0, \sqrt{2})$ [KMSW19, Remark 5]), but we will not justify this here.

Let $\widehat{Z}^{\nu}: \mathbb{N}_0 \to \mathbb{Z}$ be a bi-infinite walk with increment distribution ν started from (0,0) and conditioned so that its first coordinate stays non-negative. Let \widehat{M}^{ν} be the infinite planar map obtained from \widehat{Z}^{ν} via the KMSW procedure (i.e., the analog of the UIQBOT of Section 4). It follows from [AG21, Theorems 1.3 and 3.5] that an LQG wedge of weight $\gamma^2/2$ can be encoded by a 2d Brownian motion of correlation $-\cos(\pi\gamma^2/4)$ conditioned to stay in the right half-plane. Hence, \widehat{M}^{ν} is a discrete analog of an LQG wedge of weight $\gamma^2/2$.

Define $M_{0,\infty}^{\nu}$ as in Definition 1.3 but with $M_{-\infty,\infty}^{\nu}$ in place of $M_{-\infty,\infty}$. By the analog of Proposition 5.1 for $M_{-\infty,\infty}^{\nu}$, the submap of $M_{0,\infty}^{\nu}$ induced by the set of vertices reachable by a directed path in $M_{0,\infty}^{\nu}$ started from the initial vertex of the root edge has the same law as \widehat{M}^{ν} . By the previous paragraph, for the scaling limit of XDP distances on $M_{-\infty,\infty}^{\nu}$, the set of points reachable by a directed path from the origin should be an LQG wedge of weight $\gamma^2/2$. As explained just after (2.2), this is equivalent to $\widetilde{\theta} = \widetilde{\theta}_*(\gamma)$.

Remark 2.4. If we fix $\theta \in (0, \pi)$ and send $\gamma \to 2$, we expect that the longest-path directed LQG metrics $\mathfrak{L}_{\Phi}^{\mathrm{LDP}}$ should converge, in some sense, to a random directed metric $\widehat{\mathfrak{L}}^{\mathrm{LDP}}$ depending on θ . The longest directed paths for $\widehat{\mathfrak{L}}^{\mathrm{LDP}}$ should be closely related to longest increasing subsequences (LIS) in Brownian separable permutons [BBF⁺18].¹¹ Substantial progress on constructing $\widehat{\mathfrak{L}}^{\mathrm{LDP}}$ has been made in the recent paper [ABB⁺25], which computes (as a function of p=1-q) the growth exponent for the length of the LIS in permutations sampled from the skew Brownian permuton and shows that the length of the LIS, re-scaled appropriately, converges in law to a non-constant random variable. As explained in Remark 1.15, the techniques of [ABB⁺25] are completely different from those of the present paper.

The limiting metric $\widehat{\mathbb{L}}^{LDP}$ should have a coupling with $\gamma = 2$ -LQG decorated by CLE₄ due to the critical mating-of-trees theorem of [AHPS23]. Consequently, it can be interpreted as a directed version of the 2-LQG metric. However, in contrast to the directed metrics in Conjecture 2.2, the directed metric $\widehat{\mathcal{L}}^{LDP}$ should not be defined on \mathbb{C} , but rather on a tree-like space obtained by identifying each CLE₄ loop to a point. See [ABB⁺25, Section 1.3] for further discussion.

We are less certain about the behavior of the shortest-path directed LQG metrics $\mathfrak{L}_{\Phi}^{\text{SDP}}$ as $\gamma \to 2$. We expect that, at least for $\widetilde{\theta} \in (0, \pi)$, the scaling exponent converges to 1/2 as $\gamma \to 2$ with $\widetilde{\theta}$ fixed, but we are not sure whether there is an interesting limiting directed metric.

¹¹The Brownian separable permutons depend on a parameter $q \in (0,1)$ which should be related to $\widetilde{\theta}$ by the formula $q = (\pi - \widetilde{\theta})/\pi$. This relation is obtained by sending $\gamma \to 2$ in [ASY25, Theorem 1.1] and recalling that $\theta = \widetilde{\theta} - \pi/2$.

2.4 Parallels with directed first- and last-passage percolation

We explain why directed distances on uniform bipolar-oriented planar maps are analogous to directed first- or last-passage percolation on \mathbb{Z}^2 ; see also Figure 3. We will then discuss some parallels between directed LQG metrics and the directed landscape.

In two-dimensional directed first- or last-passage percolation, each vertex $(x, y) \in \mathbb{Z}^2$ is assigned an i.i.d. non-negative random weight $\omega_{x,y}$. Fix now a reference point $(\overline{x}, \overline{y})$. A directed path from (x, y) to $(\overline{x}, \overline{y})$ is a sequence of lattice points that starts at (x, y), ends at $(\overline{x}, \overline{y})$, and moves only in unit steps either to the right or upward. The passage time $T(\pi)$ of a directed path π is the sum of the random weights of the lattice points it visits. For a point (x, y), the last- (resp. first-) passage time is defined as

$$LPT(x,y) = \max_{\pi:(x,y)\to(\overline{x},\overline{y})} T(\pi) \quad and \quad FPT(x,y) = \min_{\pi:(x,y)\to(\overline{x},\overline{y})} T(\pi). \tag{2.3}$$

The quantities LDP and SDP from Definition 1.2 are the planar map analogs of LPT and FPT. In the case of bipolar-oriented triangulations, we do not need extra randomness, such as the weights $\omega_{x,y}$ used in the lattice setting, since directed distances are already random due to the map and orientation being random. On the other hand, we expect that adding i.i.d. weights to the vertices (with sufficiently light tails) would not change the limiting behavior of directed distances; see for instance [CL15] for a similar property for undirected planar map distances.

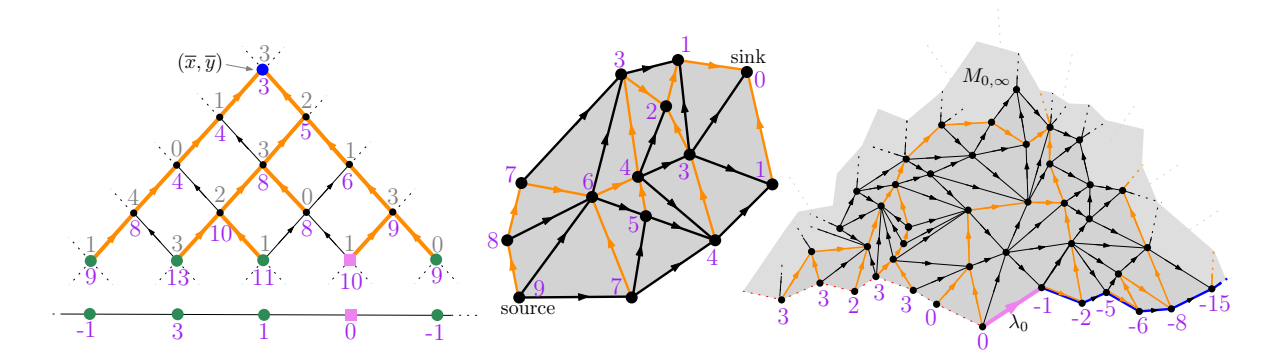
The case when the vertex weights $\omega_{x,y}$ are exponentially distributed (henceforth **exponential LPP/FPP**) is more solvable than other cases. Exponential LPP has been studied more extensively than directed exponential FPP, so we henceforth focus on this case. The existence of the Busemann function for exponential LPP (i.e., the analog of our Theorem 1.4) was established in [FP05]. In LPP, each semi-infinite geodesic is associated with a direction $\xi \in \mathbb{R}$, so there is a one-parameter family of Busemann functions, one for each ξ . This is in contrast to the case of the UIBOT, where there is only one "direction" for semi-infinite geodesics (see, e.g., Lemma 5.3), hence only one Busemann function.

The 1/3 shape fluctuation exponent for exponential LPP was first obtained in [Joh00] using the RSK correspondence. This is roughly analogous to the 3/4 scaling exponents for LDP distances in the setting of the present paper. The Busemann function for exponential LPP has i.i.d. increments, analogously to the case of the UIBOT (Theorem 1.7). This was shown in [Sep17] using the so-called Burke property from [BCS06]. It was shown in [Bus24] that the scaling limit of the Busemann function on a horizontal line is the so-called **stationary horizon**, a family of coupled Brownian motions indexed by the direction ξ . This is analogous to our Theorem 1.6, but in our setting the scaling limit is a stable Lévy process instead of a family of Brownian motions.

The full limit of exponential LPP when we re-center and re-scale appropriately (analogous to our Conjecture 2.2) was obtained in [DV21]. The limiting object is the **directed landscape**, a random directed metric $\mathfrak{L}: \mathbb{R}^2 \times \mathbb{R}^2 \to \mathbb{R} \cup \{-\infty\}$ constructed in [DOV22]. It is closely connected to the KPZ equation [KPZ86]. Intuitively speaking, for $x, y \in \mathbb{R}$ and t < s, $\mathfrak{L}(x, t; y, s)$ describes the length of the longest directed path from (x, t) to (y, s) in a certain random geometry, where here a path is considered to be directed if its second coordinate is increasing (we set $\mathfrak{L}(x, t; y, s) = -\infty$ if s < t). See, e.g., [Gan22, GH24] for expository articles on the directed landscape.

Directed first-passage percolation is believed to converge (under appropriate re-centering and re-scaling) to $-\mathfrak{L}$. This is in contrast to the setting of uniform bipolar-oriented triangulations, where LDP and SDP distances are believed to have fundamentally different scaling limits (see Conjecture 2.2).

It is shown in [RV25, Corollary 3.22] that the Busemann function in the directed landscape on a fixed horizontal line $\mathbb{R} \times \{t\}$, with geodesics going in a fixed direction, is a Brownian motion. The



Left: Last passage percolation on \mathbb{Z}^2 . A portion of \mathbb{Z}^2 , rotated counterclockwise by 45 degrees, is shown. A reference point $(\overline{x}, \overline{y})$ is shown in blue. The grey labels associated with each vertex (x,y) are the weights $\omega_{x,y}$, while the purple labels are the last-passage times LPT(x,y) introduced in (2.3). The labels on the bottom of the picture are the LPT(x,y) times of the corresponding green vertices renormalized so that the LPT time for the squared violet vertex is zero. The orange paths are LPT-geodesics, i.e. directed paths that realize the LPT times. Middle: A bipolar-oriented triangulation with its vertices labeled by their LDP distance to the sink vertex, as introduced in Definition 1.2. The orange paths are LDP geodesics from each vertex to the sink. Right: A portion of the infinite rooted submap $(M_{0,\infty},\lambda_0)$ of the UIBOT introduced in Definition 1.3. The boundary vertices are labeled in purple by the values of the Busemann function \mathcal{X} for LDP introduced in Theorem 1.4. These labels are the analogue of the bottom labels in the picture on the left when one sends the blue reference point $(\overline{x}, \overline{y})$ to infinity (recall that the limiting labels depend on the direction ξ in which we send (\bar{x}, \bar{y}) to infinity compared to the squared violet vertex). The orange paths are LDP geodesics from the boundary vertices to the sink "at infinity" in the sense of Definition 4.5. The two models in the middle and right picture are a natural version of last-passage percolation on planar maps, one in finite and one in infinite volume.

joint law of the Busemann functions on $\mathbb{R} \times \{t\}$, for all directions, has the law of the stationary horizon [BSS24, Theorem 5.3(iii)](see the above discussion on Busemann functions in different directions for exponential LPP). The coupling for the Busemann functions with different values of t is described in terms of the KPZ fixed point [BSS24, Theorem 5.1(iv)]).

For the directed $\sqrt{4/3}$ -LQG metrics as in Conjecture 2.2, the interface $\partial \eta(-\infty, t]$ (which, for t=0, is the continuum analog of the discrete interface $\partial M_{0,\infty}$) plays a role analogous to $\mathbb{R} \times \{t\}$. Theorem 1.6 suggests that the Busemann function along this interface for a fixed value of t is a certain stable Lévy process. We do not yet have a $\sqrt{4/3}$ -LQG analog of the KPZ dynamics which governs how these Busemann functions evolve when t varies (see Problem 8.2).

We expect that the directed LQG metrics have deterministic limits when $\gamma \to 0$, but it is natural to also look at the second order behavior. We have the following tantalizing question.

Problem 2.5. Do the directed LQG metrics of Conjecture 2.2 converge, in some sense, to the directed landscape when we send $\gamma \to 0$ (with some appropriate behavior for $\tilde{\theta}$) and re-center and re-scale appropriately?

A possible guess for the appropriate behavior of $\tilde{\theta}$ in Problem 2.5 is to take $\tilde{\theta} = \tilde{\theta}_*(\gamma)$ as in (2.2) and send $\gamma \to 0$. Since $\tilde{\theta}_*(\gamma) \to 0$, directed paths in this setting will converge to straight lines,

but the second-order fluctuations around these straight lines could be interesting. If the directed LQG metric does indeed converge to the directed landscape in this regime, then we would have, conjecturally, a one-parameter family of solvable models which interpolate between the directed landscape at $\gamma = 0$ and Brownian surfaces at $\gamma = \sqrt{8/3}$ (see the solid red curve in Figure 2, right).

3 KMSW bijection and conditional independence property

Sections 3.1 and 3.2 contain a review of the Kenyon-Miller-Sheffield-Wilson [KMSW19] (KMSW) bijection and its versions for various particular directed triangulations. Section 3.3 gives a conditional independence statement when we cut a Boltzmann bipolar-oriented triangulation by an XDP geodesic (Lemma 3.15). This statement is a key ingredient in the proof of the independent increments property in Theorem 1.7. Section 3.4 discusses a specialization of the KMSW bijection to so-called boundary-channeled bipolar-oriented triangulations, which will be needed for the proof of the symmetry property in Theorem 1.7.

3.1 The Kenyon-Miller-Sheffield-Wilson bijection

In this subsection, we only consider deterministic objects. Recall that we assume all planar maps in this paper are equipped with an acyclic orientation of their edges and are drawn in the plane with the edges oriented from south-west to north-east.

For a planar map \mathfrak{m} , the **external face** is the unbounded complementary connected component of the union of the edges of \mathfrak{m} . This is well-defined since we are viewing planar maps modulo orientation-preserving homeomorphisms $\mathbb{C} \to \mathbb{C}$ (instead of $\mathbb{C} \cup \{\infty\} \to \mathbb{C} \cup \{\infty\}$), recall Section 1.1. We write $\mathcal{V}(\mathfrak{m})$, $\mathcal{E}(\mathfrak{m})$, and $\mathcal{F}(\mathfrak{m})$ for the sets of vertices, edges, and non-external faces of \mathfrak{m} , respectively.

Definition 3.1. A planar map with missing edges is a planar map \mathfrak{m} with two types of edges: missing and non-missing edges (we often refer to non-missing edges simply as edges). The missing edges are always on the boundary of the external face of \mathfrak{m} and are *not* considered to be part of $\mathcal{E}(\mathfrak{m})$. A directed planar map with missing edges is a planar map \mathfrak{m} with missing edges equipped with an orientation of the edges in $\mathcal{E}(\mathfrak{m})$ that is acyclic. In particular, missing-edges are *not* oriented. See the left-hand side of Figure 4 for an example.

The planar maps \mathfrak{m} with missing edges considered in this paper will always have the boundary of their external face divided into four (possibly empty) sets of consecutive all missing or all non-missing edges. When the four sets are all non-empty, they alternate between missing and non-missing types. See again the map on the left-hand side of Figure 4 for an example.

Definition 3.2. Given an oriented planar map \mathfrak{m} with missing edges, make the following definitions (see the map on the left-hand side of Figure 4).

- The **upper-left** (resp. **lower-right**) **boundary** of \mathfrak{m} is defined to be the set of edges $e \in \mathcal{E}(\mathfrak{m})$ lying on the boundary of the external face of \mathfrak{m} which are oriented so that the external face of \mathfrak{m} is immediately to the left (resp. right) of e. For all of the maps we consider, the upper-left and lower-right boundaries of \mathfrak{m} will be (possibly empty) simple directed paths.
- The **upper-right** (resp. **lower-left**) **boundary** of \mathfrak{m} is defined to be the set of consecutive missing edges $e \notin \mathcal{E}(\mathfrak{m})$ between the terminal (resp. initial) vertex of the upper-left boundary and the terminal (resp. initial) vertex of the lower-right boundary.

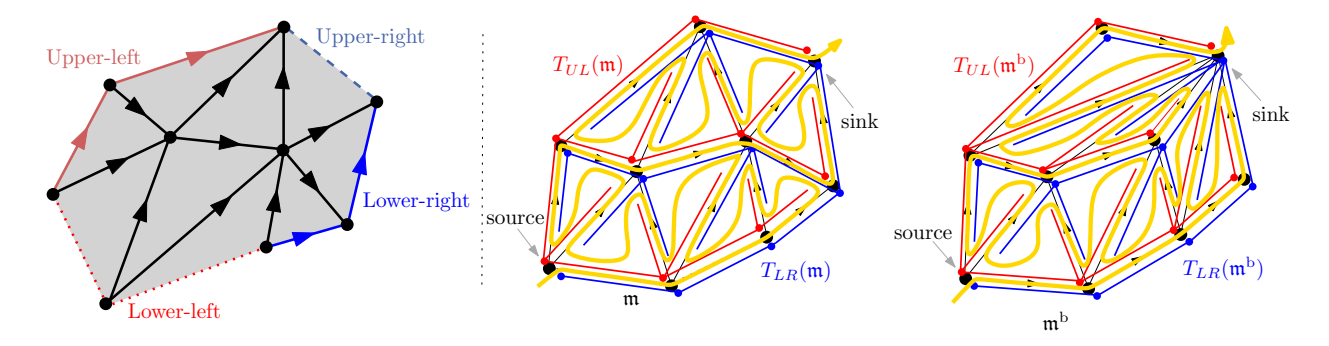


Figure 4: **Left:** An oriented planar triangulation with missing edges. The missing edges are the dotted (non-oriented) edges on the external face. The upper-left/lower-left/upper-right/lower-right boundaries of the triangulation on the left are shown in darkred/red/lightblue/blue. Note that the upper-right and lower-left boundaries are formed by missing edges. **Right:** The first bipolar-oriented triangulation \mathfrak{m} is the map on the left picture where we fixed an orientation of the missing edges (turning them into non-missing edges) to obtain a bipolar orientation. The second map \mathfrak{m}^b is a boundary-channeled bipolar-oriented triangulation (Definition 3.17). The trees $T_{UL}(\mathfrak{m})$ and $T_{LR}(\mathfrak{m})$ (resp. $T_{UL}(\mathfrak{m}^b)$ and $T_{LR}(\mathfrak{m}^b)$) introduced in the description of the inverse KMSW procedure (below Lemma 3.6) are shown in red and blue in both maps. The corresponding Peano paths are shown in gold. Note that the right-most branch of $T_{UL}(\mathfrak{m})$ has two edges that correspond to the first two right-boundary edges of \mathfrak{m} , while the right-most branch of $T_{UL}(\mathfrak{m}^b)$ has four edges that correspond to the four (and so all) right-boundary edges of \mathfrak{m}^b .

When the orientation of \mathfrak{m} is bipolar and there are no missing edges, we simply call the upper-left boundary **left** boundary and the lower-right boundary **right** boundary.

Our oriented planar maps (with possibly missing edges) will often have a single distinguished edge on the upper-left boundary of the map, called the **active edge** of the map. Note that, in particular, the active edge is in $\mathcal{E}(\mathfrak{m})$.

A key tool in the study of bipolar-oriented planar maps is the **Kenyon-Miller-Sheffield-Wilson (KMSW)** bijection [KMSW19], which encodes a bipolar-oriented planar map by means of a walk on \mathbb{Z}^2 . We will only need the case of oriented triangulations, in which case the encoding walk has increments in $\{(1,-1),(-1,0),(0,1)\}$. The following definition explains how to construct a map from a walk.

Definition 3.3 (KMSW procedure). Let $\mathfrak{Z}:[0,n]\cap\mathbb{Z}\to\mathbb{Z}^2$ be a two-dimensional walk with increments

$$\mathfrak{Z}(j) - \mathfrak{Z}(j-1) \in \{(1,-1), (-1,0), (0,1)\}.$$

The **KMSW** procedure builds a triangulation $\mathfrak{m} = \mathfrak{m}_n$ (possibly with some missing edges), equipped with an acyclic orientation, from \mathfrak{Z} through the following inductive procedure. See Figure 5 for an illustration.

¹²The map obtained via the KMSW procedure in our setting is reflected so that the left and right boundaries are swapped as compared to the map in [KMSW19]. This is to make it so that the first (resp. second) coordinate of the encoding walk corresponds to the left (resp. right) boundary length, as in the continuum setting of [DMS21]. Moreover, in this paper, we decided to draw all the maps with the orientation going from west to east (instead of from south to north as in [KMSW19]) in order to have horizontal (instead of vertical) boundaries in the figures.

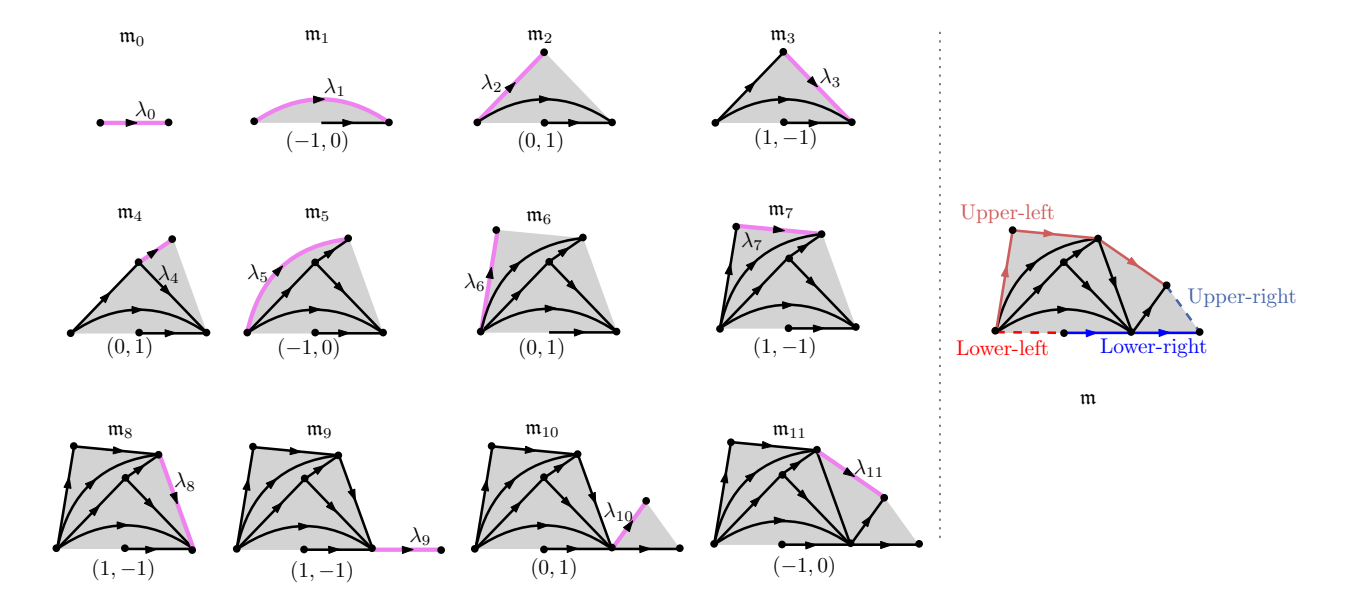


Figure 5: **Left:** The directed triangulations with missing edges $\mathfrak{m}_0, \ldots, \mathfrak{m}_{11}$ built from the KMSW procedure for a walk with 11 steps. For convenience, the lower boundary edges are drawn along a horizontal line. The steps of the walk are shown underneath the maps. The active edges λ_j are shown in violet. All edges are oriented from west to east. **Right:** The final map $\mathfrak{m} = \mathfrak{m}_{11}$ with its four special boundary segments shown in different colors as in Figure 4. Note that edges along the upper-left and lower-right boundary belong to \mathfrak{m} , but edges along the lower-left and lower-right boundary do not.

Let $(\mathfrak{m}_0, \lambda_0)$ be the map consisting of a single directed active edge λ_0 . The only non-empty boundaries of this map are the upper-left and lower-right boundaries (which coincide). We assume that this single edge is drawn in the plane so that it is oriented from west to east.

Inductively, suppose $j \in [1, n] \cap \mathbb{Z}$ and a directed map $(\mathfrak{m}_{j-1}, \lambda_{j-1})$ with an active edge $\lambda_{j-1} \in \mathcal{E}(\mathfrak{m}_{j-1})$ (and possibly missing edges) have been defined and drawn in the plane so that all its edges are oriented from south-west to north-east. We let $(\mathfrak{m}_j, \lambda_j)$ be the directed triangulation with an active edge (and possibly missing edges) obtained from $(\mathfrak{m}_{j-1}, \lambda_{j-1})$ as follows:

- If $\mathfrak{Z}(j) \mathfrak{Z}(j-1) = (1,-1)$, we construct $(\mathfrak{m}_j, \lambda_j)$ in the following way:
 - If the upper-right boundary of \mathfrak{m}_{j-1} is not empty, we consider the missing edge of the upper-right boundary of \mathfrak{m}_{j-1} immediately to the east of λ_{j-1} and construct $(\mathfrak{m}_j, \lambda_j)$ by adding this edge to the set of edges of \mathfrak{m}_{j-1} , orienting this edge from west to east and setting λ_j equal to this new edge. See, for instance, how the triangulation \mathfrak{m}_3 is obtained from the triangulation \mathfrak{m}_2 in Figure 5.
 - Otherwise, we construct $(\mathfrak{m}_j, \lambda_j)$ by adding to the set of edges of \mathfrak{m}_{j-1} a new active edge λ_j oriented from west to east, whose initial vertex coincides with the terminal vertex of λ_{j-1} . Note that λ_j does not lie on the boundary of any triangle of \mathfrak{m}_j . See, for instance, how the triangulation \mathfrak{m}_9 is obtained from the triangulation \mathfrak{m}_8 in Figure 5.
- If $\mathfrak{Z}(j) \mathfrak{Z}(j-1) = (-1,0)$, we construct $(\mathfrak{m}_j, \lambda_j)$ by adding to \mathfrak{m}_{j-1} a new triangular face t_j with a new directed edge λ_j on the boundary of t_j with the following properties: The edges λ_{j-1} and λ_j both lie on the boundary of t_j , and their terminal vertices coincide. Moreover,

- if the upper-left boundary of \mathfrak{m}_{j-1} , excluding λ_{j-1} , is not empty, the third edge on the boundary of t_j is the edge of the upper-left boundary of \mathfrak{m}_{j-1} , which lies immediately to the west of λ_{j-1} . In particular, the initial vertex of this edge coincides with the initial vertex of λ_j . See, for instance, how the triangulation \mathfrak{m}_5 is obtained from the triangulation \mathfrak{m}_4 in Figure 5;
- otherwise, the third edge on the boundary t_j is a new *missing* edge, with one vertex equal to the initial vertex of λ_{j-1} . Moreover, the other vertex of this missing edge coincides with the initial vertex of λ_j . See, for instance, how the triangulation \mathfrak{m}_1 is obtained from the map \mathfrak{m}_0 in Figure 5;
- If $\mathfrak{Z}(j) \mathfrak{Z}(j-1) = (0,1)$, we construct \mathfrak{m}_j by adding to \mathfrak{m}_{j-1} a new triangle t_j and a new directed edge λ_j with the following properties. The edges λ_{j-1} and λ_j both lie on the boundary of t_j , and their initial vertices coincide. The third edge on the boundary of λ_j is a new *missing* edge, whose initial vertex coincides with the terminal vertex of λ_j . See, for instance, how the triangulation \mathfrak{m}_2 is obtained from the triangulation \mathfrak{m}_1 in Figure 5;

We finally set $\mathfrak{m} = \mathfrak{m}_n$.

The map \mathfrak{m} produced by the KMSW procedure depends only on the increments of \mathfrak{Z} , so it is unchanged if we replace \mathfrak{Z} by $\mathfrak{Z} + z$ for any $z \in \mathbb{Z}^2$.

Remark 3.4. Let $n \in \mathbb{Z}$. The KMSW procedure can still be defined if $\mathfrak{Z}: \mathbb{Z}_{\geq n} \to \mathbb{Z}^2$ with increments in $\{(1,-1),(-1,0),(0,1)\}$. In this case, we take $\mathfrak{m}_{n,\infty}$ to be the increasing union of the triangulations $(\mathfrak{m}_j)_{j\in\mathbb{Z}_{\geq n}}$ built during the KMSW procedure of Definition 3.3, where the maps are labeled so that $(\mathfrak{m}_n,\lambda_n)$ denotes the initial map consisting of a single active oriented edge λ_n . Moreover, we set the edge in $\mathfrak{m}_{n,\infty}$ corresponding to the initial active edge λ_n to be the root edge of $\mathfrak{m}_{n,\infty}$. The boundary of $\mathfrak{m}_{n,\infty}$ is divided into four (possibly infinite or possibly empty) intervals of consecutive edges: the upper-left (resp. lower-left, lower-right, upper-right) boundary of $\mathfrak{m}_{n,\infty}$ is the set of edges that belong to the upper-left (resp. lower-left, lower-right, upper-right) boundary of \mathfrak{m}_i for infinitely many j.

The KMSW procedure can also be defined for bi-infinite walks $\mathfrak{Z}:\mathbb{Z}\to\mathbb{Z}^2$ with increments in $\{(1,-1),(-1,0),(0,1)\}$. In this case, we take $\mathfrak{m}_{-\infty,\infty}$ to be the union of the triangulations $(\mathfrak{m}_{n,\infty})_{n\in\mathbb{Z}}$ – note that these triangulations increase when n decreases – where the maps $\mathfrak{m}_{n,\infty}$ are obtained from $\mathfrak{Z}|_{[n,\infty)}$ using the KMSW procedure described in the previous paragraph. Moreover, we set the edge in $\mathfrak{m}_{-\infty,\infty}$ corresponding to the active edge λ_0 to be the root edge of $\mathfrak{m}_{-\infty,\infty}$. The boundary of $\mathfrak{m}_{-\infty,\infty}$ is divided into four (possibly-infinite and possibly-empty) intervals of consecutive edges: the upper-left (resp. lower-left, lower-right, upper-right) boundary of $\mathfrak{m}_{-\infty,\infty}$ is the set of edges that belong to the upper-left (resp. lower-left, lower-right, upper-right) boundary of $\mathfrak{m}_{-\infty,\infty}$ for infinitely many n. Note that it is possible for all four boundary intervals of $\mathfrak{m}_{-\infty,\infty}$ to be empty; in this case, $\mathfrak{m}_{-\infty,\infty}$ has no boundary.

The following is the special case of [KMSW19, Theorem 2] when we restrict to triangulations.

Theorem 3.5 ([KMSW19]). Let $l, r, n \in \mathbb{N}$. The KMSW procedure restricts to a bijection between the following two sets.

- Walks with increments in $\{(1,-1),(-1,0),(1,0)\}$ which start at (0,0), end at (l-1,-r+1), have n-1 total steps, and stay in $[0,\infty)\times[-r+1,\infty)$.
- Bipolar-oriented triangulations with n total edges, ¹³ l left boundary edges, and r right boundary edges (Definition 1.9).

 $^{^{13}\}mathrm{We}$ stress that these triangulations have no missing edges.

Note that the walk used in Figure 5 is not a valid walk for the theorem above, since the walk does not stay in the requested domain. In the setting of Definition 3.3, the lengths (and several other properties) of the four special boundary segments of $\mathfrak m$ can be recovered from the encoding walk as follows.

Lemma 3.6. Let $\mathfrak{Z} = (\mathfrak{L}, \mathfrak{R}) : [0, n] \cap \mathbb{Z} \to \mathbb{Z}^2$ be a walk with increments in $\{(1, -1), (-1, 0), (0, 1)\}$ and started at $\mathfrak{Z}(0) = (0, 0)$ and let \mathfrak{m} be its associated map via the KMSW procedure as in Definition 3.3. Define the four boundary segments of \mathfrak{m} as done in Definition 3.2.

- (i) The time $\min\{m \in \mathbb{N} : \mathfrak{L}(m) = -k\}$, is the time when the kth lower-left (missing) boundary edge of \mathfrak{m} (counting starting from the initial vertex of λ_0 and moving along the lower-left boundary) is added to \mathfrak{m} by the KMSW procedure. Moreover, this is the first time that the west vertex of this new edge is the initial vertex of an active edge (and all the other times the same fact happens are the times m such that $\mathfrak{L}(m) = -k$ and $\mathfrak{L}(j) \geq -k$ for all $j \leq m$).
- (ii) The time $\min\{m \in \mathbb{N} : \Re(m) = -k\}$, is the time when the k+1th (counting respecting the orientation) lower-right boundary edge of \mathfrak{m} is added to \mathfrak{m} by the KMSW procedure. Moreover, this is the first time that the terminal vertex of this new edge is the terminal vertex of an active edge (and all the other times the same fact happens are the times m such that $\Re(m) = -k$ and $\Re(j) \geq -k$ for all $j \leq m$).
- (iii) The kth smallest $m \in \mathbb{N}$ such that $\mathfrak{L}(j) \geq \mathfrak{L}(m) + 1$ for all $j \in [m+1,n] \cap \mathbb{Z}$ is the time when the kth (counting respecting the orientation) upper-left boundary edge of \mathfrak{m} is added to \mathfrak{m} by the KMSW procedure. Moreover, for every time $m' \leq m$ such that $\mathfrak{L}(m') = \mathfrak{L}(m)$ and $\mathfrak{L}(j) \geq \mathfrak{L}(m')$ for all $j \in [m', m] \cap \mathbb{Z}$, the corresponding active edge $\lambda_{m'}$ has the same initial vertex as the upper-left boundary edge λ_m .
- (iv) The kth smallest $m \in \mathbb{N}$ such that $\mathfrak{R}(j) \geq \mathfrak{R}(m-1) + 1$ for all $j \in [m,n] \cap \mathbb{Z}$ is the time when the kth upper-right (missing) boundary edge of \mathfrak{m} (counting starting from the terminal vertex of the lower-right boundary and moving along the upper-right boundary) is added to \mathfrak{m} by the KMSW procedure.

In particular, denoting the set of edges on the upper-left, upper-right, lower-left, and lower-right boundary segments by $\overline{\partial}_L \mathfrak{m}$, $\overline{\partial}_R \mathfrak{m}$, $\underline{\partial}_L \mathfrak{m}$, and $\underline{\partial}_R \mathfrak{m}$, respectively, we have that

$$\#\overline{\partial}_{L}\mathfrak{m} = \mathfrak{L}(n) - \min_{j \in [0,n] \cap \mathbb{Z}} \mathfrak{L}(j) + 1, \qquad \#\overline{\partial}_{R}\mathfrak{m} = \mathfrak{R}(n) - \min_{j \in [0,n] \cap \mathbb{Z}} \mathfrak{R}(j),$$

$$\#\underline{\partial}_{L}\mathfrak{m} = -\min_{j \in [0,n] \cap \mathbb{Z}} \mathfrak{L}(j), \qquad \#\underline{\partial}_{R}\mathfrak{m} = -\min_{j \in [0,n] \cap \mathbb{Z}} \mathfrak{R}(j) + 1. \tag{3.1}$$

Proof. We prove the statements for the lower-left and upper-left boundaries. The proof for the lower-right and upper-right boundaries are similar.

For $j \in [0, n] \cap \mathbb{Z}$, let \mathfrak{m}_j be the time-j map in the KMSW procedure, as in Definition 3.3. By considering each of the three possible values of $\mathfrak{Z}(j) - \mathfrak{Z}(j-1)$ in Definition 3.3, we see that for $j \geq 1$,

$$\mathfrak{L}(j) - \mathfrak{L}(j-1) = (\#\overline{\partial}_L \mathfrak{m}_j - \#\overline{\partial}_L \mathfrak{m}_{j-1}) - (\#\underline{\partial}_L \mathfrak{m}_j - \#\underline{\partial}_L \mathfrak{m}_{j-1})
= (\#\overline{\partial}_L \mathfrak{m}_j - \#\underline{\partial}_L \mathfrak{m}_j) - (\#\overline{\partial}_L \mathfrak{m}_{j-1} - \#\underline{\partial}_L \mathfrak{m}_{j-1}),$$
(3.2)

and $\mathfrak{L}(0) = 0 = (\# \overline{\partial}_L \mathfrak{m}_0 - \# \underline{\partial}_L \mathfrak{m}_0) - 1$. (We also have the analogous relation with \mathfrak{R} in place of \mathfrak{L} and "right" in place of "left", but with starting value $\mathfrak{R}(0) = 0 = (\# \overline{\partial}_R \mathfrak{m}_0 - \# \underline{\partial}_R \mathfrak{m}_0) + 1$.) Summing these relations over $i \in [0, j] \cap \mathbb{Z}$ gives

$$\mathfrak{L}(j) = \# \overline{\partial}_L \mathfrak{m}_j - \# \underline{\partial}_L \mathfrak{m}_j - 1 \quad (\text{and} \quad \mathfrak{R}(j) = \# \overline{\partial}_R \mathfrak{m}_j - \# \underline{\partial}_R \mathfrak{m}_j + 1.)$$
 (3.3)

By construction, the lower-left boundary length $\underline{\partial}_L \mathfrak{m}_j$ is non-decreasing in j (once a lower-left boundary edge is added, it can never be removed). If $j \in [0, n] \cap \mathbb{Z}$ such that $\#\underline{\partial}_L \mathfrak{m}_j > \#\underline{\partial}_L \mathfrak{m}_{j-1}$, then at time j we must add a triangle to \mathfrak{m}_{j-1} which has a new missing edge that becomes part of the lower-left boundary of \mathfrak{m}_j and a new active edge whose initial vertex v coincides with one vertex of the new missing edge (the one farthest from λ_0). By Definition 3.3, this happens if and only if $\mathfrak{Z}(j) - \mathfrak{Z}(j-1) = (-1,0)$ and the upper-left boundary of \mathfrak{m}_{j-1} consists of the single edge λ_{j-1} . By (3.3), this is the case if and only if $\mathfrak{L}(j) = -\#\underline{\partial}_L \mathfrak{m}_j = \min_{i \in [0,j] \cap \mathbb{Z}} \mathfrak{L}(i)$.

Hence, the time τ_{-k} at which \mathfrak{L} attains the running minimum -k corresponds to the times at which the kth lower-left boundary edge is added to the map. In particular, this gives the first part of Assertion (i) and the formula for $\# \underline{\partial}_L \mathfrak{m}$ in (3.1). The formula for $\# \overline{\partial}_L \mathfrak{m}$ in (3.1) follows from the formula for $\# \underline{\partial}_L \mathfrak{m}$ and (3.3).

We will now prove the rest of Assertion (i). The time τ_{-k} is obviously the first time that the vertex v (which is the west vertex of the kth lower-left boundary edge) is the initial vertex of an active edge. For all subsequent times $m \geq \tau_{-k}$ such that $\mathfrak{L}(j) \geq -k$ for all $j \leq m$, we have that $\# \underline{\partial}_L \mathfrak{m}_m = -\min_{i \in [0,m] \cap \mathbb{Z}} \mathfrak{L}(i)$ since $\underline{\partial}_L \mathfrak{m}_j$ is non-decreasing in j, and so by (3.3) and (3.1) for $\underline{\partial}_L \mathfrak{m}_m$, we have that

$$\#\overline{\partial}_L \mathfrak{m}_j - 1 = \mathfrak{L}(m) + \#\underline{\partial}_L \mathfrak{m}_m = \mathfrak{L}(m) - \min_{j \in [0,m] \cap \mathbb{Z}} \mathfrak{L}(j) = \mathfrak{L}(m) - (-k)$$
 (3.4)

is equal to the distance along the upper-left boundary between v and the initial vertex of λ_m . Hence, the vertex v is still part of the upper-left boundary of the corresponding map \mathfrak{m}_m and we have that when $\mathfrak{L}(j) \geq -k$ for all $j \leq m$ and $\mathfrak{L}(m) = -k$, the initial vertex of λ_m must be the vertex v. These are the only times this happens. Indeed, at the first subsequent time $m \geq \tau_{-k}$ such that $\mathfrak{L}(m) = -(k+1)$, using the same argument in the paragraph below (3.3), we have that the vertex v is no longer part of the upper-left boundary of the corresponding map \mathfrak{m}_m . This completes the proof of Assertion (i).

We now consider Assertion (iii). By the construction in Definition 3.3, for $m \in [0, n] \cap \mathbb{Z}$, the edge λ_m is part of the upper-left boundary of \mathfrak{m} if and only if $\mathfrak{Z}(m) - \mathfrak{Z}(m-1) = (1, -1)$ and the map obtained by applying the KMSW procedure to $\mathfrak{Z}|_{[m+1,n]}$ has no lower-left boundary edges. By (3.1) for the lower-left boundary of this map, this is the case if and only if $\mathfrak{L}(j) \geq \mathfrak{L}(m) + 1$ for all $j \in [m+1,n] \cap \mathbb{Z}$. This gives the first part of Assertion (iii). The statement about the initial vertex of λ_m follows from a similar argument as in the case of Assertion (i).

We now describe the inverse KMSW procedure, i.e., the procedure that, given a bipolar-oriented triangulation \mathfrak{m} with missing edges, returns the corresponding encoding walk \mathfrak{Z} with increments in $\{(1,-1),(-1,0),(1,0)\}$. We stress that the inverse KMSW procedure will be defined only for bipolar-oriented maps, in particular, maps having only non-missing edges. In what follows, **disconnecting** an edge from a vertex means deleting the connection between the edge and the vertex, resulting in an edge that is missing one of its vertices. See the right-hand side of Figure 4 for examples of this procedure.

Assume that \mathfrak{m} has n total edges. For each vertex v of \mathfrak{m} , we disconnect from v every incoming edge to v (including the missing ones) except for the leftmost incoming edge to v. This turns the map \mathfrak{m} into a plane tree $T_{UL}(\mathfrak{m})$ rooted at the source, which we call the **upper-left tree** of \mathfrak{m} (see the right-hand side of Figure 4). The tree $T_{UL}(\mathfrak{m})$ contains every edge of \mathfrak{m} . We denote by $\lambda_1, \ldots, \lambda_n$ the edges of \mathfrak{m} in the order that they are first visited by the counterclockwise contour exploration of $T_{UL}(\mathfrak{m})$. The tree $T_{LR}(\mathfrak{m})$, called the **lower-right tree**, can be obtained similarly from \mathfrak{m} by disconnecting every outgoing edge from each vertex but the rightmost, and is rooted at the sink. The following facts hold (see [KMSW19, Section 2.1]): The clockwise contour exploration

of $T_{LR}(\mathfrak{m})$ also visits the edges of \mathfrak{m} in the order $\lambda_1, \ldots, \lambda_n$. Moreover, one can draw $T_{UL}(\mathfrak{m})$ and $T_{LR}(\mathfrak{m})$ in the plane, one next to the other, in such a way that the interface between the two trees traces a path, called the **Peano path**, ¹⁴ from the source to the sink visiting edges $\lambda_1, \ldots, \lambda_n$ in this order. Moreover, every branch of $T_{UL}(\mathfrak{m})$ (resp. $T_{LR}(\mathfrak{m})$) is a leftmost (resp. rightmost) directed path from the source (resp. to the sink).

Definition 3.7 (Inverse KMSW procedure). Let $n \ge 1$ and \mathfrak{m} be a bipolar-oriented triangulation with n total edges, with l edges on its left boundary and r edges on its right boundary. We define the corresponding KMSW walk $\mathfrak{Z} = (\mathfrak{L}(j), \mathfrak{R}(j))_{0 \le j \le n-1}$ as follows: for $0 \le j \le n-1$,

- $\mathfrak{L}(j)$ is the height in the tree $T_{UL}(\mathfrak{m})$ of the initial vertex of λ_{j+1} (i.e. its distance in $T_{UL}(\mathfrak{m})$ from the source);
- $\Re(j)$ is the height in the tree $T_{LR}(\mathfrak{m})$ of the terminal vertex of λ_{j+1} (i.e. its distance in $T_{LR}(\mathfrak{m})$ from the sink) minus r-1.

By [KMSW19, Theorem 2], the function $\mathfrak{m} \to \mathfrak{Z}$ of Definition 3.7 is the inverse of the bijection from Theorem 3.5. That is, if \mathfrak{m} and \mathfrak{Z} are as in Definition 3.7, then \mathfrak{Z} is a walk with increments in $\{(1,-1),(-1,0),(1,0)\}$ which starts at (0,0), ends at (l-1,-r+1), has n-1 total steps, and stay in $[0,\infty) \times [-r+1,\infty)$; and applying the KMSW procedure to \mathfrak{Z} gives \mathfrak{m} .

Recall the definition of leftmost and rightmost directed paths from Section 1.2. The following lemma describes the boundary of the infinite map $(\mathfrak{m}_{n,\infty}, \lambda_n)$ introduced in Remark 3.4.

Lemma 3.8. Let $\mathfrak{Z}: \mathbb{Z} \to \mathbb{Z}^2$ be a bi-infinite walk with increments in $\{(1,-1),(-1,0),(0,1)\}$, normalized so that $\mathfrak{Z}(0)=(0,0)$. For $n\in\mathbb{Z}$, let $(\mathfrak{m}_{n,\infty},\lambda_n)$ be the rooted submap of the UIBOT obtained by applying, as detailed in Remark 3.4, the KMSW procedure to $\mathfrak{Z}|_{[n,\infty)}$.

The boundary of $\mathfrak{m}_{n,\infty}$ is the union of the root edge λ_n , the rightmost directed path in $\mathfrak{m}_{-\infty,\infty}$ from the terminal vertex of λ_n to ∞ , and the leftmost directed path in $\mathfrak{m}_{-\infty,\infty}$ from $-\infty$ to the initial vertex of λ_n . The edge λ_n and the edges on the rightmost directed path are part of $\mathfrak{m}_{n,\infty}$ and form the right boundary of $\mathfrak{m}_{n,\infty}$, whereas the edges of the leftmost directed path are not, i.e. are missing edges, and form the left boundary of $\mathfrak{m}_{n,\infty}$.

Furthermore, every vertex on the left boundary of $\mathfrak{m}_{n,\infty}$, including the initial vertex of λ_n , has at least one outgoing edge but no incoming edges (recall that missing edges are not oriented), while every other vertex of $\mathfrak{m}_{n,\infty}$ has at least one incoming and one outgoing edge. Finally, every pair of rightmost directed paths P_x and $P_{x'}$ started from a pair of boundary vertices x and x' of $\mathfrak{m}_{n,\infty}$ coalesce into each other, i.e. there is some s, s' > 0 such that $P_x(s+t) = P_{x'}(s'+t)$ for all $t \geq 0$.

Proof. This follows combining: (i) the construction in Remark 3.4 of $\mathfrak{m}_{n,\infty}$ as the increasing union of the triangulations $(\mathfrak{m}_j)_{j\in\mathbb{Z}_{\geq n}}$ built during the KMSW procedure; (ii) the construction of $\mathfrak{m}_{-\infty,\infty}$ in the same remark; and (iii) the description of the inverse KMSW procedure in Definition 3.7, recalling that every branch of $T_{UL}(\mathfrak{m}_j)$ (resp. $T_{LR}(\mathfrak{m}_j)$) is a leftmost (resp. rightmost) directed path from the source (resp. to the sink).

3.2 KMSW encodings of random bipolar-oriented triangulations

Recall from Section 1.2 that the uniform infinite bipolar-oriented triangulation (UIBOT) is the directed, edge-rooted infinite bipolar-oriented triangulation $(M_{-\infty,\infty}, \lambda_0)$ obtained as the Benjamini-Schramm [BS01] local limit in law of uniform bipolar-oriented triangulations with n edges and a fixed number of left and right boundary edges, rooted at a uniformly chosen edge. We recall the definition of this topology for directed planar maps.

¹⁴The Peano path coincides with the counter-clockwise contour exploration of $T_{UL}(\mathfrak{m})$.

Definition 3.9. Let (M, e) and $(\widetilde{M}, \widetilde{e})$ be directed planar maps, each equipped with a (directed) root edge. For $r \in \mathbb{N}$, define the graph-distance ball $\mathcal{B}_r(M)$ to be the directed submap of M consisting of the vertices of M which lie at (undirected) graph distance at most r from the initial vertex of e, together with the (directed) edges whose vertices both lie in this vertex set and the faces whose boundary vertices all lie in this vertex set. Similarly define $\mathcal{B}_r(\widetilde{M})$. The **Benjamini-Schramm local distance** between (M, e) and $(\widetilde{M}, \widetilde{e})$ is

$$D_{\mathrm{loc}}((M, e), (\widetilde{M}, \widetilde{e})) = \inf \{ 2^{-r} : \mathcal{B}_r(M) \cong \mathcal{B}_r(\widetilde{M}) \}$$

where \cong means that the two balls are isomorphic as directed planar maps.

The UIBOT can be described in terms of the KMSW procedure as follows (see [GHS20, Proposition 3.16] for the case of bipolar-oriented maps with unconstrained face degrees – the triangulation case can be treated identically).

Proposition 3.10 ([GHS20]). Let $\mathcal{Z} : \mathbb{Z} \to \mathbb{Z}^2$ be a bi-infinite random walk whose increments are i.i.d. uniform samples from $\{(1,-1),(-1,0),(0,1)\}$, normalized so that $\mathcal{Z}(0)=(0,0)$. Applying the KMSW procedure to \mathcal{Z} , as detailed in Remark 3.4, gives the UIBOT $M_{-\infty,\infty}$.

We have the following description of the KMSW encoding walk for Boltzmann bipolar-oriented planar maps with a given right boundary length (Definition 1.10).

Lemma 3.11. Let $r \in \mathbb{N}$. Let $\mathcal{Z} = (\mathcal{L}, \mathcal{R}) : \mathbb{N}_0 \to \mathbb{Z}^2$ be a walk started from (0,0) with i.i.d. increments sampled uniformly from $\{(1,-1),(-1,0),(1,0)\}$. Let τ be the smallest $n \in \mathbb{N}$ for which $\mathcal{R}(n) = -r$ and let

$$E:=\{\mathcal{L}(n)\geq 0,\,\forall n\in[0,\tau]\cap\mathbb{Z}\}.$$

Let M be the map obtained by applying the KMSW procedure to $\mathcal{Z}|_{[0,\tau-1]}$. The conditional law of M given E is that of a Boltzmann bipolar-oriented triangulation with right boundary length r (Definition 1.10).

Proof. Let \mathfrak{m} be a bipolar-oriented triangulation with l left boundary edges, r right boundary edges, and n total edges. Let \mathfrak{Z} be the corresponding encoding walk under the KMSW bijection as in Theorem 3.5. Then \mathfrak{Z} is a walk that starts at (0,0), ends at (l-1,-r+1), has n-1 total steps, and stays in $[0,\infty)\times[-r+1,\infty)$. We have $M=\mathfrak{m}$ if and only if $\mathcal{Z}|_{[0,\tau-1]}=\mathfrak{Z}$. This is the case if and only if $\mathcal{Z}|_{[0,n-1]}=\mathfrak{Z}$ and $\mathcal{Z}(n)-\mathcal{Z}(n-1)=(1,-1)$ (in which case E occurs). Since the increments of \mathcal{Z} are i.i.d.,

$$\mathbb{P}[M = \mathfrak{m}] = \mathbb{P}\left[\mathcal{Z}|_{[0,n-1]} = \mathfrak{Z}, \ \mathcal{Z}(n) - \mathcal{Z}(n-1) = (1,-1)\right] = \left(\frac{1}{3}\right)^n.$$

Since $\{M = \mathfrak{m}\} \subset E$, it follows that

$$\mathbb{P}[M = \mathfrak{m} \,|\, E] = \mathbb{P}[E]^{-1} \left(\frac{1}{3}\right)^n$$

as required.

As a consequence of Lemma 3.12, we see that the first Boltzmann distribution defined in Definition 1.10 is well-defined, in the sense that it has finite total mass. We can also establish the analogous statement for the second distribution defined in Definition 1.10.

Lemma 3.12. Assume that we are in the setting of Lemma 3.11. Then

$$\mathbb{E}[\mathcal{L}(\tau) + 1 \mid E] < \infty. \tag{3.5}$$

In particular, the Boltzmann distribution on bipolar-oriented triangulations with right boundary length r and a marked boundary edge (Definition 1.10) is well-defined.

Proof. Let $\sigma := \min\{n \geq 0 : \mathcal{L}(n) = -1\}$, so that $E = \{\sigma > \tau\}$. Let $Y(n) := (\mathcal{L}(n) + 1)\mathbb{1}_E$. One can check from the definition that Y is a martingale w.r.t. the filtration generated by $\mathcal{Z}|_{[0,n]}$ (see [BD94] for a much more general statement). The time τ is an a.s. finite stopping time for this filtration, and Y is always non-negative. By Fatou's lemma and the optional stopping theorem,

$$\mathbb{E}[(\mathcal{L}(\tau)+1)\mathbb{1}_E] = \mathbb{E}[Y(\tau)] \le \lim_{n \to \infty} \mathbb{E}[Y(\tau \land n)] = \mathbb{E}[Y(0)] = 1.$$

This gives (3.5). As explained just after Definition 1.10, the Boltzmann distribution on bipolaroriented triangulations with right boundary length r and a marked left boundary vertex is obtained by weighting the Boltzmann distribution on bipolar-oriented triangulations with right boundary length r by the left boundary length plus one. By Lemma 3.11, this corresponds to weighting the conditional law of $\mathcal{Z}|_{[0,\tau]}$ given E by $\mathcal{L}(\tau) + 1$. This is a valid weighting by (3.5).

3.3 Conditional independence for Boltzmann bipolar-oriented triangulations

Recall the notation LDP and SDP from Definition 1.2.

Definition 3.13. Let XDP \in {LDP, SDP}. Let \mathfrak{m} be a finite planar map equipped with an acyclic orientation of its edges and let $x, y \in \mathcal{V}(\mathfrak{m})$. We say that a directed path $\mathfrak{p}: [1, |\mathfrak{p}|] \cap \mathbb{Z} \to \mathcal{E}(\mathfrak{m})$ from x to y is an XDP **geodesic** if the length $|\mathfrak{p}|$ of \mathfrak{p} is equal to XDP_m(x, y) (Definition 1.2). We say that \mathfrak{p} is the **leftmost** XDP **geodesic** from x to y if every XDP geodesic in \mathfrak{m} from x to y lies weakly to the right of \mathfrak{p} if we stand at x and look toward y. That is, every XDP geodesic from x to y lies in the submap of \mathfrak{m} bounded by \mathfrak{p} , the rightmost directed path started from x, and the rightmost directed path ending at y (including the vertices and edges lying on the three paths).

It is easy to see that if there is a directed path from x to y, then there is a unique leftmost XDP geodesic from x to y.

Definition 3.14. For $l, r \in \mathbb{N}$, let $\mathcal{M}_{l,r}$ be the set of finite bipolar-oriented triangulations with boundary having l edges on their left boundary and r edges on their right boundary. We define the **Boltzmann distribution** on bipolar-oriented triangulations with left boundary length l and right boundary length r exactly as in Definition 1.10, but with both the left and right boundary lengths fixed. That is, it is the law of a random bipolar-oriented triangulation M(l,r) such that for every bipolar-oriented triangulation \mathfrak{m} with l left boundary edges, r right boundary edges, and r total edges,

$$\mathbb{P}[M(l,r) = \mathfrak{m}] = \frac{3^{-n}}{C_{l,r}},\tag{3.6}$$

where $C_{l,r}$ is a normalizing constant. Equivalently, M(l,r) is a sample from the conditional law of a Boltzmann bipolar-oriented triangulation with r right boundary edges (Definition 1.10) given that its left boundary length is l.

The following statement is the starting point of the proof that the Busemann function of Theorem 1.4 has independent increments; see Figure 6.

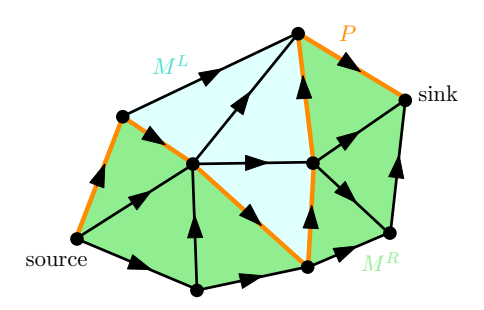


Figure 6: A Boltzmann bipolar-oriented triangulation M(l,r) with left boundary length l=3 and right boundary length r=4. In orange, the leftmost LDP geodesic P from the source to the sink, as introduced in Definition 3.13. The map M^L (resp. M^R) is the submap of M(l,r) consisting of the vertices, edges, and faces of M(l,r) in the lightblue (resp. lightgreen) region including the vertices and edges which lie on the orange leftmost XDP geodesic P. Note that the lightblue map M^L does not contain any other geodesic from the source to the sink other than P, while the lightgreen map M^R contains additional geodesics. By Lemma 3.15, the submaps M^L and M^R are conditionally independent given the length of P.

Lemma 3.15. Fix XDP \in {LDP, SDP} and $l, r \in \mathbb{N}$. Let M(l, r) be a Boltzmann bipolar-oriented triangulation with left boundary length l and right boundary length r. Let P be the leftmost XDP geodesic from the source of M(l, r) to the sink of M(l, r) (Definition 3.13). Let M^L (resp. M^R) be the submap of M(l, r) consisting of the vertices, edges, and faces of M(l, r) that lie to the left (resp. right) of P, including the vertices and edges that lie on P. Then M^L and M^R are conditionally independent given $|P| = \text{XDP}_{M(l,r)}(\text{source}, \text{sink})$.

Proof. Fix $s \ge \max\{l,r\}$ (if XDP = LDP) or $s \le \min\{l,r\}$ (if XDP = SDP). We will show that M^L and M^R are conditionally independent given $\{|P| = s\}$. Let $\mathcal{M}_{l,s}^L$ be the set of bipolar-oriented triangulations with l edges on their left boundary and s edges on their right boundary, with the further property that the right boundary is the unique XDP geodesic from the source to the sink. Let $\mathcal{M}_{s,r}^R$ be the set of bipolar-oriented triangulations with s edges on their left boundary and r edges on their right boundary, with the further property that the left boundary is an XDP geodesic from the source to the sink (not necessarily unique). The asymmetry in the definitions is because we consider the leftmost XDP geodesic. Finally, let $\mathcal{M}_{l,r,s}$ be the set of all bipolar-oriented triangulations in $\mathcal{M}_{l,r}$ with the property that XDP(source, sink) = s.

Consider the map Φ from $M_{l,s}^L \times M_{s,r}^R$ to $M_{l,r}$ that takes $(\mathfrak{m}^L, \mathfrak{m}^R) \in M_{l,s}^L \times M_{l,s}^R$ to the map $\Phi(\mathfrak{m}^L, \mathfrak{m}^R) \in M_{l,r}$ obtained by identifying the right boundary of \mathfrak{m}^L with the left boundary of \mathfrak{m}^R . One can easily check that Φ is a bijection from $M_{l,s}^L \times M_{s,r}^R$ to $M_{l,r,s}$. The inverse bijection is given by cutting an element of $M_{l,r,s}$ along its leftmost XDP geodesic from the source to the sink.

If $\mathfrak{m} \in \mathcal{M}_{l,r,s}$ and $(\mathfrak{m}^L, \mathfrak{m}^R) = \Phi^{-1}(\mathfrak{m})$, then the edge set of \mathfrak{m} is the union of the edge sets of \mathfrak{m}^L and \mathfrak{m}^R . This is a disjoint union, except that the s edges along the leftmost LDP geodesic of \mathfrak{m} are counted twice, hence

$$\#\mathcal{E}(\mathfrak{m}) = \#\mathcal{E}(\mathfrak{m}^L) + \#\mathcal{E}(\mathfrak{m}^R) - s. \tag{3.7}$$

From this, we obtain

$$\mathbb{P}\Big[M(l,r)=\mathfrak{m}\ \Big|\ |P|=s\Big]\stackrel{(3.6)}{=}\frac{3^{-\#\mathcal{E}(\mathfrak{m})}}{C_{l\,r}\mathbb{P}[|P|=s]}\stackrel{(3.7)}{=}\frac{3^s}{C_{l\,r}\mathbb{P}[|P|=s]}3^{-\#\mathcal{E}(\mathfrak{m}^L)}3^{-\#\mathcal{E}(\mathfrak{m}^R)}.$$

This is the product of a constant times something depending only on \mathfrak{m}^L times something depending only on \mathfrak{m}^R , which gives the desired conditional independence.

Remark 3.16. Exactly the same proof gives analogs of Lemma 3.15 for bipolar-oriented planar maps with other face degree distributions. This includes the biased face degree distributions considered in [KMSW19, Remark 5] (which are expected to be in the universality class of γ -LQG for $\gamma \in (0, \sqrt{2})$ with γ depending on the particular model).

3.4 KMSW bijection for boundary-channeled bipolar-oriented triangulations

Recall from Definition 3.14 that for $l, r \in \mathbb{N}$, we denote by $\mathcal{M}_{l,r}$ the set of bipolar-oriented triangulations with l left boundary edges and r right boundary edges. In this section, we discuss a special subset of $\mathcal{M}_{l,r}$ that will be used in Section 5.6 for the purpose of proving the symmetry property from Theorem 1.7. The reader can skip this section on a first read.

Definition 3.17. Let $\mathcal{M}_{l,r}^b$ be the set of bipolar-oriented triangulations $\mathfrak{m} \in \mathcal{M}_{l,r}$ with the following property: each vertex on the boundary of \mathfrak{m} , except for the sink vertex, has no incoming edges other than boundary edges. Equivalently, every boundary vertex, other than the source and the sink, has exactly one incoming edge. We call the maps in $\mathcal{M}_{l,r}^b$ boundary-channeled bipolar-oriented triangulations with left boundary length l and right boundary length r.

The reason for our interest in $\mathcal{M}_{l,r}^{b}$ is the following symmetry, which will be used in Section 5.6 to prove Property (iv) of Theorem 1.4.

Lemma 3.18. Let $\mathcal{M}_{l,r}^{b}$ be as above. For $\mathfrak{m} \in \mathcal{M}_{l,r}^{b}$, let $\mathfrak{x}_{0}, \ldots, \mathfrak{x}_{r}$ be the vertices on the right boundary of \mathfrak{m} , enumerated in order so that \mathfrak{x}_{0} is the source and \mathfrak{x}_{r} is the sink. For $k \in \{1, \ldots, r-1\}$, let $\Phi_{k}(\mathfrak{m})$ be the directed planar map obtained from \mathfrak{m} by reversing the orientation of the edges $(\mathfrak{x}_{0},\mathfrak{x}_{1}),\ldots,(\mathfrak{x}_{k-1},\mathfrak{x}_{k})$. Then Φ_{k} is a bijection from $\mathcal{M}_{l,r}^{b}$ to $\mathcal{M}_{l+k,r-k}^{b}$.

Proof. We claim that $\Phi_k(\mathfrak{m})$ is a bipolar-oriented map with source \mathfrak{x}_k and sink \mathfrak{x}_r . Since Φ_k does not change the orientation of any non-boundary edge, this implies that Φ_k maps $\mathcal{M}_{l,r}^b$ to $\mathcal{M}_{l+k,r-k}^b$. It is clear that Φ_k has an inverse map (defined in the same way with left and right interchanged), so this will prove the lemma.

It remains to prove the claim. Since Φ_k does not alter the orientations of any edges incident to the sink \mathfrak{x}_r , there are no outgoing edges from \mathfrak{x}_r on $\Phi_k(\mathfrak{m})$. Since \mathfrak{x}_k does not have any non-boundary incoming edges on \mathfrak{m} (by the definition of $\mathcal{M}_{l,r}^{\mathrm{b}}$), it follows that \mathfrak{x}_k has no incoming edges at all on $\Phi_k(\mathfrak{m})$. Every boundary vertex of $\Phi_k(\mathfrak{m})$ other than \mathfrak{x}_k and \mathfrak{x}_r has at least one incoming edge and at least one outgoing edge, namely the two boundary edges incident to it. Since Φ_k does not change the orientations of the non-boundary edges, every non-boundary vertex of Φ_k still has at least one incoming and at least one outgoing edge.

It remains to show that the orientation on $\Phi_k(\mathfrak{m})$ is acyclic. Suppose by way of contradiction that there are edges e_1, \ldots, e_m which form a directed cycle on $\Phi_k(\mathfrak{m})$. Since the orientation on \mathfrak{m} is acyclic, at least one of the edges e_1, \ldots, e_m must be one of the boundary edges whose orientation we changed. The boundary of $\Phi_k(\mathfrak{m})$ is not a directed cycle, so at least one of e_1, \ldots, e_m must be a non-boundary edge. Moreover, none of these edges can be incident to the sink \mathfrak{x}_r since it only has incoming edges incident to it. Hence, by re-labeling, we can assume without loss of generality that e_1 is a non-boundary edge and e_2 is a boundary edge. But then e_1 is non-boundary edge whose terminal vertex is a boundary vertex different from \mathfrak{x}_r . This contradicts the fact that $\mathfrak{m} \in \mathcal{M}_{l,r}^b$. \square

We now explain how elements of $\mathcal{M}_{l,1}^{b}$ can be obtained by applying the KMSW procedure to certain specific walks.

Lemma 3.19. Let $l, n \in \mathbb{N}$. The KMSW procedure restricts to a bijection between the following two sets:

- Walks \mathfrak{Z}_l^b with increments in $\{(1,-1),(-1,0),(1,0)\}$ and n total steps, which start at (l-1,0) and end at (0,0), and stay in $[0,\infty)\times[0,\infty)$.
- Maps \mathfrak{m}' of $\mathcal{M}_{l,1}^{b}$ having n-1 non-boundary edges, i.e. N=n+l total edges, with all of its left boundary edges except for the left boundary edge whose terminal vertex is the sink vertex declared to be missing.

Proof. Let $\widetilde{\mathfrak{m}}$ be any bipolar-oriented triangulation. By the definition of the tree $T_{UL}(\widetilde{\mathfrak{m}})$ (above Definition 3.7), we have that the rightmost branch of $T_{UL}(\widetilde{\mathfrak{m}})$ coincides with the right boundary of $\widetilde{\mathfrak{m}}$ if and only if every right boundary vertex of $\widetilde{\mathfrak{m}}$, other than the source and the sink, has exactly one incoming edge (necessarily a boundary edge); see the right-hand side of Figure 4.

In particular, by Definition 3.7 and Theorem 3.5, given $\overline{\mathfrak{m}} \in \mathcal{M}_{1,r}^{\mathrm{b}}$ with N total edges, the corresponding KMSW encoding walk $\overline{\mathfrak{J}}$ is a walk with increments in $\{(1,-1),(-1,0),(1,0)\}$ and N-1 total steps, starting at (0,0) and ending at (0,-(r-1)), staying in $[0,\infty)\times[-(r-1),\infty)$; with the additional constraint that the first r steps are (1,-1)-steps. Removing the first r-1 steps from $\overline{\mathfrak{J}}$ and shifting the walk so that it ends at (0,0), we obtain a walk $\overline{\mathfrak{J}}_r^{\mathrm{b}}$ with increments in $\{(1,-1),(-1,0),(1,0)\}$ and N-r total steps, starting at (r-1,0) and ending at (0,0), staying in $[0,\infty)\times[0,\infty)$. Moreover, the triangulation $\overline{\mathfrak{m}}$ with all its right boundary edges declared to be missing except for the edge having the sink vertex as the terminal vertex, coincides with the triangulation obtained from $\overline{\mathfrak{J}}_r^{\mathrm{b}}$ by applying the KMSW procedure.

Now, given $\mathfrak{m} \in \mathcal{M}_{l,1}^{b}$, we can apply the bijection Φ_{l-1} from Lemma 3.18, to obtain a triangulation $\Phi_{l-1}(\mathfrak{m}) \in \mathcal{M}_{1,l}^{b}$. Using the bijection in the last paragraph, we obtain an encoding walk \mathfrak{Z}_{l}^{b} with increments in $\{(1,-1),(-1,0),(1,0)\}$ and N-l=n total steps, starting at (l-1,0) and ending at (0,0), staying in $[0,\infty)\times[0,\infty)$. Moreover, the triangulation $\Phi_{l-1}(\mathfrak{m})$ with all its right boundary edges declared to be missing except for the edge having the sink vertex as the terminal vertex, coincides with the triangulation \mathfrak{m}' obtained from \mathfrak{Z}_{l}^{b} by applying the KMSW procedure. This gives the lemma statement.

4 Cut vertices and geodesics in the UIQBOT

4.1 Definitions and results

Throughout this section, we fix $XDP \in \{LDP, SDP\}$.

Let $\mathcal{Z}=(\mathcal{L},\mathcal{R}):\mathbb{N}_0\to\mathbb{Z}^2$ be a walk whose increments are i.i.d. uniform samples from the set of steps $\{(1,-1),(-1,0),(0,1)\}$. For $z=(x,y)\in\mathbb{Z}^2$, we write \mathbb{P}_z for the law of \mathcal{Z} starting from z. Let $\widehat{\mathcal{Z}}=(\widehat{\mathcal{L}},\widehat{\mathcal{R}})$ be the random walk obtained from \mathcal{Z} by conditioning \mathcal{L} to stay non-negative for all time in the sense of [BD94]. To describe this process more explicitly, for $z\in\mathbb{N}_0\times\mathbb{Z}$, we write $\widehat{\mathbb{P}}_z$ for the law of $\widehat{\mathcal{Z}}$ starting from z. The process $\widehat{\mathcal{Z}}$ is a Markov process, and for each $n\geq 0$, the $\widehat{\mathbb{P}}_z$ -law of $\widehat{\mathcal{Z}}|_{[0,n]}$ is obtained by weighting the \mathbb{P}_z -law of $\mathcal{Z}|_{[0,n]}$ by

$$(x+1)^{-1}(\mathcal{L}(n)+1)\mathbb{1}\{\mathcal{L}(j)\geq 0, \forall j\in [0,n]\cap \mathbb{Z}\}.$$
 (4.1)

In this section, we will study the following infinite bipolar-oriented triangulation.

Definition 4.1. Assume that $\widehat{\mathcal{Z}}$ starts from (0,0), i.e. we are working under $\widehat{\mathbb{P}}_{(0,0)}$. Let \widehat{M} be the infinite bipolar-oriented triangulation obtained from $\widehat{\mathcal{Z}}$ via the KMSW procedure (Definition 3.3 and

Remark 3.4). We call \widehat{M} the uniform infinite quarter-plane bipolar-oriented triangulation (UIQBOT). The root edge of \widehat{M} is the edge $\widehat{\lambda}_0$ where the KMSW procedure starts.

The map \widehat{M} is equipped with an acyclic orientation with a unique source, which is the initial vertex of the root edge of \widehat{M} , and no sink (the sink is "at ∞ "). We stress that the map \widehat{M} has no missing edges (as opposed to $M_{0,\infty}$); this follows from Assertions (i) and (iv) of Lemma 3.6. Analogously to Definition 3.2, we define the **left** (resp. **right**) **boundary** of \widehat{M} to be the path on the boundary of the external face of \widehat{M} from the source vertex to ∞ with the external face immediately to the left (resp. right). For later convenience, we note that the left (resp. right) boundary edges of \widehat{M} are upper-left (resp. lower-right) boundary edges according to Definition 3.2.

The reason for the name "quarter plane" is that we will eventually show that the UIQBOT has the same law as the "first quadrant" in the UIBOT bounded by the rightmost directed path from the terminal vertex of the root edge (i.e. the right boundary of $M_{0,\infty}$) and the leftmost directed path from the initial vertex of the root edge (Proposition 5.1).

We expect that \widehat{M} arises as the Benjamini-Schramm local limit around the source vertex of Boltzmann bipolar-oriented triangulations with given left and right boundary lengths (see (3.6)) as the left and right boundary lengths approach ∞ . We will not prove this here, but see Lemma 4.13.

The first main result of this subsection is that the UIQBOT a.s. has infinitely many cut vertices, defined as follows.

Definition 4.2. A vertex v of \widehat{M} is a **cut vertex** of \widehat{M} if v lies on both the left and right boundaries of \widehat{M} . Equivalently, v is a cut vertex if and only if either v is the source vertex or removing v disconnects \widehat{M} .

Proposition 4.3. Almost surely, the UIQBOT \widehat{M} has infinitely many cut vertices.

We will prove Proposition 4.3 in Section 4.2 using estimates for the walk $\widehat{\mathcal{Z}}$. Proposition 4.3 will play an essential role in the proof of the existence of the Busemann function (Theorem 1.4). The reason is that the existence of cut vertices forces any two sufficiently long directed paths in \widehat{M} to have a vertex in common. Taking these paths to be XDP geodesics will allow us to verify the condition in (1.2) of Theorem 1.4.

Remark 4.4. Proposition 4.3 may be surprising in light of known facts in the continuum. Indeed, from mating of trees theory (see, e.g., [AG21, Theorems 1.3 and 3.5]) the map \widehat{M} is the discrete analog of a weight $\gamma^2/2 = 2/3$ LQG wedge, with $\gamma = \sqrt{4/3}$. The walk $\widehat{\mathcal{Z}}$ is the discrete analog of the left/right boundary length process for an $\mathrm{SLE}_{12}(2;0)$ curve on this LQG wedge. Weight $\gamma^2/2$ is exactly the critical weight for an LQG wedge to have cut points: an LQG wedge of weight $W \geq \gamma^2/2$ is homeomorphic to the half-plane, whereas an LQG wedge of weight $W < \gamma^2/2$ is homeomorphic to a countable string of domains that are homeomorphic to a disk with two marked points, glued together end-to-end [DMS21, Sections 4.2 and 4.4]. Intuitively, the reason why our infinite planar map \widehat{M} has cut vertices whereas its continuum counterpart is homeomorphic to the half-plane is that the cut vertices of \widehat{M} are very sparse, so they disappear when one passes to the scaling limit.

As an easy consequence of Proposition 4.3, we get that infinite XDP geodesics in the UIQBOT exist. The following definition generalizes Definition 3.13 to infinite planar maps.

Definition 4.5. Let \mathfrak{m} be an infinite planar map equipped with an acyclic orientation. A directed path $\mathfrak{p}: \mathbb{N} \to \mathcal{E}(\mathfrak{m})$ started from $x \in \mathcal{V}(\mathfrak{m})$ is an XDP **geodesic from** x **to** ∞ if for any integers $1 \le a \le b < \infty$, the path $\mathfrak{p}|_{[a,b]}$ is the longest (if XDP = LDP) or shortest (if XDP = SDP) directed

path between its starting and terminal vertices. We say that \mathfrak{p} is a **leftmost** XDP **geodesic from** x **to** ∞ if any other infinite XDP geodesic from x to ∞ lies (weakly) to the right of \mathfrak{p} . That is, any such XDP geodesic is contained in the submap of \mathfrak{m} lying to the right of \mathfrak{p} and to the left of the rightmost directed path started from x (including the vertices and edges on these paths).

Lemma 4.6. Let \widehat{M} be the UIQBOT as in Definition 4.1. For each $x \in \mathcal{V}(\widehat{M})$, there is a (unique) leftmost LDP geodesic from x to ∞ in \widehat{M} .

Lemma 4.6 will be proven at the end of Section 4.2. The second main result of this section is the following proposition, which extends Lemma 3.15 to the infinite map \widehat{M} .

Proposition 4.7. Let \widehat{P} be the leftmost XDP geodesic from the source vertex to ∞ in the UIQBOT \widehat{M} , as provided by Lemma 4.6. Let \widehat{M}^L and \widehat{M}^R be the submaps of \widehat{M} lying (weakly) to the left and right of \widehat{P} , respectively. Then \widehat{M}^L and \widehat{M}^R are independent.

Proposition 4.7 will be proven in Section 4.3.

4.2 Existence of cut vertices in the UIQBOT

In this subsection, we will prove Proposition 4.3. For $n \in \mathbb{N}_0$, let $\widehat{\lambda}_n$ be the time-n active edge of the KMSW procedure for \widehat{M} (Definition 3.3). Just below, we will prove the following statement using basic observations about the KMSW procedure.

Lemma 4.8. For $n \in \mathbb{N}_0$, let $\widehat{\lambda}_n^-$ be the initial vertex of $\widehat{\lambda}_n$. The following are equivalent.

- $\widehat{\lambda}_n^-$ is a cut vertex for \widehat{M} and $\widehat{\lambda}_j^- \neq \widehat{\lambda}_n^-$ for each $j \leq n-1$.
- The event $A_n \cap B_n$ occurs, where

$$A_n := \left\{ \widehat{\mathcal{R}}(n) \le \widehat{\mathcal{R}}(j) - 1, \ \forall j \le n - 1 \right\} \quad and \quad B_n := \left\{ \widehat{\mathcal{L}}(j) \ge \widehat{\mathcal{L}}(n), \ \forall j \ge n \right\}. \tag{4.2}$$

Proof. Assume that $A_n \cap B_n$ occurs. By Assertion (ii) of Lemma 3.6 (recall also Remark 3.4), the occurrence of A_n implies that $\widehat{\lambda}_n^-$ lies on the right boundary of \widehat{M} and $\widehat{\lambda}_j^- \neq \widehat{\lambda}_n^-$ for each $j \leq n-1$. Furthermore, by Assertion (iii) of Lemma 3.6, the occurrence of B_n implies that $\widehat{\lambda}_n^-$ lies on the left boundary of \widehat{M} . The converse is checked similarly.

By Lemma 4.8, Proposition 4.3 is equivalent to the statement that a.s. there are infinitely many $n \in \mathbb{N}$ such that $A_n \cap B_n$ occurs. To prove this statement, we will first observe that the set of such n is a discrete-time renewal process (Lemma 4.9). We will then show using basic estimates for random walk that $\sum_{n=1}^{\infty} \mathbb{P}[A_n \cap B_n] = \infty$ (Lemma 4.12). This implies that a.s. $\sum_{n=1}^{\infty} \mathbb{1}_{A_n \cap B_n} = \infty$ by a standard argument for discrete-time renewal processes.

Lemma 4.9. Let $T_0 = 0$ and for $m \in \mathbb{N}$, let T_m be the mth smallest time $n \in \mathbb{N}$ for which $A_n \cap B_n$ occurs, or $T_m = \infty$ if there are fewer than m such times. Equivalently, by Lemma 4.8, T_m is the mth smallest $n \in \mathbb{N}$ for which $\widehat{\lambda}_n^-$ is a cut vertex of \widehat{M} which is visited by $\widehat{\lambda}^-$ for the first time at time n. On the event $\{T_m < \infty\}$, the conditional law of $(\widehat{\mathcal{Z}}(\cdot + T_m) - \widehat{\mathcal{Z}}(T_m))|_{[0,\infty)}$ given $\widehat{\mathcal{Z}}|_{[0,T_m]}$ is the same as the law $\widehat{\mathbb{P}}_{(0,0)}$ of $\widehat{\mathcal{Z}}$.

Proof. We have $T_m = n$ if and only if the following is true:

• $\widehat{\mathcal{R}}$ attains a running minimum at time n, i.e., A_n occurs.

- There are exactly m times $j \in [1, n] \cap \mathbb{Z}$ such that $\widehat{\mathcal{R}}$ attains a running minimum at time j and $\widehat{\mathcal{L}}(i) \geq \widehat{\mathcal{L}}(j)$ for each $i \in [j, n] \cap \mathbb{Z}$.
- $\widehat{\mathcal{L}}(j) \geq \widehat{\mathcal{L}}(n)$ for each $j \geq n$, i.e., B_n occurs.

The first two itemized conditions depend only on $\widehat{\mathcal{Z}}|_{[0,n]}$. Hence, conditioning on $\widehat{\mathcal{Z}}|_{[0,n]}$ and $\{T_m = n\}$ is the same as conditioning on $\widehat{\mathcal{Z}}|_{[0,n]}$ and the event B_n . By the Markov property, the conditional law of $(\widehat{\mathcal{Z}}(\cdot + n) - \widehat{\mathcal{Z}}(n))|_{[0,\infty)}$ given $\widehat{\mathcal{Z}}|_{[0,n]}$ and $\{T_m = n\}$ is that of a random walk started at (0,0) with the same increment distribution as \mathcal{Z} conditioned so that its first component stays non-negative. That is, its conditional law is the same as the law $\widehat{\mathbb{P}}_{(0,0)}$ of $\widehat{\mathcal{Z}}$.

As noted above, to show that a.s. there exist infinitely many n such that $A_n \cap B_n$ occurs, we want to show that $\sum_{n=1}^{\infty} \mathbb{P}[A_n \cap B_n] = \infty$. To accomplish this, we will prove a lower bound for the conditional probability of B_n given A_n (Lemma 4.10) and then combine this with a lower bound for the number of values of n for which A_n occurs (Lemma 4.12).

Lemma 4.10. Recall that $\widehat{\mathbb{P}}_{(x,y)}$ denotes the law of the (conditioned) walk $\widehat{\mathcal{Z}}$ started from (x,y). For $x \geq 0$ and $s \in [0,x] \cap \mathbb{Z}$,

$$\widehat{\mathbb{P}}_{(x,y)} \Big[\widehat{\mathcal{L}}(j) \ge x - s, \, \forall j \ge 0 \Big] = \frac{s+1}{x+1}.$$

Proof. For $k \in \mathbb{N}$, let

$$\widehat{\sigma}_k = \min \Big\{ n \in \mathbb{N} : \widehat{\mathcal{L}}(n) \ge k \Big\},$$

and similarly define σ_k with the unconditioned walk \mathcal{L} in place of $\widehat{\mathcal{L}}$. By the definition of $\widehat{\mathcal{Z}}$ from (4.1), for $k \geq x + 1$,

$$\widehat{\mathbb{P}}_{(x,y)}\Big[\widehat{\mathcal{L}}(j) \ge x - s, \, \forall j \in [0,\widehat{\sigma}_k] \cap \mathbb{Z}\Big] = \frac{1}{x+1} \mathbb{E}_{(x,y)}[(\mathcal{L}(\sigma_k) + 1)\mathbb{1}\{\mathcal{L}(j) \ge x - s, \, \forall j \in [0,\sigma_k] \cap \mathbb{Z}\}]$$
$$= \frac{k+1}{x+1} \mathbb{P}_{(x,y)}[\mathcal{L}(j) \ge x - s, \, \forall j \in [0,\sigma_k] \cap \mathbb{Z}].$$

Since \mathcal{L} is a lazy random walk, by the standard Gambler's ruin formula, the probability in the last line above is equal to (s+1)/(k-x+s+1). Sending $k \to \infty$ and using [BD94, Theorem 1] concludes the proof.

We will need the following fact, which is a special case of the much more general result [DW15b, Theorem 2].

Lemma 4.11 ([DW15b]). Under $\widehat{\mathbb{P}}_{(0,0)}$, the re-scaled walk $\{n^{-1/2}\widehat{\mathcal{Z}}(\lfloor tn \rfloor)\}_{t\geq 0}$ converges in law with respect to the topology of uniform convergence on compact subsets of $[0,\infty)$. The limiting process is $\sqrt{2/3}$ times a 2d Brownian motion of correlation -1/2 started from (0,0) and conditioned to stay in the right half-plane, i.e., it is described as follows. Let \mathcal{A} be a 3d Bessel process and let \mathcal{B} be an independent standard linear Brownian motion. Then consider the process $\sqrt{2/3}(\mathcal{A}, \frac{\sqrt{3}}{2}\mathcal{B} - \frac{1}{2}\mathcal{A})$.

Proof. Apply [DW15b, Theorem 2] with the cone equal to the half-plane $\{(x,y) \in \mathbb{R}^2 : x \geq 0\}$, to the random walk obtained by applying a linear transformation to make the coordinates of \mathcal{Z} uncorrelated. The constant $\sqrt{2/3}$ appears because the variance of each coordinate of \mathcal{Z} is 2/3. \square

Lemma 4.12. With A_n and B_n as in (4.2),

$$\sum_{n=1}^{\infty} \widehat{\mathbb{P}}_{(0,0)}[A_n \cap B_n] = \infty.$$

Proof. For $n \in \mathbb{N}$, let

$$F_n := A_n \cap \left\{ \widehat{\mathcal{L}}(n) \in \left[\frac{1}{100} n^{1/2}, 100 n^{1/2} \right] \right\}. \tag{4.3}$$

In words, F_n is the event that $\widehat{\mathcal{R}}$ attains a running minimum at time n and $\widehat{\mathcal{L}}(n)$ is comparable to $n^{1/2}$.

By the Markov property, if we condition on $\widehat{\mathcal{Z}}|_{[0,n]}$, then the conditional law of $\widehat{\mathcal{Z}}(\cdot+n)|_{[0,\infty)}$ is $\widehat{\mathbb{P}}_{\widehat{\mathcal{Z}}(n)}$. By Lemma 4.10 applied with s=0, the conditional probability given $\widehat{\mathcal{Z}}|_{[0,n]}$ that the event B_n occurs is $1/(\widehat{\mathcal{L}}(n)+1)$. Since $\widehat{\mathcal{L}}(n) \leq 100n^{1/2}$ on F_n ,

$$\widehat{\mathbb{P}}_{(0,0)}[B_n \mid F_n] \ge \frac{1}{101} n^{-1/2}.$$
(4.4)

We will now argue that there are many times n for which $\widehat{\mathbb{P}}_{(0,0)}[F_n]$ is bounded below. For $N \in \mathbb{N}$, let E_N be the event that the following is true:

- 1. $\widehat{\mathcal{L}}(n) \in \left[\frac{1}{100}n^{1/2}, 100n^{1/2}\right]$ for each $n \in [N/2, N] \cap \mathbb{Z}$;
- 2. $\min_{n \in [0, N/2] \cap \mathbb{Z}} \widehat{\mathcal{R}}(n) \ge -N^{1/2}$;
- 3. $\widehat{\mathcal{R}}(N) \leq -2N^{1/2}$.

The limiting process in Lemma 4.11 has a positive chance to stay arbitrarily close (in the uniform distance) to any given deterministic path $[0,1] \to [0,\infty) \times \mathbb{R}$ for one unit of time. By Lemma 4.11, there is a universal constant $p \in (0,1)$ such that $\widehat{\mathbb{P}}_{(0,0)}[E_N] \geq p$ for each $N \geq 100$, say (we can decrease p to deal with finitely many small values of N). If E_N occurs, then there are at least $N^{1/2}$ times $n \in [N/2, N]$ at which $\widehat{\mathcal{R}}$ attains a running minimum. By (4.3) and the definition of E_N , the event F_n occurs for each of these times n. Consequently,

$$pN^{1/2} \le \widehat{\mathbb{P}}_{(0,0)}[E_N]N^{1/2} \le \widehat{\mathbb{E}}_{(0,0)} \left[\sum_{n=\lceil N/2 \rceil}^N \mathbb{1}_{F_n} \right] = \sum_{n=\lceil N/2 \rceil}^N \widehat{\mathbb{P}}_{(0,0)}[F_n]. \tag{4.5}$$

Recall that $F_n \subset A_n$. By combining (4.4) and (4.5), we find that there is a universal constant c > 0 such that for every $N \ge 100$,

$$c \leq \sum_{n=\lceil N/2 \rceil}^{N} \widehat{\mathbb{P}}_{(0,0)}[B_n \mid F_n] \, \widehat{\mathbb{P}}_{(0,0)}[F_n] \leq \sum_{n=\lceil N/2 \rceil}^{N} \widehat{\mathbb{P}}_{(0,0)}[A_n \cap B_n].$$

Applying this with $N = 2^k$ and summing over k concludes the proof.

Proof of Proposition 4.3. Let S be the set of $n \in \mathbb{N}_0$ for which $A_n \cap B_n$ occurs. By Lemma 4.8, it suffices to show that $\widehat{\mathbb{P}}_{(0,0)}$ -a.s. $\#S = \infty$. With T_m as in Lemma 4.9,

$$\#S = \min\{m \in \mathbb{N} : T_m = \infty\}.$$

By Lemma 4.9, if $\widehat{\mathbb{P}}_{(0,0)}[\#S < \infty] > 0$, then $\widehat{\mathbb{P}}_{(0,0)}[T_1 = \infty] > 0$ and for each $m \in \mathbb{N}$, on the event $\{T_{m-1} < \infty\}$,

$$\widehat{\mathbb{P}}_{(0,0)} \left[T_m = \infty \, \middle| \, \mathcal{Z}|_{[0,T_{m-1}]} \right] = \widehat{\mathbb{P}}_{(0,0)} [T_1 = \infty] > 0. \tag{4.6}$$

By (4.6), if $\widehat{\mathbb{P}}_{(0,0)}[\#S < \infty] > 0$, then #S has a geometric distribution with positive success probability, so $\widehat{\mathbb{E}}_{(0,0)}[\#S] < \infty$. But, Lemma 4.12 implies that $\widehat{\mathbb{E}}_{(0,0)}[\#S] = \infty$. Hence we conclude that $\widehat{\mathbb{P}}_{(0,0)}[\#S < \infty] = 0$.

We conclude this section by providing the proof of Lemma 4.6 regarding the existence of infinite geodesics in \widehat{M} .

Proof of Lemma 4.6. Define the times T_m as in Lemma 4.9, so that $\widehat{\lambda}_{T_m}^-$ is the *m*th cut vertex of \widehat{M} (we know that $T_m < \infty$ a.s. for every $m \in \mathbb{N}$ by Proposition 4.3).

Fix $x \in \mathcal{V}(\widehat{M})$ and consider the infinite rightmost directed path from x in \widehat{M} . This path has to visit a cut vertex. Let m_0 be the smallest $m \in \mathbb{N}$ for which this path visits the cut vertex $\widehat{\lambda}_{T_m}^-$. For $m \geq m_0$, let \widehat{P}_m be the leftmost XDP geodesic from x to $\widehat{\lambda}_{T_m}^-$ (Definition 3.13). By the definition of a cut vertex, for $m' \geq m \geq m_0$, the path $\widehat{P}_{m'}$ must visit the vertex $\widehat{\lambda}_{T_m}^-$. By the uniqueness of leftmost XDP geodesics between finite points, the portion of $\widehat{P}_{m'}$ up to the time when it hits $\widehat{\lambda}_{T_m}^-$ coincides with \widehat{P}_m . Hence we can define a leftmost XDP geodesic \widehat{P} from x to ∞ by declaring that \widehat{P} coincides with \widehat{P}_m until the first time when it hits $\widehat{\lambda}_{T_m}^-$, for each $m \geq m_0$. This leftmost XDP geodesic is unique since the leftmost XDP geodesic from x to $\widehat{\lambda}_{T_m}^-$ is unique for each $m \geq m_0$. \square

4.3 Independence in the UIQBOT

In this subsection, we will only consider walks started from (0,0), so we just write $\mathbb{P}=\widehat{\mathbb{P}}_{(0,0)}$. The idea of the proof of Proposition 4.7 is as follows. Let \widehat{P} be the leftmost XDP geodesic from the source vertex to ∞ in the UIQBOT \widehat{M} , as provided by Lemma 4.6. Using the existence of cut vertices of \widehat{M} (Proposition 4.3), we can find arbitrarily large finite submaps of \widehat{M} that have the law of a Boltzmann bipolar-oriented triangulation conditional on their left and right boundary lengths (Lemma 4.13). By Lemma 3.15, the leftmost XDP geodesic \widehat{P} of \widehat{M} divides each of these submaps into two pieces that are conditionally independent given the length of the portion of \widehat{P} in the submap (Lemma 4.14). It remains to send the size of the submap to ∞ and get rid of the conditioning. We do this using a combination of the backward martingale convergence theorem and the Hewitt-Savage zero-one law (the latter is applied to the i.i.d. submaps of \widehat{M} between its successive cut vertices).

Define the times T_m as in Lemma 4.9, so that $\widehat{\lambda}_{T_m}^-$ is the mth cut vertex of \widehat{M} . For $k \in \mathbb{N}_0$, let

$$\tau_k^R = \min \left\{ n \in \mathbb{N} : \widehat{\mathcal{R}}(n) = -k \right\},\tag{4.7}$$

so that $\widehat{\lambda}_{\tau_k^R}$ is the k+1th edge on the right boundary of \widehat{M} thanks to Assertion (ii) in Lemma 3.6. For $k \in \mathbb{N}_0$, let

$$m_k := \max \left\{ m : T_m \le \tau_k^R \right\}. \tag{4.8}$$

That is, $\widehat{\lambda}_{T_{m_k}}^-$ is the last cut vertex along the right boundary of \widehat{M} which comes before $\widehat{\lambda}_{\tau_k^R}$ in directed order. Let

$$\widehat{M}(T_{m_k}) := \widehat{M}_{0, T_{m_k} - 1}$$

be the submap of \widehat{M} obtained by applying the KMSW procedure to $\widehat{Z}|_{[0,T_{m_k}-1]}$. Then $\widehat{M}(T_{m_k})$ is a bipolar-oriented triangulation with the same source as \widehat{M} and sink equal to $\widehat{\lambda}_{T_{m_k}}^-$. See Figure 7 for an illustration.

Lemma 4.13. Let $k \in \mathbb{N}$ and let $\widehat{M}(T_{m_k})$ be the map defined just above. If we condition on $\widehat{\mathcal{Z}}(\cdot + T_{m_k})|_{[0,\infty)}$ (which in particular determines $\widehat{\mathcal{Z}}(T_{m_k})$), then the conditional law of $\widehat{\mathcal{Z}}|_{[0,T_{m_k}]}$ is that of a random walk with the law of \mathcal{Z} started at (0,0), conditioned to first hit $\mathbb{R} \times [\widehat{\mathcal{R}}(T_{m_k}), \infty)$ at $(\widehat{\mathcal{L}}(T_{m_k}), \widehat{\mathcal{R}}(T_{m_k}))$ and to stay in $[0,\infty) \times [\widehat{\mathcal{R}}(T_{m_k}),\infty)$ until this hitting time. Under the same

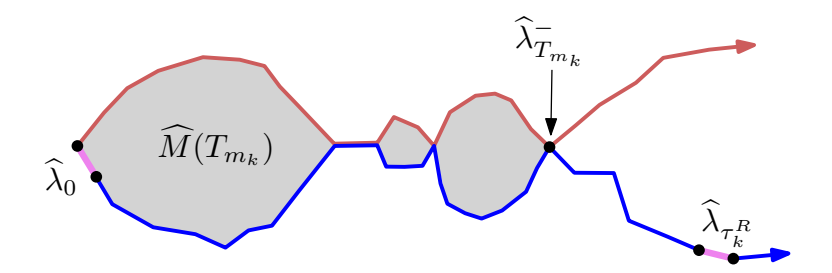


Figure 7: Illustration of the map $\widehat{M}(T_{m_k})$, in grey, defined just after (4.8). We show in Lemma 4.13 that the conditional law of $\widehat{M}(T_{m_k})$ given its left and right boundary lengths is that of a Boltzmann bipolar-oriented triangulation with given left and right boundary lengths (Definition 3.14).

conditioning, the conditional law of $\widehat{M}(T_{m_k})$ is that of a Boltzmann bipolar-oriented triangulation with left and right boundary lengths $\widehat{\mathcal{L}}(T_{m_k})$ and $-\widehat{\mathcal{R}}(T_{m_k})$, respectively (Definition 3.14).

Proof. Define the times τ_k^R as in (4.7). By the definition of T_m from Lemma 4.9, $\{T_m\}_{m\in\mathbb{N}_0}\subset\{\tau_k^R\}_{k\in\mathbb{N}_0}$. Fix $l,r\geq 1$ with $r\leq k$. Define the event

$$E_{l,r} = E_{l,r}(k) := \left\{ \widehat{\mathcal{Z}}(T_{m_k}) = (l, -r) \right\} = \left\{ T_{m_k} = \tau_r^R, \, \widehat{\mathcal{L}}(\tau_r^R) = l \right\}.$$

By unpacking the definitions of τ_r^R and T_{m_k} and noting that $T_{m_k} \leq \tau_k^R$ by definition, we see that $E_{l,r}$ is the same as the event that the following is true:

- $\widehat{\mathcal{L}}(\tau_r^R) = l;$
- $\widehat{\mathcal{L}}(j) \geq l$ for each $j \geq \tau_r^R$ (combined with the first item, this is the event $B_{\tau_r^R}$ in (4.2) and, by the definitions of τ_r^R and T_m , this ensures that $\tau_r^R = T_m$ for some $m \in \mathbb{N}_0$);
- there are no numbers $s \in [r+1,k] \cap \mathbb{Z}$ such that $\widehat{\mathcal{L}}(n) \geq \widehat{\mathcal{L}}(\tau_s^R)$ for each $n \geq \tau_s^R$ (by (4.8), this ensures that $T_{m_k} = \tau_r^R$, instead of $T_{m_k} = \tau_s^R$ for some $s \in [r+1,k] \cap \mathbb{Z}$).

The first itemized condition depends only on $\widehat{\mathcal{Z}}(\tau_r^R)$ and the other two itemized conditions depend only on $\widehat{\mathcal{Z}}(\cdot + \tau_r^R)|_{[0,\infty)}$. By the strong Markov property, $\widehat{\mathcal{Z}}|_{[0,\tau_r^R]}$ is conditionally independent from $\widehat{\mathcal{Z}}(\cdot + \tau_r^R)|_{[0,\infty)}$ given $\widehat{\mathcal{Z}}(\tau_r^R)$. Hence, on the event $E_{l,r}$, the conditional law of $\widehat{\mathcal{Z}}|_{[0,\tau_r^R]} = \widehat{\mathcal{Z}}|_{[0,T_{m_k}]}$ given $\widehat{\mathcal{Z}}(\cdot + \tau_r^R)|_{[0,\infty)}$ is the same as the conditional law of $\widehat{\mathcal{Z}}|_{[0,\tau_r^R]}$ given only $\{\widehat{\mathcal{L}}(\tau_r^R) = l\}$. By the definition (4.7) of τ_r^R , we get the desired description of the conditional law of $\widehat{\mathcal{Z}}|_{[0,T_{m_k}]}$. The description of the conditional law of $\widehat{\mathcal{M}}(T_{m_k})$ then follows by applying Lemma 3.11 and conditioning on the left boundary length.

By Definition 4.2 of a cut vertex, the leftmost XDP geodesic \widehat{P} from the source vertex to ∞ in \widehat{M} must pass through the cut vertex $\widehat{\lambda}_{T_m}^-$ for each $m \in \mathbb{N}$. Note that $\widehat{\lambda}_{T_0}^- = \widehat{\lambda}_0^-$ is the source vertex of \widehat{M} . For $k \geq 1$, define the σ -algebra

$$\mathcal{F}_k := \sigma \Big(\widehat{\mathcal{Z}}(\cdot + T_{m_k})|_{[0,\infty)}, \, \mathrm{XDP}_{\widehat{M}} \Big(\widehat{\lambda}_0^-, \widehat{\lambda}_{T_{m_k}}^- \Big) \Big). \tag{4.9}$$

Lemma 4.14. Let $\widehat{M}^L(T_{m_k})$ and $\widehat{M}^R(T_{m_k})$ be the submaps of $\widehat{M}(T_{m_k})$ lying to the left and right of \widehat{P} , respectively, both including the vertices and edges which lie on $\widehat{P} \cap \widehat{M}(T_{m_k})$. Then $\widehat{M}^L(T_{m_k})$ and $\widehat{M}^R(T_{m_k})$ are conditionally independent given the σ -algebra \mathcal{F}_k of (4.9).

Proof. Recall that the source of $\widehat{M}(T_{m_k})$ is the same as the source $\widehat{\lambda}_0^-$ of \widehat{M} , and the sink of $\widehat{M}(T_{m_k})$ is the vertex $\widehat{\lambda}_{T_{m_k}}^-$. Since \widehat{P} must visit the cut vertex $\widehat{\lambda}_{T_{m_k}}^-$, the portion of \widehat{P} which lies in $\widehat{M}(T_{m_k})$ is the leftmost XDP geodesic from the source to the sink of $\widehat{M}(T_{m_k})$, and the length of this portion of \widehat{P} is $\mathrm{XDP}_{\widehat{M}}(\widehat{\lambda}_0^-, \widehat{\lambda}_{T_{m_k}}^-)$. The lemma then follows by combining the description of the conditional law of $\widehat{M}(T_{m_k})$ given $\widehat{\mathcal{Z}}(\cdot + T_{m_k})|_{[0,\infty)}$ from Lemma 4.13 with the conditional independence statement of Lemma 3.15.

Lemma 4.15. The σ -algebras \mathcal{F}_k of (4.9) are decreasing in k, i.e., $\mathcal{F}_K \subset \mathcal{F}_k$ whenever K > k. Moreover, any event in the intersection σ -algebra $\bigcap_{k>0} \mathcal{F}_k$ has probability zero or one.

Proof. The monotonicity is proven essentially by inspection, but we give the details. Let K > k. Define the walk

$$\widehat{\mathcal{Z}}' = (\widehat{\mathcal{L}}', \widehat{\mathcal{R}}') := \widehat{\mathcal{Z}}(\cdot + T_{m_k})|_{[0,\infty)}.$$

By definition, $\widehat{\mathcal{Z}}'$ is \mathcal{F}_k -measurable. The time $T_{m_K} - T_{m_k}$ is determined by $\widehat{\mathcal{Z}}'$: indeed, to recover $T_{m_K} - T_{m_k}$ from $\widehat{\mathcal{Z}}'$, we first let $\acute{\tau}_K^R$ be the smallest $n \in \mathbb{N}$ for which $\widehat{\mathcal{R}}'(n) = -K$. Then $T_{m_K} - T_{m_k}$ is the largest $n \leq \acute{\tau}_K^R$ at which the event $A_n \cap B_n$ of (4.2) occurs with $\widehat{\mathcal{Z}}'$ in place of $\widehat{\mathcal{Z}}$. We also note that $\widehat{\lambda}_{T_{m_k}}^-$ is the source vertex for the map constructed from $\widehat{\mathcal{Z}}'$ via the KMSW procedure. From this, it follows that $\mathrm{XDP}_{\widehat{M}}(\widehat{\lambda}_{T_{m_k}}^-, \widehat{\lambda}_{T_{m_K}}^-)$ is determined by $\widehat{\mathcal{Z}}'$. Since \widehat{P} must pass through each of the cut vertices $\widehat{\lambda}_{T_m}^-$,

$$XDP_{\widehat{M}}(\widehat{\lambda}_{0}^{-}, \widehat{\lambda}_{T_{m_{K}}}^{-}) = XDP_{\widehat{M}}(\widehat{\lambda}_{0}^{-}, \widehat{\lambda}_{T_{m_{k}}}^{-}) + XDP_{\widehat{M}}(\widehat{\lambda}_{T_{m_{k}}}^{-}, \widehat{\lambda}_{T_{m_{K}}}^{-}).$$

$$(4.10)$$

Since $\text{XDP}_{\widehat{M}}(\widehat{\lambda}_{T_{m_k}}^-, \widehat{\lambda}_{T_{m_K}}^-)$ is determined by $\widehat{\mathcal{Z}}'$, it follows from (4.10) and the definition (4.9) of \mathcal{F}_k that $\text{XDP}_{\widehat{M}}(\widehat{\lambda}_0^-, \widehat{\lambda}_{T_{m_K}}^-)$ is \mathcal{F}_k -measurable. Clearly, $\widehat{\mathcal{Z}}(\cdot + T_{m_K})|_{[0,\infty)}$ is also \mathcal{F}_k -measurable. Therefore, $\mathcal{F}_K \subset \mathcal{F}_k$.

To prove the tail triviality, we will argue using the Hewitt-Savage zero-one law. We will apply this result to the collection of i.i.d. random variables $(Z_j)_{j\in\mathbb{N}}$, given by the walk segments

$$Z_{j} := \left(\widehat{\mathcal{Z}}(\cdot + T_{j-1}) - \widehat{\mathcal{Z}}(T_{j-1})\right)|_{[0,T_{j} - T_{j-1}]}, \quad j \in \mathbb{N},$$
(4.11)

which are i.i.d. by Lemma 4.9. The *j*th walk segment Z_j determines the submap of \widehat{M} between the cut vertices $\widehat{\lambda}_{T_{j-1}}^-$ and $\widehat{\lambda}_{T_j}^-$ via the KMSW procedure, so in particular it determines $\text{XDP}_{\widehat{M}}(\widehat{\lambda}_{T_{j-1}}^-, \widehat{\lambda}_{T_j}^-)$. Since the XDP geodesic \widehat{P} must pass through each of the cut vertices $\widehat{\lambda}_{T_m}^-$,

$$\widehat{\mathcal{Z}}(T_m) = \sum_{j=1}^{m} (\widehat{\mathcal{Z}}(T_j) - \widehat{\mathcal{Z}}(T_{j-1})) \quad \text{and} \quad XDP_{\widehat{M}}(\widehat{\lambda}_0^-, \widehat{\lambda}_{T_m}^-) = \sum_{j=1}^{m} XDP_{\widehat{M}}(\widehat{\lambda}_{T_{j-1}}^-, \widehat{\lambda}_{T_j}^-). \tag{4.12}$$

Consequently, $\widehat{\mathcal{Z}}(T_m)$ and $\mathrm{XDP}_{\widehat{M}}(\widehat{\lambda}_0^-, \widehat{\lambda}_{T_m}^-)$ remain unchanged if we make any finite permutation of the first m walk segments $(Z_j)_{j\in[1,m]\cap\mathbb{Z}}$. This implies that $\widehat{\mathcal{Z}}(\cdot+T_m)|_{[0,\infty)}$ also remains unchanged if we make any finite permutation of the first m walk segments $(Z_j)_{j\in[1,m]\cap\mathbb{Z}}$. The σ -algebra \mathcal{F}_k of (4.9) is generated by $\widehat{\mathcal{Z}}(\cdot+T_m)|_{[0,\infty)}$ and $\mathrm{XDP}_{\widehat{M}}(\widehat{\lambda}_0^-,\widehat{\lambda}_{T_m}^-)$ and with $m=m_k$, so any \mathcal{F}_k -measurable event is invariant under finite permutations of the first m_k walk segments $(Z_j)_{j\in[1,m_k]\cap\mathbb{Z}}$; indeed, such permutations cannot change the value of m_k . Since $m_k \to \infty$ as $k \to \infty$ by Proposition 4.3, any $\bigcap_{k=0}^{\infty} \mathcal{F}_k$ -measurable event must be invariant under finite permutations of the walk segments $(Z_j)_{j\in\mathbb{N}}$. Since these walk segments are i.i.d., the Hewitt-Savage zero-one law implies that any such event has probability zero or one.

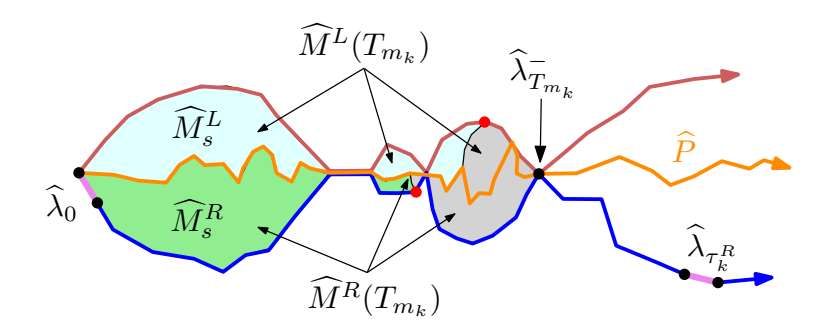


Figure 8: Illustration for the proof of Proposition 4.7. To get that the submaps \widehat{M}^L and \widehat{M}^R lying (weakly) to the left and right of \widehat{P} are independent, we first fix s and send $k \to \infty$ to deduce the independence of \widehat{M}^L_s and \widehat{M}^R_s ; highlighted in light blue and green, respectively (the red vertices are the sth vertices along the left and right boundaries of \widehat{M}). We then send $s \to \infty$.

Proof of Proposition 4.7. See Figure 8 for an illustration. Fix $s \in \mathbb{N}$. Let \widehat{M}_s^L be the submap of \widehat{M}^L consisting of all vertices of \widehat{M}^L which can be joined to the sth vertex on the left boundary of \widehat{M}^L by a directed path in \widehat{M}^L , and all edges and faces of \widehat{M}^L whose vertices are all of this type. Similarly define \widehat{M}_s^R with "right" in place of "left". On the event

$$E_k = E_k(s) := \left\{ \min\{\widehat{\mathcal{L}}(T_{m_k}), -\widehat{\mathcal{R}}(T_{m_k})\} \ge s + 1 \right\}, \tag{4.13}$$

the cut vertex $\widehat{\lambda}_{T_{m_k}}^-$ comes after the sth vertex on both the left and right boundaries of \widehat{M} . Hence on E_k , we have $\widehat{M}_s^L \subset \widehat{M}^L(T_{m_k})$ and $\widehat{M}_s^R \subset \widehat{M}^R(T_{m_k})$, where we are using the same notation as in Lemma 4.14. Moreover, on E_k the map \widehat{M}_s^L is determined by $\widehat{M}^L(T_{m_k})$: indeed, the definition of \widehat{M}_s^L with $\widehat{M}^L(T_{m_k})$ in place of \widehat{M}_s^L gives us the same map. The same is true for \widehat{M}_s^R .

Let \mathcal{F}_k be as in (4.9) and note that the event E_k of (4.13) is \mathcal{F}_k -measurable. By Lemma 4.14 and the previous paragraph, we get that on E_k , the maps \widehat{M}_s^L and \widehat{M}_s^R are conditionally independent given \mathcal{F}_k . Hence, if X^L and X^R are bounded real-valued random variables which are a.s. given by measurable functions of \widehat{M}_s^L and \widehat{M}_s^R , respectively, then

$$\mathbb{E}\left[X^{L}X^{R} \mid \mathcal{F}_{k}\right] \mathbb{1}_{E_{k}} = \mathbb{E}\left[X^{L} \mid \mathcal{F}_{k}\right] \mathbb{E}\left[X^{R} \mid \mathcal{F}_{k}\right] \mathbb{1}_{E_{k}}.$$
(4.14)

By Lemma 4.15 and the backward martingale convergence theorem, we get the a.s. convergence $\mathbb{E}[X^LX^R \mid \mathcal{F}_k] \to \mathbb{E}[X^LX^R]$ as $k \to \infty$, and similarly for the other two conditional expectations in (4.14). By the definition of T_m in the statement of Lemma 4.9, $\min\{\widehat{\mathcal{L}}(T_{m_k}), -\widehat{\mathcal{R}}(T_{m_k})\}$ is strictly increasing in k, hence goes to ∞ as $k \to \infty$. Therefore, $\mathbb{P}[E_k] \to 1$ as $k \to \infty$. Taking the limit as $k \to \infty$ in (4.14) therefore gives $\mathbb{E}\left[X^LX^R\right] = \mathbb{E}\left[X^L\right]\mathbb{E}\left[X^R\right]$. Since this holds for any possible choices of X^L and X^R , we get that \widehat{M}_s^L and \widehat{M}_s^R are independent. As $s \to \infty$, \widehat{M}_s^L and \widehat{M}_s^R increase to \widehat{M}_s^L and \widehat{M}_s^R , respectively. Sending $s \to \infty$ now concludes the proof.

5 Existence and basic properties of the Busemann function

5.1 Setup and outline

In this section, we will prove Theorems 1.4 and 1.7. We consider the following setup. Fix XDP \in {LDP, SDP}. Let $\mathcal{Z} = (\mathcal{L}, \mathcal{R}) : \mathbb{Z}^2 \to \mathbb{Z}$ be the encoding walk for the UIBOT $(M_{-\infty,\infty}, \lambda_0)$ as in

Proposition 3.10. For $n \in \mathbb{Z}$, let

$$\lambda_n = (\lambda_n^-, \lambda_n^+)$$

be the active edge of the KMSW procedure at time n, with the indexing chosen so that λ_0 is the root edge.

For $n \in \mathbb{Z}$, let $M_{n,\infty}$ be the infinite acyclic-oriented triangulation with missing edges obtained by applying the KMSW procedure to $(\mathcal{Z}(\cdot + n) - \mathcal{Z}(n))|_{[n,\infty)}$. By Remark 3.4, $M_{-\infty,\infty}$ can be recovered from $(M_{n,\infty})_{n\in\mathbb{Z}}$ by taking their union. Boundary edges to the west of λ_n are not part of $M_{n,\infty}$, i.e. are missing edges.

Let $\widehat{M}_{n,\infty}$ be the submap of $M_{n,\infty}$ induced by the vertices of $M_{n,\infty}$ which are reachable by a directed path in $M_{n,\infty}$ started from the initial vertex λ_n^- . That is, $\widehat{M}_{n,\infty}$ consists of this vertex set, all of the edges of $M_{n,\infty}$ whose vertices are both in this vertex set, and all of the faces of $\widehat{M}_{n,\infty}$ whose three boundary vertices are all in this vertex set.

The left and right boundaries of $\widehat{M}_{n,\infty}$ are the leftmost and rightmost directed paths in $M_{n,\infty}$ from λ_n^- to ∞ (note that these two paths are *not* disjoint in general). In particular, $\widehat{M}_{n,\infty}$ has no missing edges. The rightmost directed path in $M_{n,\infty}$ from λ_n^- to ∞ is just the set of non-missing boundary edges of $M_{n,\infty}$, i.e. all the boundary edges to the east of λ_n , including λ_n itself. We denote the leftmost directed path from λ_n^- to ∞ in $M_{n,\infty}$ by

$$\beta_n: \mathbb{N} \to \mathcal{E}(M_{n,\infty}),$$
 (5.1)

noting that such a path exists thanks to the final claim in Lemma 3.8. By definition, all of the edges of β_n are included in $\widehat{M}_{n,\infty}$.

Let $\widehat{M}'_{n,\infty}$ be the submap of $M_{n,\infty}$ obtained by removing from $M_{n,\infty}$ all of the vertices, edges, and faces of $\widehat{M}_{n,\infty}$ (including the ones on β_n). Then $\widehat{M}'_{n,\infty}$ is a directed triangulation with missing edges (every boundary edge of $\widehat{M}'_{n,\infty}$ is a missing edge). See Figure 9 for an illustration of the above definitions.

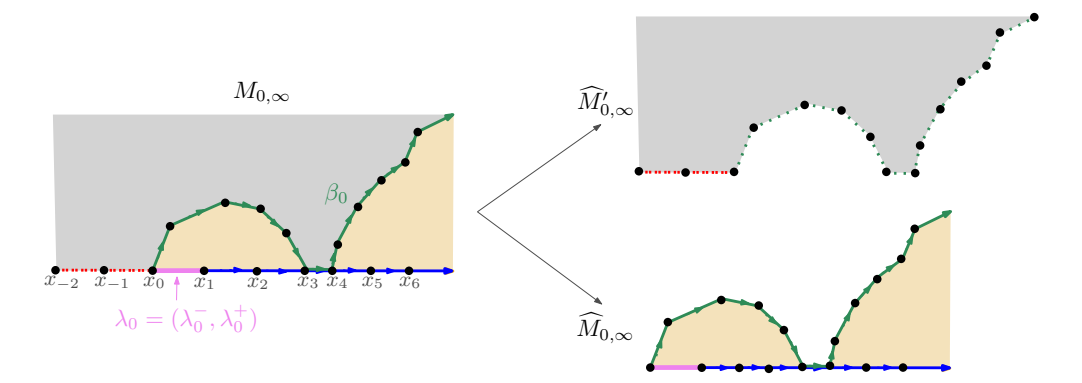


Figure 9: Illustration of the definitions of the maps $\widehat{M}_{n,\infty}$, $\widehat{M}'_{n,\infty}$ obtained from $M_{n,\infty}$ and β_n , in the case when n=0. The edges on β_0 belong to $\widehat{M}_{0,\infty}$ but not to $\widehat{M}'_{0,\infty}$.

The following proposition makes the connection between the results of Section 4 and the UIBOT.

Proposition 5.1. For each $n \in \mathbb{Z}$, the maps $\widehat{M}_{n,\infty}$ and $\widehat{M}'_{n,\infty}$ are independent. Furthermore, the map $\widehat{M}_{n,\infty}$ has the same law as the UIQBOT \widehat{M} of Definition 4.1.

We will prove Proposition 5.1 in Section 5.5 using the KMSW bijection.

As in Theorem 1.4, we let $\{x_k\}_{k\in\mathbb{Z}}$ be the boundary vertices of $M_{0,\infty}$, enumerated in directed order in such a way that $x_0 = \lambda_0^+$ and $x_1 = \lambda_0^+$ are the initial and terminal vertices of λ_0 , respectively. For $k \in \mathbb{Z}$, let

$$\tau_k := \min\{n \in \mathbb{N}_0 : x_k \text{ is the initial vertex of } \lambda_n\}. \tag{5.2}$$

Recalling Definition 3.2, it is easy to see from the Assertions (i) and (ii) of Lemma 3.6 (note that in Assertions (i) we are counting in the reversed order compared to how boundary vertices are enumerated in $M_{0,\infty}$; this is why we have $\mathcal{L}(n) = k$ instead of $\mathcal{L}(n) = -k$ in the last case of (5.3)) that

$$\tau_{k} = \begin{cases}
0, & k = 0 \\
\min\{n \in \mathbb{N} : \mathcal{R}(n) = -k\}, & k \ge 1 \\
\min\{n \in \mathbb{N} : \mathcal{L}(n) = k\}, & k \le -1.
\end{cases}$$
(5.3)

In particular, τ_k is increasing for $k \geq 0$ and decreasing for $k \leq 0$.

In Section 5.2, we will prove Theorem 1.4 using the existence of cut vertices in the UIQBOT (Proposition 4.3). More precisely, we will force long directed paths started from boundary vertices of $M_{0,\infty}$ to pass through the cut vertices of one of the maps $\widehat{M}_{\tau_k,\infty}$ (which has the law of the UIQBOT by Proposition 5.1 and the strong Markov property of \mathcal{Z}).

In Section 5.3, we will use the left and right independence property of Proposition 4.7 (applied to the UIQBOTs \widehat{M}_{τ_k}), together with the strong Markov property of \mathcal{Z} , to prove the independent and stationary increments properties in Theorem 1.7 (Properties (i) and (ii)). Property (iii) follows from elementary monotonicity considerations.

What remains is then to prove Property (iv). To do this, in Section 5.4 we introduce a new infinite acyclically-oriented triangulation with boundary, which we call the uniform infinite boundary-channeled half-plane bipolar-oriented triangulation (UIBHBOT; Definition 5.8). The UIBHBOT describes the local limit of uniformly sampled finite boundary-channeled triangulations (Definition 3.17) around a uniform boundary edge (Proposition 5.16). Moreover, the UIBHBOT admits submaps which have the same law as $M_{0,\infty}$ (Lemma 5.10). Using the symmetry in Lemma 3.18, one can show that the law of the UIBHBOT is invariant under applying an orientation-reversing homeomorphism from $\mathbb{C} \to \mathbb{C}$ (Proposition 5.9). Combining these last two facts leads to Property (iv).

5.2 Existence of the Busemann function

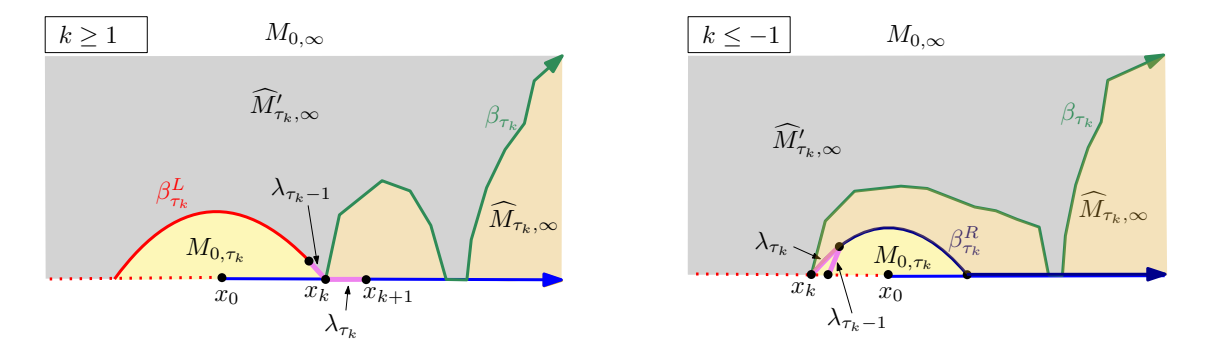


Figure 10: Illustration of the proof of Lemma 5.2 in the case when $k \ge 1$ (left) and $k \le -1$ (right).

Lemma 5.2. Define τ_k as in (5.2). For each $k \in \mathbb{Z}$, the map $M_{\tau_k,\infty}$ has the same law as the map $M_{0,\infty}$ and the map $\widehat{M}_{\tau_k,\infty}$ has the same law as the UIQBOT (Definition 4.1). Furthermore, every directed path in $M_{0,\infty}$ started from x_k is contained in the map $\widehat{M}_{\tau_k,\infty}$ defined just above (5.1).

Proof. See Figure 10 for an illustration of the proof. By (5.3), each τ_k is a stopping time for \mathcal{Z} . By the strong Markov property, the map $M_{\tau_k,\infty}$ (which is determined by $(\mathcal{Z}(\cdot + \tau_k) - \mathcal{Z}(\tau_k))|_{[0,\infty)}$) has the same law as $M_{0,\infty}$. By this and Proposition 5.1, $\widehat{M}_{\tau_k,\infty}$ has the law of the UIQBOT.

It remains to prove the statement about directed paths. This statement holds by definition for k = 0, so we only need to prove it for $k \neq 0$. We first argue that for $k \in \mathbb{Z} \setminus \{0\}$, every directed path in $M_{0,\infty}$ started from x_k is contained in $M_{\tau_k,\infty}$. Let P be such a directed path.

First, consider the case when $k \geq 1$. Let $\beta_{\tau_k}^L$ be the path formed by the missing edges on the boundary of $M_{\tau_k,\infty}$ lying to the west of $\lambda_{\tau_k}^- = x_k$. By Lemma 3.8, $\beta_{\tau_k}^L$ is the leftmost directed path in $M_{-\infty,\infty}$ ending at x_k and every vertex on $\beta_{\tau_k}^L$ has no incoming edges in $M_{\tau_k,\infty}$. Since $\beta_{\tau_k}^L$ is the leftmost directed path ending at x_k , all of the edges of $M_{0,\infty} \setminus M_{\tau_k,\infty}$ incident to x_k must be oriented toward x_k . Therefore, the first step of P must be from x_k to a vertex of $M_{\tau_k,\infty}$, and P cannot visit any vertex on $\beta_{\tau_k}^L$ after its first step. The path $\beta_{\tau_k}^L$ disconnects $M_{0,\infty} \setminus M_{\tau_k,\infty}$ from ∞ in $M_{0,\infty}$. Hence P cannot enter $M_{0,\infty} \setminus M_{\tau_k,\infty}$, so P must be contained in $M_{\tau_k,\infty}$.

Next, consider the case when $k \leq -1$. Let $\beta_{\tau_k}^R$ be the path formed by the edges in the boundary of $M_{\tau_k,\infty}$ lying to the east of the terminal vertex $\lambda_{\tau_k}^+$ of λ_{τ_k} (see the dark blue path on the right-hand side of Figure 10). By Lemma 3.8, $\beta_{\tau_k}^R$ is the rightmost directed path in $M_{0,\infty}$ started from $\lambda_{\tau_k}^+$. It follows that P cannot cross $\beta_{\tau_k}^R$: indeed, otherwise concatenating part of $\beta_{\tau_k}^R$ with the portion of P lying to the right of $\beta_{\tau_k}^R$ would yield a directed path started from $\lambda_{\tau_k}^+$ which lies partially to the right of $\beta_{\tau_k}^R$.

By (5.2), τ_k is the first non-negative time at which x_k is the initial vertex of λ_n , and $M_{0,\infty}$ does not contain the edges along its left boundary since they are missing. Consequently, there are no non-missing edges of $M_{0,\tau_k-1} = M_{0,\infty} \setminus M_{\tau_k,\infty}$ incident to x_k . In particular, the first edge of P is not in M_{0,τ_k-1} . Since P is a directed path and the orientation on $M_{0,\infty}$ is acyclic, P can visit x_k only once. It follows that P cannot visit a edge of M_{0,τ_k-1} without crossing $\beta_{\tau_k}^R$. We already saw that P cannot cross $\beta_{\tau_k}^R$, so P cannot visit a edge of M_{0,τ_k-1} .

Recall that $\widehat{M}_{\tau_k,\infty}$ is the submap of $M_{\tau_k,\infty}$ induced by the set of vertices of $M_{\tau_k,\infty}$ reachable by a directed path in $M_{\tau_k,\infty}$ started from x_k . Since every such directed path in $M_{0,\infty}$ started from x_k is contained in $M_{\tau_k,\infty}$, any such directed path is in fact contained in $\widehat{M}_{\tau_k,\infty}$.

The following lemma tells us that any finite collection of sufficiently long directed paths started from vertices on the boundary of $M_{0,\infty}$ must have a vertex in common. This will be the key tool for the proof of the existence of the Busemann function (Theorem 1.4).

Lemma 5.3. Let $\{x_k\}_{k\in\mathbb{Z}}$ be the sequence of boundary vertices as in Theorem 1.4. For each $k,k'\in\mathbb{Z}$ with k< k', there exists a sequence of distinct vertices $\{v_m\}_{m\in\mathbb{N}}$ of $M_{0,\infty}$ with the following property. Let $l\in[k,k']\cap\mathbb{Z}$ and let $\{w_j\}_{j\in\mathbb{N}}$ be any sequence of distinct vertices of $M_{0,\infty}$ which can each be reached by a directed path in $M_{0,\infty}$ started from x_l . Then for each $m\in\mathbb{N}$, it holds for each sufficiently large $j\in\mathbb{N}$ that every directed path in $M_{0,\infty}$ from x_l to w_j visits v_m .

Proof. The proof is based on the fact that the UIQBOT has infinitely many cut vertices (Proposition 4.3). Let τ_k be as in (5.2). By Lemma 5.2, the map $\widehat{M}_{\tau_k,\infty}$ has the same law as the UIQBOT. Let $k, k' \in \mathbb{Z}$ with k < k'. Since the KMSW procedure only explores finitely many edges between times τ_k and $\tau_{k'}$, the right boundaries of the maps $M_{\tau_l,\infty}$ for $l \in [k, k'] \cap \mathbb{Z}$ (equivalently, the right boundaries of the maps $\widehat{M}_{\tau_l,\infty}$ for $l \in [k, k'] \cap \mathbb{Z}$) coincide except for finitely many edges.

In particular, there is an infinite directed path $\beta_{\tau_k,\tau_{k'}}^R$ which is part of the right boundary of $\widehat{M}_{\tau_l,\infty}$ for each $l \in [k,k'] \cap \mathbb{Z}$. Almost surely, the right boundary of $\widehat{M}_{\tau_k,\infty}$ has infinitely many cut vertices (Proposition 4.3). So, a.s. there are infinitely many cut vertices of $\widehat{M}_{\tau_k,\infty}$ which lie on $\beta_{\tau_k,\tau_{k'}}^R$. Let $\{v_m\}_{m\in\mathbb{N}}$ be the ordered sequence of these cut vertices.

For $l \in [k, k'] \cap \mathbb{Z}$, the leftmost directed path β_{τ_l} of (5.1) (which is the left boundary of $\widehat{M}_{\tau_l, \infty}$) cannot cross β_{τ_k} (which is the left boundary of $\widehat{M}_{\tau_k, \infty}$). Hence every cut vertex of $\widehat{M}_{\tau_k, \infty}$ which lies on $\beta_{\tau_k, \tau_{k'}}^R$ (i.e., each of the vertices v_m) is also a cut vertex of $\widehat{M}_{\tau_l, \infty}$. By Lemma 5.2, every directed path in $M_{0,\infty}$ started from x_l must be contained in $\widehat{M}_{\tau_l, \infty}$. For each $m \in \mathbb{N}$, there are only finitely many vertices of $\widehat{M}_{\tau_l, \infty}$ which are not disconnected from x_l when we remove the cut vertex v_m . It follows that there are only finitely many vertices of $M_{0,\infty}$ which are reachable by a directed path started from x_l in $M_{0,\infty}$ which does not visit v_m . If $\{w_j\}_{j\in\mathbb{N}}$ is as in the lemma statement, then if j is sufficiently large, w_j is not equal to any of these finitely many vertices, for any $l \in [k, k'] \cap \mathbb{Z}$. This implies the lemma statement.

Proof of Theorem 1.4. Let XDP \in {LDP, SDP} and $K \in \mathbb{N}$. By Lemma 5.3, there exists a vertex z = z(K) of $M_{0,\infty}$ with the following property. Let $k \in [-K, K] \cap \mathbb{Z}$ and let $\{w_j\}_{j \in \mathbb{N}}$ be a sequence of distinct vertices of $M_{0,\infty}$ which can each be reached from x_k by a directed path in $M_{0,\infty}$. Then, it holds for each sufficiently large $j \in \mathbb{N}$ that every directed path in $M_{0,\infty}$ from x_k to w_j visits z. Indeed, we can take z to be one of the vertices v_m in Lemma 5.3 (with -K and K in place of k and k'). We define

$$\mathcal{X}(k) := XDP_{M_{0,\infty}}(x_k, z) - XDP_{M_{0,\infty}}(x_0, z), \quad \forall k \in [-K, K] \cap \mathbb{Z}.$$

$$(5.4)$$

We claim that the function defined in (5.4) satisfies the defining property (1.2) from the theorem statement for all $k, k' \in [-K, K] \cap \mathbb{Z}$. Indeed, let $\{w_j\}_{j \in \mathbb{Z}}$ be a (new) sequence of distinct vertices which can be reached by a directed path in $M_{0,\infty}$ started from x_k or started from $x_{k'}$ Then for each sufficiently large j, each XDP geodesic in $M_{0,\infty}$ from x_k to w_j visits z, which implies that

$$XDP_{M_{0,\infty}}(x_k, w_j) = XDP_{M_{0,\infty}}(x_k, z) + XDP_{M_{0,\infty}}(z, w_j)$$

The analogous relation also holds with k' in place of k. By subtracting these two relations, we obtain that for each sufficiently large j,

$$\mathcal{X}(k') - \mathcal{X}(k) = XDP_{M_{0,\infty}}(x_{k'}, w_j) - XDP_{M_{0,\infty}}(x_k, w_j),$$

which is (1.2).

It is clear that there is a at most one function satisfying $\mathcal{X}(0) = 0$ and (1.2) with k, k' restricted to lie in $[-K, K] \cap \mathbb{Z}$. Since we have constructed such a function on $[-K, K] \cap \mathbb{Z}$ for an arbitrary $K \in \mathbb{N}$, we have proven the theorem statement.

5.3 Independent and stationary increments

In this section, we will prove Properties (i) through (iii) of Theorem 1.7. We first observe that leftmost XDP geodesics to ∞ in $M_{0,\infty}$ (Definition 4.5) exist and satisfy a coalescence property.

Lemma 5.4. Let $\{x_k\}_{k\in\mathbb{Z}}$ be the ordered sequence of boundary vertices as in Theorem 1.4. Almost surely, for each $k\in\mathbb{Z}$, there exists a (unique) leftmost XDP geodesic P_{x_k} from x_k to ∞ in $M_{0,\infty}$. These leftmost XDP geodesics coalesce, in the sense that for any $k, k' \in \mathbb{Z}$, there exists $\theta, \theta' \in \mathbb{N}$ such that $P_{x_k}(t+\theta) = P_{x_{k'}}(t+\theta')$ for each $t \in \mathbb{N}$.

Proof. Define $\{\tau_k\}_{k\in\mathbb{Z}}$ as in (5.2). Since $\widehat{M}_{\tau_k,\infty}$ has the law of the UIQBOT (Lemma 5.2), Lemma 4.6 implies that there is a unique leftmost XDP geodesic P_{x_k} from x_k to ∞ in $\widehat{M}_{\tau_k,\infty}$. Since every directed path from x_k to ∞ in $M_{0,\infty}$ is contained in \widehat{M}_{τ_k} (Lemma 5.2), the path P_{x_k} is in fact the unique leftmost XDP geodesic from x_k to ∞ in $M_{0,\infty}$.

By Lemma 5.3, if we define the sequence of vertices $\{v_m\}_{m\in\mathbb{N}}$ for x_k and $x_{k'}$ as in that lemma, then each of P_{x_k} and $P_{x_{k'}}$ must visit v_m for every $m\in\mathbb{N}$. In particular, P_{x_k} and $P_{x_{k'}}$ have at least one vertex in common. By the uniqueness of leftmost XDP geodesics, P_{x_k} and $P_{x_{k'}}$ coincide after the first time they meet. This gives the coalescence property.

The following lemma is the main input in the proofs of the independent and stationary increments properties in Theorem 1.7 (Properties (i) and (ii)). It is a consequence of Proposition 4.7.

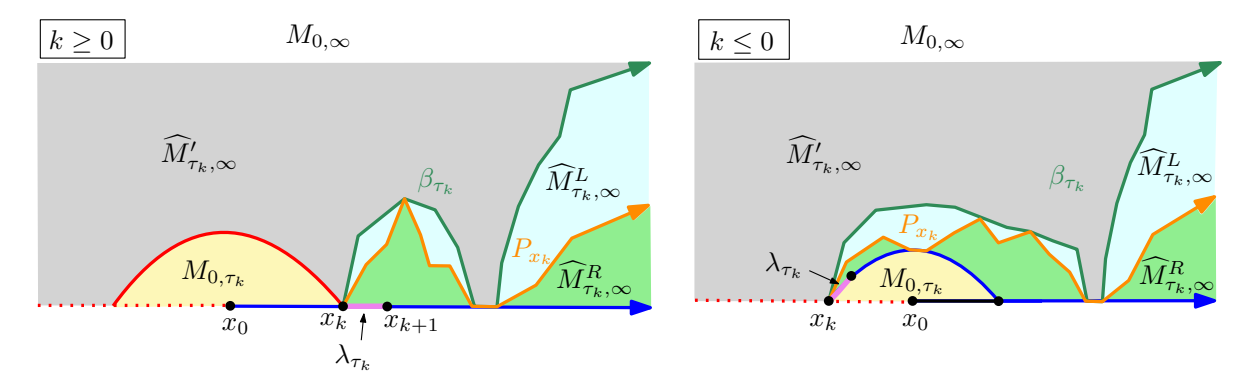


Figure 11: Illustration of the submaps used in the proof of Lemma 5.5 in the case when $k \ge 0$ (left) and the case when $k \le 0$ (right).

Lemma 5.5. For $k \in \mathbb{Z}$, let $\mathring{M}_{x_k,\infty}^L$ (resp. $\mathring{M}_{x_k,\infty}^R$) be the submap of $M_{0,\infty}$ lying to the left (resp. right) of the leftmost XDP geodesic P_{x_k} of Lemma 5.4, including the vertices and edges lying on P_{x_k} . Then $\mathring{M}_{x_k,\infty}^L$ and $\mathring{M}_{x_k,\infty}^R$ are independent. Furthermore, if $k \geq 0$ then $\mathring{M}_{x_k,\infty}^R \stackrel{d}{=} \mathring{M}_{x_0,\infty}^R$ and if $k \leq 0$ then $\mathring{M}_{x_k,\infty}^L \stackrel{d}{=} \mathring{M}_{x_0,\infty}^L$.

Proof. See Figure 11 for an illustration.

Define τ_k as in (5.2). Let M_{0,τ_k} be the submap of $M_{0,\infty}$ obtained by applying the KMSW procedure to $\mathcal{Z}|_{[0,\tau_k]}$ (Definition 3.3). By (5.3), each τ_k is a stopping time for \mathcal{Z} . Since M_{0,τ_k} is determined by $\mathcal{Z}|_{[0,\tau_k]}$ and $M_{\tau_k,\infty}$ is determined by $(\mathcal{Z}(\cdot + \tau_k) - \mathcal{Z}(\tau_k))|_{[0,\infty)}$, the maps M_{0,τ_k} and $M_{\tau_k,\infty}$ are independent.

Define the maps $\widehat{M}_{\tau_k,\infty}$ and $\widehat{M}'_{\tau_k,\infty}$ as in the discussion just above Proposition 5.1. By Proposition 5.1 and Lemma 5.2, the maps $\widehat{M}_{\tau_k,\infty}$ and $\widehat{M}'_{\tau_k,\infty}$ are independent and their joint law does not depend on k. Since the maps $\widehat{M}_{\tau_k,\infty}$ and $\widehat{M}'_{\tau_k,\infty}$ are a.s. determined by $M_{\tau_k,\infty}$, combining this with the previous paragraph shows that the triple $(M_{0,\tau_k},\widehat{M}_{\tau_k,\infty},\widehat{M}'_{\tau_k,\infty})$ is independent.

By Lemma 5.2, P_{x_k} is the leftmost XDP geodesic from x_k to ∞ in $\widehat{M}_{\tau_k,\infty}$. By Lemma 5.2, the map $\widehat{M}_{\tau_k,\infty}$ has the same law as the UIQBOT. Hence, Proposition 4.7 implies the following. Let $\widehat{M}_{\tau_k,\infty}^L$ (resp. $\widehat{M}_{\tau_k,\infty}^R$) be the submap of $\widehat{M}_{\tau_k,\infty}$ consisting of the vertices, edges, and faces lying to the left (resp. right) of P_{x_k} , including the vertices and edges lying on P_{x_k} . Then $\widehat{M}_{\tau_k,\infty}^L$ and $\widehat{M}_{\tau_k,\infty}^R$ are independent. By combining this with the previous paragraph, we get that the 4-tuple

 $(M_{0,\tau_k},\widehat{M}_{\tau_k,\infty}^L,\widehat{M}_{\tau_k,\infty}^R,\widehat{M}_{\tau_k,\infty}^R)$ is independent. Moreover, the laws of $\widehat{M}_{\tau_k,\infty}^L,\widehat{M}_{\tau_k,\infty}^R$, and $\widehat{M}_{\tau_k,\infty}^I$ do not depend on k.

When $k \geq 0$, the map $\mathring{M}^R_{x_k,\infty}$ is equal to $\widehat{M}^R_{\tau_k,\infty}$. The map $\mathring{M}^L_{x_k,\infty}$ is obtained by removing the edge (x_k,x_{k+1}) from M_{0,τ_k} to get M_{0,τ_k-1} , then identifying the maps M_{0,τ_k-1} , $\widehat{M}^L_{\tau_k,\infty}$, and $\widehat{M}'_{\tau_k,\infty}$ together along their boundaries. In particular, the upper boundary of M_{0,τ_k-1} (Definition 3.3) is identified with a segment of the left boundary of $\widehat{M}'_{\tau_k,\infty}$ starting from the vertex x_k , and the right boundary of $\widehat{M}'_{\tau_k,\infty}$ is identified with the left boundary of $\widehat{M}^L_{\tau_k,\infty}$. By the independence statement from the previous paragraph and the fact that the law of $\widehat{M}^R_{\tau_k,\infty}$ does not depend on k, we get the lemma statement in the case when $k \geq 0$.

In the case when $k \leq 0$, the map $\mathring{M}_{x_k,\infty}^L$ is obtained by identifying the right boundary of $\widehat{M}_{\tau_k}^{\prime}$ with the left boundary of $\widehat{M}_{\tau_k,\infty}^L$. The map $\mathring{M}_{x_k,\infty}^R$ is obtained by identifying the upper boundary of M_{0,τ_k} with a segment of the right boundary of $\widehat{M}_{\tau_k,\infty}^R$ started at x_k . Thus the lemma statement similarly follows in this case.

For $k \in \mathbb{Z}$, let P_{x_k} be the leftmost XDP geodesic from x_k to ∞ in $M_{0,\infty}$, as in Lemma 5.4. We will now use Lemma 5.5 to decompose $M_{0,\infty}$ into countably many independent "geodesic slices" lying between successive leftmost XDP geodesics $P_{x_{k-1}}$ and P_{x_k} . For $k \in \mathbb{Z}$, let $\theta_k^-, \theta_k \in \mathbb{N}_0$ be the smallest numbers such that

$$P_{x_{k-1}}(t+\theta_k^-) = P_{x_k}(t+\theta_k), \quad \forall t \in \mathbb{N}. \tag{5.5}$$

Such numbers exist by Lemma 5.4.

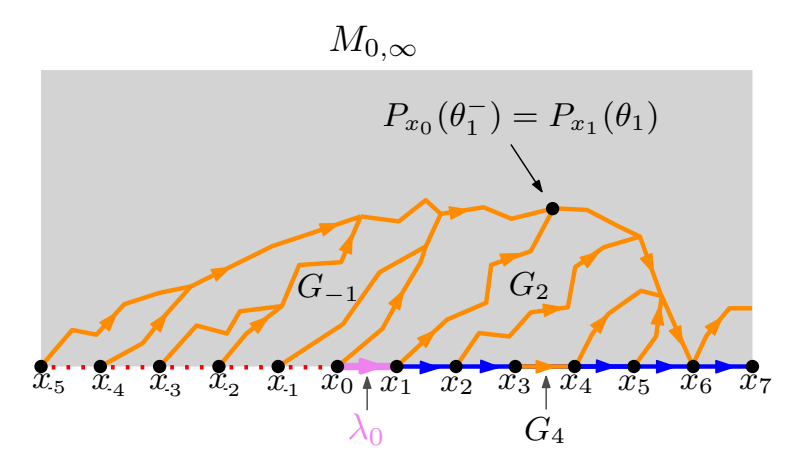


Figure 12: Illustration of the XDP geodesic slices G_k defined in Lemma 5.6 (regions between the orange paths). For $k \geq 0$, G_k can consist of a single edge (which means that $\theta_k^- = 1$ and $\theta_k = 0$) as shown for G_4 , but for $k \leq -1$ this is not possible since $M_{0,\infty}$ does not include the boundary edges to the left of x_0 .

Lemma 5.6. Let G_k be the (directed) submap of $M_{0,\infty}$ consisting of the vertices, edges, and faces of $M_{0,\infty}$ which lie between $P_{x_{k-1}}([1,\theta_k^-])$ and $P_{x_k}([1,\theta_k])$, including the vertices and edges which lie on these XDP geodesic segments. We call G_k an XDP geodesic slice (see Figure 12). The maps $\{G_k\}_{k\in\mathbb{Z}}$ are independent. Furthermore, the maps $\{G_k\}_{k\geq 1}$ all have the same law, and the maps $\{G_k\}_{k\leq 0}$ all have the same law.

Proof. Define the maps $\mathring{M}^L_{x_k,\infty}$ and $\mathring{M}^R_{x_k,\infty}$ as in Lemma 5.5. Since leftmost XDP geodesics cannot cross each other, for $k \in \mathbb{Z}$, the maps $\{G_j\}_{j \leq k}$ are a.s. determined by $\mathring{M}^L_{x_k,\infty}$ and the maps $\{G_j\}_{j \geq k+1}$ are a.s. determined by $\mathring{M}^R_{x_k,\infty}$. By the independence part of Lemma 5.5, the sequence of maps $\{G_j\}_{j \leq k}$ is independent from the sequence of maps $\{G_j\}_{j \geq k+1}$. Since this holds for every $k \in \mathbb{Z}$, the sequence of maps $\{G_k\}_{k \in \mathbb{Z}}$ are independent from each other. To get the stationarity property, we observe that G_k is determined by each of $\mathring{M}^L_{x_k,\infty}$ and $\mathring{M}^R_{x_{k-1},\infty}$ in a manner which does not depend on k. The stationarity property for G_k therefore follows from the stationarity part of Lemma 5.5.

The Busemann function can be expressed in terms of the geodesic slices G_k as follows.

Lemma 5.7. Let θ_k^- and θ_k be as in (5.5). Then the Busemann function (Theorem 1.4) satisfies

$$\mathcal{X}(k) - \mathcal{X}(k-1) = \theta_k - \theta_k^-. \tag{5.6}$$

Proof. Let w_0 be the terminal vertex of $P_{x_k}(\theta_k)$, equivalently, the terminal vertex of $P_{x_{k-1}}(\theta_k^-)$. Let $\{w_j\}_{j\in\mathbb{N}}$ be the ordered sequence of vertices visited by P_{x_k} (equivalently, $P_{x_{k-1}}$) after w_0 . Since P_{x_k} and $P_{x_{k-1}}$ are XDP geodesics, for each $j\in\mathbb{N}$,

$$XDP_{M_{0,\infty}}(x_k, w_j) = XDP_{M_{0,\infty}}(x_k, w_0) + XDP_{M_{0,\infty}}(w_0, w_j)$$

and the same is true with x_{k-1} in place of x_k . Therefore,

$$XDP_{M_{0,\infty}}(x_k, w_j) - XDP_{M_{0,\infty}}(x_{k-1}, w_j) = XDP_{M_{0,\infty}}(x_k, w_0) - XDP_{M_{0,\infty}}(x_{k-1}, w_0) = \theta_k - \theta_k^-$$

By the definition of \mathcal{X} from Theorem 1.4, this implies (5.6).

Proof of Theorem 1.7, Properties (i) through (iii). By Lemma 5.7, the increment $\mathcal{X}(k) - \mathcal{X}(k-1)$ is a function of the XDP geodesic slice map G_k of Lemma 5.6. Therefore, the independent increments and stationary increments properties (i) and (ii) follow from Lemma 5.6. To get Property (iii), let $k \geq 1$. Use Theorem 1.4 to find $w \in M_{0,\infty}$ such that

$$\mathcal{X}(k) - \mathcal{X}(k-1) = XDP_{M_{0,\infty}}(x_k, w) - XDP_{M_{0,\infty}}(x_{k-1}, w).$$

$$(5.7)$$

Since the directed edge (x_{k-1}, x_k) is part of $M_{0,\infty}$, Property (iii) is immediate from (5.7).

5.4 Symmetry via the UIBHBOT

To prove Theorem 1.7, it remains to prove Property (iv). For this purpose, we will introduce an auxiliary infinite directed planar map, which we now define. Let $\mathcal{Z}^b = (\mathcal{L}^b, \mathcal{R}^b) : \mathbb{Z} \to \mathbb{Z}^2$ be a bi-infinite walk such that $\mathcal{Z}^b(0) = (0,0)$; $\mathcal{Z}^b|_{[0,\infty)} \stackrel{d}{=} \mathcal{Z}|_{[0,\infty)}$; and

$$\mathcal{Z}^{\mathrm{b}}|_{(-\infty,0]}$$
 has the law of $\mathcal{Z}|_{(-\infty,0]}$ conditioned so that $\mathcal{L}(n) \geq 1$ for every $n \leq -1$.

To be concrete, one way to construct $\mathcal{Z}^b|_{(-\infty,0]}$ is as follows. Let $\{\widetilde{\mathcal{Z}}_k(\cdot)\}_{k\in\mathbb{Z}}$ be an i.i.d. collection of random walk paths such that $\widetilde{\mathcal{Z}}_k$ has the same law as $\mathcal{Z}|_{[0,\tau_{-1}]}$, where $\tau_{-1}=\min\{n\in\mathbb{N}:\mathcal{L}(n)=-1\}$ (as in (5.3)). Let $\mathcal{Z}^b:\mathbb{Z}\to\mathbb{Z}^2$ be obtained by concatenating the paths $\widetilde{\mathcal{Z}}_k$ end-to-end in order, in such a way that $\mathcal{Z}^b(0)=(0,0)$ and 0 is the time at which we start traversing the path $\widetilde{\mathcal{Z}}_0$. Then for $k\in\mathbb{Z}$, the path $\widetilde{\mathcal{Z}}_k$ is the segment of \mathcal{Z}^b between the first time that \mathcal{L}^b hits -k and the first time that \mathcal{L}^b hits -k-1. It follows from the strong Markov property that $\mathcal{Z}^b|_{[0,\infty)}\stackrel{d}{=}\mathcal{Z}|_{[0,\infty)}$. It

can be seen from Lemma 5.14 below that $\mathcal{Z}^b|_{(-\infty,0]}$ has the same law as the process obtained from $\mathcal{Z}|_{(-\infty,0]}$ by conditioning $\mathcal{L}|_{(-\infty,1]}$ to stay positive in the sense of [BD94] (but we will not need to use this latter fact).

By Definition 3.3 and Remark 3.4, we can apply the KMSW procedure to \mathcal{Z}^b to produce an infinite bipolar-oriented triangulation M^b . As we will explain just below, M^b has an infinite boundary, and all of its boundary edges are missing (i.e. it only has an infinite lower-left boundary); see Figure 13 for an illustration of M^b .

We describe $M^{\mathbf{b}}$ more precisely. For $k \in \mathbb{Z}$, let

$$\tau_k^{\mathbf{b}} := \min \left\{ n \in \mathbb{Z} : \mathcal{L}^{\mathbf{b}}(n) = k \right\}. \tag{5.8}$$

By the definition of \mathcal{Z}^b , $\{\tau_k^b\}_{k\in\mathbb{Z}}$ is a decreasing sequence of times and $\tau_0^b = 0$. By Assertion (i) of Lemma 3.6, for each $k \in \mathbb{Z}$, the time τ_k^b is the time when the triangle of M^b whose boundary includes the kth lower-left (missing) boundary edge of M^b is added to M^b by the KMSW procedure, with the lower-left boundary edges enumerated from west to east. Hence, the (missing) boundary edges are added from east to west by the KMSW procedure. Since, a.s.,

$$\liminf_{n \to \infty} \mathcal{L}^{\mathbf{b}}(n) = \liminf_{n \to \infty} \mathcal{R}^{\mathbf{b}}(n) = \liminf_{n \to -\infty} \mathcal{R}^{\mathbf{b}}(n) = -\infty,$$

Lemma 3.6 and Remark 3.4 imply that a.s. all of the boundary edges of $M^{\rm b}$ belong to the lower-left boundary.

Let $\{x_k^b\}_{k\in\mathbb{Z}}$ be the vertices along the (lower-left) boundary of M^b , enumerated so that (x_k^b, x_{k+1}^b) is the edge corresponding to time τ_k^b . Since, as explained above, the edges $\{(x_k^b, x_{k+1}^b)\}_{k\in\mathbb{Z}}$ are enumerated from west to east, the vertices $\{x_k^b\}_{k\in\mathbb{Z}}$ are also enumerated from west to east. We write $e^b = (x_0^b, x_1^b)$ and call it the **root edge** of M^b . Note that here we are not respecting the usual convention that maps are rooted at λ_0 , the reason being that λ_0 is not a boundary edge for M^b (rather, its initial vertex is x_0^b and its terminal vertex is not on the boundary). Also note that e^b is a missing edge of M^b .

Definition 5.8. The uniform infinite boundary-channeled half-plane bipolar-oriented triangulation (UIBHBOT) is the edge-rooted triangulation with boundary (M^b, e^b) defined just above.

The reason for the name is that the UIHBHBOT arises as the Benjamini-Schramm local limit of certain uniform boundary-channeled bipolar-oriented triangulations, as defined in Definition 3.17, around a uniformly chosen boundary edge (see Proposition 5.16 below). For the purposes of proving Theorem 1.7, the main fact about the UIBHBOT which we need is the following non-trivial symmetry.

Proposition 5.9. Let (M^b, e^b) be the UIBHBOT. Let $(\widetilde{M}^b, \widetilde{e}^b)$ be the directed, edge-rooted triangulation with missing boundary edges obtained from (M^b, e^b) by applying an orientation-reversing homeomorphism $\mathbb{C} \to \mathbb{C}$. Then $(\widetilde{M}^b, \widetilde{e}^b)$ has the same law as (M^b, e^b) .

Recall that a planar map is viewed modulo *orientation-preserving* homeomorphisms from \mathbb{C} to \mathbb{C} . Applying an orientation-reversing homeomorphism to (M^b, e^b) gives us a different planar map. Proposition 5.9 tells us that this new planar map has the same law as (M^b, e^b) .

In the setting of Proposition 5.9, each (non-missing) edge of $\widetilde{M}^{\rm b}$ is equipped with the same orientation as the corresponding edge of $M^{\rm b}$ (it is only the orientation of the plane which is reversed, not the orientation of the edges of the map).

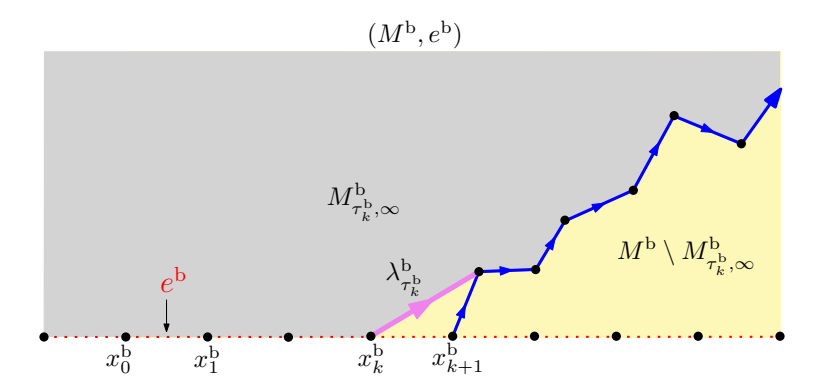


Figure 13: The UIBHBOT $M^{\rm b}$ and the submap $M_{\tau_k^{\rm b},\infty}^{\rm b} \stackrel{d}{=} M_{0,\infty}$ for a typical value of $k \in \mathbb{Z}$. The KMSW procedure first explores the yellow region and then the grey region. The triangles containing a boundary edge are explored in east to west order. Also shown is the active edge for the KMSW procedure at time $\tau_k^{\rm b}$ with the corresponding triangle having a (missing) boundary edge. Note that all the boundary edges of the UIBHBOT are missing. By, e.g., Proposition 5.16 below, each of the boundary vertices of the UIBHBOT has no incoming edges.

Proposition 5.9 is not obvious from the definition of the UIBHBOT in terms of the KMSW procedure. Indeed, the KMSW encoding walk corresponding to $(\widetilde{M}^{\rm b}, \widetilde{e}^{\rm b})$ is coupled with the original KMSW encoding walk $\mathcal{Z}^{\rm b}$ in a highly non-trivial way. Reversing the orientation of \mathbb{C} swaps west and east, so if $\{x_k^{\rm b}\}_{k\in\mathbb{Z}}$ is the west to east ordered sequence of boundary vertices of $M^{\rm b}$, as in the discussion just above (5.8), then $\{x_{-k}^{\rm b}\}_{k\in\mathbb{Z}}$ is the west to east ordered sequence of boundary vertices of $\widetilde{M}^{\rm b}$.

We will prove Proposition 5.9 in Section 5.6 using a symmetry for finite boundary-channeled bipolar-oriented triangulations (Lemma 3.18) and a limiting argument. For the time being, we use Proposition 5.9 to conclude the proof of Theorem 1.7.

Lemma 5.10. Let (M^b, e^b) be the UIBHBOT (Definition 5.8). For $k \in \mathbb{Z}$, let τ_k^b be as in (5.8) and let $\{x_k^b\}_{k\in\mathbb{Z}}$ be the sequence of boundary vertices as in the discussion just after (5.8). Let $M_{\tau_k^b,\infty}^b$ be the submap of M^b obtained by applying the KMSW procedure to $(\mathcal{Z}^b(\cdot + \tau_k^b) - \mathcal{Z}^b(\tau_k^b))|_{[0,\infty)}$. Then $M_{\tau_k^b,\infty} \stackrel{d}{=} M_{0,\infty}$. Furthermore, for each $l \leq k$, each directed path in M^b from x_l^b to ∞ is contained in $M_{\tau_k^b,\infty}$.

Proof. In the construction of \mathcal{Z}^{b} described at the beginning of Section 5.4, the process $(\mathcal{Z}^{\mathrm{b}}(\cdot + \tau_k^{\mathrm{b}}) - \mathcal{Z}^{\mathrm{b}}(\tau_k^{\mathrm{b}}))|_{[0,\infty)}$ is obtained by concatenating the walk paths $\widetilde{\mathcal{Z}}_j$ for $j \geq -k$. By the strong Markov property of \mathcal{Z} , this implies that $(\mathcal{Z}^{\mathrm{b}}(\cdot + \tau_k^{\mathrm{b}}) - \mathcal{Z}^{\mathrm{b}}(\tau_k^{\mathrm{b}}))|_{[0,\infty)} \stackrel{d}{=} \mathcal{Z}|_{[0,\infty)}$. Hence $M_{\tau_k^{\mathrm{b}},\infty}^{\mathrm{b}} \stackrel{d}{=} M_{0,\infty}$. The statement that each directed path in M^{b} from x_l^{b} to ∞ is contained in $M_{\tau_k^{\mathrm{b}},\infty}$ follows from a similar argument as in the $k \leq -1$ case of Lemma 5.2.

From Lemma 5.10, we can obtain the analog of Theorem 1.4 for the UIBHBOT.

Proposition 5.11. Let $\{x_k^b\}_{k\in\mathbb{Z}}$ be the boundary vertices of the UIBHBOT as in the discussion just after (5.8). There exists a unique function $\mathcal{X}^b: \mathbb{Z} \to \mathbb{Z}$, called the **Busemann function**, such that $\mathcal{X}^b(0) = 0$ and the following is true. Let $k, k' \in \mathbb{Z}$ and let $\{w_j\}_{j\in\mathbb{N}}$ be a sequence of distinct

vertices of M^b such that for each $j \in \mathbb{N}$, each of x_k^b and $x_{k'}^b$ can be joined to w_j by a directed path in M^b . Then

 $\mathcal{X}^{\mathrm{b}}(k') - \mathcal{X}^{\mathrm{b}}(k) = \mathrm{XDP}_{M^{\mathrm{b}}}(x_{k'}, w_j) - \mathrm{XDP}_{M^{\mathrm{b}}}(x_k, w_j),$ for each sufficiently large $j \in \mathbb{N}$. (5.9) Furthermore, the increments $\mathcal{X}^{\mathrm{b}}(k) - \mathcal{X}^{\mathrm{b}}(k-1)$ are i.i.d., and if \mathcal{X} is the Busemann function for $M_{0,\infty}$ as in Theorem 1.4, then

$$\mathcal{X}^{b}(k) - \mathcal{X}^{b}(k-1) \stackrel{d}{=} \mathcal{X}(0) - \mathcal{X}(-1). \tag{5.10}$$

Proof. For $K \in \mathbb{Z}$, define the time $\tau_K^{\rm b}$ and the map $M_{\tau_K^{\rm b},\infty}^{\rm b}$ as in Lemma 5.10. By Lemma 5.10, $M_{\tau_K^{\rm b},\infty}^{\rm b} \stackrel{d}{=} M_{0,\infty}$ and for $k \leq K$, each directed path in $M^{\rm b}$ from $x_k^{\rm b}$ to ∞ is contained in $M_{\tau_K^{\rm b},\infty}^{\rm b}$. By applying Theorem 1.4 to $M_{\tau_K^{\rm b},\infty}^{\rm b}$, we find that there exists a unique $\mathcal{X}^{\rm b}: (-\infty,K] \cap \mathbb{Z} \to \mathbb{Z}$ satisfying (5.9) for $k,k' \leq K$. Furthermore, by applying Properties (i) and (ii) of Theorem 1.7 (which we have already proven) to $M_{\tau_K^{\rm b},\infty}^{\rm b}$, we find that the increments $\mathcal{X}^{\rm b}(k) - \mathcal{X}^{\rm b}(k-1)$ for $k \leq K$ are i.i.d. and have the same law as the increment $\mathcal{X}(0) - \mathcal{X}(-1)$. Since K can be made arbitrarily large, this proves the proposition.

Proof of Theorem 1.7, Property (iv). Let (M^b, e^b) be the UIBHBOT and let \mathcal{X}^b be its Busemann function as in Proposition 5.11. By Proposition 5.9, the law of (M^b, e^b) is invariant under applying an orientation-reversing homeomorphism from \mathbb{C} to \mathbb{C} (while keeping the directions of the edges fixed). Applying such an orientation-reversing homeomorphism has the effect of reversing the order of the boundary vertices of M^b , which by (5.9) has the effect of replacing \mathcal{X}^b by its time reversal $\mathcal{X}^b(-\cdot)$. Consequently, the increments of \mathcal{X}^b and its time reversal have the same law, i.e., $\mathcal{X}^b(k) - \mathcal{X}^b(k-1) \stackrel{d}{=} \mathcal{X}^b(k-1) - \mathcal{X}^b(k)$. By (5.10), this implies that $\mathcal{X}(0) - \mathcal{X}(-1) \stackrel{d}{=} \mathcal{X}(-1) - \mathcal{X}(0)$. Since the negative-time increments of \mathcal{X} all have the same law (Property (ii)), this implies Property (iv).

5.5 Proof of Proposition 5.1: Relation between the UIBOT and the UIQBOT

The idea of the proof of Proposition 5.1 is to look at the excursions that the KMSW exploration λ_n makes to the left and right of the leftmost directed path β_0 of (5.1). In Lemma 5.12, we give a description in terms of the KMSW encoding walk \mathcal{Z} of the times n when $\lambda_n \in \widehat{M}_{0,\infty}$ and times n when $\lambda_n \in \widehat{M}_{0,\infty}$ (recall the definitions of $\widehat{M}_{0,\infty}$ and $\widehat{M}'_{0,\infty}$ from the beginning of Section 5.1). We then concatenate the increments of \mathcal{Z} corresponding to times when $\lambda_n \in \widehat{M}_{0,\infty}$ (resp. $\lambda_n \in \widehat{M}'_{0,\infty}$) to obtain two KMSW encoding walks $\widehat{\mathcal{Z}}$ and $\widehat{\mathcal{Z}}'$ for $\widehat{M}_{0,\infty}$ and $\widehat{M}'_{0,\infty}$, respectively (Lemma 5.13). In Lemma 5.14, we describe the joint law of $(\widehat{\mathcal{Z}}, \widehat{\mathcal{Z}}')$, with the help of an elementary lemma about lazy random walks (Lemma 5.15). This description immediately yields Proposition 5.1.

We will often use in this section the following two aspects of the definitions of $\widehat{M}_{0,\infty}$ and $\widehat{M}'_{0,\infty}$: (i) $\widehat{M}_{0,\infty}$ is the submap of $M_{0,\infty}$ induced by the vertices of $M_{0,\infty}$ which are reachable by a directed path in $M_{0,\infty}$ started from the initial vertex λ_0^- ; (ii) the edges of the leftmost directed path β_0 of (5.1) are non-missing edges in $\widehat{M}_{0,\infty}$ and missing edges in $\widehat{M}'_{0,\infty}$.

Lemma 5.12. Let $N_1^R = 0$. Inductively, for $k \in \mathbb{N}$, let N_k^L be the smallest $n \geq N_k^R + 1$ for which $\lambda_n \notin \widehat{M}_{0,\infty}$ (i.e., $\lambda_n \in \widehat{M}'_{0,\infty}$) and let N_{k+1}^R be the smallest $n \geq N_k^L + 1$ for which $\lambda_n \in \widehat{M}_{0,\infty}$. Then

$$N_k^L = \min \left\{ n \ge N_k^R + 1 : \mathcal{L}(n) = \mathcal{L}(N_k^R) - 1 \right\}$$

$$N_{k+1}^R = \min \left\{ n \ge N_k^L + 1 : \mathcal{R}(n) = \mathcal{R}(N_k^L) - 1 \right\}.$$
(5.11)

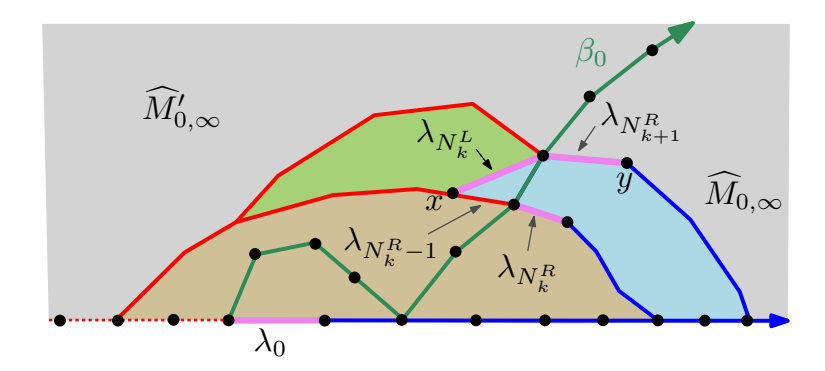


Figure 14: The times N_k^R , N_k^L , and N_{k+1}^R appearing in Lemma 5.12 and the active edges at these times. The KMSW procedure explores the light brown region, then the light blue region, then the light green region, and then the gray region.

In particular:

(i) At each of the times N_k^R for $k \geq 2$,

$$\mathcal{Z}(N_k^R) - \mathcal{Z}(N_k^R - 1) = (1, -1), \tag{5.12}$$

and the KMSW procedure for $M_{0,\infty}$ adds at time N_k^R a new single non-missing edge (rather than a triangular face) to M_{0,N_k^R-1} . This edge is $\lambda_{N_k^R}$.

(ii) At each of the times N_k^L for $k \ge 1$,

$$\mathcal{Z}(N_k^L) - \mathcal{Z}(N_k^L - 1) = (-1, 0),$$
 (5.13)

and the KMSW procedure for $M_{0,\infty}$ creates a triangular face T contained in $\widehat{M}'_{0,\infty}$ whose boundary consists of the edge $\lambda_{N_k^L-1}$, the (new active) edge $\lambda_{N_k^L}$, and the (previously active) edge $\lambda_{N_k^L-1}$ along the path β_0 .

Proof. The lemma is essentially a re-statement of [GHS16, Lemma 2.1], but [GHS16] has a slightly different setup as compared to this paper, so we will give a proof. Our proof is based on the forward KMSW bijection, in contrast to [GHS16] which uses the reverse KMSW bijection. See Figure 14 for an illustration.

We proceed by induction on k. Assume that $k \in \mathbb{N}$ and the claimed description of the time N_k^R has been proven. Let x be the vertex on the boundary of $M_{N_k^R,\infty}$ lying immediately to the west of the initial vertex $\lambda_{N_k^R}^-$ of $\lambda_{N_k^R}$. We claim that $x \notin \widehat{M}_{0,\infty}$. For k=1, in which case $N_1^R=0$, the claim follows from the fact that β_0 cannot hit the boundary of $M_{0,\infty}$ strictly to the west of its initial vertex λ_0^- , which in turn follows from the fact that vertices on the left boundary of $M_{0,\infty}$ have no incoming edges in $M_{0,\infty}$ (Lemma 3.8).

If $k \geq 2$, then (5.11) with k-1 in place of k implies (5.12) since \mathcal{Z} has increments in $\{(1,-1),(-1,0),(0,1)\}.$

By the KMSW procedure, this means that at time N_k^R we add a new non-missing edge (rather than a triangular face) to M_{0,N_k^R-1} . This edge is $\lambda_{N_k^R}$. By the definition of N_k^R , the edge $\lambda_{N_k^R}$ lies in $\widehat{M}_{0,\infty}$. Furthermore, the edge on the boundary of $M_{N_k^R,\infty}$ immediately to the west of $\lambda_{N_k^R}$ is

 $\lambda_{N_k^R-1}$, which (by the definition of N_k^R) is not in $\widehat{M}_{0,\infty}$. Hence $\lambda_{N_k^R-1}=(x,\lambda_{N_k^R}^-)\notin\mathcal{E}(\widehat{M}_{0,\infty})$ and so $x\notin\mathcal{V}(\widehat{M}_{0,\infty})$.

By the definition of N_k^L , the time N_k^L is at most the first time $n \ge N_k^R + 1$ at which x is a vertex of λ_n . From Assertion (i) of Lemma 3.6 (applied to the walk $(\mathcal{Z}(N_k^R + \cdot) - \mathcal{Z}(N_k^R))|_{[0,\infty)}$ and the corresponding map $M_{N_k^R,\infty}$), this time is

$$\min \left\{ n \ge N_k^R + 1 : \mathcal{L}(n) = \mathcal{L}(N_k^R) - 1 \right\}. \tag{5.14}$$

Conversely, assume that $n \geq N_k^R + 1$ and n is strictly smaller than the time (5.14). We make the following preliminary observation: Fix $m \geq 0$. Let N > m be the first time such that $\mathcal{L}(N) < \mathcal{L}(m)$. Thanks to Assertion (i) of Lemma 3.6 (applied to the walk $(\mathcal{Z}(m+\cdot)-\mathcal{Z}(m))|_{[0,N-1)}$ and the corresponding map $M_{m,N-1}$), the map $M_{m,N-1}$ does not have any edge on the lower-left boundary. Hence, the vertex λ_m^- remains on the lower-left boundary of the map $M_{m',\infty}$ for all times m' such that $m \leq m' < N$.

Since we assume that n is strictly smaller than the time (5.14), we deduce from the latter observation that $\lambda_{N_k}^-$ lies on the lower-left boundary of $M_{n,\infty}$, i.e. to the boundary to the west of λ_n (possibly $\lambda_{N_k}^-$ is the initial vertex of λ_n). Moreover, there is a directed path in $M_{0,\infty}$ from $\lambda_{N_k}^-$ to the initial vertex of λ_n , namely a segment of the boundary of $M_{n,\infty}$. Therefore, $\lambda_n \in \widehat{M}_{N_k^R,\infty}$ because $\widehat{M}_{N_k}^-$ is, by definition, the submap of $M_{N_k}^-$ induced by the vertices of $M_{N_k}^-$ which are reachable by a directed path in $M_{N_k}^-$ started from the initial vertex $\lambda_{N_k}^-$. Since $\widehat{M}_{N_k}^ \subset \widehat{M}_{0,\infty}$, we conclude that $n < N_k^L$. Hence N_k^L is equal to the time (5.14), as stated in (5.11), and we also proved Assertion (i).

Now we consider N_{k+1}^R . Let y be the vertex on the boundary of $M_{N_k^L,\infty}$ lying immediately to the east of the terminal vertex $\lambda_{N_k^L}^+$ of $\lambda_{N_k^L}$. By the description of N_k^L proven just above, we have (5.13) since $\mathcal Z$ has increments in $\{(1,-1),(-1,0),(0,1)\}$. By the KMSW procedure, at time N_k^L , we add a triangle with two of its edges on the boundary of $M_{N_k^L-1,\infty}$, and $\lambda_{N_k^L}$ is the other edge of this triangle. In particular, $\lambda_{N_k^L}^+$ is equal to $\lambda_{N_k^L-1}^+$, which is in $\widehat{M}_{0,\infty}$. Since $\lambda_{N_k^L} \notin \widehat{M}_{0,\infty}$, the vertex $\lambda_{N_k^L}^+$ must in fact lie on the left boundary β_0 of $\widehat{M}_{0,\infty}$. Furthermore, we note the following fact for future reference: since β_0 cannot cross the left or right boundaries of $M_{N_k^L,\infty}$, the part of β_0 contained in $M_{N_k^L,\infty}$ consists only of edges of β_0 traversed after it hits $\lambda_{N_k^L}^+$.

The edge $(\lambda_{N_k}^+, y)$ is directed, and so, since $\lambda_{N_k}^+ \in \widehat{M}_{0,\infty}$, this edge also belongs to $\widehat{M}_{0,\infty}$. By the definition of N_{k+1}^R , we thus have that N_{k+1}^R is at most the first time $n \geq N_k^L + 1$ for which $\lambda_n = (\lambda_{N_k}^+, y)$. By Assertion (ii) of Lemma 3.6 (applied to the walk $(\mathcal{Z}(N_k^L + \cdot) - \mathcal{Z}(N_k^L))|_{[0,\infty)}$ and the corresponding map $M_{N_k}^-$, ∞), this time is

$$\min \left\{ n \ge N_k^L + 1 : \mathcal{R}(n) = \mathcal{R}(N_k^L) - 1 \right\}. \tag{5.15}$$

Conversely, if $n \geq N_k^L + 1$ and n is strictly smaller than the time (5.15), then $\lambda_{N_k}^+$ lies on the lower-left boundary of $M_{n,\infty}$, i.e. to the boundary to the east of λ_n (possibly $\lambda_{N_k}^+$ is the terminal vertex of λ_n); this follows using the same idea we used below (5.14). We also make the following observation for future reference: the segment of the boundary of $M_{n,\infty}$ from λ_n^+ to $\lambda_{N_k}^+$ is a directed path between these two vertices in $M_{0,\infty}$. Since the orientation on $M_{-\infty,\infty}$ is acyclic, there is no

directed path in $M_{-\infty,\infty}$ from $\lambda_{N_k^L}^+$ to λ_n^+ . Since $(\lambda_n^-, \lambda_n^+)$ is directed, there is also no directed path in $M_{-\infty,\infty}$ from $\lambda_{N_k^L}^+$ to λ_n^- .

We now show that $N_{k+1}^R > n$. Since $\lambda_{N_{k+1}^R - 1} \notin \widehat{M}_{0,\infty}$, $\lambda_{N_{k+1}^R} \in \widehat{M}_{0,\infty}$, and $\lambda_{N_{k+1}^R - 1}$ and $\lambda_{N_{k+1}^R}$ share a vertex, at least one of the vertices of $\lambda_{N_{k+1}^R}$ must lie on β_0 (we will see a posteriori that $\lambda_{N_{k+1}^R}^-$ has to be the shared vertex, but for the moment it may be $\lambda_{N_{k+1}^R}^-$ or $\lambda_{N_{k+1}^R}^+$). As we noted at the end of the paragraph after (5.13), $\lambda_{N_k}^+$ is the first vertex of $M_{N_k}^L$, hit by β_0 . So, one of the vertices of $\lambda_{N_{k+1}^R}$ is hit by β_0 after $\lambda_{N_k}^+$. Since β_0 is a directed path, this gives a directed path from $\lambda_{N_k}^+$ to either $\lambda_{N_{k+1}^R}^-$ or $\lambda_{N_{k+1}^R}^+$, which combined with the result in the previous paragraph shows that $N_{k+1}^R > n$. Hence N_{k+1}^R is equal to the time (5.15), as stated in (5.11), and we also proved Assertion (ii).

We will now describe the KMSW encoding walks for the maps $\widehat{M}_{0,\infty}$ and $\widehat{M}'_{0,\infty}$ in terms of \mathcal{Z} . For $m \in \mathbb{N}_0$, let $S_m, S'_m \in \mathbb{N}_0$ be the smallest integers such that

$$m = \#\{n \le S_m : \lambda_n \in \widehat{M}_{0,\infty}\} = \#\{n \le S'_m : \lambda_n \in \widehat{M}'_{0,\infty}\}.$$
 (5.16)

Define $\widehat{\mathcal{Z}} = (\widehat{\mathcal{L}}, \widehat{\mathcal{R}}) : \mathbb{N}_0 \to \mathbb{Z}$ by $\widehat{\mathcal{Z}}(0) = (0, 0)$ and

$$\widehat{\mathcal{Z}}(m) - \widehat{\mathcal{Z}}(m-1) := \mathcal{Z}(S_m) - \mathcal{Z}(S_m-1), \quad \forall m \in \mathbb{N}.$$
 (5.17)

In other words, $\widehat{\mathcal{Z}}(m)$ is obtained by summing the first m increments of \mathcal{Z} corresponding to times n such that $\lambda_n \in \widehat{M}_{0,\infty}$.

Similarly, with N_k^L as in Lemma 5.12, we define $\widehat{\mathcal{Z}}' = (\widehat{\mathcal{L}}', \widehat{\mathcal{R}}') : \mathbb{N}_0 \to \mathbb{Z}$ so that $\widehat{\mathcal{Z}}'(0) = (0,0)$ and

$$\widehat{\mathcal{Z}}'(m) - \widehat{\mathcal{Z}}'(m-1) := \begin{cases} \mathcal{Z}(S'_m) - \mathcal{Z}(S'_m - 1), & S'_m \notin \{N_k^L\}_{k \in \mathbb{N}} \\ (0, 1), & S'_m \in \{N_k^L\}_{k \in \mathbb{N}}, \end{cases} \quad \forall m \in \mathbb{N}.$$
 (5.18)

In other words, $\widehat{Z}'(m)$ is obtained by summing the first m increments of \mathcal{Z} corresponding to times n such that $\lambda_n \in \widehat{M}'_{0,\infty}$, except that for each of the times N_k^L , we replace the corresponding increment $\mathcal{Z}(N_k^L) - \mathcal{Z}(N_k^L - 1) = (-1,0)$ by (0,1). The reason we do this is explained in the proof of the next lemma.

Lemma 5.13. The maps $\widehat{M}_{0,\infty}$ and $\widehat{M}'_{0,\infty}$ are obtained by applying the KMSW procedure (Definition 3.3) to the walks $\widehat{\mathcal{Z}}$ and $\widehat{\mathcal{Z}}'$, respectively.

Proof. The fact that $\widehat{\mathcal{Z}}$ (resp. $\widehat{\mathcal{Z}}'$) is the correct KMSW walk for $\widehat{M}_{0,\infty}$ (resp. $\widehat{M}'_{0,\infty}$) is obvious when $S_m \notin \{N_k^R\}_{k\geq 2}$ (resp. $S'_m \notin \{N_k^L\}_{k\geq 1}$), i.e. when the KMSW exploration of $M_{0,\infty}$ is not crossing β_0 . We now justify why the definitions in (5.17) and (5.18) are the correct definitions also when $S_m \in \{N_k^R\}_{k\geq 2}$ and $S'_m \in \{N_k^L\}_{k\geq 1}$. We first look at the case $S'_m \in \{N_k^L\}_{k\geq 1}$.

By Assertion (ii) of Lemma 5.12, at each of the times N_k^L for $k \geq 1$, the KMSW procedure for $M_{0,\infty}$ creates a triangular face T contained in $\widehat{M}'_{0,\infty}$ whose boundary consists of the edge $\lambda_{N_k^R-1}$, the (new active) edge $\lambda_{N_k^L}$, and the (previously active) edge $e = \lambda_{N_k^L-1}$ along the path β_0 ; see the triangle to the west of β_0 in the light-blue region in Figure 14. Now, since the edges along β_0 are missing edges in $\widehat{M}'_{0,\infty}$, the KMSW procedure for $\widehat{M}'_{0,\infty}$ never activates the missing edge e. On the other hand, the KMSW procedure for $\widehat{M}'_{0,\infty}$ adds the triangular face T by adding it directly to

the edge $\lambda_{N_k^R-1}$ and creating the new (non-missing) edge $\lambda_{N_k^L}$ and the new (missing) edge e. This corresponds to a (0,1) step for the KMSW encoding walk of $\widehat{M}'_{0,\infty}$ (instead of a (-1,0) step for the KMSW encoding walk of $M_{0,\infty}$).

We finally explain why, for the walk $\widehat{\mathcal{Z}}$ in (5.17), we do not have to make a modification similar to the one we had to make for $\widehat{\mathcal{Z}}'$ in (5.18). By Assertion (i) of Lemma 5.12, at each of the times N_k^R for $k \geq 2$, the KMSW procedure for $M_{0,\infty}$ adds at time N_k^R a new single non-missing edge (rather than a triangular face) to M_{0,N_k^R-1} . This edge is $\lambda_{N_k^R}$; see the pink edge on the lower boundary of the light-blue region in Figure 14. Now, noting that the KMSW procedure for $\widehat{M}_{0,\infty}$ must add the edge $\lambda_{N_k^R}$ using the same procedure, i.e. adding a new single non-missing edge (rather than a triangular face), we get that the step (1,-1) taken by the $\mathcal Z$ walk is the correct step also for the $\widehat{\mathcal Z}$ walk. This completes the proof of the lemma.

The walks $\widehat{\mathcal{Z}}$ and $\widehat{\mathcal{Z}}'$ can equivalently be described in terms of the times N_k^R, N_k^L for $k \geq 1$ defined in Lemma 5.12. Indeed, by definition of N_k^R and N_k^L , the collections of times n such that $\lambda_n \in \widehat{M}_{0,\infty}$ and $\lambda_n \in \widehat{M}'_{0,\infty}$ are respectively

$$\bigcup_{k=1}^{\infty} [N_k^R, N_k^L - 1] \cap \mathbb{Z} \quad \text{and} \quad \bigcup_{k=1}^{\infty} [N_k^L, N_{k+1}^R - 1] \cap \mathbb{Z}.$$
 (5.19)

By (5.17) and (5.19), $\widehat{\mathcal{Z}}$ can be obtained by concatenating the random walk paths

$$\mathcal{Z}|_{[0,N_1^L-1]}$$
 and $\left(\mathcal{Z}(\cdot+N_k^R-1)-\mathcal{Z}(N_k^R-1)\right)|_{[0,N_k^L-N_k^R]}$, for $k \ge 2$. (5.20)

That is, to get $\widehat{\mathcal{Z}}(m)$ we sum the first m increments of these paths in order. Similarly, by (5.18) and (5.19), $\widehat{\mathcal{Z}}'$ can be obtained by concatenating the random walk paths

$$\left(\mathcal{Z}(\cdot + N_k^L - 1) - \mathcal{Z}(N_k^L - 1) + (1, 1) \, \mathbb{1}_{[1, \infty)}(\cdot) \right) |_{[0, N_{k+1}^R - N_k^L]} \quad \text{for } k \ge 1.$$
 (5.21)

Here, adding $(1,1) \mathbbm{1}_{[1,\infty)}(\cdot)$ is equivalent to replacing the first walk step $\mathbb{Z}(N_k^L) - \mathbb{Z}(N_k^L - 1) \stackrel{(5.13)}{=} (-1,0)$ of each walk path by (0,1); which accounts for the special rule at the times N_k^L in (5.18). The following lemma is the key input in the proof of Proposition 5.1.

Lemma 5.14. The walks $\widehat{\mathcal{Z}}$ and $\widehat{\mathcal{Z}}'$ of (5.17) and (5.18) are independent. The walk $\widehat{\mathcal{Z}}$ has the same law as the walk obtained by conditioning \mathcal{Z} so that its first coordinate stays non-negative (defined as in (4.1)). As for the walk $\widehat{\mathcal{Z}}'$, we have $\widehat{\mathcal{Z}}'(0) = (0,0)$, $\widehat{\mathcal{Z}}'(1) = (1,0)$, and $(\widehat{\mathcal{Z}}'(\cdot+1) - \widehat{\mathcal{Z}}'(1))|_{[0,\infty)}$ has the same law as the walk obtained by conditioning \mathcal{Z} so that its second coordinate stays non-negative (defined as in (4.1) with \mathcal{R} in place of \mathcal{L}).

For the proof of Lemma 5.14, we need the following random walk analog of Pitman's theorem for Brownian motion.

Lemma 5.15. Let \mathcal{L} be a random walk with i.i.d. increments which are uniform on $\{-1,0,1\}$. For $n \in \mathbb{N}$, define

$$\widehat{\mathcal{L}}(n) := \mathcal{L}(n) - 2 \min_{j \in [0, n] \cap \mathbb{Z}} \mathcal{L}(j).$$
(5.22)

In words, to obtain $\widehat{\mathcal{L}}$, every time \mathcal{L} attains a running minimum (at which time it has a -1 step), we flip the -1 step to a +1 step. Then $\widehat{\mathcal{L}}$ is a random walk started from 0 and conditioned to stay non-negative in the sense of [BD94] (see (4.1)).

Proof. Let \mathcal{W}_n be the set of n-step paths $\mathfrak{L}:[0,n]\cap\mathbb{Z}\to\mathbb{Z}$ such that $\mathfrak{L}(0)=0$ and $\mathfrak{L}(j)-\mathfrak{L}(j-1)\in\{-1,0,1\}$ for each $j\in\{1,\ldots,n\}$. Let $\widehat{\mathcal{W}}_n$ be the set of $\mathfrak{L}\in\mathcal{W}_n$ such that $\mathfrak{L}(j)\geq 0$ for each $j\in\{0,\ldots,n\}$. We define a function $\Phi_n:\mathcal{W}_n\to\widehat{\mathcal{W}}_n$ by

$$\Phi_n \mathfrak{L}(j) := \mathfrak{L}(j) - 2 \min_{i \in [0,j] \cap \mathbb{Z}} \mathfrak{L}(i).$$

In words, to obtain $\Phi_n \mathcal{L}$, every time \mathcal{L} attains a running minimum (at which time it has a -1 step), we flip the -1 step to a +1 step.

For $\widehat{\mathfrak{L}} \in \widehat{\mathcal{W}}_n$ and $k \in \{0, \dots, \widehat{\mathfrak{L}}(n)\}$, we also define $\Psi_{n,k}\widehat{\mathfrak{L}} \in \mathcal{W}_n$ by

$$\Psi_{n,k}\widehat{\mathfrak{L}}(j) := \widehat{\mathfrak{L}}(j) - 2\min\bigg\{k, \min_{i \in [j,n] \cap \mathbb{Z}} \widehat{\mathfrak{L}}(i)\bigg\}.$$

In words, to obtain $\Psi_{n,k}\widehat{\mathfrak{L}}$, for $r \in \{0,\ldots,k-1\}$, we look at the last time that $\widehat{\mathfrak{L}}$ hits r before time n, at which time it has a +1 step. We flip each of these +1 steps to a -1 step.

From the step-flipping descriptions of Φ_n and $\Psi_{n,k}$, for any $\widehat{\mathfrak{L}} \in \widehat{\mathcal{W}}_n$ and $k \in \{0, \dots, \widehat{\mathfrak{L}}(k)\}$, we have $\Phi_n \Psi_{n,k} \widehat{\mathfrak{L}} = \widehat{\mathfrak{L}}$. Furthermore, if $\mathcal{L} \in \mathcal{W}_n$ and $k = \min_{j \in [0,n] \cap \mathbb{Z}} \mathcal{L}(j)$, then $\Psi_{n,k} \Phi_n \mathfrak{L} = \mathfrak{L}$. These two facts imply that if $\widehat{\mathfrak{L}} \in \widehat{\mathcal{W}}_n$, then

$$\Phi_n^{-1}\widehat{\mathfrak{L}} = \{\Psi_{n,k}\widehat{\mathfrak{L}} : k \in \{0,\dots,\widehat{\mathfrak{L}}(n)\}\}.$$

Consequently, $\#\Phi_n^{-1}\widehat{\mathfrak{L}} = \widehat{\mathfrak{L}}(n) + 1$.

For each $n \in \mathbb{N}$, the walk $\mathcal{L}|_{[0,n]}$ is a uniform sample from \mathcal{W}_n . We have $\widehat{\mathcal{L}}|_{[0,n]} = \Phi_n(\mathcal{L}|_{[0,n]})$, so the previous paragraph implies that $\widehat{\mathcal{L}}|_{[0,n]}$ is sampled from the uniform measure on $\widehat{\mathcal{W}}_n$ weighted by $\widehat{\mathfrak{L}}(n) + 1$. By the definition (4.1), this means that $\widehat{\mathcal{L}}$ is the walk obtained by conditioning \mathcal{L} to stay non-negative.

Proof of Lemma 5.14. By Lemma 5.12 and the strong Markov property, the sequences of random walk paths

$$\left\{ \left(\mathcal{Z}(\cdot + N_k^L) - \mathcal{Z}(N_k^L) \right) |_{[0, N_{k+1}^R - N_k^L]} \right\}_{k \ge 1} \quad \text{and} \quad \left\{ \left(\mathcal{Z}(\cdot + N_k^R) - \mathcal{Z}(N_k^R) \right) |_{[0, N_k^L - N_k^R]} \right\}_{k \ge 1} \quad (5.23)$$

are independent. By definition of N_k^L and N_k^R in Lemma 5.12, the first (resp. second) sequence in (5.23) has the law of a collection of i.i.d. samples from the law of \mathcal{Z} stopped at the first time that \mathcal{R} (resp. \mathcal{L}) hits -1. Consequently, concatenating the elements of the first (resp. second) sequence in (5.23) in order gives a walk $\mathring{\mathcal{Z}}' = (\mathring{\mathcal{L}}', \mathring{\mathcal{R}}')$ (resp. $\mathring{\mathcal{Z}} = (\mathring{\mathcal{L}}, \mathring{\mathcal{R}})$) with the same law as $\mathcal{Z}|_{[0,\infty)}$. Furthermore, the walks $\mathring{\mathcal{Z}}$ and $\mathring{\mathcal{Z}}'$ are independent.

The kth path $\left(\mathcal{Z}(\cdot+N_k^L)-\mathcal{Z}(N_k^L)\right)|_{[0,N_{k+1}^R-N_k^L]}$ from the first sequence in (5.23) coincides with the segment of $\mathring{\mathcal{Z}}'$ between the first time that $\mathring{\mathcal{R}}$ hits -(k-1) and the first time that $\mathring{\mathcal{R}}$ hits -k. Similarly, the kth path $\left(\mathcal{Z}(\cdot+N_k^R)-\mathcal{Z}(N_k^R)\right)|_{[0,N_k^L-N_k^R]}$ from the second sequence in (5.23) coincides with the segment of $\mathring{\mathcal{Z}}$ between the first time that $\mathring{\mathcal{L}}$ hits -(k-1) and the first time that $\mathring{\mathcal{L}}$ hits -k.

From (5.12) and (5.13) in Lemma 5.12, we have that the last step of the two paths

$$\left(\mathcal{Z}(\cdot+N_k^L)-\mathcal{Z}(N_k^L)\right)|_{[0,N_{k+1}^R-N_k^L]} \quad \text{and} \quad \left(\mathcal{Z}(\cdot+N_k^R)-\mathcal{Z}(N_k^R)\right)|_{[0,N_k^L-N_k^R]}$$

are respectively

$$\mathcal{Z}(N_{k+1}^R) - \mathcal{Z}(N_{k+1}^R - 1) = (1, -1)$$
 and $\mathcal{Z}(N_k^L) - \mathcal{Z}(N_k^L - 1) = (-1, 0)$.

Hence, recalling (5.21), \hat{Z}' can be obtained from \mathring{Z}' in the following manner. We set \hat{Z}' to be the walk starting at (0,0), taking a first (1,0) step (this is because the first walk path in (5.21) has an additional starting (1,0) step compared to the first walk path in the first sequence in (5.23)), and then exactly following the steps of the following modified version of \mathring{Z}' . For each of the times at which $\mathring{\mathcal{R}}'$ attains a running minimum, replace the corresponding step $\mathcal{Z}(N_{k+1}^R) - \mathcal{Z}(N_{k+1}^R) -$

Similarly, recalling (5.20), we find that $\widehat{\mathcal{Z}}$ can be obtained from $\mathring{\mathcal{Z}}$ in the following manner. For each of the times at which $\mathring{\mathcal{L}}$ attains a running minimum, replace the corresponding step $\mathcal{Z}(N_k^L) - \mathcal{Z}(N_k^L - 1) = (-1,0)$, which is the last step of the kth excursion in the second sequence in (5.23), by the step $\mathcal{Z}(N_{k+1}^R) - \mathcal{Z}(N_{k+1}^R - 1) = (1,-1)$, which is the first step of the k+1th excursion in (5.20). Note that in this case we do not need to do any special modification for the first step of the walk since the first step of the first walk path in (5.20) is $\mathcal{Z}(1) - \mathcal{Z}(0)$ and the first step of the first walk path in the second sequence in (5.23) is $\mathcal{Z}(N_1^R + 1) - \mathcal{Z}(N_1^R) = \mathcal{Z}(1) - \mathcal{Z}(0)$ since $N_1^R = 0$ by Lemma 5.12.

Since $\hat{\mathcal{Z}}$ and $\hat{\mathcal{Z}}'$ are independent and $\hat{\mathcal{Z}}$ and $\hat{\mathcal{Z}}'$ are functions of $\mathring{\mathcal{Z}}$ and $\mathring{\mathcal{Z}}'$, respectively, $\hat{\mathcal{Z}}$ and $\hat{\mathcal{Z}}'$ are independent.

The marginal law of $\mathring{\mathcal{R}}'$ is that of a random walk with i.i.d. increments each sampled uniformly from $\{-1,0,1\}$. Therefore, the previous paragraph together with Lemma 5.15 implies that $\widehat{\mathcal{R}}'$ has the same law as \mathcal{R}' conditioned to stay non-negative and taking a first 0 step (this is because of the first (1,0) step of $\widehat{\mathcal{Z}}'$). Since the steps of $\widehat{\mathcal{R}}'$ determine the steps of $\widehat{\mathcal{L}}'$, this implies that $\widehat{\mathcal{Z}}'$ has the desired law. \square

Proof of Proposition 5.1. Thanks to Lemma 5.13, the maps $\widehat{M}_{0,\infty}$ and $\widehat{M}'_{0,\infty}$ can be built using the KMSW procedure on the walks $\widehat{\mathcal{Z}}$ and $\widehat{\mathcal{Z}}'$ of Lemma 5.14, respectively. Hence, Lemma 5.14 implies that $\widehat{M}_{0,\infty}$ and $\widehat{M}'_{0,\infty}$ are independent. Furthermore, by Definition 4.1 and the description of the law of $\widehat{\mathcal{Z}}$ from Lemma 5.14, we get that $\widehat{M}_{0,\infty}$ has the law of the UIQBOT.

5.6 Proof of Proposition 5.9: Symmetry for the UIBHBOT

Recall the set of boundary-channeled bipolar-oriented triangulations $\mathcal{M}_{l,r}^{b}$ with l left boundary edges and r right boundary edges from Definition 3.17. For $n \in \mathbb{N}$, let $\mathcal{M}_{l,r}^{b}(n)$ be the set of maps in $\mathcal{M}_{l,r}^{b}$ having n non-boundary edges. To prove Proposition 5.9, we will first show that the UIBHBOT arises as the local limit of uniformly sampled elements of $\mathcal{M}_{l,1}^{b}(n)$. Proposition 5.9 will then be an easy consequence of the left/right symmetry property of $\mathcal{M}_{l,r}^{b}$ (Lemma 3.18).

The following proposition justifies the terminology in Definition 5.8.

Proposition 5.16. Let $\{l_n\}_{n\in\mathbb{N}}$ be a sequence of positive integers. Assume there exists A>1 such that $l_n\in[A^{-1}n^{1/2},An^{1/2}]$ for each $n\in\mathbb{N}$. For $n\in\mathbb{N}$, let M_n^b be the map obtained by starting with a uniform sample from $\mathcal{M}_{l_n+1,1}^b(n-1)$ (as defined just above), then declaring all of its left boundary edges, except for the left boundary edge whose terminal vertex is the sink vertex, to be missing. Conditional on M_n^b , let e_n^b be a uniform sample from the l_n missing edges on the (lower-left) boundary of M_n^b . Then (M_n^b, e_n^b) converges in law to the UIBHBOT of Definition 5.8 with respect to the (directed) Benjamini-Schramm topology (Definition 5.8).

We will prove Proposition 5.16 via a standard argument based on Cramér's large deviation theorem [DZ10, Theorem 2.1.24]; see, e.g., [DS11, Section 4.2] for a similar argument.

Let $\mathcal{Z}_n^{\rm b} = (\mathcal{L}_n^{\rm b}, \mathcal{R}_n^{\rm b})$ be the walk which encodes $M_n^{\rm b}$ via the KMSW bijection as in Lemma 3.19. By Lemma 3.19, the walk $\mathcal{Z}_n^{\rm b}$ is a uniform sample from the set of walks with increments in the set

 $\{(1,-1),(-1,0),(0,1)\}$ which start at $(l_n,0)$, stay in $[0,\infty)^2$ until time n, and end up at (0,0) at time n. Let $K_n \in [1,l_n] \cap \mathbb{Z}$ be chosen so that e_n^b is the K_n th missing edge in order on the lower-left boundary of M_n^b (starting from the missing edge next to the unique lower-right boundary edge). Since e_n^b is chosen uniformly from the missing boundary edges of M_n^b , the integer K_n is a uniform sample from $[1,l_n] \cap \mathbb{Z}$, independent from \mathcal{Z}_n^b . Let T_n be the stopping time

$$T_n := \min \{ j \in [1, n] \cap \mathbb{Z} : \mathcal{L}_n^{\mathrm{b}}(j) - \mathcal{L}_n^{\mathrm{b}}(0) = -K_n \}.$$
 (5.24)

By Assertion (i) of Lemma 3.6, T_n is the same as the time at which the KMSW exploration associated with $\mathcal{Z}_n^{\mathrm{b}}$ explores the triangle of M_n^{b} with e_n^{b} on its boundary.

The main technical step in the proof of Proposition 5.16 is to show that the probability of the event that we condition on to get the law of \mathcal{Z}_n^b decays slower than exponentially in l_n . We will in fact prove a power-law lower bound.

Lemma 5.17. Recall from Section 4 that $\mathbb{P}_{(l,0)}$ denotes the law of a walk \mathcal{Z} with i.i.d. increments sampled uniformly from $\{(1,-1),(-1,0),(0,1)\}$, started from (l,0). For $n \in \mathbb{N}$, let

$$E_n := \left\{ \mathcal{Z}[0, n] \subset [0, \infty)^2, \ \mathcal{Z}(n) = (0, 0) \right\}. \tag{5.25}$$

For each A > 1, there exist c > 0 such that

$$\mathbb{P}_{(l_n,0)}[E_n] \ge cn^{-3}, \quad \forall n \in \mathbb{N}, \quad \forall l_n \in [A^{-1}n^{1/2}, An^{1/2}] \cap \mathbb{Z}.$$
 (5.26)

Proof. This is a fairly straightforward consequence of the results of [DW15a, DW15b], but these results do not exactly apply in our setting so we will explain how to extract (5.26) from the results of [DW15a, DW15b]. Whenever we apply results from [DW15a, DW15b], we need to apply an affine transformation which maps \mathcal{Z} to an uncorrelated random walk, see [DW15a, Example 2]. In our setting, the correlation of the coordinates of \mathcal{Z} is -1/2, so the parameter p from [DW15a, DW15b] is 3.

It suffices to prove the lemma only for $n \geq 100$. Let $n_1, n_2, n_3 \in \mathbb{N}$ be chosen so that

$$n_1 + n_2 + n_3 = n, \quad n_1, n_2, n_3 \ge n/4, \quad n_2 \in 3\mathbb{Z}.$$
 (5.27)

The reason for requiring that $n_2 \in 3\mathbb{Z}$ is that \mathcal{Z} is periodic of period 3.

We will lower-bound the probabilities of three events, depending on the restrictions of \mathcal{Z} to intervals of length n_1, n_2, n_3 , whose intersection is contained in E_n . To this end, we define

$$\mathcal{Z}^{1}(j) := \mathcal{Z}(j), \quad j \in [0, n_{1}] \cap \mathbb{Z}$$
$$\mathcal{Z}^{2}(j) := \mathcal{Z}(j + n_{1}) - \mathcal{Z}(n_{1}), \quad j \in [0, n_{2}] \cap \mathbb{Z}$$
$$\mathcal{Z}^{3}(j) := \mathcal{Z}(n - j) - \mathcal{Z}(n), \quad j \in [0, n_{3}] \cap \mathbb{Z}$$

Then $\mathcal{Z}^1, \mathcal{Z}^2$, and \mathcal{Z}^3 are independent, and the laws of \mathcal{Z}^2 and \mathcal{Z}^3 do not depend on the starting point for \mathcal{Z} .

Define the events

$$\begin{split} E_n^1 &:= \left\{ \mathcal{Z}^1(j) \in [0,\infty)^2, \ \forall j \in [0,n_1] \cap \mathbb{Z} \right\} \cap \left\{ \mathcal{Z}^1(n_1) \in [n^{1/2},2n^{1/2}]^2 \right\} \\ E_n^2 &:= \left\{ \mathcal{Z}^2(j) + \mathcal{Z}^1(n_1) \in [0,\infty)^2, \ \forall j \in [0,n_2] \cap \mathbb{Z} \right\} \cap \left\{ \mathcal{Z}^2(n_2) = \mathcal{Z}^3(n_3) - \mathcal{Z}^1(n_1) \right\} \\ E_n^3 &:= \left\{ \mathcal{Z}^3(j) \in [0,\infty)^2, \ \forall j \in [0,n_3] \cap \mathbb{Z} \right\} \cap \left\{ \mathcal{Z}^3(n_3) \in [3n^{1/2},4n^{1/2}]^2 \right\}. \end{split}$$

Then $E_n^1 \cap E_n^2 \cap E_n^3 \subset E_n$. We also note that E_n^1 and E_n^3 are determined by \mathcal{Z}^1 and \mathcal{Z}^3 , respectively, so these events are independent.

We first consider the event E_n^1 . By a standard estimate for one-dimensional random walk, there exists $c_1 > 0$ such that for all $l, n \in \mathbb{N}$,

$$\mathbb{P}_{(0,0)}[F_n^1] \ge c_1 n^{-1/2}, \text{ where } F_n^1 := \{ \mathcal{R}(j) \ge 0, \, \forall j \in [0, n_1] \cap \mathbb{Z} \}.$$
 (5.28)

By [DW15b, Theorem 1], applied with the cone equal to the upper half-plane, under $\mathbb{P}_{(0,0)}[\cdot \mid F_n^1]$, the re-scaled walk $n_1^{-1/2} \mathbb{Z}(\lfloor n_1 \cdot \rfloor)|_{[0,1]}$ converges as $n_1 \to \infty$ to a correlated two-dimensional Brownian motion (with correlation -1/2) started at (0,0) and conditioned to stay in the upper half-plane for one unit of time. For any $l_n \in [A^{-1}n^{1/2},An^{1/2}]$ and each small enough $\varepsilon > 0$ (depending on A), such a conditioned Brownian motion has a positive chance (uniformly over the choice of l_n) to stay in $[-n_1^{-1/2}l_n + \varepsilon, \infty) \times [0, \infty)$ until time 1 and end up in $(-n_1^{-1/2}l_n, 0) + [2(1+\varepsilon), \sqrt{2}(2-\varepsilon)]^2$ at time 1. By shifting by $(l_n, 0)$, noting that $n^{1/2}/2 \le n_1^{1/2} \le n^{1/2}/\sqrt{2}$ by (5.27), and applying the preceding sentence together with (5.28), we find that there exists $c_2 > 0$ such that for any $n \in \mathbb{N}$ and $l_n \in [A^{-1}n^{1/2}, An^{1/2}] \cap \mathbb{Z}$,

$$\mathbb{P}_{(l_n,0)} \left[E_n^1 \right] \ge c_2 n^{-1/2}. \tag{5.29}$$

Next we consider E_n^3 . By [DW15a, Theorem 1], applied to the time reversal of \mathcal{Z} , there exists $c_3 > 0$ such that for any $n \in \mathbb{N}$,

$$\mathbb{P}\left[\mathcal{Z}^{3}(j) \in [0, \infty)^{2}, \, \forall j \in [0, n_{3}] \cap \mathbb{Z}\right] \ge c_{3} n^{-3/2}. \tag{5.30}$$

By [DW15b, Theorem 1], applied as in the argument just above (5.29), this implies that we can find $c_4 > 0$ such that for any $n \in \mathbb{N}$ and $l_n \in [A^{-1}n^{1/2}, An^{1/2}] \cap \mathbb{Z}$,

$$\mathbb{P}_{(l_n,0)}\left[E_n^3\right] \ge c_4 n^{-3/2}.\tag{5.31}$$

To deal with E_n^2 , we first observe that on $E_n^1 \cap E_n^3$,

$$\mathcal{Z}^3(n_3) - \mathcal{Z}^1(n_1) \in [n^{1/2}, 3n^{1/2}]^2.$$

Recall that \mathbb{Z}^2 is independent from $(\mathbb{Z}^1, \mathbb{Z}^2)$. The walk \mathbb{Z} is periodic of period 3, but the walk $\mathbb{Z}^3(3\cdot)$ is strongly aperiodic since $\mathbb{P}_{(0,0)}[\mathbb{Z}(3)=0]>0$ [Spi76, Section 5, P1]. Since n_2 was chosen to be a multiple of 3, we can apply a standard local limit result for unconditioned random walk (see, e.g., [Spi76, Section 7, P9]) to get that there exists $c_5>0$ such that on $E_n^1\cap E_n^3$,

$$\mathbb{P}_{(l_n,0)} \left[\mathcal{Z}^2(n_2) = \mathcal{Z}^3(n_3) - \mathcal{Z}^1(n_1) \, \middle| \, \mathcal{Z}^1, \mathcal{Z}^2 \right] \ge c_5 n^{-1}. \tag{5.32}$$

We now use the convergence of random walk conditioned on its endpoints to two-dimensional Brownian bridge (see, e.g., [Lig70, Theorem 3]), together with the fact that for any S > 1 and $z, w \in [1/S, S]^2$, a (correlated) Brownian bridge from z to w has a uniformly positive chance to stay in $[0, \infty)^2$. We infer from (5.32) that there exists $c_6 > 0$ such that on $E_n^1 \cap E_n^3$,

$$\mathbb{P}_{(l_n,0)} \left[E_n^2 \mid \mathcal{Z}^1, \mathcal{Z}^2 \right] \ge c_6 n^{-1}. \tag{5.33}$$

Combining (5.29), (5.31), and (5.33) and recalling that E_n^1 and E_n^3 are independent concludes the proof.

Recall the discussion above (5.24).

Lemma 5.18. For $n \in \mathbb{N}$, let E_n be as in (5.25). Let $\{l_n\}_{n \in \mathbb{N}}$ be a sequence of positive integers. Assume there exists A > 1 such that $l_n \in [A^{-1}n^{1/2}, An^{1/2}]$ for each $n \in \mathbb{N}$. Let $\mathcal{Z}_n^b = (\mathcal{L}_n^b, \mathcal{R}_n^b)$ be a walk from $(l_n, 0)$ to (0, 0) in $[0, \infty)^2$ sampled from the $\mathbb{P}_{(l_n, 0)}$ -conditional law of \mathcal{Z} given E_n . Also let K_n be sampled uniformly from $[1, l_n] \cap \mathbb{Z}$, independently from \mathcal{Z}_n^b and let T_n be as in (5.24). For each fixed $N \in \mathbb{N}$, the law of

 $\left(\mathcal{Z}_n^{\mathrm{b}}(\cdot + T_n) - \mathcal{Z}_n^{\mathrm{b}}(T_n)\right)|_{[-N,N]} \tag{5.34}$

converges in the total variation sense as $n \to \infty$ to the law of $\mathcal{Z}^b|_{[-N,N]}$, where \mathcal{Z}^b is the encoding walk for the UIBHBOT, as defined at the beginning of Section 5.4.

Proof. Fix $m \in \mathbb{N}$. We will send $n \to \infty$ then send $m \to \infty$. We first study the unconditional law of \mathcal{Z} sampled from $\mathbb{P}_{(l_n,0)}$. Let $\sigma_0 = 0$ and for $k \in \mathbb{N}$, let

$$\sigma_k := \min\{j \in \mathbb{N} : \mathcal{L}(j) - \mathcal{L}(0) = -k\}. \tag{5.35}$$

Note that T_n in (5.24) is equal to σ_{K_n} (with \mathcal{L} replaced by $\mathcal{L}_n^{\mathrm{b}}$). Furthermore, for $s \in \mathbb{N}$, the stopped walk paths

$$Z_s := \left(\mathcal{Z}(\cdot + \sigma_{(s-1)m}) - \mathcal{Z}(\sigma_{(s-1)m}) \right) |_{[0,(\sigma_{sm} - \sigma_{(s-1)m}) \land m^{100}]}$$
(5.36)

are i.i.d. paths. The reason why we stop after m^{100} steps is to ensure that Z_s takes values in a finite set (namely, the set of paths in \mathbb{Z}^2 started from (0,0) with increments in $\{(1,-1),(0,1),(-1,0)\}$ which go for at most m^{100} steps). We also note that the definition of the stopping times σ_k in (5.35) and the increments in (5.36) does not depend on the starting point for \mathbb{Z} .

By Cramér's larger deviation theorem [DZ10, Theorem 2.1.24], the empirical distribution for $Z_1, \ldots, Z_{\lfloor l_n/m \rfloor}$ is exponentially concentrated around the actual distribution of Z_1 as $n \to \infty$. That is, for any possible realization \mathfrak{z} of Z_1 , let $p_{l_n}(\mathfrak{z})$ be the fraction of values of $s \in [1, l_n/m] \cap \mathbb{Z}$ for which $Z_s = \mathfrak{z}$. Then for each $\delta > 0$, there exists $c = c(m, \delta) > 0$ such that 15

$$\mathbb{P}_{(l_n,0)}\left[\sup_{\mathfrak{z}}\left|p_{l_n}(\mathfrak{z}) - \mathbb{P}_{(l_n,0)}[Z_1 = \mathfrak{z}]\right| > \delta\right] = O(e^{-c\,l_n}), \quad \text{as } n \to \infty, \tag{5.37}$$

where the supremum is over all possible realizations \mathfrak{z} of Z_1 .

By Lemma 5.17, $\mathbb{P}_{(l_n,0)}[E_n]$ decays like a negative power of n. In particular, since l_n is comparable to $n^{1/2}$, this probability decays slower than exponentially in l_n . Hence (5.38) implies that

$$\mathbb{P}_{(l_n,0)}\left[\sup_{\mathfrak{z}}\left|p_{l_n}(\mathfrak{z}) - \mathbb{P}_{(l_n,0)}[Z_1 = \mathfrak{z}]\right| > \delta \left|E_n\right| = O(e^{-c'l_n}), \quad \text{as } n \to \infty,$$
 (5.38)

for a slightly smaller constant $c' = c'(\delta, m) > 0$.

Let K_n be as in the lemma statement and let $S_n \in [1, l_n/m] \cap \mathbb{Z}$ be chosen so that $K_n \in [(S_n-1)m, S_nm] \cap \mathbb{Z}$ (we take S_n to be a graveyard point in the probability space if $K_n \in [m \lfloor l_n/m \rfloor + 1, l_n]$). By (5.38), the total variation distance between the conditional law of Z_{S_n} given E_n and the unconditional law of Z_1 goes to zero as $n \to \infty$ (it would in fact decay exponentially, it not for the possibility that $K_n \in [m \lfloor l_n/m \rfloor + 1, l_n]$).

¹⁵The law of Z_s in (5.36) does not depend on s, so (5.37) is equivalent to the analogous statement with $\mathbb{P}_{(r,0)}$ in place of $\mathbb{P}_{(l_n,0)}$ for any $r \in \mathbb{Z}$.

It remains to transfer from a statement about the law of Z_{S_n} to a statement about the law of (5.34). To this end, let $\varepsilon \in (0,1)$ and $N \in \mathbb{N}$. Since σ_{sm} is the hitting time of -sm for the lazy random walk $\mathcal{L}-\mathcal{L}(0)$, if we choose m large enough (depending on ε) then for every $s \in [1, l_n/m] \cap \mathbb{Z}$, the unconditional $\mathbb{P}_{(l_n,0)}$ -probability that $\sigma_{sm} - \sigma_{(s-1)m}$ is larger than m^{100} is at most $\varepsilon/2$. By the previous paragraph, if m is chosen to be large enough (depending on ε) and n is large enough (depending on m and ε), then

$$\mathbb{P}_{(l_n,0)}\left[\sigma_{S_n m} - \sigma_{(S_n-1)m} \le m^{100} \,\middle|\, E_n\right] \ge 1 - \varepsilon. \tag{5.39}$$

Furthermore, if m is large enough (depending on ε and N) and n is large enough (depending on N, m, and ε), then the conditional probability given E_n that $[K_n - N, K_n + N] \subset [(S_n - 1)m, S_n m]$ is at least $1 - \varepsilon$. By this and (5.39), we can choose $m = m(\varepsilon, N) \in \mathbb{N}$ large enough so that when n is sufficiently large (recall that T_n in (5.24) is equal to σ_{K_n}),

$$\mathbb{P}_{(l_n,0)} \Big[[T_n - N, T_n + N] \subset \Big[\sigma_{(S_n - 1)m}, \sigma_{(S_n - 1)m} + (\sigma_{S_n m} - \sigma_{(S_n - 1)m}) \wedge m^{100} \Big] \, \Big| \, E_n \Big] \ge 1 - 2\varepsilon.$$

In other words, under the conditional law given E_n , it holds with probability at least $1-2\varepsilon$ that the walk path (5.34) (defined with \mathcal{Z} in place of $\mathcal{Z}_n^{\rm b}$) is determined by Z_{S_n} and $K_n-(S_n-1)m$. By combining this with the previous paragraph and recalling that $\mathcal{Z}_n^{\rm b}$ is sampled from the conditional law of \mathcal{Z} given E_n , we get the following. When n and m are sufficiently large, the total variation distance between the laws of the following two processes is at most 2ε : the process (5.34) and the law of $(\mathcal{Z}(\cdot + \sigma_M) - \mathcal{Z}(\sigma_M))|_{[-N,N]}$, where M is sampled uniformly from $[0,m] \cap \mathbb{Z}$ (recall the definition of Z_1 from (5.36). By the construction of $\mathcal{Z}^{\rm b}$ at the beginning of Section 5.4, this concludes the proof.

Proof of Proposition 5.16. This is an easy consequence of Lemma 5.18, but we spell out the details for completeness. Recall the discussion above (5.24). Let (M^b, e^b) be the UIBHBOT and let \mathcal{Z}^b be its KMSW encoding walk, as in the discussion just above Definition 5.8. For $a, b \in \mathbb{Z}$ with a < b, let $M^b_{a,b}$ be the submap of M^b obtained by applying the KMSW procedure to $(\mathcal{Z}^b(\cdot + a) - \mathcal{Z}^b(a))|_{[a,b]}$. For $r \in \mathbb{N}$, define the **graph distance ball** $\mathcal{B}_r(M^b)$ to be the submap of M^b consisting of the vertices of M^b which lie at graph distance at most r from the initial vertex of e^b , along with the edges of M^b whose vertices both satisfy this condition, and the faces of M^b whose boundary vertices all satisfy this condition. For any $\varepsilon > 0$ and $r \in \mathbb{N}$, we can choose $N = N(r, \varepsilon) \in \mathbb{N}$ sufficiently large so that

$$\mathbb{P}\left[\mathcal{B}_r(M^{\mathrm{b}}) \subset M_{-N,N}^{\mathrm{b}}\right] \ge 1 - \varepsilon.$$

By the total variation convergence in Lemma 5.18, this implies that for large enough $n \in \mathbb{N}$, it holds with probability at least $1 - 2\varepsilon$ that the graph distance ball $\mathcal{B}_r(M_n^b)$ of radius r in M_n^b centered at the initial vertex of e_n^b is completely explored by the KMSW procedure for M_n^b during the time interval $[T_n - N, T_n + N] \cap \mathbb{Z}$ (the latter is determined by the walk $\mathcal{Z}_n^b|_{[T_n - N, T_n + N]}$). Note that Lemma 5.18 guarantees that we can choose the same N for all values of n. By applying Lemma 5.18 again, this implies the desired Benjamini-Schramm convergence.

Proof of Proposition 5.9. Assume that we are in the setting of Proposition 5.16. Let $(\widetilde{M}_n^b, \widetilde{e}_n^b)$ be the edge-rooted directed map obtained from (M_n^b, e_n^b) by applying an orientation-reversing homeomorphism from $\mathbb C$ to $\mathbb C$. By the definition of M_n^b (see Proposition 5.16), the map \widetilde{M}_n^b can be obtained by starting with a uniform sample from $\mathcal{M}_{1,l_n+1}^b(n)$ (as defined just above Proposition 5.16), then declaring all of the right boundary edges to be missing except for the one whose terminal vertex

is the sink vertex. Furthermore, $\widetilde{e}_n^{\rm b}$ is a uniformly sampled missing boundary edge of $\widetilde{M}_n^{\rm b}$. By Lemma 3.18 (applied with $(l,r)=(1,l_n+1)$ and $k=l_n$),

$$(M_n^{\mathbf{b}}, e_n^{\mathbf{b}}) \stackrel{d}{=} (\widetilde{M}_n^{\mathbf{b}}, \widetilde{e}_n^{\mathbf{b}}). \tag{5.40}$$

By Proposition 5.16, $(M_n^{\rm b}, e_n^{\rm b}) \to (M^{\rm b}, e^{\rm b})$ in law with respect to the Benjamini-Schramm topology. By applying an orientation-reversing homeomorphism, we get that also $(\widetilde{M}_n^{\rm b}, \widetilde{e}_n^{\rm b}) \to (\widetilde{M}^{\rm b}, \widetilde{e}^{\rm b})$ in law with respect to the Benjamini-Schramm topology, where $(\widetilde{M}^{\rm b}, \widetilde{e}^{\rm b})$ is as in the proposition statement. By (5.40), this shows that $(M^{\rm b}, e^{\rm b}) \stackrel{d}{=} (\widetilde{M}^{\rm b}, \widetilde{e}^{\rm b})$, as required.

6 Recursive equations, tail asymptotics, and scaling exponents

In this section, we prove Theorem 1.8 about the tail asymptotics of the increments of the Busemann function \mathcal{X} when XDP \in {LDP, SDP}. We will prove Items (va) and (vb) of Theorem 1.8 separately in Sections 6.1 and 6.2, respectively.

Recall from Lemma 3.8 that for $n \in \mathbb{Z}$, the infinite rooted bipolar-oriented triangulation with missing edges $(M_{n,\infty}, \lambda_n)$ is the submap of the UIBOT obtained by applying the KMSW procedure to $\mathcal{Z}|_{[n,\infty)}$, where $\mathcal{Z}: \mathbb{Z} \to \mathbb{Z}^2$ is a bi-infinite random walk whose increments are i.i.d. uniform samples from $\{(1,-1),(-1,0),(0,1)\}$, normalized so that $\mathcal{Z}(0)=(0,0)$.

By the stationarity of \mathcal{Z} , we have that

$$M_{1,\infty} \stackrel{d}{=} M_{0,\infty}. \tag{6.1}$$

Therefore, the Busemann function \mathcal{X}^1 associated with $M_{1,\infty}$ has the same law as \mathcal{X} . Also, recall the notation

$$f(x) := \mathbb{P}[\mathcal{X}(0) - \mathcal{X}(-1) = x] \quad \text{and} \quad g(y) := \mathbb{P}[\mathcal{X}(1) - \mathcal{X}(0) = y].$$
 (6.2)

Since the Busemann function \mathcal{X} introduced in Theorem 1.4 is normalized so that $\mathcal{X}(0) = 0$, we equivalently have that $f(x) = \mathbb{P}[-\mathcal{X}(-1) = x]$ and $g(y) = \mathbb{P}[\mathcal{X}(1) = y]$. Our main goal will be to determine the tail behavior of f and g for XDP $\in \{\text{LDP}, \text{SDP}\}$.

Using the fact that $\mathcal{X}^1 \stackrel{d}{=} \mathcal{X}$ and the properties in Theorem 1.7 proved in the previous section, we will obtain a recursive equation for f and g (see Proposition 6.5 for the LDP case and Proposition 6.11 for the SDP case), which will later be converted into a functional equation for the characteristic functions F and G of f and g, respectively. We then reach our goal by first studying the asymptotics of the characteristic functions F and G (see Proposition 6.2 for the LDP case and Proposition 6.8 for the SDP case) and then transferring the estimates to f and g using the following Tauberian type result, whose proof can be found in Appendix A.

Proposition 6.1. Let X be a non-negative integer-valued random variable. Define the characteristic function $\varphi(t) = \mathbb{E}[e^{itX}]$. Consider the following two sets of assumptions:

1. For some $c \in \mathbb{C} \setminus i\mathbb{R}$ and $\nu \in (0,1)$,

$$\varphi(t) = 1 + (c\mathbb{1}_{(t>0)} + \overline{c}\mathbb{1}_{(t<0)})|t|^{\nu} + o(t^{\nu}), \quad as \ t \to 0.$$
(6.3)

2. For some $c_1 > 0$, $c_2 \in \mathbb{C} \setminus \mathbb{R}$, and $\nu \in (0,1)$,

$$\varphi(t) = 1 + ic_1t + (c_2\mathbb{1}_{(t>0)} + \overline{c}_2\mathbb{1}_{(t<0)})|t|^{1+\nu} + o(t^{1+\nu}), \quad as \ t \to 0.$$
 (6.4)

Then:

1. In the case of Assumption 1, $\operatorname{Re}(c) < 0$ and $\operatorname{Im}(c) > 0$, and setting $a = -\frac{\operatorname{Re}(c)}{\Gamma(1-\nu)} \sec\left(\frac{\pi\nu}{2}\right) > 0$,

$$\mathbb{P}[X > R] = aR^{-\nu} + o(R^{-\nu}), \quad as \ R \to \infty. \tag{6.5}$$

2. In the case of Assumption 2, $\operatorname{Im}(c_2) < 0$ and setting $a = -\frac{\nu \operatorname{Im}(c_2)}{\Gamma(1-\nu)} \sec\left(\frac{\pi\nu}{2}\right) > 0$,

$$\mathbb{P}[X > R] = aR^{-\nu - 1} + o(R^{-\nu - 1}), \quad as \ R \to \infty.$$
 (6.6)

6.1 The LDP case

We start by looking at the case when XDP = LDP. Thanks to Items (iii) and (iv) of Theorem 1.7, we know that f is a symmetric distribution on \mathbb{Z} , and g is a distribution on $\mathbb{Z}_{\leq -1}$. We introduce the three characteristic functions

$$F(t) := \sum_{x \in \mathbb{Z}} f(x) e^{itx}, \qquad F^{-}(t) := \sum_{x \in \mathbb{Z}_{<-1}} f(x) e^{itx}, \qquad G(s) := \sum_{y \in \mathbb{Z}_{<-1}} g(y) e^{isy}. \tag{6.7}$$

By the symmetry of f, we have $F(t) \in \mathbb{R}$. Moreover, since every characteristic function $\varphi(t)$ satisfies $\varphi(-t) = \overline{\varphi(t)}$, in what follows, we only focus on the case $t \geq 0$.

Proposition 6.2 (Asymptotics of the characteristic functions, LDP case). Setting

$$\kappa := 3 + f(0) > 0,$$

it holds that as $t \downarrow 0$,

$$F(t) = 1 - \left(\frac{\kappa}{2}\right)^{1/3} t^{2/3} + o(t^{2/3}),$$

$$F^{-}(t) = \frac{1}{2}(1 - f(0)) + \frac{-1 - i\sqrt{3}}{2} \left(\frac{\kappa}{2}\right)^{1/3} t^{2/3} + o(t^{2/3}),$$

$$G(t) = 1 + \frac{-1 - i\sqrt{3}}{2} \left(\frac{\kappa}{2}\right)^{1/3} t^{2/3} + o(t^{2/3}).$$

Before proving Proposition 6.2, we note that it immediately implies Item (va) of Theorem 1.8.

Proof of Item (va) of Theorem 1.8 (assuming Proposition 6.2). We combine Proposition 6.2 with the Tauberian result in Proposition 6.1. The asymptotic expansion of F(t) in Proposition 6.2 ensures that $f(0) \neq 1$. Recalling the notation in (6.2), in the case of f, we apply Proposition 6.1 to the random variable X with $\mathbb{P}[X=x] = \frac{2}{1-f(0)}f(x)$ for all $x \geq 1$, so that X is non-negative (recall that f(x) = f(-x)). Since the characteristic function of X for t > 0 is

$$\varphi_X(t) = \frac{2}{1 - f(0)} (F(t) - F^-(t) - f(0))$$
$$= 1 + \frac{-1 + i\sqrt{3}}{1 - f(0)} \left(\frac{3 + f(0)}{2}\right)^{1/3} t^{2/3} + o(t^{2/3}),$$

we obtain that

$$\mathbb{P}[X > R] = \frac{1}{1 - f(0)} \left(\frac{3 + f(0)}{2}\right)^{1/3} \frac{1}{\Gamma(1 - 2/3)} \sec\left(\frac{\pi}{3}\right) R^{-2/3} + o(R^{-2/3})$$
$$= \frac{\sqrt{3}\Gamma(2/3)}{\pi(1 - f(0))} \left(\frac{3 + f(0)}{2}\right)^{1/3} R^{-2/3} + o(R^{-2/3})$$

Hence, recalling that $f(x) = \mathbb{P}[\mathcal{X}(0) - \mathcal{X}(-1) = x]$ for all $x \in \mathbb{Z}$,

$$\mathbb{P}[|\mathcal{X}(0) - \mathcal{X}(-1)| > R] = \frac{\sqrt{3}\Gamma(2/3)}{\pi} \left(\frac{3 + f(0)}{2}\right)^{1/3} R^{-2/3} + o(R^{-2/3}). \tag{6.8}$$

In the case of g, we apply Proposition 6.1 to the random variable Y with $\mathbb{P}[Y=y]=g(-y)$ for all $y \geq 1$, so that Y is non-negative. Since the characteristic function of Y for t > 0 is

$$\varphi_Y(t) = G(-t) = \overline{G(t)} = 1 + \frac{-1 + i\sqrt{3}}{2} \left(\frac{3 + f(0)}{2}\right)^{1/3} t^{2/3} + o(t^{2/3})$$

we obtain that

$$\mathbb{P}[Y > R] = \frac{1}{2} \left(\frac{3 + f(0)}{2}\right)^{1/3} \frac{1}{\Gamma(1 - 2/3)} \sec\left(\frac{\pi}{3}\right) R^{-2/3} + o(R^{-2/3})$$
$$= \frac{\sqrt{3}\Gamma(2/3)}{2\pi} \left(\frac{3 + f(0)}{2}\right)^{1/3} R^{-2/3} + o(R^{-2/3})$$

Hence, recalling that $g(y) = \mathbb{P}[\mathcal{X}(1) - \mathcal{X}(0) = y]$ for all $y \in \mathbb{Z}_{\leq -1}$,

$$\mathbb{P}[\mathcal{X}(1) - \mathcal{X}(0) < -R] = \frac{\sqrt{3}\Gamma(2/3)}{2\pi} \left(\frac{3 + f(0)}{2}\right)^{1/3} R^{-2/3} + o(R^{-2/3}). \tag{6.9}$$

Setting $c_1 = \frac{\sqrt{3} \Gamma(2/3)}{2\pi} \left(\frac{3+f(0)}{2}\right)^{1/3}$ in (6.8) and (6.9) gives the expressions in the statement of the theorem.

Remark 6.3. Note that we do not know the exact value of $c_1 = \frac{\sqrt{3}\Gamma(2/3)}{2\pi} \left(\frac{3+f(0)}{2}\right)^{1/3}$ because we do not know the value of f(0).

To prove Proposition 6.2, we first express \mathcal{X} in terms of the Busemann function \mathcal{X}^1 of $M_{1,\infty}$.

Lemma 6.4 (Express \mathcal{X} in terms of \mathcal{X}^1 in the LDP case). Let XDP = LDP. Define the KMSW encoding walk $\mathcal{Z}: \mathbb{Z} \to \mathbb{Z}^2$, the infinite directed triangulations $M_{0,\infty} \stackrel{d}{=} M_{1,\infty}$, and their associated Busemann functions \mathcal{X} and \mathcal{X}^1 as at the beginning of Section 6.

• If
$$\mathcal{Z}(1) - \mathcal{Z}(0) = (1, -1)$$
, then
$$\left(\mathcal{X}(-1), \mathcal{X}(1)\right) = \left(\mathcal{X}^{1}(-2) - \max\{\mathcal{X}^{1}(-1), 1\}, -\max\{\mathcal{X}^{1}(-1), 1\}\right). \tag{6.10}$$

• If
$$Z(1) - Z(0) = (-1, 0)$$
, then

$$\left(\mathcal{X}(-1), \mathcal{X}(1)\right) = \left(-\mathcal{X}^{1}(1) - 1, -1\right). \tag{6.11}$$

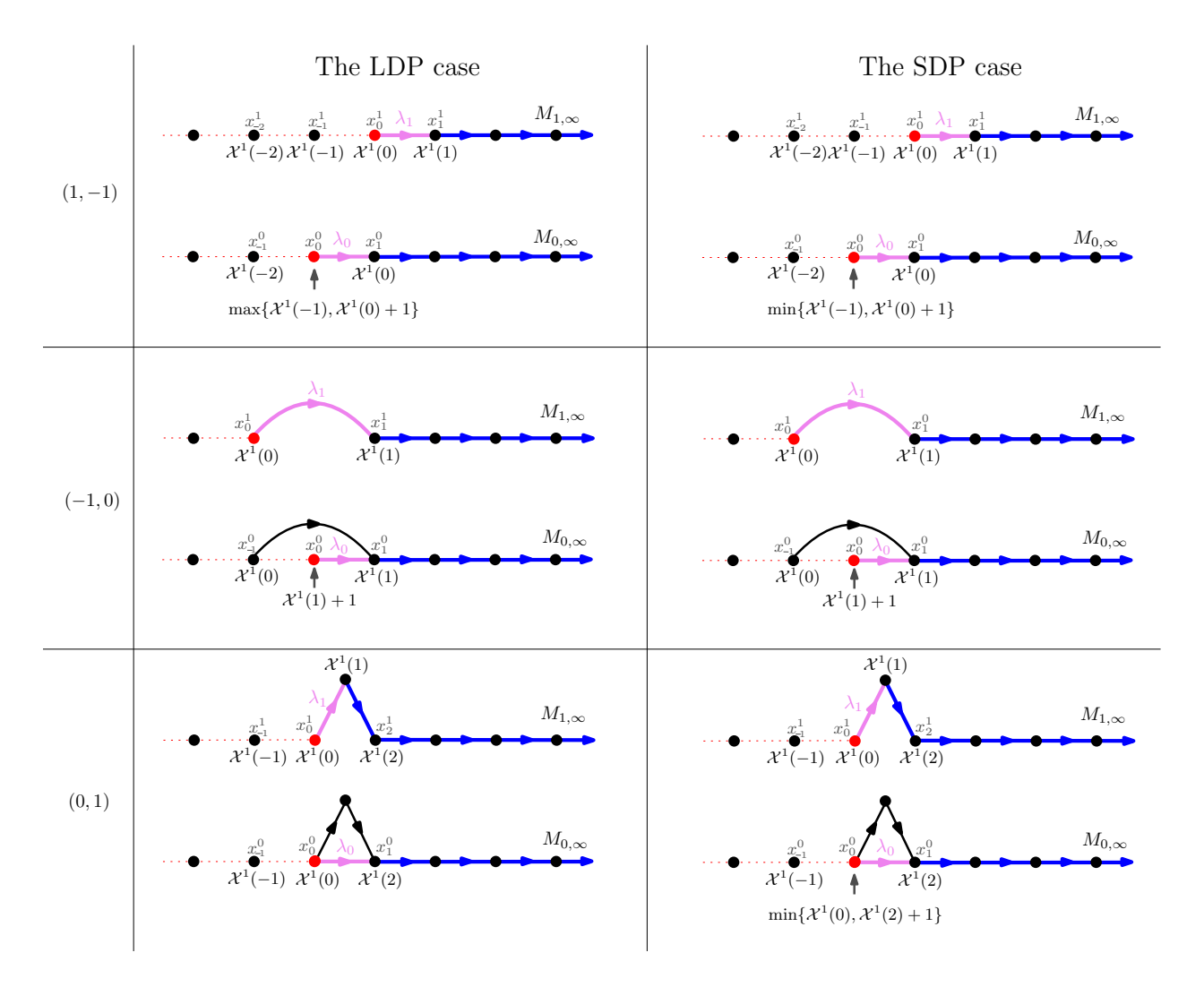


Figure 15: A schema for the proof of Lemmas 6.4 and 6.10. The left-hand side is for the LDP case, while the right-hand side is for the SDP case. The three rows correspond to the three different steps $\{(1,-1),(-1,0),(0,1)\}$ the walk \mathcal{Z} can take between time 0 and 1. The violet edges correspond to the root edges of the maps, the red vertex is the vertex x_0^0 (resp. x_0^1 for the map $M_{1,\infty}$), with the vertices $(x_i^0)_{i\geq 1}$ (resp. $(x_i^1)_{i\geq 1}$) on the right and the vertices $(x_i^0)_{i\leq 1}$ (resp. $(x_i^1)_{i\leq 1}$) on the left. On the maps $M_{1,\infty}$, we show some of the values of the Busemann function \mathcal{X}^1 below each vertex. On the maps $M_{0,\infty}$, we show some of the values of the shifted Busemann function $\widetilde{\mathcal{X}}$ of (6.14) in terms of \mathcal{X}^1 . We have $\mathcal{X}(\cdot) = \widetilde{\mathcal{X}}(\cdot) - \widetilde{\mathcal{X}}(0)$.

• If
$$\mathcal{Z}(1) - \mathcal{Z}(0) = (0, 1)$$
, then
$$\left(\mathcal{X}(-1), \mathcal{X}(1)\right) = \left(\mathcal{X}^{1}(-1), \mathcal{X}^{1}(2)\right). \tag{6.12}$$

Proof. Recall that $M_{0,\infty}$ and $M_{1,\infty}$ are constructed via the KMSW procedure from $\mathcal{Z}|_{[0,\infty)}$ and $\mathcal{Z}|_{[1,\infty)}$, respectively. We label the boundary vertices of $M_{0,\infty}$ from left to right by $\{x_k^0\}_{k\in\mathbb{Z}}$ so that $\lambda_0=(x_0^0,x_1^0)$ and the boundary vertices of $M_{1,\infty}$ from left to right by $\{x_k^1\}_{k\in\mathbb{Z}}$ so that $\lambda_1=(x_0^1,x_1^1)$.

By Theorem 1.4 (applied to, e.g., a sequence of vertices along the right boundary of $M_{1,\infty}$), there exists $w \in \mathcal{V}(M_{1,\infty})$ such that

$$LDP_{M_{j,\infty}}(x_{k'}^j, w) - LDP_{M_{j,\infty}}(x_k^j, w) = \mathcal{X}^j(k') - \mathcal{X}^j(k), \quad \forall j \in \{0, 1\}, \quad \forall k, k' \in [-2, 2] \cap \mathbb{Z}.$$
 (6.13)

We will analyze how the Busemann function changes when we perform one backward step of the KMSW procedure (Definition 3.3) to get $M_{0,\infty}$ from $M_{1,\infty}$. Since \mathcal{X}^1 is normalized so that $\mathcal{X}^1(0) = 0$, to facilitate the comparison, it is convenient to introduce

$$\widetilde{\mathcal{X}}(k) := \mathcal{X}(k) + \text{LDP}_{M_{0,\infty}}(x_0^0, w) - \text{LDP}_{M_{1,\infty}}(x_0^1, w) = \text{LDP}_{M_{0,\infty}}(x_k^0, w) - \text{LDP}_{M_{1,\infty}}(x_0^1, w).$$
(6.14)

Then $\mathcal{X}(\cdot) = \widetilde{\mathcal{X}}(\cdot) - \widetilde{\mathcal{X}}(0)$. We will express $\widetilde{\mathcal{X}}(-1)$, $\widetilde{\mathcal{X}}(0)$, and $\widetilde{\mathcal{X}}(1)$ in terms of \mathcal{X}^1 , then subtract $\widetilde{\mathcal{X}}(0)$ from $\widetilde{\mathcal{X}}(-1)$ and $\widetilde{\mathcal{X}}(1)$ to get an expression for $\mathcal{X}(-1)$ and $\mathcal{X}(1)$ in terms of \mathcal{X}^1 .

If $\mathcal{Z}(1) - \mathcal{Z}(0) = (1, -1)$, then the edges on the boundary of $M_{0,\infty}$ are the same as the edges on the boundary of $M_{1,\infty}$, with the only difference being that the root edge λ_0 of $M_{0,\infty}$ is the missing edge to the left of the root edge λ_1 of $M_{1,\infty}$; see the top-left diagram in Figure 15. In this case, an LDP geodesic in $M_{0,\infty}$ from the vertex $x_{-1}^0 = x_{-2}^1$ to w must be an LDP geodesic in $M_{1,\infty}$ from the vertex x_{-2}^0 to w because the vertex x_{0}^0 has only outgoing edges in $M_{0,\infty}$ thanks to the last claim in Lemma 3.8. Hence, in the notation (6.14),

$$\widetilde{\mathcal{X}}(-1) = \mathcal{X}^1(-2).$$

An LDP geodesic in $M_{0,\infty}$ from $x_0^0 = x_{-1}^1$ to w must be the longest between an LDP geodesic in $M_{1,\infty}$ from x_{-1}^1 to w and an LDP geodesic in $M_{1,\infty}$ from x_0^1 to w with the additional edge λ_0 prepended. Recalling that $\mathcal{X}^1(0) = 0$, this gives

$$\widetilde{\mathcal{X}}(0) = \max \Big\{ \mathcal{X}^1(-1), 1 \Big\}.$$

An LDP geodesic in $M_{0,\infty}$ started from $x_1^0 = x_0^1$ cannot use the edge λ_0 (which is incoming to x_0^0), so $\tilde{\mathcal{X}}(1) = \mathcal{X}^1(0) = 0$. Writing $\mathcal{X}(-1) = \tilde{\mathcal{X}}(-1) - \tilde{\mathcal{X}}(0)$ and $\mathcal{X}(1) = \tilde{\mathcal{X}}(1) - \tilde{\mathcal{X}}(0)$ and plugging in the above relations gives (6.10).

If $\mathcal{Z}(1) - \mathcal{Z}(0) = (-1,0)$, then the edges on the boundary of $M_{0,\infty}$ are the same as the edges on the boundary of $M_{1,\infty}$, with the only difference being that the root edge λ_1 of $M_{1,\infty}$ is replaced in the boundary of $M_{0,\infty}$ by a path of length two with the following properties. The first edge in the path is a missing edge whose initial vertex coincides with the initial vertex of λ_1 . The second edge in the path is the new root edge λ_0 whose terminal vertex coincides with the terminal vertex of λ_1 ; see the middle-left diagram in Figure 15. From this, we obtain

$$\widetilde{\mathcal{X}}(-1) = \mathcal{X}^1(0) = 0, \quad \widetilde{\mathcal{X}}(0) = \mathcal{X}^1(1) + 1, \quad \widetilde{\mathcal{X}}(1) = \mathcal{X}^1(1)$$

where in the case of $\widetilde{\mathcal{X}}(0)$ we used that an LDP geodesic in $M_{0,\infty}$ from x_0^0 to w must be an LDP geodesic in $M_{1,\infty}$ from x_1^1 to w, with the additional edge λ_0 prepended. Subtracting gives (6.11).

If $\mathcal{Z}(1) - \mathcal{Z}(0) = (0, 1)$, then the edges on the boundary of $M_{0,\infty}$ are the same as the edges on the boundary of $M_{1,\infty}$, with the only difference being that the root edge λ_1 of $M_{1,\infty}$ and the edge e immediately to the right of it are replaced in the boundary of $M_{0,\infty}$ by the new root edge λ_0 whose initial vertex coincides with the initial vertex of λ_1 and whose terminal vertex coincides with the terminal vertex of e; see the bottom-left diagram in Figure 15. This leads to

$$\widetilde{\mathcal{X}}(-1) = \mathcal{X}^1(-1), \quad \widetilde{\mathcal{X}}(0) = \mathcal{X}^1(0) = 0, \quad \widetilde{\mathcal{X}}(1) = \mathcal{X}^1(2),$$

where here we used that there is a directed path of length two in $M_{1,\infty}$ between the two vertices of λ_0 , so no LDP geodesic in $M_{0,\infty}$ can traverse λ_0 . Subtracting gives (6.12).

Lemma 6.4 immediately implies the following recursive equation for the distributions f and g.

Proposition 6.5 (LDP recursive equation). For all $x \in \mathbb{Z}$ and $y \in \mathbb{Z}_{\leq -1}$,

$$3f(x)g(y) = f(x)f(y) + f(x) \sum_{j=1}^{-y-1} g(y+j)g(-j) + \mathbb{1}_{\{y=-1\}} \left(\sum_{j\geq 0} f(j+x+1)f(-j) + g(-x-1) \right).$$
(6.15)

Proof. Fix $x \in \mathbb{Z}$ and $y \in \mathbb{Z}_{\leq -1}$. Using the fact that $\mathcal{X}^1 \stackrel{d}{=} \mathcal{X}$ (which follows from the fact that $M_{0,\infty} \stackrel{d}{=} M_{1,\infty}$), we can write

$$\mathbb{P}\left[\left(\mathcal{X}^{1}(-1)\,,\,\mathcal{X}^{1}(1)\right)=(x,y)\right]=\mathbb{P}\left[\left(\mathcal{X}(-1)\,,\,\mathcal{X}(1)\right)=(x,y)\right].$$

Thanks to Lemma 6.4, we have that

$$\mathbb{P}\left[\left(\mathcal{X}(-1), \mathcal{X}(1)\right) = (x, y)\right] = \frac{1}{3}\mathbb{P}\left[\left(\mathcal{X}^{1}(-2) - \max\{\mathcal{X}^{1}(-1), 1\}, -\max\{\mathcal{X}^{1}(-1), 1\}\right) = (x, y)\right]
+ \frac{1}{3}\mathbb{P}\left[\left(-\mathcal{X}^{1}(1) - 1, -1\right) = (x, y)\right]
+ \frac{1}{3}\mathbb{P}\left[\left(\mathcal{X}^{1}(-1), \mathcal{X}^{1}(2)\right) = (x, y)\right].$$
(6.16)

By stationarity (recall (6.1) and (6.2)) and the fact that $\mathcal{X}(0) = \mathcal{X}^1(0) = 0$,

$$f(x) = \mathbb{P}[-\mathcal{X}(-1) = x] = \mathbb{P}\left[-\mathcal{X}^1(-1) = x\right] \quad \text{and} \quad g(y) = \mathbb{P}[\mathcal{X}(1) = y] = \mathbb{P}\left[\mathcal{X}^1(1) = y\right].$$

Furthermore, the increments $\{\mathcal{X}^1(k) - \mathcal{X}^1(k-1)\}_{k \in \mathbb{Z}}$ are independent, the increments $\{\mathcal{X}^1(k) - \mathcal{X}^1(k-1)\}_{k \geq 1}$ all have the same distribution, and the increments $\{\mathcal{X}^1(k) - \mathcal{X}^1(k-1)\}_{k \leq 0}$ all have the same distribution (Properties (i) and (ii) in Theorem 1.7). Applying these facts in (6.16) gives

$$3f(-x)g(y) = f(-x)f(y) + \mathbb{1}_{\{y=-1\}} \sum_{j \le 0} f(j-x-1)f(-j) + \mathbb{1}_{\{y=-1\}} g(-x-1) + f(-x) \sum_{j=1}^{-y-1} g(y+j)g(-j),$$

where the first probability on the right-hand side of (6.16) involving the maximum was computed by distinguishing the cases when $\mathcal{X}^1(-1) \leq 0$ and $\mathcal{X}^1(-1) \geq 1$. Using the fact that f(x) = f(-x), we obtain the expression stated in the proposition.

We now proceed with the proof of Proposition 6.2 by first establishing some preliminary results.

Lemma 6.6. Let $Y \sim f$. Then Y is not a.s. constant and $\mathbb{P}(Y = 0) = f(0) > 0$.

Proof. We first prove that Y is not a.s. constant. Since f(x) = f(-x), it is enough to show that f(0) = 1 is not a solution to (6.15). Assume for contradiction that f(0) = 1. Then f(k) = 0 for all $k \neq 0$. Fixing x = 0 in (6.15), we obtain that for all $y \leq -1$,

$$3g(y) = f(y) + \sum_{j=1}^{-y-1} g(y+j)g(-j) + \mathbf{1}_{\{y=-1\}} \left(\sum_{j\geq 0} f(j+1)f(-j) + g(-1) \right).$$
 (6.17)

First, take y = -1. Since f(-1) = 0 and f(j+1) = 0 for all $j \ge 0$, (6.17) gives 3g(-1) = g(-1), and so g(-1) = 0. Now let $y \le -2$. The indicator term vanishes and f(y) = 0 since $y \ne 0$, so (6.17) becomes

$$3g(y) = \sum_{j=1}^{-y-1} g(y+j)g(-j). \tag{6.18}$$

For y = -2, the right-hand side is g(-1)g(-1) = 0, hence g(-2) = 0. Inductively, one obtains that g(y) = 0 for all $y \le -1$. A contradiction since g is a probability distribution supported on $\mathbb{Z}_{<-1}$.

We now prove that f(0) > 0. Fixing y = -1 and summing (6.15) over all $x \in \mathbb{Z}$, we get using the symmetry of f,

$$3g(-1) = f(-1) + \frac{1 + f(0)}{2} + 1, (6.19)$$

and so $g(-1) \ge \frac{1}{2}$. Now take x = 0, y = -1 in (6.15):

$$3f(0)g(-1) = f(0)f(-1) + \sum_{j>0} f(j+1)f(j) + g(-1),$$

again using the symmetry of f. If f(0) = 0, this gives $g(-1) \le 0$, resulting in a contradiction.

To simplify computations, we introduce the auxiliary characteristic function:

$$\overline{G}(s) := \sum_{y \in \mathbb{Z}_{\geq 1}} g(-y) e^{isy}, \tag{6.20}$$

that is, $\overline{G}(-s) = G(s)$, where G(s) was introduced in (6.7). Multiplying (6.15) by $e^{i(tx-sy)}$ and summing over $x \in \mathbb{Z}$ and $y \in \mathbb{Z}_{<-1}$, we obtain the functional equation

$$3\overline{G}(s)F(t) = F(t)\left(F^{-}(-s) + \overline{G}(s)^{2}\right) + e^{is-it}\left(F(t)\left(F^{-}(t) + f(0)\right) + \overline{G}(t)\right). \tag{6.21}$$

Setting s=0 in (6.21) and using $F^-(0)=\frac{1}{2}(1-f(0))$ and $\overline{G}(0)=1$, gives

$$3F(t) = F(t)\left(\frac{3-f(0)}{2}\right) + e^{-it}\left(F(t)\left(F^{-}(t) + f(0)\right) + \overline{G}(t)\right). \tag{6.22}$$

Solving (6.22) for $\overline{G}(t)$ yields

$$\overline{G}(t) = -F(t)\,\hat{F}^{-}(t), \qquad \hat{F}^{-}(t) := F^{-}(t) + c(t), \qquad c(t) := f(0) - \frac{\kappa}{2}\,e^{it},$$
 (6.23)

where we recall that $\kappa = 3 + f(0) > 0$. Now set t = 0 in (6.21) and substitute the expression for $\overline{G}(t)$ in (6.23). After some algebra, we obtain the quadratic equation \widehat{F} in the variable \widehat{F} :

$$F^{2}(\widehat{F}^{-})^{2} + (3F - 1)\widehat{F}^{-} + F = 0.$$
(6.24)

Lemma 6.7 ($\widehat{F}^-(t)$ has non-trivial imaginary part). Let $\Delta(F) := (3F-1)^2 - 4F^3$ be the discriminant of (6.24). Then there exists $\delta > 0$ such that for all t with $0 < t < \delta$,

$$\Delta(F(t)) < 0$$
,

hence the two roots of (6.24) are non-real complex conjugates. In particular, writing

$$\widehat{F}^{-}(t) = \alpha(t) + i\beta(t) \tag{6.25}$$

with a continuous choice of branch, one has $\beta(t) \neq 0$ for $0 < t < \delta$.

¹⁶Just performing the substitution, one gets a minus sign on the left-hand side of (6.24) that we removed for simplicity.

Proof. We have F(0) = 1, F is continuous, and $\Delta(1) = \Delta'(1) = 0$, $\Delta''(1) = -6 < 0$. Thus

$$\Delta(1+\varepsilon) \le -C\,\varepsilon^2\tag{6.26}$$

for sufficiently small $\varepsilon \in \mathbb{R} \setminus \{0\}$ and some C > 0. Let $Y \sim f$ and d be the lattice span of Y, i.e.

$$d := \gcd\{x - y : f(x) > 0, \ f(y) > 0\}.$$

Since Y is not a.s. constant by Lemma 6.6, we have $d < \infty$. Since f(0) > 0 thanks to Lemma 6.6, a simple argument for the characteristic function of integer-valued random variables gives

$$F(t) = 1$$
 if and only if $t \in \frac{2\pi}{d}\mathbb{Z}$. (6.27)

So there exists $\delta_1 \in (0, 2\pi/d)$ such that $F(t) \neq 1$ for all $0 < t < \delta_1$. By continuity, there exists $\delta_2 > 0$ such that $|F(t) - 1| < \eta$ whenever $t < \delta_2$, with $\eta > 0$ small enough to ensure the estimate in (6.26) applies. Setting $\delta := \min\{\delta_1, \delta_2\}$, we get that for all $0 < t < \delta$,

$$F(t) \neq 1,$$
 $\Delta(F(t)) \leq -C(F(t) - 1)^2 < 0.$

Thus $\Delta(F(t)) < 0$ for $0 < |t| < \delta$, so the two roots of (6.24) are non-real conjugates with nonzero imaginary part.

We are now ready to complete the proof of Proposition 6.2.

Proof of Proposition 6.2. Recall that $F(t) \in \mathbb{R}$ and write

$$F(t) = f(0) + F^{-}(t) + \overline{F^{-}(t)} \stackrel{(6.23)}{=} f(0) + (\widehat{F}^{-}(t) - c(t)) + \overline{(\widehat{F}^{-}(t) - c(t))} = f(0) - 2\operatorname{Re}(c(t)) + 2\operatorname{Re}(\widehat{F}^{-}(t)).$$

We set

$$K(t) := f(0) - 2\operatorname{Re}(c(t)) \stackrel{\text{(6.23)}}{=} -f(0) + \kappa \cos t,$$

so that K(t) encodes the part of F(t) that is independent of $\widehat{F}^{-}(t)$ (which we recall is our indeterminate in (6.24)) and

$$\operatorname{Re}(\widehat{F}^{-}(t)) = \frac{F(t) - K(t)}{2}.$$
 (6.28)

Hence, thanks to Lemma 6.7,

$$\hat{F}^{-}(t) \stackrel{(6.25)}{=} \alpha(t) + i\beta(t) \stackrel{(6.28)}{=} \frac{F(t) - K(t)}{2} + i\beta(t),$$

with $\beta(t) \neq 0$ for $0 < t < \delta$.

Now, taking the imaginary part in (6.24), we obtain the equation

$$\beta(F^3 - KF^2 + 3F - 1) = 0,$$

and since $\beta(t) \neq 0$ for $0 < t < \delta$, we get that for $0 < t < \delta$,

$$F^3 - KF^2 + 3F - 1 = 0. (6.29)$$

The Taylor expansion of K(t) around t = 0 is

$$K(t) = 3 - \frac{\kappa}{2}t^2 + O(t^4).$$

Writing $F(t) = 1 + \varepsilon(t)$ with $\varepsilon(t) \to 0$ as $t \downarrow 0$, we get from (6.29) that

$$0 = \varepsilon^3 + \frac{\kappa}{2} t^2 (\varepsilon^2 + 2\varepsilon + 1) + O(t^4). \tag{6.30}$$

Now, since $\kappa > 0$ (and so $\kappa \neq 0$), we claim that as $t \downarrow 0$,

$$\varepsilon(t) = -\left(\frac{\kappa}{2}\right)^{1/3} t^{2/3} + o(t^{2/3}). \tag{6.31}$$

Indeed, set $\varepsilon(t) = t^{2/3}s(t)$. Dividing (6.30) by t^2 gives as $t \downarrow 0$,

$$0 = s^{3} + \frac{\kappa}{2}(1 + 2st^{2/3} + s^{2}t^{4/3}) + O(t^{2}) = s^{3} + \frac{\kappa}{2} + o(1), \tag{6.32}$$

where in the last equality we used that $\varepsilon(t) = t^{2/3}s(t) \to 0$ as $t \downarrow 0$. Hence $s(t) = -\left(\frac{\kappa}{2}\right)^{1/3} + o(1)$ and so (6.31) holds. This completes the proof for the expansion of F(t).

We now determine the expansions of $F^-(t)$ and $\overline{G}(t)$. Solving the quadratic equation (6.24), the two possible continuous choices of branch for $\widehat{F}^-(t)$ are

$$\hat{F}_{\pm}^{-}(t) = \frac{1 - 3F \pm \sqrt{\Delta(F)}}{2F^2}, \quad \text{with } \Delta(F) = (3F - 1)^2 - 4F^3,$$

and recalling (6.23), we obtain that the two possible continuous choices of branch for $F^-(t)$ are

$$F_{\pm}^{-}(t) = \frac{1 - 3F \pm \sqrt{\Delta(F)}}{2F^{2}} - c(t), \quad \text{with } \Delta(F) = (3F - 1)^{2} - 4F^{3}.$$
 (6.33)

Moreover, from (6.23), we have that the two possible continuous choices of branch for $\overline{G}(t)$ are

$$\overline{G}_{\pm}(t) = -F(t)\,\widehat{F}_{\pm}^{-}(t).$$
 (6.34)

Therefore, since $F(t) = 1 - (\frac{\kappa}{2})^{1/3} t^{2/3} + o(t^{2/3})$ as $t \downarrow 0$, we get from (6.23) and (6.33) that

$$F_{\pm}^{-}(t) = \left(\frac{1 - f(0)}{2}\right) + \frac{1}{2}(-1 \pm i\sqrt{3})\left(\frac{\kappa}{2}\right)^{1/3}t^{2/3} + o(t^{2/3}),$$

and from (6.34),

$$\overline{G}_{\pm}(t) = 1 + \frac{1}{2}(-1 \mp i\sqrt{3})\left(\frac{\kappa}{2}\right)^{1/3}t^{2/3} + o(t^{2/3}).$$

Noting that $\overline{G}(t)$, introduced in (6.20), is the characteristic function of a non-negative integer-valued random variable, and using Proposition 6.1, we have that the only admissible expression is

$$\overline{G}(t) = 1 + \frac{1}{2}(-1 + i\sqrt{3})\left(\frac{\kappa}{2}\right)^{1/3}t^{2/3} + o(t^{2/3}),$$

and so

$$F^{-}(t) = \left(\frac{1 - f(0)}{2}\right) + \frac{1}{2}(-1 - i\sqrt{3})\left(\frac{\kappa}{2}\right)^{1/3}t^{2/3} + o(t^{2/3}).$$

This completes the proof for the expansion of $F^-(t)$ and $\overline{G}(t)$ as $t \downarrow 0$. To recover the expansion of G(t), it is enough to note that $G(t) = \overline{G}(-t)$ and the latter is just the complex conjugate of $\overline{G}(t)$.

6.2 The SDP case

We now move to the case when XDP = SDP. The proof is very similar to the LDP case. We use the same notation as in Section 6.1, but now everything is defined with SDP instead of LDP.

Thanks to Properties (iii) and (iv) of Theorem 1.7 we know that f is a symmetric distribution on \mathbb{Z} and g is a distribution on $\mathbb{Z}_{\geq -1}$. We introduce the three characteristic functions

$$F(t) := \sum_{x \in \mathbb{Z}} f(x) e^{itx}, \qquad F^{-}(t) := \sum_{x \in \mathbb{Z}_{<-1}} f(x) e^{itx}, \qquad G(s) := \sum_{y \in \mathbb{Z}_{>-1}} g(y) e^{isy}. \tag{6.35}$$

By the symmetry of f, we note that $F(t) \in \mathbb{R}$. Moreover, since every characteristic function $\varphi(t)$ satisfies $\varphi(-t) = \overline{\varphi(t)}$, in what follows, we only focus on the case $t \geq 0$.

Proposition 6.8 (Asymptotics of the characteristic functions, SDP case). Setting

$$\kappa := 3 - 6g(-1)^2 - f(0),$$

it holds that $\kappa = 0$, and, as $t \downarrow 0$,

$$F(t) = 1 - g(-1)^{2/3} t^{4/3} + o(t^{4/3}),$$

$$F^{-}(t) = \frac{1}{2} (1 - f(0)) - 2i g(-1)^{2} t + \frac{-1 + i\sqrt{3}}{2} g(-1)^{2/3} t^{4/3} + o(t^{4/3}),$$

$$G(t) = 1 + \frac{-1 - i\sqrt{3}}{2} g(-1)^{2/3} t^{4/3} + o(t^{4/3}).$$

Moreover, g(-1) > 0.

Before proving Proposition 6.8, we note that it immediately implies Item (vb) of Theorem 1.8.

Proof of Item (vb) of Theorem 1.8 (assuming Proposition 6.8). We first combine Proposition 6.8 with Proposition 6.1 to prove the claimed tail behaviors. The asymptotic expansions of F(t) and G(t) in Proposition 6.8 ensures that $f(0) \neq 1$ and $g(-1) \neq 1$. Moreover, $g(-1) \neq 0$ as stated in Proposition 6.8. Recalling the notation introduced in (6.2), in the case of f, we apply Proposition 6.1 to the random variable X with $\mathbb{P}[X=x] = \frac{2}{1-f(0)}f(x)$ for all $x \geq 1$, so that X is non-negative (recall that f(x) = f(-x)). Since the characteristic function of X for t > 0 is

$$\varphi_X(t) = \frac{2}{1 - f(0)} \Big(F(t) - F^-(t) - f(0) \Big)$$

$$= 1 + \frac{4i g(-1)^2}{1 - f(0)} t + \frac{(-1 - i\sqrt{3}) g(-1)^{2/3}}{1 - f(0)} t^{4/3} + o(t^{4/3}),$$

we obtain that

$$\mathbb{P}[X > R] = \frac{\sqrt{3} g(-1)^{2/3}}{1 - f(0)} \frac{4}{3\Gamma(1 - 4/3)} \sec\left(\frac{2\pi}{3}\right) R^{-4/3} + o(R^{-4/3})$$
$$= \frac{4\Gamma(1/3) g(-1)^{2/3}}{3\pi(1 - f(0))} R^{-4/3} + o(R^{-4/3}).$$

Hence, recalling that $f(x) = \mathbb{P}[\mathcal{X}(0) - \mathcal{X}(-1) = x]$ for all $x \in \mathbb{Z}$,

$$\mathbb{P}[|\mathcal{X}(0) - \mathcal{X}(-1)| > R] = \frac{4\Gamma(1/3)g(-1)^{2/3}}{3\pi}R^{-4/3} + o(R^{-4/3}). \tag{6.36}$$

In the case of g, we apply Proposition 6.1 to the random variable Y with $\mathbb{P}[Y=y] = \frac{1}{1-g(-1)}g(y)$ for all $y \geq 0$, so that Y is non-negative. Since the characteristic function of Y for t > 0 is

$$\varphi_Y(t) = \frac{1}{1 - g(-1)} \Big(G(t) - g(-1)e^{-it} \Big) = 1 + \frac{i g(-1)}{1 - g(-1)} t + \frac{g(-1)^{2/3}(-1 - i\sqrt{3})}{2(1 - g(-1))} t^{4/3} + o(t^{4/3}),$$

where we used that $e^{-it} = 1 - it + O(t^2)$, we obtain that

$$\mathbb{P}[Y > R] = \frac{\sqrt{3} g(-1)^{2/3}}{2(1 - g(-1))} \frac{4}{3\Gamma(1 - 4/3)} \sec\left(\frac{2\pi}{3}\right) R^{-4/3} + o(R^{-4/3})$$
$$= \frac{4\Gamma(1/3) g(-1)^{2/3}}{6\pi(1 - g(-1))} R^{-4/3} + o(R^{-4/3})$$

Hence, recalling that $g(y) = \mathbb{P}[\mathcal{X}(1) - \mathcal{X}(0) = y]$ for all $y \in \mathbb{Z}_{\geq -1}$,

$$\mathbb{P}[\mathcal{X}(1) - \mathcal{X}(0) > R] = \frac{4\Gamma(1/3)g(-1)^{2/3}}{6\pi}R^{-4/3} + o(R^{-4/3}). \tag{6.37}$$

Setting $c_2 = \frac{4\Gamma(1/3) g(-1)^{2/3}}{6\pi}$ in (6.36) and (6.37) gives the expressions in the statement of the theorem.

The tail expansions (6.36) and (6.37), together with the stationarity property (ii) of Theorem 1.7, imply that $\mathbb{E}[|\mathcal{X}(k) - \mathcal{X}(k-1)|] < \infty$ for every $k \in \mathbb{Z}$. From the expansions of F(t) and G(t) in Proposition 6.8, we get F'(0) = G'(0) = 0, which implies that $\mathbb{E}[\mathcal{X}(k) - \mathcal{X}(k-1)] = 0$ for every $k \in \mathbb{Z}$.

Remark 6.9. Also in this case, we do not know the exact value of $c_2 = \frac{4\Gamma(1/3)g(-1)^{2/3}}{6\pi}$ because we do not know the value of g(-1).

As in Section 6.1, the first step in the proof of Proposition 6.8 is to express \mathcal{X} in terms of \mathcal{X}^1 .

Lemma 6.10 (Express \mathcal{X} in terms of \mathcal{X}^1 in the SDP case). Let XDP = SDP. Define the KMSW encoding walk $\mathcal{Z}: \mathbb{Z} \to \mathbb{Z}^2$ and the infinite directed triangulations $M_{0,\infty} \stackrel{d}{=} M_{1,\infty}$ and their associated Busemann functions \mathcal{X} and \mathcal{X}^1 as at the beginning of Section 6.

• If
$$\mathcal{Z}(1) - \mathcal{Z}(0) = (1, -1)$$
, then
$$\left(\mathcal{X}(-1), \mathcal{X}(1)\right) = \left(\mathcal{X}^1(-2) - \min\{\mathcal{X}^1(-1), 1\}, -\min\{\mathcal{X}^1(-1), 1\}\right). \tag{6.38}$$

• If Z(1) - Z(0) = (-1, 0), then

$$(\mathcal{X}(-1), \mathcal{X}(1)) = (-\mathcal{X}^1(1) - 1, -1).$$
 (6.39)

• If Z(1) - Z(0) = (0,1), then

$$\left(\mathcal{X}(-1)\,,\,\mathcal{X}(1)\right) = \left(\mathcal{X}^1(-1) - \min\{0,\mathcal{X}^1(2) + 1\}\,,\,\mathcal{X}^1(2) - \min\{0,\mathcal{X}^1(2) + 1\}\right). \tag{6.40}$$

Proof. Recall that $M_{0,\infty}$ and $M_{1,\infty}$ are constructed via the KPZ procedure from $\mathcal{Z}|_{[0,\infty)}$ and $\mathcal{Z}|_{[1,\infty)}$, respectively. We label the boundary vertices of $M_{0,\infty}$ from left to right by $\{x_k^0\}_{k\in\mathbb{Z}}$ so that $\lambda_0 = (x_0^0, x_1^0)$ and the boundary vertices of $M_{1,\infty}$ from left to right by $\{x_k^1\}_{k\in\mathbb{Z}}$ so that $\lambda_1 = (x_0^1, x_1^1)$.

By Theorem 1.4 (applied to, e.g., a sequence of vertices along the right boundary of $M_{1,\infty}$), there exists $w \in \mathcal{V}(M_{1,\infty})$ such that

$$SDP_{M_{j,\infty}}(x_{k'}^j, w) - SDP_{M_{j,\infty}}(x_k^j, w) = \mathcal{X}^j(k') - \mathcal{X}^j(k), \quad \forall j \in \{0, 1\}, \quad \forall k, k' \in [-2, 2] \cap \mathbb{Z}.$$
 (6.41)

We analyze how the Busemann function changes when we perform one backward step of the KMSW procedure (Definition 3.3), to get $M_{0,\infty}$ from $M_{1,\infty}$. Exactly as in the LDP case (6.14), we introduce

$$\widetilde{\mathcal{X}}(k) := \mathcal{X}(k) + \text{SDP}_{M_{0,\infty}}(x_0^0, w) - \text{SDP}_{M_{1,\infty}}(x_0^1, w) = \text{SDP}_{M_{0,\infty}}(x_k^0, w) - \text{SDP}_{M_{1,\infty}}(x_0^1, w).$$
 (6.42)

Then $\mathcal{X}(\cdot) = \widetilde{\mathcal{X}}(\cdot) - \widetilde{\mathcal{X}}(0)$. We will express $\widetilde{\mathcal{X}}(-1), \widetilde{\mathcal{X}}(0)$, and $\widetilde{\mathcal{X}}(1)$ in terms of \mathcal{X}^1 , then subtract $\widetilde{\mathcal{X}}(0)$ from $\widetilde{\mathcal{X}}(-1)$ and $\widetilde{\mathcal{X}}(1)$ to get an expression for $\mathcal{X}(-1)$ and $\mathcal{X}(1)$ in terms of \mathcal{X}^1 .

If $\mathcal{Z}(1) - \mathcal{Z}(0) = (1, -1)$, then the edges on the boundary of $M_{0,\infty}$ are the same as the edges on the boundary of $M_{1,\infty}$, with the only difference being that the root edge λ_0 of $M_{0,\infty}$ is the missing edge to the left of the root edge λ_1 of $M_{1,\infty}$; see the top-right diagram in Figure 15. In this case, an SDP geodesic in $M_{0,\infty}$ from the vertex $x_{-1}^0 = x_{-2}^1$ to w must be an SDP geodesic in $M_{1,\infty}$ from the vertex x_{-2}^1 to w because the vertex x_0^1 has only outgoing edges in $M_{0,\infty}$ thanks to the last claim in Lemma 3.8. Hence, in the notation (6.42),

$$\widetilde{\mathcal{X}}(-1) = \mathcal{X}^1(-2).$$

An SDP geodesic in $M_{0,\infty}$ from $x_0^0 = x_{-1}^1$ to w must be the shortest between an SDP geodesic in $M_{1,\infty}$ from x_{-1}^1 to w and an SDP geodesic in $M_{1,\infty}$ from x_0^1 to w with the additional edge λ_0 prepended. Recalling that $\mathcal{X}^1(0) = 0$, this gives

$$\widetilde{\mathcal{X}}(0) = \min \Big\{ \mathcal{X}^1(-1), 1 \Big\}.$$

Since the edge λ_0 is incoming to $x_1^0 = x_0^0$, we also have $\widetilde{\mathcal{X}}(1) = \mathcal{X}^1(0) = 0$. Subtracting now gives (6.38).

If $\mathcal{Z}(1) - \mathcal{Z}(0) = (-1,0)$, then the edges on the boundary of $M_{0,\infty}$ are the same as the edges on the boundary of $M_{1,\infty}$, with the only difference being that the root edge λ_1 of $M_{1,\infty}$ is replaced in the boundary of $M_{0,\infty}$ by a path of length two with the following properties. The first edge in the path is a missing edge whose initial vertex coincides with the initial vertex of λ_1 . The second edge in the path is the new root edge λ_0 whose terminal vertex coincides with the terminal vertex of λ_1 ; see the middle-right diagram in Figure 15. In this case,

$$\widetilde{\mathcal{X}}(-1) = \mathcal{X}^1(0) = 0, \quad \widetilde{\mathcal{X}}(0) = \mathcal{X}^1(1) + 1, \quad \widetilde{\mathcal{X}}(1) = \mathcal{X}^1(1),$$

where for $\widetilde{\mathcal{X}}(0)$ we used that an SDP geodesic in $M_{0,\infty}$ from x_0^0 to w must be an SDP geodesic in $M_{1,\infty}$ from x_1^1 to w with the additional edge λ_0 prepended. Subtracting gives (6.39).

If $\mathcal{Z}(1) - \mathcal{Z}(0) = (0, 1)$, then the edges on the boundary of $M_{0,\infty}$ are the same as the edges on the boundary of $M_{1,\infty}$, with the only difference being that the root edge λ_1 of $M_{1,\infty}$ and the edge e immediately to the right of it are replaced in the boundary of $M_{0,\infty}$ by the new root edge λ_0 whose initial vertex coincides with the initial vertex of λ_1 and whose terminal vertex coincides with the terminal vertex of e; see the bottom-right diagram in Figure 15. In this case, an SDP geodesic in $M_{0,\infty}$ from the vertex $x_{-1}^0 = x_{-1}^1$ to w must be an SDP geodesic in $M_{1,\infty}$ from the vertex x_{-1}^1 to w because the vertex x_0^0 has only outgoing edges in $M_{0,\infty}$ thanks to the last claim in Lemma 3.8. Hence,

$$\widetilde{\mathcal{X}}(-1) = \mathcal{X}^1(-1).$$

An SDP geodesic in $M_{0,\infty}$ from $x_0^0 = x_0^1$ to w must be the shortest between an SDP geodesic in $M_{1,\infty}$ from x_0^1 to w and an SDP geodesic in $M_{1,\infty}$ from x_0^1 to w with the additional edge λ_0 prepended. Recalling that $\mathcal{X}^1(0) = 0$, this gives

$$\widetilde{\mathcal{X}}(0) = \min \left\{ 0, \mathcal{X}^1(2) + 1 \right\}.$$

Since λ_0 is incoming to $x_1^0 = x_2^1$, we also have $\widetilde{\mathcal{X}}(1) = \mathcal{X}^1(2)$. Subtracting gives (6.40).

Lemma 6.10 immediately implies the following recursive equation for the distributions f and g.

Proposition 6.11 (SDP recursive equation). For all $x \in \mathbb{Z}$ and $y \in \mathbb{Z}_{>-1}$.

$$3 f(x)g(y) = f(x) \left(f(y) + \sum_{j=-1}^{y+1} g(j)g(y-j) \right) + \mathbb{1}_{\{y=-1\}} \left(\sum_{j \le -2} f(j)f(x-j-1) + g(-1)^2 f(x+1) + g(x-1) \right).$$

$$(6.43)$$

Proof. Fix $x \in \mathbb{Z}$ and $y \in \mathbb{Z}_{\geq -1}$. Using the fact that $\mathcal{X}^1 \stackrel{d}{=} \mathcal{X}$ (which follows from the fact that $M_{0,\infty} \stackrel{d}{=} M_{1,\infty}$), we can write

$$\mathbb{P}\left[\left(\mathcal{X}^{1}(-1)\,,\,\mathcal{X}^{1}(1)\right)=\left(x,y\right)\right]=\mathbb{P}\left[\left(\mathcal{X}(-1)\,,\,\mathcal{X}(1)\right)=\left(x,y\right)\right].$$

Thanks to Lemma 6.10, we have that

$$\mathbb{P}\Big[\Big(\mathcal{X}(-1)\,,\,\mathcal{X}(1)\Big) = (x,y)\Big) = \frac{1}{3}\mathbb{P}\Big(\Big(\mathcal{X}^{1}(-2) - \min\{\mathcal{X}^{1}(-1),1\}\,,\,-\min\{\mathcal{X}^{1}(-1),1\}\Big] = (x,y)\Big) \\
+ \frac{1}{3}\mathbb{P}\Big[\Big(-\mathcal{X}^{1}(1) - 1\,,\,-1\Big) = (x,y)\Big] \\
+ \frac{1}{3}\mathbb{P}\Big[\Big(\mathcal{X}^{1}(-1) - \min\{0,\mathcal{X}^{1}(2) + 1\}\,,\,\mathcal{X}^{1}(2) - \min\{0,\mathcal{X}^{1}(2) + 1\}\Big) = (x,y)\Big].$$

By stationarity (recall (6.1) and (6.2)) and the fact that $\mathcal{X}(0) = \mathcal{X}^1(0) = 0$,

$$f(x) = \mathbb{P}[-\mathcal{X}(-1) = x] = \mathbb{P}\left[-\mathcal{X}^1(-1) = x\right] \quad \text{and} \quad g(y) = \mathbb{P}[\mathcal{X}(1) = y] = \mathbb{P}\left[\mathcal{X}^1(1) = y\right].$$

Furthermore, the increments $\{\mathcal{X}^1(k) - \mathcal{X}^1(k-1)\}_{k \in \mathbb{Z}}$ are independent, the increments $\{\mathcal{X}^1(k) - \mathcal{X}^1(k-1)\}_{k \geq 1}$ all have the same distribution, and the increments $\{\mathcal{X}^1(k) - \mathcal{X}^1(k-1)\}_{k \leq 0}$ all have the same distribution (thanks to Items (i) and (ii) in Theorem 1.7). Applying these facts in (6.44) gives

$$\begin{split} 3f(-x)g(y) &= f(-x)f(y) + \mathbbm{1}_{\{y=-1\}} \sum_{j \leq -2} f(-x-j-1)f(j) \\ &+ \mathbbm{1}_{\{y=-1\}} g(-x-1) \\ &+ f(-x) \sum_{j=-1}^{y+1} g(j)g(y-j) + \mathbbm{1}_{\{y=-1\}} g(-1)^2 f(-x+1), \end{split}$$

where the first probability on the right-hand side of (6.44) involving the minimum was computed by distinguishing the cases when $\mathcal{X}^1(-1) \leq 0$ and $\mathcal{X}^1(-1) \geq 1$, and the second probability involving the minimum was computed by distinguishing the cases when $\mathcal{X}^1(2) \geq -1$ and $\mathcal{X}^1(2) = -2$ (since we must have that $\mathcal{X}^1(2) \geq -2$ because g is supported on $\mathbb{Z}_{\geq -1}$). Changing -x to x, we obtain the expression in the statement of the lemma.

We now proceed with the proof of Proposition 6.8 by first establishing some preliminary results.

Lemma 6.12. Let $Y \sim f$. Then Y is not a.s. constant and $\mathbb{P}(Y = 0) = f(0) > 0$. Moreover, g(-1) > 0.

Proof. We first prove that Y is not a.s. constant. Since f(x) = f(-x), it is enough to prove that f(0) < 1. Assume for contradiction that f(0) = 1. Setting x = 0 in (6.43) gives, for all $y \ge -1$,

$$3g(y) = f(y) + \sum_{j=-1}^{y+1} g(j)g(y-j) + \mathbb{1}_{\{y=-1\}} g(-1).$$
(6.45)

Take y = -1 in (6.45). Noting f(-1) = 0 (since f(0) = 1) and that the sum reduces to 2g(-1)g(0), we obtain

$$3g(-1) = 2g(-1)g(0) + g(-1) \implies g(-1) = g(-1)g(0).$$

Hence either g(-1) = 0 or g(0) = 1. If g(0) = 1, taking y = 0 in (6.45) yields 3 = 1 + 1, a contradiction; thus g(-1) = 0. Taking y = 0 in (6.45):

$$3g(0) = 1 + g(0)^2 \implies g(0) = \frac{1}{2}(3 - \sqrt{5}) \le \frac{1}{2}.$$

Next take y=1 in (6.45). The only nonzero terms in the sum are j=0,1, so 3g(1)=2g(0)g(1), which forces g(1)=0 because $g(0)\leq \frac{1}{2}$. An induction using (6.45) shows that for every $y\geq 2$ the sum again reduces to 2g(0)g(y) and hence g(y)=0. Therefore g(k)=0 for all $k\geq 1$, and since also g(-1)=0 we have $\sum_k g(k)=g(0)\leq \frac{1}{2}\neq 1$; a contradiction.

We now prove that f(0) > 0 and g(-1) > 0. Fixing y = -1 in (6.43) and summing over $x \in \mathbb{Z}$, we obtain

$$3g(-1) = f(-1) + 2g(-1)g(0) + \sum_{j \le -2} f(j) + g(-1)^2 + 1.$$
(6.46)

By symmetry of f, we have that $f(-1) + \sum_{j \le -2} f(j) = \frac{1-f(0)}{2}$, so from (6.46),

$$3g(-1) = \frac{3 - f(0)}{2} + 2g(-1)g(0) + g(-1)^{2} \ge \frac{3 - f(0)}{2}.$$
 (6.47)

In particular, g(-1) > 0. Now, evaluate (6.43) at (x, y) = (0, -1):

$$3f(0)g(-1) = f(0)\big(f(-1) + 2g(-1)g(0)\big) + \sum_{j \le -2} f(j)f(-j-1) + g(-1)^2f(1) + g(-1) \ge g(-1).$$

If f(0) = 0, the last equation gives a contradiction because g(-1) > 0.

Now, multiplying (6.43) by $e^{i(tx+sy)}$ and summing over $x \in \mathbb{Z}$ and $y \in \mathbb{Z}_{\geq -1}$, we get the equation

$$3F(t)G(s) = F(t)\left[F(s) - F^{-}(s) + f(-1)e^{-is} + G^{2}(s) - g(-1)^{2}e^{-2is}\right] + e^{-is}\left[e^{it}F^{-}(t)F(t) - f(-1)F(t) + g(-1)^{2}F(t)e^{-it} + G(t)e^{it}\right].$$
(6.48)

Setting t=0 and using that F(0)=1, $F^{-}(0)=(1-f(0))/2$ and G(0)=1, we get that

$$3G(s) = \left[F(s) - F^{-}(s) + G^{2}(s) - g(-1)^{2}e^{-2is} \right] + e^{-is} \left[(1 - f(0))/2 + g(-1)^{2} + 1 \right]. \tag{6.49}$$

Similarly, setting s = 0, we get that

$$3F(t) = F(t) \left[2 - (1 - f(0))/2 - g(-1)^2 \right] + \left[e^{it} F^-(t) F(t) + g(-1)^2 F(t) e^{-it} + G(t) e^{it} \right].$$

This latter equation allows us to write G(t) in terms of F(t) and $F^{-}(t)$. More precisely, we have that

$$G(t) = -F(t)\,\hat{F}^{-}(t) \tag{6.50}$$

where

$$\widehat{F}^{-}(t) := F^{-}(t) + c(t) \tag{6.51}$$

and

$$c(t) := \frac{2g(-1)^2 + e^{it}(-3 - 2g(-1)^2 + f(0))}{2e^{2it}}.$$
(6.52)

Substituting (6.50) in (6.49), one obtains the quadratic equation \hat{F}^{-} :

$$F^{2}(\hat{F}^{-})^{2} + (3F - 1)\hat{F}^{-} + F = 0.$$
(6.53)

Note that this is exactly the same equation that we obtained in (6.24) in the LDP case (but c(t) is defined differently).

We are now ready to complete the proof of Proposition 6.8.

Proof of Proposition 6.8. The fact that g(-1) > 0 follows from Lemma 6.12. We now determine the asymptotic expansions. Recalling that $F(t) \in \mathbb{R}$ and writing

$$F(t) = f(0) + F^{-}(t) + \overline{F^{-}(t)} \stackrel{(6.51)}{=} f(0) + (\widehat{F}^{-}(t) - c(t)) + \overline{(\widehat{F}^{-}(t) - c(t))} = f(0) - 2\operatorname{Re}(c(t)) + 2\operatorname{Re}(\widehat{F}^{-}(t)),$$

we set

$$K(t) := f(0) - 2\operatorname{Re}(c(t)) \stackrel{(6.52)}{=} f(0) + (3 + 2g(-1)^2 - f(0))\cos(t) - 2g(-1)^2\cos(2t),$$

so that K(t) encodes the part of F(t) that is independent of $\widehat{F}^{-}(t)$ (which we recall is our indeterminate in (6.53)) and

$$\operatorname{Re}(\widehat{F}^{-}(t)) = \frac{F(t) - K(t)}{2}.$$
 (6.54)

Hence, thanks to Lemma 6.7 (which is valid also in this SDP case thanks to Lemma 6.12), we can write

$$\hat{F}^{-}(t) = \alpha(t) + i\beta(t) \stackrel{(6.54)}{=} \frac{F(t) - K(t)}{2} + i\beta(t),$$

and there exists $\delta > 0$ such that $\beta(t) \neq 0$ for $0 < t < \delta$.

Now, taking the imaginary part in (6.53), we obtain the equation

$$\beta(F^3 - KF^2 + 3F - 1) = 0,$$

and since $\beta(t) \neq 0$ for $0 < t < \delta$, we get that for $0 < t < \delta$,

$$F^3 - KF^2 + 3F - 1 = 0, (6.55)$$

¹⁷Just performing the substitution, one gets a minus sign on the left-hand side of (6.53) that we removed for simplicity.

The Taylor expansion of K(t) around t = 0 is

$$K(t) = 3 - \frac{\kappa}{2}t^2 + \left(\frac{\kappa}{24} - g(-1)^2\right)t^4 + O(t^6),$$

where we recall that $\kappa = 3 - 6g(-1)^2 - f(0)$. Writing $F(t) = 1 + \varepsilon(t)$ with $\varepsilon(t) \to 0$ as $t \downarrow 0$, we get from (6.55) that

$$0 = \varepsilon^3 + \frac{\kappa}{2}t^2(\varepsilon^2 + 2\varepsilon + 1) - \left(\frac{\kappa}{24} - g(-1)^2\right)t^4(\varepsilon^2 + 2\varepsilon + 1) + O(\varepsilon^4 + t^6 + t^4\varepsilon).$$

Now, to ensure that the right-hand side of the latter equation tends to zero as t decreases to zero:

- If $\kappa = 0$, we must have that $\varepsilon^3(1 + o(1)) = -g(-1)^2t^4(1 + o(1))$ as $t \downarrow 0$, and so $\varepsilon(t) = -g(-1)^{2/3}t^{4/3} + o(t^{4/3})$ as $t \downarrow 0$.
- If $\kappa \neq 0$, we must have that $\varepsilon^3(1+o(1)) = -\frac{\kappa}{2} t^2(1+o(1))$ as $t \downarrow 0$. Since F is real, F(0) = 1, and $|F(t)| \leq 1$ for all $t \in \mathbb{R}$, it must be that $\kappa > 0$ and so $\varepsilon(t) = -(\frac{\kappa}{2})^{1/3} t^{2/3} + o(t^{2/3})$ as $t \downarrow 0$.

The above two items complete the proof for the expansion of F(t).

We now determine the expansions of $F^-(t)$ and G(t). Solving the quadratic equation (6.53), the two possible continuous choices of branch for $\widehat{F}^-(t)$ are

$$\hat{F}_{\pm}^{-}(t) = \frac{1 - 3F \pm \sqrt{\Delta(F)}}{2F^2}, \quad \text{with } \Delta(F) = (3F - 1)^2 - 4F^3,$$

and recalling (6.51), we obtain that the two possible continuous choices of branch for $F^-(t)$ are

$$F_{\pm}^{-}(t) = \frac{1 - 3F \pm \sqrt{\Delta(F)}}{2F^{2}} - c(t), \quad \text{with } \Delta(F) = (3F - 1)^{2} - 4F^{3}.$$
 (6.56)

Moreover, from (6.50), we have that the two possible continuous choices of branch for G(t) are

$$G_{\pm}(t) = -F(t)\,\hat{F}_{\pm}^{-}(t).$$
 (6.57)

Therefore,

• If $\kappa = 0$, since $F(t) = 1 - g(-1)^{2/3} t^{4/3} + o(|t|^{4/3})$ as $t \downarrow 0$, we get from (6.52) and (6.56) that

$$F_{\pm}^{-}(t) = \left(\frac{1-f(0)}{2}\right) - 2ig(-1)^2t + \frac{1}{2}(-1 \pm i\sqrt{3})g(-1)^{2/3}t^{4/3} + o(t^{4/3}),$$

and from (6.57),

$$G_{\pm}(t) = 1 + \frac{1}{2} \left(-g(-1)^{2/3} \mp i\sqrt{3}g(-1)^{2/3} \right) t^{4/3} + o(t^{4/3}).$$

• If $\kappa > 0$, since $F(t) = 1 - \left(\frac{\kappa}{2}\right)^{1/3} t^{2/3} + o(t^{2/3})$ as $t \downarrow 0$, we get from (6.52) and (6.56) that

$$F_{\pm}^{-}(t) = \left(\frac{1 - f(0)}{2}\right) + \frac{1}{2}(-1 \pm i\sqrt{3})\left(\frac{\kappa}{2}\right)^{1/3} t^{2/3} + o(t^{2/3})$$
(6.58)

and from (6.57),

$$G_{\pm}(t) = 1 + \frac{1}{2}(-1 \mp i\sqrt{3})\left(\frac{\kappa}{2}\right)^{1/3}t^{2/3} + o(t^{2/3}).$$

Noting that the conjugate of $F^-(t)$ is the characteristic function of a non-negative integer-valued random variable, and using Proposition 6.1, we have that the only admissible expressions when $\kappa = 0$ are the ones in the proposition statement.

Hence, it remains to prove that the case $\kappa > 0$ is not possible. This does not appear to follow from the recursive equation of Proposition 6.11, and it is the only part of the proof that is not directly parallel to the LDP case. If $\kappa > 0$, then the asymptotics in (6.58) combined with Proposition 6.1 give that as $x \to \infty$,

$$\mathbb{P}[|\mathcal{X}(0) - \mathcal{X}(-1)| \ge x] = c x^{-2/3} + o(x^{-2/3}), \tag{6.59}$$

for some c > 0.

Recall from Theorem 1.4 that $\{x_k\}_{k\in\mathbb{Z}}$ is the sequence of boundary vertices of $M_{0,\infty}$, ordered from left to right so that $\lambda_0 = (x_0, x_1)$. The idea of the proof is to show that $\mathcal{X}(-k)$ is bounded above by O(k) with high probability, which will violate the heavy-tailed central limit theorem if $\kappa > 0$. We will do this using the triangle inequality and the fact that the rightmost directed path started from x_{-k} typically takes O(k) units of time to coalesce into the rightmost directed path started from x_1 (i.e., the right boundary of $M_{0,\infty}$). See Figure 16 for an illustration.

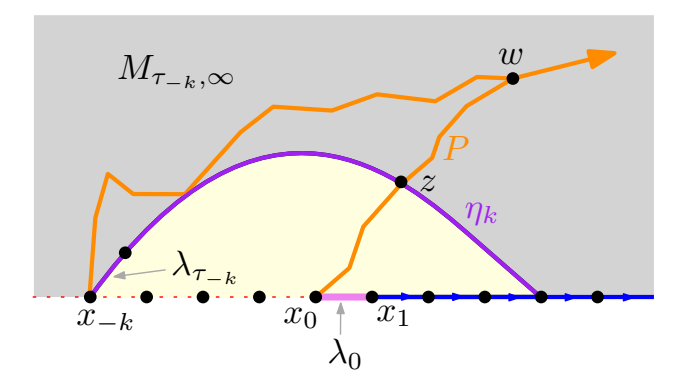


Figure 16: Illustration for the proof that $\kappa > 0$ is not admissible.

For $k \in \mathbb{N}$, let τ_{-k} be the smallest $n \in \mathbb{N}$ which x_{-k} is the initial vertex of λ_n , as in (5.2). By (5.3), τ_{-k} can equivalently be defined as the smallest $n \in \mathbb{N}$ for which $\mathcal{L}(n) = -k$. By the convergence of the re-scaled encoding walk $k^{-1}\mathcal{Z}(\lfloor k^2 \cdot \rfloor)$ to a (correlated) two-dimensional Brownian motion, for each $\delta \in (0,1)$, there exists A > 1 such that for every $k \in \mathbb{N}$, it holds with probability at least $1 - \delta$ that

$$\max_{n \in [0, \tau_{-k}] \cap \mathbb{Z}} |\mathcal{R}(n)| \le Ak. \tag{6.60}$$

Let η_k be the path on the boundary of $M_{\tau_{-k},\infty}$ from x_{-k} to the point where the right boundaries of $M_{\tau_{-k},\infty}$ and $M_{0,\infty}$ meet. Equivalently, η_k consists of the edge $\lambda_{\tau_{-k}}$ followed by the upper-right boundary of the submap of $M_{0,\infty}$ obtained by applying the KMSW procedure to $\mathcal{Z}|_{[0,\tau_{-k}]}$. By Lemma 3.8, η_k is a directed path in $M_{\tau_{-k},\infty}$ started from x_k . By (3.1) of Lemma 3.6, if (6.60) holds, then the length of η_k is at most 2Ak+1. Hence

$$\mathbb{P}[|\eta_k| \le 2Ak + 1] \ge 1 - \delta. \tag{6.61}$$

By Theorem 1.4, there exists a vertex $w = w(k) \in \mathcal{V}(M_{\tau_{-k},\infty})$ such that the SDP Busemann function satisfies

$$SDP_{M_{0,\infty}}(x_{-k}, w) - SDP_{M_{0,\infty}}(x_0, w) = \mathcal{X}(-k) - \mathcal{X}(0) = \mathcal{X}(-k).$$
 (6.62)

Let P be an SDP geodesic from x_0 to w in $M_{0,\infty}$. Since η_k is a path in $M_{0,\infty}$ from x_{-k} to x_r for some $r \geq 0$, topological considerations imply that P must hit a vertex on η_k . Let z be such a vertex. Then

$$SDP_{M_{0,\infty}}(x_0, w) = SDP_{M_{0,\infty}}(x_0, z) + SDP_{M_{0,\infty}}(z, w).$$
(6.63)

On the other hand, concatenating the segment of η_k from x_{-k} to z with the segment of P from z to w gives a directed path from x_{-k} to w. Hence

$$SDP_{M_{0,\infty}}(x_{-k}, w) \le |\eta_k| + SDP_{M_{0,\infty}}(z, w).$$
 (6.64)

We therefore obtain that with probability at least $1 - \delta$,

$$\mathcal{X}(-k) = \text{SDP}_{M_{0,\infty}}(x_{-k}, w) - \text{SDP}_{M_{0,\infty}}(x_0, w)$$
 by (6.62)

$$\leq |\eta_k| - \text{SDP}_{M_{0,\infty}}(x_0, z)$$
 by (6.63) and (6.64)

$$\leq |\eta_k| \leq 2Ak + 1$$
 by (6.61).

Since $\delta \in (0,1)$ is arbitrary, any possible limit in law of the random variable $k^{-3/2}\mathcal{X}(-k)$ is a.s. non-positive. Since $\mathcal{X}(-k) \stackrel{d}{=} -\mathcal{X}(-k)$ by Item (iv) of Theorem 1.7, this implies that $k^{-3/2}\mathcal{X}(-k)$ converges in probability to zero. By the heavy-tailed central limit theorem, this shows that the increments $\mathcal{X}(-k+1) - \mathcal{X}(-k) \stackrel{d}{=} \mathcal{X}(0) - \mathcal{X}(-1)$ for $k \leq 0$ cannot have the tail asymptotic in (6.59). This shows that the case $\kappa > 0$ is not admissible, concluding the entire proof.

Proof of Theorem 1.6. This is immediate from Theorems 1.7 and 1.8 and the heavy-tailed functional central limit theorem (see, e.g., [JS03, Chapter VII]). □

7 The case of finite triangulations

The goal of this section is to prove the finite-volume versions of our results, i.e. Theorems 1.11-1.13. We will first prove the statements for size-n KMSW cells (Theorems 1.12 and 1.13), then use these to deduce the statement for Boltzmann bipolar-oriented triangulations (Theorem 1.11).

7.1 LDP in size-n KMSW cells

Recall that $M_{-\infty,\infty}$ denotes the UIBOT, the random walk $\mathcal{Z} = (\mathcal{L}, \mathcal{R}) : \mathbb{Z} \to \mathbb{Z}^2$ is its KMSW encoding walk as in Proposition 3.10, $\{x_k\}_{k\in\mathbb{Z}}$ is the ordered sequence of boundary vertices of $M_{0,\infty}$ (as in Theorem 1.4), and τ_k (introduced in (5.2)) is the smallest $n \in \mathbb{N}$ such that x_k is the initial vertex of the active edge λ_n .

For $n \in \mathbb{N}$, let $M_{0,n}$ be the submap of $M_{0,\infty}$ obtained by applying the KMSW procedure (Definition 3.3) to $\mathcal{Z}|_{[0,n]}$, as in Section 1.3.2. In this subsection we will deduce Theorem 1.12 from our results for the UIBOT.

We will only be working with longest directed paths in this subsection, so in what follows we assume that \mathcal{X} is the Busemann function in Theorem 1.4 with XDP = LDP. The following deterministic lemma is the main input in the proof of the lower bound for LDP distances in $M_{0,n}$.

Lemma 7.1. Let $l, k \in \mathbb{N}$ with l < k and recall that τ_{-k} is the time from (5.2). There is a directed path contained in $M_{0,\tau_{-k}}$ with length at least

$$\max\{\mathcal{X}(-l) - \mathcal{X}(-k), 0\}.$$

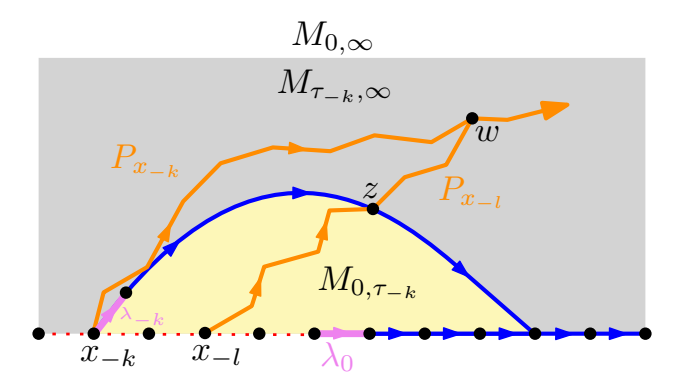


Figure 17: Illustration of the proof of Lemma 7.1. We prove a lower bound for the length of the segment of the leftmost LDP geodesic $P_{x_{-l}}$ before it hits z.

Proof. This is an elementary geometric argument. See Figure 17 for an illustration. To lighten notation, we abbreviate LDP = LDP_{$M_{0,\infty}$}. Let $P_{x_{-l}}$ and $P_{x_{-k}}$ be the leftmost LDP geodesics in $M_{0,\infty}$ from x_{-l} and x_{-k} to ∞ , as in Lemma 5.4.

Let T be the smallest time for which the edge $P_{x_{-l}}(T+1)$ does not belong to $M_{0,\tau_{-k}}$ and let z be the initial vertex of $P_{x_{-l}}(T+1)$. Then $P_{x_{-l}}|_{[0,T]}$ is a directed path in $M_{0,\tau_{-k}}$ from x_{-l} to z, of length $T = \text{LDP}(x_{-l}, z)$. We will prove a lower bound for this length.

Let w be any vertex with the property that the segments of $P_{x_{-l}}$ and $P_{x_{-k}}$ after they hit w are identical (such a vertex exists by Lemma 5.4). By the definition of the Busemann function in Theorem 1.4, we can choose w so that

$$LDP(x_{-l}, w) - LDP(x_{-k}, w) = \mathcal{X}(-l) - \mathcal{X}(-k). \tag{7.1}$$

The vertices x_{-k} and z each lie on the right boundary of $M_{\tau_{-k},\infty}$. The segment of this right boundary between x_{-k} and z is a directed path from x_{-k} to z in $M_{0,\infty}$. Therefore,

$$LDP(z, w) \le LDP(x_{-k}, w). \tag{7.2}$$

Since z and w are both hit by the LDP geodesic $P_{x_{-1}}$,

$$LDP(x_{-l}, w) = LDP(x_{-l}, z) + LDP(z, w).$$

$$(7.3)$$

We have

$$LDP(x_{-l}, z) = LDP(x_{-l}, w) - LDP(z, w)$$
 by (7.3)

$$= \mathcal{X}(-l) - \mathcal{X}(-k) + LDP(x_{-k}, w) - LDP(z, w)$$
 by (7.1)

$$\geq \mathcal{X}(-l) - \mathcal{X}(-k)$$
 by (7.2).

As we saw above, the directed path $P_{x_{-l}}|_{[0,T]}$ is a directed path in $M_{0,\tau_{-k}}$ with length LDP (x_{-l},z) , so this concludes the proof.

We can now prove the lower bound in Theorem 1.12. We actually obtain a slightly more quantitative statement.

Lemma 7.2. For each $n \in \mathbb{N}$ and A > 1,

$$\mathbb{P}\left[M_{0,n} \text{ contains a directed path of length at least } A^{-1}n^{3/4}\right] \ge 1 - A^{-2/3 + o(1)}, \tag{7.5}$$

where the o(1) goes to zero as $A \to \infty$, at a rate which is uniform in n.

Proof. Fix $\varepsilon > 0$, which we will eventually send to zero to get the o(1) error in (7.5). By Theorem 1.7, the increments $\mathcal{X}(-k+1) - \mathcal{X}(-k)$ for $k \ge 1$ are i.i.d. By Theorem 1.8, there is a universal constant $c_1 > 0$ such that for all $k \ge 1$

$$\mathbb{P}\left[\mathcal{X}(-k+1) - \mathcal{X}(-k) \ge A^{-1}n^{3/4}\right] \ge c_1 A^{2/3} n^{-1/2}.$$
 (7.6)

By multiplying the bound (7.6) over $|A^{-2/3+\varepsilon}n^{1/2}|$ values of k, we obtain

$$\mathbb{P}\left[\max\left\{\mathcal{X}(-k+1) - \mathcal{X}(-k) : k \in [1, A^{-2/3 + \varepsilon} n^{1/2}] \cap \mathbb{Z}\right\} \ge A^{-1} n^{3/4}\right] \\
\ge 1 - \left(1 - c_1 A^{2/3} n^{-1/2}\right)^{\lfloor A^{-2/3 + \varepsilon} n^{1/2} \rfloor} \\
\ge 1 - c_2 e^{-c_3 A^{\varepsilon}} \tag{7.7}$$

for constants $c_2, c_3 > 0$ depending only on ε .

The process \mathcal{L} is a random walk with i.i.d. increments sampled uniformly from $\{-1,0,1\}$. By (5.3), the time τ_{-k} is the first positive time at which \mathcal{L} hits -k. By standard estimates for random walk,

$$\mathbb{P}\left[\tau_{-\lfloor A^{-2/3+\varepsilon}n^{1/2}\rfloor} \le n\right] \ge 1 - c_4 A^{-2/3+\varepsilon},\tag{7.8}$$

for a universal constant $c_4 > 0$.

By Lemma 7.1, if the event in (7.7) occurs, then the map $M_{0,\tau_{-\lfloor A^{-2/3+\varepsilon_n 1/2}\rfloor}}$ contains a directed path of length at least $A^{-1}n^{3/4}$. If the event in (7.8) also occurs, then $M_{0,n}$ also contains a directed path of length at least $A^{-1}n^{3/4}$. These events occur simultaneously with probability at least $1 - O(A^{-2/3+\varepsilon})$. Since $\varepsilon > 0$ is arbitrary, this gives (7.5).

We now turn our attention to the upper bound. The main input is the following elementary estimate for the maximum of the Busemann function.

Lemma 7.3. For each $k \in \mathbb{N}$ and A > 1,

$$\mathbb{P}\left[\max_{l\in[-k,k]\cap\mathbb{Z}}|\mathcal{X}(l)| \le Ak^{3/2}\right] \ge 1 - O(A^{-2/3}),\tag{7.9}$$

with the implicit constant in the O(1) uniform in k.

Proof. By Theorems 1.7 and 1.8, the increments $\mathcal{X}(l) - \mathcal{X}(l-1)$ are independent and each $|\mathcal{X}(l) - \mathcal{X}(l-1)|$ is stochastically dominated by a positive 2/3-stable random variable (the scale parameter for this stable random variable can be taken to be uniform in l by the stationarity property in Theorem 1.7). Hence, we can couple \mathcal{X} with a collection $\{Y_l\}_{l\in\mathbb{Z}}$ of i.i.d. stable random variables in such a way that $|\mathcal{X}(l) - \mathcal{X}(l-1)| \leq Y_l$ for each $l \in \mathbb{Z}$. Under this coupling,

$$\max_{l \in [-k,k] \cap \mathbb{Z}} |\mathcal{X}(l)| \le \sum_{l=-k+1}^{k} Y_l,$$

which has the same law as $(2k)^{3/2}Y_0$ by the stability property. The bound (7.9) then follows from the standard tail estimate for the stable distribution.

Lemma 7.4. For each $n \in \mathbb{N}$ and A > 1,

$$\mathbb{P}\left[\max\left\{\text{LDP}_{M_{0,n}}(x,y): x, y \in \mathcal{V}(M_{0,n})\right\} \le An^{3/4}\right] \ge 1 - A^{-2/3 + o(1)}$$
(7.10)

where the o(1) goes to zero as $A \to \infty$, uniformly in n, and we set $LDP_{M_{0,n}}(x,y) = -\infty$ if there is no directed path in $M_{0,n}$ from x to y.

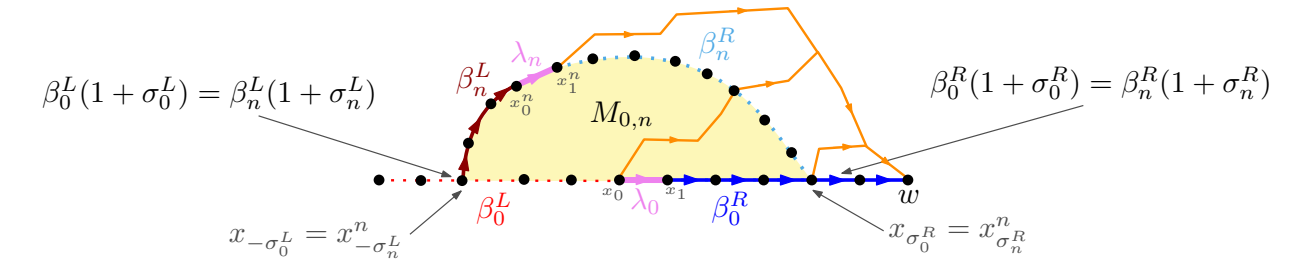


Figure 18: Illustration of the proofs of Lemmas 7.4 and 7.8. The edge λ_0 is part of β_0^R and the edge λ_n is part of β_n^R .

Proof. Recall that $M_{n,\infty}$ is the submap of $M_{-\infty,\infty}$ obtained by applying the KMSW procedure to $(\mathcal{Z}(\cdot+n)-\mathcal{Z}(n))|_{[0,\infty)}$. Let \mathcal{X}_n be the Busemann function for $M_{n,\infty}$, defined in the same way as \mathcal{X} but with $M_{n,\infty}$ in place of $M_{0,\infty}$. Since $M_{n,\infty}\stackrel{d}{=}M_{0,\infty}$, we have $\mathcal{X}\stackrel{d}{=}\mathcal{X}_n$. The basic idea of the proof is as follows. By (3.1) of Lemma 3.6, the number of edges on the boundary of $M_{0,n}$ is bounded above by $2\max_{j\in[0,n]\cap\mathbb{Z}}|\mathcal{Z}(j)|+1$ (with $|\mathcal{Z}(j)|$ denoting the Euclidean norm), which is typically of order $n^{1/2}$. Using Lemma 7.3, we can therefore upper-bound the maximal values of each of $|\mathcal{X}|$ and $|\mathcal{X}_n|$ at the times corresponding to vertices on the boundary of $M_{0,n}$ by $O(n^{3/4})$ (see (7.13)). If there is a long directed path between two vertices of $M_{0,n}$, then by concatenating paths we would find that the values of $|\mathcal{X}_n|$ on the upper boundary of $M_{0,n}$ are much larger than the values of $|\mathcal{X}|$ on the lower boundary of $M_{0,n}$. This would violate our bounds for \mathcal{X} and \mathcal{X}_n . We now proceed with the details. See Figure 18 for an illustration.

Step 1: bounds for \mathcal{X} and \mathcal{X}_n . Recall that $M_{0,n} = M_{0,\infty} \setminus M_{n+1,\infty}$. Let β_0^R (resp. β_n^R) be the directed path which traverses the portion of the boundary of $M_{0,\infty}$ (resp. $M_{n,\infty}$) lying to the right of the initial vertex of λ_0 (resp. initial vertex of λ_n). Let σ_0^R and σ_n^R be chosen so that $\beta_0^R|_{[0,\sigma_0^R]}$ and $\beta_n^R|_{[0,\sigma_n^R]}$ traverse the entirety of the upper-right and lower-right boundaries of $M_{0,n}$, respectively (recall Definition 3.3). Then

$$\beta_0^R(k + \sigma_0^R) = \beta_n^R(k + \sigma_n^R), \quad \forall k \ge 1.$$

$$(7.11)$$

In an exactly analogous manner, we also define the left boundary paths β_0^L and β_n^L and the times σ_0^L and σ_n^L , for which (7.11) holds with L in place of R.

By (3.1) of Lemma 3.6, σ_0^R , σ_n^R , σ_0^L , σ_n^L are each bounded above by $2 \max_{j \in [0,n] \cap \mathbb{Z}} |\mathcal{Z}(j)| + 1$. By Hoeffding's inequality for sums of i.i.d. bounded random variables, for any fixed $\varepsilon \in (0,1)$,

$$\mathbb{P}\left[\max\left\{\sigma_0^R, \sigma_n^R, \sigma_0^L, \sigma_n^L\right\} \le A^{\varepsilon} n^{1/2}\right] \ge 1 - c_1 e^{-c_2 A^{2\varepsilon}} \tag{7.12}$$

for universal constants $c_1, c_2 > 0$.

By (7.12) combined with Lemma 7.3 (applied once for each of \mathcal{X} and \mathcal{X}_n and with $k = A^{\varepsilon} n^{1/2}$), it holds with probability at least $1 - O(A^{-2(1-\varepsilon)/3})$ that

$$\max \left\{ \max_{l \in [-\sigma_0^L, \sigma_0^R] \cap \mathbb{Z}} |\mathcal{X}(l)|, \max_{l \in [-\sigma_n^L, \sigma_n^R] \cap \mathbb{Z}} |\mathcal{X}_n(l)| \right\} \le An^{3/4}. \tag{7.13}$$

Step 2: relating \mathcal{X} and \mathcal{X}_n to longest directed paths. Henceforth assume that the event in (7.13) occurs. Let $\{x_k^n\}_{k\in\mathbb{Z}}$ (resp. $\{x_k\}_{k\in\mathbb{Z}}$) be the vertices on the boundary of $M_{n,\infty}$ (resp. $M_{0,\infty}$),

enumerated in west to east order so that $\lambda_n = (x_0^n, x_1^n)$ (resp. $\lambda_0 = (x_0, x_1)$). By (7.11) and its analog with L in place of R,

$$x_{k+\sigma_0^R} = x_{k+\sigma_n^R}^n$$
 and $x_{-k-\sigma_0^L} = x_{-k-\sigma_n^L}^n$, $\forall k \ge 0$. (7.14)

By the definition of the Busemann function in Theorem 1.4, applied, e.g., to a sequence of points $\{w_i\}_{i\in\mathbb{N}}$ on the right boundary of $M_{0,\infty}$, we can find a vertex w of $M_{0,\infty}$ such that

$$\mathcal{X}(l) = \mathrm{LDP}_{M_{0,\infty}}(x_l, w) - \mathrm{LDP}_{M_{0,\infty}}(x_0, w), \quad \forall l \in [-\sigma_0^L, \sigma_0^R] \cap \mathbb{Z} \quad \text{and}$$

$$\mathcal{X}_n(l) = \mathrm{LDP}_{M_{n,\infty}}(x_l^n, w) - \mathrm{LDP}_{M_{n,\infty}}(x_0^n, w), \quad \forall l \in [-\sigma_n^L, \sigma_n^R] \cap \mathbb{Z}. \tag{7.15}$$

We claim that every directed path in $M_{0,\infty}$ started from $x_{\sigma_n^R}^n$ must stay in $M_{n,\infty}$. Indeed, such a path cannot hit the boundary of $M_{n,\infty}$ to the west of $x_{\sigma_n^R}^n$ since this would create a directed cycle in $M_{-\infty,\infty}$. Such a path cannot cross the boundary of $M_{n,\infty}$ to the east of $x_{\sigma_n^R}^n$ since by the definition of σ_n^R , the portion of the boundary of $M_{n,\infty}$ to the right of $x_{\sigma_n^R}^n$ is also part of the boundary of $M_{0,\infty}$. By (7.14), $x_{\sigma_n^R}^n = x_{\sigma_0^R}$. Hence

$$LDP_{M_{n,\infty}}(x_{\sigma_n^R}^n, w) = LDP_{M_{0,\infty}}(x_{\sigma_0^R}, w).$$

$$(7.16)$$

We thus obtain that with probability at least $1 - O(A^{-2(1-\varepsilon)/3})$

$$\begin{aligned} \left| \text{LDP}_{M_{n,\infty}}(x_0^n, w) - \text{LDP}_{M_{0,\infty}}(x_0, w) \right| \\ &\leq \left| \text{LDP}_{M_{n,\infty}}(x_{\sigma_n^R}^n, w) - \text{LDP}_{M_{0,\infty}}(x_{\sigma_0^R}, w) \right| + \left| \mathcal{X}_n(\sigma_n^R) - \mathcal{X}(\sigma_0^R) \right| & \text{by (7.15)} \\ &= \left| \mathcal{X}_n(\sigma_n^R) - \mathcal{X}(\sigma_0^R) \right| & \text{by (7.16)} \\ &\leq 2An^{3/4} & \text{by (7.13).} \end{aligned}$$

Step 3: bound for paths in $M_{0,n}$. Now let $x, y \in \mathcal{V}(M_{0,n})$ be vertices which can be joined by a directed path in $M_{0,n}$. There is a vertex on $\partial M_{0,n} \cap \partial M_{0,\infty}$, i.e., a vertex x_l for $l \in [-\sigma_0^L, \sigma_0^R] \cap \mathbb{Z}$, which can be joined to x by a directed path in $M_{0,n}$. Indeed, it is enough to consider a segment of the upper-left boundary of $M_{0,j}$ (whose edges are included in $M_{0,j}$), where $j \in [0,n] \cap \mathbb{Z}$ is chosen so that x is one of the vertices of λ_j . Similarly, there exists $k \in [-\sigma_n^L, \sigma_n^R]$ such that y can be joined to x_k^n by a directed path in $M_{0,n}$. By concatenating paths from x_l to x to y to x_k^n to x, we get

$$LDP_{M_{0,\infty}}(x_l, w) \ge LDP_{M_{0,n}}(x, y) + LDP_{M_{n,\infty}}(x_k^n, w).$$

Re-arranging gives that with probability at least $1 - O(A^{-2(1-\varepsilon)/3})$

$$LDP_{M_{0,n}}(x,y) \leq LDP_{M_{0,\infty}}(x_l, w) - LDP_{M_{n,\infty}}(x_k^n, w)
= LDP_{M_{0,\infty}}(x_0, w) - LDP_{M_{n,\infty}}(x_0^n, w) + \mathcal{X}(l) - \mathcal{X}_n(k) \quad \text{by (7.15)}
\leq 4An^{3/4} \quad \text{by (7.13) and (7.17)}.$$

Since $\varepsilon > 0$ is arbitrary, this gives (7.10).

Proof of Theorem 1.12. Combine Lemmas 7.2 and 7.4. \Box

7.2 SDP in size-n KMSW cells

In this section, we prove Theorem 1.13. Throughout, we assume that \mathcal{X} is the Busemann function of Theorem 1.4 with XDP = SDP. We also let $\{x_k\}_{k\in\mathbb{Z}}$ be the ordered sequence of vertices on the boundary of $M_{0,\infty}$, as in Theorem 1.4, so that x_0 is the initial vertex of the root edge. We begin with a lower bound for shortest directed paths.

Lemma 7.5. Almost surely, for each $l, k \in \mathbb{Z}_{>0}$ with l < k,

$$SDP_{M_{0,\infty}}(x_l, x_k) \ge \mathcal{X}(l) - \mathcal{X}(k). \tag{7.18}$$

Proof. By the definition of the Busemann function (Theorem 1.4), we can find $w \in M_{0,\infty}$ (depending on l and k) such that

$$\mathcal{X}(k) - \mathcal{X}(l) = \text{SDP}_{M_{0,\infty}}(x_k, w) - \text{SDP}_{M_{0,\infty}}(x_l, w). \tag{7.19}$$

Concatenating a directed path from x_l to x_k with a directed path from x_k to w gives a directed path from x_l to w, so

$$SDP_{M_{0,\infty}}(x_l, w) \le SDP_{M_{0,\infty}}(x_k, w) + SDP(x_l, x_k). \tag{7.20}$$

(Note that there is at least one directed path from x_l to x_k , namely a segment of the right boundary of $M_{0,\infty}$.) By re-arranging (7.20), then applying (7.19), we get (7.18).

Lemma 7.6. Recall the definition of the lower-right boundary of $M_{0,n}$ from Definition 3.3, and recall that $M_{0,n}$ contains all of the edges on its lower-right boundary. For each $\delta > 0$, there exists $A = A(\delta) > 1$ such that for each $n \in \mathbb{N}$, the following is true. With probability at least $1 - \delta$, there exists a vertex y on the lower-right boundary of $M_{0,n}$ such that

$$SDP_{M_{0,n}}(x_0, y) \ge A^{-1}n^{3/8}.$$

Proof. By Theorem 1.6, the re-scaled Busemann function $k^{-3/4}\mathcal{X}(\lfloor k \cdot \rfloor)$ restricted to positive times converges in the scaling limit when $k \to \infty$ to a 4/3-stable Lévy process with only positive jumps. Such a process has probability zero to stay positive during any positive-length time interval. From this, we get that there exists $A = A(\delta) > 1$ and $k_* = k_*(\delta) \in \mathbb{N}$ such that for each $k \geq k_*$, (the choice of $A^{-1/2}$ is for later convenience)

$$\mathbb{P}\left[\exists r \in [0, k] \cap \mathbb{Z} \text{ such that } \mathcal{X}(r) \le -A^{-1/2}k^{3/4}\right] \ge 1 - \delta/2. \tag{7.21}$$

The second coordinate \mathcal{R} of the KMSW encoding function is a random walk with i.i.d. increments sampled uniformly from $\{-1,0,1\}$. By (5.3), when $k \geq 1$, the time τ_k (which is the smallest time j that x_k is the initial vertex of λ_j) is the first positive time at which \mathcal{R} it hits -k. By standard estimates for random walks, there exists $A = A(\delta) > 1$ such that (7.21) holds and for each large enough $n \in \mathbb{N}$ (how large depends only on δ),

$$\mathbb{P}\left[\tau_{\lceil A^{-1/2}n^{1/2}\rceil} \le n\right] \ge 1 - \delta/2. \tag{7.22}$$

If $\tau_{\lceil A^{-1/2}n^{1/2}\rceil} \leq n$, then the vertices $x_1, \ldots, x_{\lceil A^{-1/2}n^{1/2}\rceil}$ all lie on the lower-right boundary of $M_{0,n}$. By (7.21) (with $k = \lceil A^{-1/2}n^{1/2}\rceil$) and (7.22), for each sufficiently large $n \in \mathbb{N}$ (how large depends only on δ), the following is true. It holds with probability at least $1 - \delta$ that there exists

 $r \in \mathbb{N}$ such that x_r lies on the lower-right boundary of $M_{0,n}$ and $\mathcal{X}(r) \leq -A^{-1}n^{3/8}$. By Lemma 7.5 (applied with (0,r) in place of (l,k)), this implies that

$$SDP_{M_{0,\infty}}(x_0, x_r) \ge A^{-1} n^{3/8}.$$
 (7.23)

Since $M_{0,n} \subset M_{0,\infty}$, we have $SDP_{M_{0,n}}(x_0,x_r) \geq SDP_{M_{0,\infty}}(x_0,x_r)$, which concludes the proof after enlarging the constant A so that the bound in (7.23) holds for all $n \in \mathbb{N}$ (this is always possible because $SDP_{M_{0,n}}(x_0,x_1) \geq 1$ since $\lambda_0 = (x_0,x_1)$ is in $M_{0,n}$ for all $n \in \mathbb{N}$).

Next we prove an upper bound for the SDP in $M_{0,n}$, which will be done via a similar argument as in the LDP case (Lemma 7.4).

Lemma 7.7. For each $k \in \mathbb{N}$, it holds with probability tending to 1 as $A \to \infty$ (uniformly in k) that

$$\max_{l \in [-k,k] \cap \mathbb{Z}} |\mathcal{X}(l)| \le Ak^{3/4}. \tag{7.24}$$

Proof. This is immediate from the fact that $k^{-3/4}X(\lfloor k \cdot \rfloor)$ converges in law to a stable Lévy process (Theorem 1.6).

Lemma 7.8. For each $n \in \mathbb{N}$, it holds with probability tending to 1 as $A \to \infty$ (uniformly in n) that the following is true:

- For every vertex x on the lower boundary of $M_{0,n}$, there exists a vertex y on the upper boundary of $M_{0,n}$ such that $SDP_{M_{0,n}}(x,y) \leq An^{3/8}$.
- For every vertex y on the upper boundary of $M_{0,n}$, there exists a vertex x on the lower boundary of $M_{0,n}$ such that $SDP_{M_{0,n}}(x,y) \leq An^{3/8}$.

Proof. The proof is very similar to that of Lemma 7.4, except for some minor changes in Step 3. So, we will be brief. See again Figure 18 for an illustration. Let \mathcal{X}_n be the Busemann function for $M_{n,\infty}$, defined in the same way as \mathcal{X} but with $M_{n,\infty}$ in place of $M_{0,\infty}$. Since $M_{n,\infty} \stackrel{d}{=} M_{0,\infty}$, we have $\mathcal{X} \stackrel{d}{=} \mathcal{X}_n$.

Step 1: bounds for \mathcal{X} and \mathcal{X}_n . Let β_0^R (resp. β_n^R) be the directed path which traverses the portion of the boundary of $M_{0,\infty}$ (resp. $M_{n,\infty}$) lying to the right of the initial vertex of λ_0 (resp. λ_n). Let σ_0^R and σ_n^R be chosen so that $\beta_0^R|_{[0,\sigma_0^R]}$ and $\beta_n^R|_{[0,\sigma_n^R]}$ traverse the entirety of the upper-right and lower-right boundaries of $M_{0,n}$, respectively (recall Definition 3.3). Then

$$\beta_0^R(k+\sigma_0^R) = \beta_n^R(k+\sigma_n^R), \quad \forall k \ge 1. \tag{7.25}$$

In an exactly analogous manner, we also define the left boundary paths β_0^L and β_n^L and the times σ_0^L and σ_n^L , for which (7.11) holds with L in place of R.

By Lemma 7.7, applied exactly as in the proof of (7.13) from Lemma 7.4, it holds with probability tending to 1 as $A \to \infty$ (uniformly in n) that

$$\max \left\{ \max_{l \in [-\sigma_L^I, \sigma_0^R] \cap \mathbb{Z}} |\mathcal{X}(l)|, \max_{l \in [-\sigma_L^I, \sigma_n^R] \cap \mathbb{Z}} |\mathcal{X}_n(l)| \right\} \le An^{3/8}. \tag{7.26}$$

Step 2: relating \mathcal{X} and \mathcal{X}_n to longest directed paths. Henceforth assume that the event in (7.26) occurs. Let $\{x_k\}_{k\in\mathbb{Z}}$ be the vertices on the boundary of $M_{0,\infty}$, enumerated in west to east order so

that $\lambda_0 = (x_0, x_1)$. Similarly, let $\{x_k^n\}_{k \in \mathbb{Z}}$ be the vertices on the boundary of $M_{n,\infty}$, enumerated in west to east order so that $\lambda_n = (x_0^n, x_1^n)$. By (7.11) and its analog with L in place of R,

$$x_{k+\sigma_0^R} = x_{k+\sigma_n^R}^n \quad \text{and} \quad x_{-k-\sigma_0^L} = x_{-k-\sigma_n^L}^n, \quad \forall k \ge 0.$$
 (7.27)

By the definition of the Busemann function in Theorem 1.4, applied, e.g., to a sequence of points $\{w_i\}_{i\in\mathbb{N}}$ on the right boundary of $M_{0,\infty}$, we can find a vertex w of $M_{0,\infty}$ such that

$$\mathcal{X}(l) = \mathrm{SDP}_{M_{0,\infty}}(x_l, w) - \mathrm{SDP}_{M_{0,\infty}}(x_0, w), \quad \forall l \in [-\sigma_0^L, \sigma_0^R] \cap \mathbb{Z} \quad \text{and}$$

$$\mathcal{X}_n(l) = \mathrm{SDP}_{M_{n,\infty}}(x_l^n, w) - \mathrm{SDP}_{M_{n,\infty}}(x_0^n, w), \quad \forall l \in [-\sigma_n^L, \sigma_n^R] \cap \mathbb{Z}. \tag{7.28}$$

By the same argument leading to (7.16),

$$SDP_{M_{n,\infty}}(x_{\sigma_n^R}^n, w) = SDP_{M_{0,\infty}}(x_{\sigma_n^R}, w). \tag{7.29}$$

By exactly the same calculation as in (7.17), we then obtain with probability tending to 1 as $A \to \infty$ (uniformly in n)

$$\begin{aligned} \left| \operatorname{SDP}_{M_{n,\infty}}(x_0^n, w) - \operatorname{SDP}_{M_{0,\infty}}(x_0, w) \right| \\ &\leq \left| \operatorname{SDP}_{M_{n,\infty}}(x_{\sigma_n^R}^n, w) - \operatorname{SDP}_{M_{0,\infty}}(x_{\sigma_0^R}, w) \right| + \left| \mathcal{X}_n(\sigma_n^R) - \mathcal{X}(\sigma_0^R) \right| & \text{by (7.28)} \\ &= \left| \mathcal{X}_n(\sigma_n^R) - \mathcal{X}(\sigma_0^R) \right| & \text{by (7.29)} \\ &\leq 2An^{3/8} & \text{by (7.26).} \end{aligned}$$

Step 3: bound for paths in $M_{0,n}$. Let x be a vertex on the lower boundary $M_{0,n}$. Let $P_x : \mathbb{N} \to \mathcal{E}(M_{0,\infty})$ be an SDP geodesic from x to ∞ in $M_{0,\infty}$ (which exists by Lemma 5.4). Let T be the smallest time for which $P_x(T+1) \notin M_{0,n}$ and let z be the initial vertex of $P_x(T+1)$. Then z lies on the upper boundary $M_{0,n}$. Since z is hit by the SDP geodesic P_x ,

$$SDP_{M_{0,n}}(x,z) = SDP_{M_{0,\infty}}(x,z) = SDP_{M_{0,\infty}}(x,w) - SDP_{M_{0,\infty}}(z,w).$$
 (7.31)

We can write $x = x_l$ and $z = x_k^n$ for some $l \in [-\sigma_0^L, \sigma_0^R] \cap \mathbb{Z}$ and $k \in [-\sigma_n^L, \sigma_n^R] \cap \mathbb{Z}$. We then have with probability tending to 1 as $A \to \infty$ (uniformly in n)

$$SDP_{M_{0,n}}(x,z) = SDP_{M_{0,\infty}}(x_l, w) - SDP_{M_{0,\infty}}(x_k^n, w)$$
 by (7.31)

$$= \mathcal{X}(l) - \mathcal{X}_n(k) + SDP_{M_{0,\infty}}(x_0, w) - SDP_{M_{0,\infty}}(x_0^n, w)$$
 by (7.28)

$$\leq 4An^{3/8}$$
 by (7.26) and (7.30).

Since A > 1 is arbitrary, we get that with probability tending to 1 as $n \to \infty$, each vertex on the lower boundary of $M_{0,n}$ can be joined to the upper boundary by a directed path of length at most $An^{3/8}$.

The statement with the upper and lower boundaries revered follows since the law of $M_{0,n}$ is invariant under reversing the orientations of the edges and applying an orientation-reversing homeomorphism $\mathbb{C} \to \mathbb{C}$. This, in turn, follows since $\mathcal{Z}(n-\cdot)-\mathcal{Z}(n)$ has the same law as $(\mathcal{R}(\cdot),\mathcal{L}(\cdot))$.

7.3 Boltzmann bipolar-oriented triangulations

In this section we will prove Theorem 1.11. The key idea is to find a submap $\widehat{M}(r) \subset M_{0,\infty}$ with a marked left boundary vertex $\widehat{z}(r)$ such that $(\widehat{M}(r), \widehat{z}(r))$ has the same law as the pair (M(r), z(r)) from the theorem statement; see Lemma 7.9. Once we have done this, the proof of Theorem 1.11 will proceed by comparing the map $\widehat{M}(r)$ to the map $M_{0,n}$ from Theorems 1.12 and 1.13, with n chosen to be comparable to r^2 .

To find the map $\widehat{M}(r)$, we first let $\widehat{M}_{0,\infty} \subset M_{0,\infty}$ be as in Proposition 5.1, so that $\widehat{M}_{0,\infty}$ has the law of the UIQBOT (Definition 4.1). Recall that \mathcal{Z} is the KMSW encoding walk for the UIBOT $M_{-\infty,\infty}$ as in Proposition 3.10. Let $\widehat{\mathcal{Z}} = (\widehat{\mathcal{L}}, \widehat{\mathcal{R}})$ be the KMSW encoding walk for $\widehat{M}_{0,\infty}$, so that $\widehat{\mathcal{Z}}$ is obtained by conditioning \mathcal{Z} on the event that its first coordinate stays non-negative for all time (Definition 4.1).

We couple $\widehat{\mathcal{Z}}$ and \mathcal{Z} together as in (5.17): that is, for $m \in \mathbb{N}$ let $S_m \in \mathbb{N}_0$ be the smallest number for which

$$m = \# \left\{ n \le S_m : \lambda_n \in \widehat{M}_{0,\infty} \right\}. \tag{7.32}$$

Then we can take $\widehat{\mathcal{Z}}(0) = (0,0)$ and

$$\widehat{\mathcal{Z}}(m) - \widehat{\mathcal{Z}}(m-1) = \mathcal{Z}(S_m) - \mathcal{Z}(S_m-1), \quad \forall m \ge 1.$$
(7.33)

By Lemma 5.13, the walk defined by (7.33) is indeed the KMSW encoding walk for $\widehat{M}_{0,\infty}$.

We now identify a submap of $M_{0,\infty}$ which has the same law as the Boltzmann map of Theorem 1.11. See Figure 19 for an illustration.

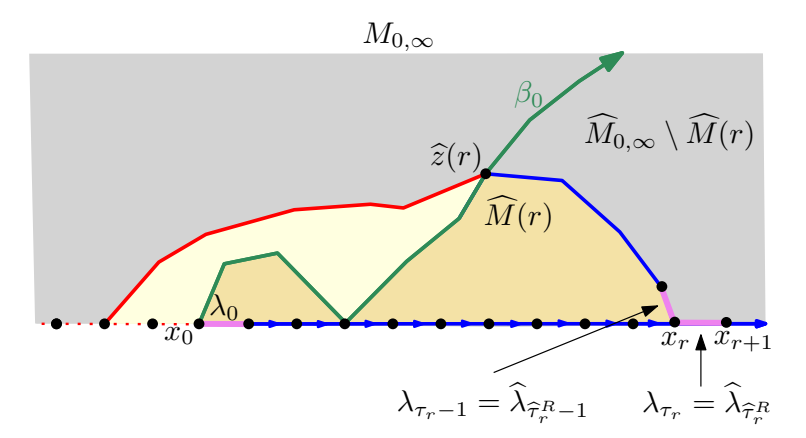


Figure 19: The map $\widehat{M}(r) \subset \widehat{M}_{0,\infty}$, which has sink x_0 , source x_r , and marked left boundary vertex $\widehat{z}(r)$. We show in Lemmas 7.9 that $(\widehat{M}(r), \widehat{z}(r))$ has the same law as a Boltzmann bipolar-oriented triangulation with right boundary length r and a marked left boundary vertex.

Lemma 7.9. For
$$r \ge 1$$
, let
$$\widehat{\tau}_r^R := \min \left\{ n \in \mathbb{N} : \widehat{\mathcal{R}}(n) = -r \right\}. \tag{7.34}$$

Let $\widehat{M}(r)$ be the submap of $\widehat{M}_{0,\infty}$ obtained by applying the KMSW procedure to $\widehat{\mathcal{Z}}|_{[0,\widehat{\tau}_r^R-1]}$. Also, let $\widehat{z}(r)$ be the last (in directed order) vertex on the left boundary of $\widehat{M}(r)$ which also lies on the left boundary of $\widehat{M}_{0,\infty}$. Then the law of $(\widehat{M}(r),\widehat{z}(r))$ is the Boltzmann distribution on bipolar-oriented triangulations with right boundary length r and a marked left boundary vertex (Definition 1.10).

In particular, $\widehat{M}(r)$ is a bipolar-oriented map with no missing edges. Moreover, with probability tending to one as $A \to \infty$, uniformly in the choice of r,

$$A^{-1}r^2 \le \#\mathcal{E}(\widehat{M}(r)) \le Ar^2. \tag{7.35}$$

Proof. Recalling the comment immediately after Definition 1.10, it is enough to show the following:

- $\widehat{M}(r)$ is sampled from the Boltzmann distribution on bipolar-oriented triangulations with right boundary length r (Definition 1.10), weighted by (a constant times) L+1, where L is the left boundary length.
- Conditional on $\widehat{M}(r)$, $\widehat{z}(r)$ is uniformly sampled from the set of left boundary vertices of $\widehat{M}(r)$.

We start by determining the marginal law of $\widehat{M}(r)$. For $r \geq 1$, as in (5.2) and (5.3), let τ_r be the smallest $n \in \mathbb{N}$ for which the unconditioned walk \mathcal{Z} satisfies $\mathcal{R}(n) = -r$. By the definition of $\widehat{\mathcal{Z}}$ (recall (4.1)), the law of $\widehat{\mathcal{Z}}|_{[0,\widehat{\tau}_r^R]}$ is the same as the law of $\mathcal{Z}|_{[0,\tau_r]}$ weighted by the Radon-Nikodym derivative

$$(\mathcal{L}(\tau_r) + 1)\mathbb{1}\{\mathcal{L}(j) \ge 0, \ \forall j \in [0, \tau_r] \cap \mathbb{Z}\}.$$

Since the event in the indicator function is the same as the conditioning event in Lemma 3.11, this lemma implies that the marginal law of $\widehat{M}(r)$ is as described in the first item above.

We now show that the conditional law of $\widehat{z}(r)$ given $\widehat{M}(r)$ is uniform on the set of left boundary vertices of $\widehat{M}(r)$. The map $\widehat{M}(r)$ has $\widehat{\mathcal{L}}(\widehat{\tau}_r^R)+1$ vertices on its left boundary. Let $\widehat{l}_r \in \mathbb{N}_0$ be chosen so that $\widehat{z}(r)$ is the \widehat{l}_r th vertex in order along the left boundary of $\widehat{M}(r)$. By Assertion (i) of Lemma 3.6 applied to the walk $\widehat{\mathcal{Z}}|_{\widehat{\tau}_r^R-1,\infty}$ and since $\widehat{\mathcal{Z}}(\widehat{\tau}_r^R)-\widehat{\mathcal{Z}}(\widehat{\tau}_r^R-1)=(1,-1)$, i.e. $\widehat{\mathcal{L}}(\widehat{\tau}_r^R)-\widehat{\mathcal{L}}(\widehat{\tau}_r^R-1)=1$,

$$\widehat{l}_r = \min \left\{ \widehat{\mathcal{L}}(j) : j \ge \widehat{\tau}_r^R - 1 \right\} = \min \left\{ \widehat{\mathcal{L}}(j) : j \ge \widehat{\tau}_r^R \right\}. \tag{7.36}$$

By the strong Markov property, the conditional law of $\widehat{\mathcal{Z}}(\cdot + \widehat{\tau}_r^R)|_{[0,\infty)}$ given $\widehat{\mathcal{Z}}|_{[0,\widehat{\tau}_r^R]}$ is that of a random walk with the same increment distribution as \mathcal{Z} started at $(\widehat{\mathcal{L}}(\widehat{\tau}_r^R), -r)$ and conditioned so that its first coordinate stays non-negative. By Lemma 4.10 and (7.36), for each $s \in [0, \widehat{\mathcal{L}}(\widehat{\tau}_r^R)] \cap \mathbb{Z}$,

$$\begin{split} \mathbb{P}\left[\widehat{l}_r \leq s \, \middle| \, \widehat{\mathcal{Z}}|_{[0,\widehat{\tau}_r^R]} \right] &= 1 - \mathbb{P}\left[\widehat{l}_r > s \, \middle| \, \widehat{\mathcal{Z}}|_{[0,\widehat{\tau}_r^R]} \right] \\ &= 1 - \mathbb{P}\left[\widehat{\mathcal{L}}(j) \geq \widehat{\mathcal{L}}(\widehat{\tau}_r^R) - (\widehat{\mathcal{L}}(\widehat{\tau}_r^R) - s - 1), \forall j \geq \tau_r^R \, \middle| \, \widehat{\mathcal{Z}}|_{[0,\widehat{\tau}_r^R]} \right] \\ &= 1 - \frac{\widehat{\mathcal{L}}(\widehat{\tau}_r^R) - s}{\widehat{\mathcal{L}}(\widehat{\tau}_r^R) + 1} = \frac{s + 1}{\widehat{\mathcal{L}}(\widehat{\tau}_r^R) + 1}. \end{split}$$

Hence, the conditional law of \widehat{l}_r given $\widehat{\mathcal{Z}}|_{[0,\widehat{\tau}_r^R]}$ is uniform on $[0,\widehat{\mathcal{L}}(\widehat{\tau}_r^R)] \cap \mathbb{Z}$, which implies that the conditional law of $\widehat{z}(r)$ given $\widehat{M}(r)$ is uniform on the set of left boundary vertices of \widehat{M}_r .

It remains to show (7.35). By the convergence of $n^{-1/2}\widehat{\mathcal{Z}}(\lfloor n \cdot \rfloor)$ to a correlated two-dimensional Brownian motion started at (0,0) and conditioned to stay in the upper half-plane (Lemma 4.11), with probability tending to one as $A \to \infty$, uniformly in the choice of r,

$$A^{-1}r^2 \le \widehat{\tau}_r^R \le Ar^2.$$

Hence, with probability tending to one as $A \to \infty$, uniformly in the choice of r, the map $\widehat{M}(r)$ (which is obtained by applying the KMSW procedure to $\widehat{\mathcal{Z}}|_{[0,\widehat{\tau}_R^R-1]}$) satisfies (7.35).

Let $(\widehat{M}(r), \widehat{z}(r))$ be as in Lemma 7.9. Since $(\widehat{M}(r), \widehat{z}(r))$ has the same law of (M(r), z(r)) from Theorem 1.11, it will suffice to prove Theorem 1.11 with $(\widehat{M}(r), \widehat{z}(r))$ in place of (M(r), z(r)).

The vertices along the right boundary of the UIQBOT $M_{0,\infty}$, starting from the source vertex, are the same as the vertices along the right boundary of $M_{0,\infty}$, starting from the initial vertex of λ_0 . As in Theorem 1.4, we call these vertices x_0, x_1, \ldots By Assertion (ii) of Lemma 3.6, the time $\widehat{\tau}_r^R$ of (7.34) is the smallest $m \in \mathbb{N}_0$ for which the initial vertex of $\widehat{\lambda}_m$ is x_r in the map $\widehat{M}(r)$. In particular, the source and sink vertices of $\widehat{M}(r)$ are the vertices x_0 and x_r , respectively.

Let τ_r be as in (5.2), so that τ_r is the smallest $n \in \mathbb{N}_0$ for which the initial vertex of λ_n is x_r . By the coupling (7.33),

$$\tau_r = S_{\widehat{\tau}_r^R}.\tag{7.37}$$

We will now prove upper and lower bounds for LDPs and SDPs in $\widehat{M}(r)$.

Lemma 7.10. With probability tending to one as $A \to \infty$, uniformly in the choice of r,

$$LDP_{\widehat{M}(r)}(x_0, x_r) \le Ar^{3/2}. (7.38)$$

Proof. By (5.3), the time τ_r is the smallest $n \in \mathbb{N}$ such that $\mathcal{R}(n) \leq -r$. Since \mathcal{R} is a lazy random walk, it holds with probability tending to one as $A \to \infty$, uniformly in the choice of r, that $\tau_r \leq A^{2/3}r^2$ (the reason for the choice of $A^{2/3}$ will be clearer later). By (7.37), if this is the case, then

$$\widehat{M}(r) \subset M_{0,|A^{2/3}r^2|},$$
 (7.39)

where here we recall that $M_{0,n}$ is the submap of $M_{0,\infty}$ obtained by applying the KMSW procedure to $\mathcal{Z}|_{[0,n]}$. By Theorem 1.12 (with $A^{1/2}$ in place of A and $\lfloor A^{2/3}r^2 \rfloor$ in place of n), it holds with probability tending to one as $A \to \infty$, uniformly in the choice of r, that every directed path in $M_{0,\lfloor A^{2/3}r^2 \rfloor}$ has length at most $Ar^{3/2}$. Since also (7.39) holds with probability tending to one as $A \to \infty$, uniformly in the choice of r, we obtain the lemma statement.

Lemma 7.11. With probability tending to one as $A \to \infty$, uniformly in the choice of r,

$$LDP_{\widehat{M}(r)}(x_0, x_r) \ge A^{-1}r^{3/2}.$$
(7.40)

Proof. Fix $\delta \in (0,1)$. We will show that if A is chosen to be large enough (depending only on δ), then (7.40) holds with probability at least $1 - \delta$.

Recall that $\widehat{\tau}_r^R$ is the first time that $\widehat{\mathcal{R}}$ reaches -r. The idea of the proof is to argue that for a suitably chosen C > 1, depending on δ , the law of the walk segment

$$\left(\widehat{\mathcal{Z}}(\cdot+\widehat{\tau}_{\lfloor r/2\rfloor}^R) - \widehat{\mathcal{Z}}(\widehat{\tau}_{\lfloor r/2\rfloor}^R)\right)|_{[0,\lfloor r^2/C\rfloor]}$$
(7.41)

is absolutely continuous with respect to the law of $\mathcal{Z}|_{[0,\lfloor r^2/C\rfloor]}$, with a Radon-Nikodym derivative which can be controlled independently of r. We will then apply the lower bound in Theorem 1.12 to get that, if A and C are chosen appropriately, then with high probability, the submap of $\widehat{M}_{0,\infty}$ obtained by applying the KMSW procedure to (7.41) contains a directed path of length at least $A^{-1}r^{3/2}$ and is contained in $\widehat{M}(r)$. This will give us a directed path of length at least $A^{-1}r^{3/2}$ contained in $\widehat{M}(r)$, which is sufficient since any vertex of $\widehat{M}(r)$ can be joined by directed paths from the source and to the sink.

Step 1: reducing to a lower bound for an event depending on a segment of $\widehat{\mathcal{Z}}$. Let $\varepsilon \in (0,1)$ be a small number, which we will eventually choose to be small enough depending only on δ . For C > 1, let $G_r = G_r(C)$ be the event that $\tau_{\lceil r/2 \rceil} \ge r^2/C$ and there is a directed path in $M_{0,\lceil r^2/C \rceil}$

with length at least $A^{-1}r^{3/2}$. By an elementary estimate for the lazy random walk \mathcal{R} , followed by Theorem 1.12, we can find $C = C(\varepsilon) > 1$ and $A = A(\varepsilon) > 1$ such that

$$\mathbb{P}[G_r] \ge 1 - \varepsilon, \quad \forall r \in \mathbb{N}. \tag{7.42}$$

Let \widehat{G}_r be defined in the same manner as the event G_r of (7.42) but with the walk (7.41) in place of $\mathcal{Z}|_{[0,\tau_{\lceil r/2 \rceil}]}$. That is, \widehat{G}_r is the event that $\widehat{\tau}_r^R - \widehat{\tau}_{\lceil r/2 \rceil}^R \ge r^2/C$ and the map obtained by applying the KMSW procedure to the walk (7.41) contains a directed path of length at least $A^{-1}r^{3/2}$.

If \widehat{G}_r occurs, then $\widehat{\tau}_r^R - \widehat{\tau}_{\lfloor r/2 \rfloor}^R \ge r^2/C$, which implies that the map in the definition of \widehat{G}_r is a submap of $\widehat{M}(r)$. Hence on \widehat{G}_r , the map $\widehat{M}(r)$ contains a directed path of length at least $A^{-1}r^{3/2}$. The longest directed path in a bipolar-oriented map is between the source and the sink, so if \widehat{G}_r occurs, then (7.40) holds.

The left side of (7.40) is always at least one, so it suffices to prove the lemma statement only for sufficiently large values of r (finitely many small values of r can be dealt with by increasing A). Hence it suffices to prove that for each sufficiently large $r \in \mathbb{N}$ (how large can depend on δ),

$$\mathbb{P}[\widehat{G}_r] \ge 1 - \delta. \tag{7.43}$$

Step 2: conditional law given $\widehat{\mathcal{Z}}|_{[0,\tau_{\lfloor r/2\rfloor}]}$. For $l\in\mathbb{N}$, by the strong Markov property, the conditional law of $\widehat{\mathcal{Z}}(\cdot+\widehat{\tau}^R_{\lfloor r/2\rfloor})|_{[0,\infty)}$ given $\widehat{\mathcal{Z}}|_{[0,\widehat{\tau}^R_{\lfloor r/2\rfloor}]}$ on the event $\{\widehat{\mathcal{L}}(\widehat{\tau}^R_{\lfloor r/2\rfloor})=l\}$ is that of a random walk with the same increment distribution as \mathcal{Z} started from $(l,-\lfloor r/2\rfloor)$ and conditioned so that its first coordinate is non-negative for all time.

By combining this with (4.1), we find that the conditional law of $\widehat{\mathcal{Z}}(\cdot + \widehat{\tau}^R_{\lfloor r/2 \rfloor})|_{[0,\lfloor r^2/C \rfloor]}$ given $\widehat{\mathcal{Z}}|_{[0,\widehat{\tau}^R_{\lfloor r/2 \rfloor}]}$ on the event $\{\widehat{\mathcal{L}}(\widehat{\tau}^R_{\lfloor r/2 \rfloor}) = l\}$ is described as follows. Let $\mathcal{Z}' = (\mathcal{L}',\mathcal{R}')$ be a random walk with the same increment distribution as \mathcal{Z} but started from $(l,-\lfloor r/2 \rfloor)$. Consider the law of $\mathcal{Z}'|_{[0,r^2/C]}$ weighted by

$$(l+1)^{-1}(\mathcal{L}'(\lfloor r^2/C \rfloor) + 1)\mathbb{1}\Big\{\mathcal{L}'(j) \ge 0, \ \forall j \in [0, r^2/C] \cap \mathbb{Z}\Big\}.$$

By shifting space by $-(l, -\lfloor r/2 \rfloor)$, we get that the conditional law of the walk (7.41) given $\widehat{\mathcal{Z}}|_{[0,\widehat{\tau}_{\lfloor r/2 \rfloor}^R]}$ on the event $\{\widehat{\mathcal{L}}(\widehat{\tau}_{\lfloor r/2 \rfloor}^R) = l\}$ is the same as the law of the walk $\mathcal{Z}|_{[0,\lfloor r^2/C \rfloor]}$ weighted by $(l+1)^{-1}(\mathcal{L}(\lfloor r^2/C \rfloor)+1)\mathbb{1}_{F_{l,r}}$, where

$$F_{l,r} := \left\{ \mathcal{L}(j) \ge -l, \ \forall j \in [0, r^2/C] \cap \mathbb{Z} \right\}. \tag{7.44}$$

Step 3: bounding the Radon-Nikodym derivative. Recall the events G_r and \widehat{G}_r defined immediately before and after (7.42). By the previous paragraph, on the event $\{\widehat{\mathcal{L}}(\widehat{\tau}_{|r/2|}^R) = l\}$,

$$\mathbb{P}\left[\widehat{G}_r^c \left| \widehat{\mathcal{Z}} \right|_{[0,\widehat{\tau}_{\lfloor r/2 \rfloor}^R]}\right] = (l+1)^{-1} \mathbb{E}\left[(\mathcal{L}(\lfloor r^2/C \rfloor) + 1) \mathbb{1}_{F_{l,r}} \mathbb{1}_{G_r^c} \right].$$
 (7.45)

Since \mathcal{L} is a lazy random walk and C > 1,

$$\mathbb{E}\left[\left(\mathcal{L}(\lfloor r^2/C\rfloor) + 1\right)^2\right] \le 2r^2. \tag{7.46}$$

We apply the Cauchy-Schwarz inequality to the right-hand side of (7.45), followed by (7.42) and (7.46). We get that, on $\{\widehat{\mathcal{L}}(\widehat{\tau}_{\lceil r/2 \rceil}^R) = l\}$,

$$\mathbb{P}\left[\hat{G}_{r}^{c} \middle| \widehat{\mathcal{Z}}|_{[0,\widehat{\tau}_{\lfloor r/2 \rfloor}^{R}]}\right] \leq (l+1)^{-1} \mathbb{E}\left[(\mathcal{L}(\lfloor r^{2}/C \rfloor) + 1)^{2} \mathbb{1}_{F_{l,r}} \right]^{1/2} \mathbb{P}[G_{r}^{c}]^{1/2} \\
\leq 2(l+1)^{-1} r \varepsilon^{1/2}.$$
(7.47)

By the convergence of $n^{-1/2}\widehat{\mathcal{Z}}(\lfloor n \cdot \rfloor)$ to conditioned Brownian motion (Lemma 4.11), there exists $c_{\delta} > 0$ such that for each sufficiently large $r \in \mathbb{N}$ (how large depends only on δ),

$$\mathbb{P}\left[\widehat{\mathcal{L}}(\widehat{\tau}_{\lfloor r/2 \rfloor}^R) \ge c_{\delta} r\right] \ge 1 - \delta/2. \tag{7.48}$$

By (7.47) and (7.48), for each such r,

$$\mathbb{P}\left[\widehat{G}_r^c\right] \leq \mathbb{P}\left[\widehat{G}_r^c \middle| \widehat{\mathcal{L}}(\widehat{\tau}_{\lfloor r/2 \rfloor}^R) \geq c_{\delta}r\right] + \mathbb{P}\left[\widehat{\mathcal{L}}(\widehat{\tau}_{\lfloor r/2 \rfloor}^R) < c_{\delta}r\right] \\
\leq 2(c_{\delta}r + 1)^{-1}r\varepsilon^{1/2} + \delta/2. \tag{7.49}$$

If we choose ε to be small enough (and hence A and C to be large enough), depending on δ , then the right side of (7.49) is at most δ for every $r \in \mathbb{N}$. This implies (7.43) for all sufficiently large $r \in \mathbb{N}$, as required.

Lemma 7.12. With probability tending to one as $A \to \infty$, uniformly in the choice of r, there exists a vertex y on the right boundary of $\widehat{M}(r)$ such that

$$SDP_{\widehat{M}(r)}(x_0, y) \ge A^{-1}r^{3/4}.$$
 (7.50)

Proof. Since \mathcal{R} is a lazy random walk and τ_r is the first time it hits -r, it holds with probability tending to one as $A \to \infty$, uniformly in the choice of r, that $\tau_r \geq A^{-1/2}r^2$. By (7.37), if this is the case, then

$$M_{0,|A^{-1/2}r^2|} \cap \widehat{M}_{0,\infty} \subset \widehat{M}(r). \tag{7.51}$$

Since the lower-right boundary of $M_{0,\lfloor A^{-1/2}r^2\rfloor}$ is a subset of the right boundary of $M_{0,\infty}$, which equals the right boundary of $\widehat{M}_{0,\infty}$, if (7.51) holds, then the right boundary of $M_{0,\lfloor A^{-1/2}r^2\rfloor}$ is a subset of the right boundary of $\widehat{M}(r)$.

By the proof of Lemma 7.6 (with $A^{1/2}$ in place of A), see in particular (7.23), it holds with probability tending to one as $A \to \infty$, uniformly in the choice of r, that there exists a vertex y on the right boundary of $M_{0,|A^{-1/2}r^2|}$ such that

$$SDP_{M_{0,\infty}}(x_0, y) \ge A^{-1}r^{3/4}$$
.

Since $SDP_{\widehat{M}(r)}(x_0, y) \ge SDP_{M_{0,\infty}}(x_0, y)$, combining this with the previous paragraph concludes the proof.

Lemma 7.13. With probability tending to one as $A \to \infty$, uniformly in the choice of r,

$$SDP_{\widehat{M}(r)}(x_0, x_r) \le Ar^{3/4}.$$
 (7.52)

Proof. Let I_r (resp. J_r) be the set of vertices and edges along the left boundary of $\widehat{M}(r)$ which lie between x_0 and $\widehat{z}(r)$ (resp. $\widehat{z}(r)$ and x_r), including the endpoints.

Step 1: path from x_0 to J_r . We first argue that with probability tending to one as $A \to \infty$, uniformly in the choice of r,

$$\exists y \in J_r \text{ such that } SDP_{\widehat{M}(r)}(x_0, y) \le Ar^{3/4}. \tag{7.53}$$

We will eventually combine (7.53) with a forward/reverse symmetry argument for $\widehat{M}(r)$ to obtain (7.52).

As in the proof of Lemma 7.10, see (7.39), it holds with probability tending to one as $A \to \infty$, uniformly in the choice of r, that

$$\widehat{M}(r) \subset M_{0,|A^{4/3}r^2|}.$$
 (7.54)

By the first item of Theorem 1.13 (applied with $A^{1/2}$ in place of A and with $\lfloor A^{4/3}r^2 \rfloor$ in place of n) it holds with probability tending to one as $A \to \infty$, uniformly in the choice of r, that there exists a directed path P from x_0 to the upper boundary of $M_{0,\lfloor A^{4/3}r^2\rfloor}$ with length at most $Ar^{3/4}$. Now assume that this is the case and (7.54) holds. We will show that (7.53) holds.

The path P is a directed path in $M_{0,\infty}$ started from x_0 , so by the definition of $\widehat{M}_{0,\infty}$ (third paragraph of Section 5.1), P is contained in $\widehat{M}_{0,\infty}$. By the definition of $\widehat{z}(r)$ in Lemma 7.9, the vertices in J_r form a (directed) path in $\widehat{M}_{0,\infty}$ from the left boundary of $\widehat{M}_{0,\infty}$ to x_r . By planarity and (7.54), the path P must intersect J_r . Thus (7.53) holds.

Step 2: path from x_0 to x_r via symmetry. Recall from Lemma 7.9 that the law of $(\widehat{M}(r), \widehat{z}(r))$ is the Boltzmann distribution on bipolar-oriented triangulations with right boundary length r and a marked left boundary vertex. By this and Definition 1.10, reversing all of the orientations of the edges of $\widehat{M}(r)$, then applying an orientation-reversing homeomorphism $\mathbb{C} \to \mathbb{C}$, gives us another decorated map with the same law as $(\widehat{M}(r), \widehat{z}(r))$. This procedure has the effect of switching the source and the sink and also switching I_r with J_r . Hence the main result of Step 1 (see (7.53)) implies that with probability tending to one as $A \to \infty$, uniformly in the choice of r,

$$\exists y' \in I_r \text{ such that } SDP_{\widehat{M}(r)}(y', x_r) \le Ar^{3/4}. \tag{7.55}$$

By planarity, any path from x_0 to a vertex of J_r and any path from a vertex of I_r to x_r must have a vertex in common. By concatenating a segment of the first path with a segment of the second path, we obtain from (7.53) and (7.55) that with probability tending to one as $A \to \infty$, uniformly in the choice of r,

$$SDP_{\widehat{M}(r)}(x_0, x_r) \le 2Ar^{3/4}.$$
 (7.56)

Applying this with A/2 in place of A concludes the proof.

Proof of Theorem 1.11. Recall from Lemma 7.9 that the map $\widehat{M}(r)$ has the same law as the map M(r) in the theorem statement. The theorem therefore follows from Lemmas 7.10, 7.11, 7.12, and 7.13.

8 Open problems

We discuss some additional open problems besides the ones already mentioned in Section 2. As discussed in Section 2.3, uniform bipolar-oriented triangulations can be viewed as discrete analogs of a hypothetical directed version of the $\sqrt{4/3}$ -LQG metric.

Problem 8.1. Construct two directed metrics on \mathbb{C} which describe the scaling limits of longest and shortest directed path distances in the UIBOT. Obtain a natural coupling of these directed metrics with a $\sqrt{4/3}$ -LQG cone together with a pair of coupled SLE₁₂ curves.

A potential approach to constructing a full scaling limit for directed distances on the UIBOT is to understand the joint scaling limit of the Busemann functions at different times. For $n \in \mathbb{Z}$, let \mathcal{X}_n be the XDP Busemann function on the boundary of the map $M_{n,\infty}$ obtained by applying the KMSW procedure (Definition 3.3) to $(\mathcal{Z}(\cdot + n) - \mathcal{Z}(n))|_{[0,\infty)}$. We have $M_{n,\infty} \stackrel{d}{=} M_{0,\infty}$, so $\mathcal{X}_n \stackrel{d}{=} \mathcal{X}_0$. Hence, Theorem 1.6 implies that each \mathcal{X}_n converges in law to a stable Lévy process of index 2/3 (in the LDP case) or 4/3 (in the SDP case).

Problem 8.2. Describe the scaling limit of the joint law of the collection of Busemann functions $\{\mathcal{X}_n\}_{n\in\mathbb{Z}}$ as a collection of coupled stable Lévy processes. Even a non-trivial joint scaling limit of two of these Busemann functions would be interesting.

It is possible to show that a variety of different random planar maps in the γ -LQG universality have the same exponent for undirected graph distances. This can be done using a strong coupling of their encoding walks with Brownian motion [KMT76, Zai98]; see [GHS20, DG20]. Moreover, this exponent is known to be the reciprocal of the dimension of the γ -LQG metric space [GP22, Corollary 1.7]. It would be interesting to prove analogous results for directed distances (the argument of [GHS20] does not carry over in an obvious way).

Problem 8.3. Prove that the exponents for LDP and SDP distances obtained in this paper are equal to analogous exponents for other models of bipolar-oriented planar maps in the $\sqrt{4/3}$ -LQG universality class (e.g., quadrangulations or maps with unconstrained face degree). Also relate the exponents in this paper to exponents for continuum models. E.g., the longest increasing subsequence for a size-n permutation sampled from the skew Brownian permuton of parameters $(\rho, q) = (-1/2, 1/2)$ [Bor23] should grow like $n^{3/4}$.

There is a substantial literature concerning bounds for Hausdorff dimensions of special sets associated with LQG or with the directed landscape, see, e.g., the surveys [DDG23, GH24]. One can ask analogous questions for uniform bipolar-oriented triangulations.

Problem 8.4. Compute the scaling exponents for the sizes of various special sets associated with longest and shortest directed paths on uniform bipolar-oriented triangulations, e.g. the following.

- The intersection of an XDP geodesic with a rightmost (or leftmost) directed path.
- The set of k-star points for $k \geq 2$, defined as vertices which are the starting points of k macroscopically distinct XDP geodesics.
- For two specified vertices x and y, the set of vertices z for which the XDPs from x to z and from y to z are equal.

Theorem 1.6 gives an exact scaling limit result for directed distances in the UIBOT, but in the finite-volume setting we only have up-to-constants bounds (Theorems 1.11, 1.12, and 1.13).

Problem 8.5. Prove a scaling limit result for some natural observable related to directed distances in finite uniform bipolar-oriented triangulations.

The most important combinatorial tool for analyzing distance on uniform planar maps (or triangulations, quadrangulations, etc.) is the Schaeffer bijection [CV81, Sch97]. This bijection encodes planar maps via labeled trees, where the labels exactly correspond to graph distances to a special root vertex. It is the key tool in the proof that uniform random planar maps converge in the scaling limit to the Brownian map [Le 13, Mie13].

Problem 8.6. Is there an analog of the Schaeffer bijection for uniform bipolar-oriented triangulations (or bipolar-oriented maps with other face degree distributions), where the labels correspond to the lengths of longest (or shortest) directed paths?

A Proof of the Tauberian result

We prove the Tauberian result in Proposition 6.1. Most of our arguments apply to general non-negative real-valued random variables; therefore, we will consider this general setting and restrict ourselves to integer-valued random variables (as stated in Proposition 6.1) only when necessary, i.e. in Section A.2.

Throughout this section, let X be a non-negative real-valued random variable. For $z \in \mathbb{C}$ with $|z| \leq 1$, define

$$\phi(z) = \mathbb{E}[z^X] \tag{A.1}$$

so that the characteristic function of X (as in the statement of Proposition 6.1) is $\varphi(t) = \varphi(e^{it})$.

A.1 Proofs for the tail exponent asymptotics

In this section, after proving the preliminary result of Lemma A.1, we prove in Lemmas A.2 and A.3 the two main claims of Proposition 6.1, i.e. the ones in (6.5) and (6.6), postponing the justification of the claim about the positivity of the imaginary part of the constant c in (6.5) to Section A.2.

We start with the following lemma.

Lemma A.1. Let $\mathbb{D} = \{z \in \mathbb{C} : |z| < 1\}$. Let $\psi : \overline{\mathbb{D}} \to \mathbb{C}$ be holomorphic on \mathbb{D} and continuous on $\overline{\mathbb{D}}$. Assume that there exists $\nu \in (0,1)$ and $c \in \mathbb{C} \setminus i\mathbb{R}$ such that

$$\psi(e^{it}) = 1 + (c\mathbb{1}_{(t>0)} + \overline{c}\mathbb{1}_{(t<0)})|t|^{\nu} + o(t^{\nu}), \quad as \ t \to 0.$$
(A.2)

Then setting $b = \operatorname{Re}(c) \sec\left(\frac{\pi\nu}{2}\right) \in \mathbb{R} \setminus \{0\},\$

$$\psi(1-r) = 1 + br^{\nu} + o(r^{\nu}), \quad as \ r \to 0.$$
 (A.3)

Proof. It is convenient to change coordinate to the upper half-plane so that we can use a scaling argument. So, we define

$$\widetilde{\psi}(z) := \psi\left(\frac{i-z}{i+z}\right).$$
 (A.4)

The function $\widetilde{\psi}$ is bounded, holomorphic on the upper-half plane $\mathbb{H} := \{z \in \mathbb{C} : \operatorname{Im} z > 0\}$, and continuous on $\overline{\mathbb{H}}$. The fractional linear transformation with which we pre-composed ψ maps 0 to 1, maps the real line to the unit circle, and is smooth in a neighborhood of the origin. From this, we see that (A.2) is equivalent to

$$\widetilde{\psi}(x) = 1 + \chi(x)|x|^{\nu} + o(x^{\nu}), \text{ as } \mathbb{R} \ni x \to 0, \text{ where } \chi(x) := (c2^{\nu}\mathbb{1}_{(x>0)} + \overline{c}2^{\nu}\mathbb{1}_{(x<0)})$$
 (A.5)

since if $t \in (-\pi, \pi)$ and $e^{it} = \frac{i-x}{i+x}$ then $t = 2\arctan(x) \sim 2x$; and (A.3) is equivalent to

$$\widetilde{\psi}(iy) = 1 + b2^{\nu}y^{\nu} + o(y^{\nu}), \quad \text{as } \mathbb{R}_{+} \ni y \to 0$$
 (A.6)

since if $1 - r = \frac{i - iy}{i + iy}$ then $r = \frac{2y}{1 + y} \sim 2y$.

Since ψ is holomorphic, its real and imaginary parts are harmonic. We may therefore use the formula for the Poisson kernel on the half-plane to write

$$\widetilde{\psi}(iy) = \frac{1}{\pi} \int_{-\infty}^{\infty} \frac{y}{x^2 + y^2} \widetilde{\psi}(x) \, dx. \tag{A.7}$$

Let

$$h(y) := \frac{1}{\pi} \int_{-\infty}^{\infty} \frac{\chi(x)|x|^{\nu} y}{x^2 + y^2} dx$$
 (A.8)

with $\chi(x)$ as in (A.5). By making the change of variables u = yx, du = y dx, we see that $h(y) = y^{\nu}h(1)$. We also note that h(y) is real (the imaginary parts of c' and \overline{c}' cancel by symmetry) and non-zero (since Re c' is non-zero).

We are going to compare $\widetilde{\psi}(iy)$ to 1+h(y). Given $\varepsilon>0$, we use (A.5) to choose $\delta>0$ small enough so that

$$|\widetilde{\psi}(x) - 1 - \chi(x)x^{\nu}| < \varepsilon |x|^{\nu}, \quad \forall x \in [-\delta, \delta].$$
 (A.9)

By (A.7), writing $\|\widetilde{\psi}\|_{\infty}$ for the (finite) L^{∞} norm of $\widetilde{\psi}$, we have

$$\left| \widetilde{\psi}(iy) - \frac{1}{\pi} \int_{-\delta}^{\delta} \frac{(1 + \chi(x)|x|^{\nu})y}{x^2 + y^2} \, dx \right| = \left| \frac{1}{\pi} \int_{\mathbb{R} \setminus [-\delta, \delta]} \frac{y}{x^2 + y^2} \widetilde{\psi}(x) \, dx - \frac{1}{\pi} \int_{-\delta}^{\delta} \frac{(1 + \chi(x)|x|^{\nu} - \widetilde{\psi}(x))y}{x^2 + y^2} \, dx \right|$$

$$\leq \frac{\|\widetilde{\psi}\|_{\infty}}{\pi} \int_{\mathbb{R} \setminus [-\delta, \delta]} \frac{y}{x^2 + y^2} \, dx + \frac{\varepsilon}{\pi} \int_{-\delta}^{\delta} \frac{|x|^{\nu}y}{x^2 + y^2} \, dx, \tag{A.10}$$

where the last estimate follows from (A.9). For a fixed value of $\delta > 0$,

$$\int_{\mathbb{R}\setminus[-\delta,\delta]} \frac{(1+|x|^{\nu})y}{x^2+y^2} \, dx = O(y). \tag{A.11}$$

By (A.11) and the fact that $\frac{1}{\pi} \int_{-\infty}^{\infty} \frac{y}{x^2 + y^2} dx = 1$, the integral inside the absolute value on the left side of (A.10) satisfies

$$\frac{1}{\pi} \int_{-\delta}^{\delta} \frac{(1+\chi(x)|x|^{\nu})y}{x^2+y^2} dx = \frac{1}{\pi} \int_{-\infty}^{\infty} \frac{(1+\chi(x)|x|^{\nu})y}{x^2+y^2} dx - \frac{1}{\pi} \int_{\mathbb{R}\setminus[-\delta,\delta]} \frac{(1+\chi(x)|x|^{\nu})y}{x^2+y^2} dx
= 1+h(y)+O(y).$$
(A.12)

By (A.11), the first term on the right side of (A.10) is at most O(y). As for the second term on the right side, we bound it above by $C\varepsilon h(y) = C\varepsilon h(1)y^{\nu}$, where h(y) is as in (A.8) and C > 0 is a constant (coming from the factor $\chi(x)$ in (A.8)). Plugging (A.12) into the left-hand side of (A.10) and using these estimates for the right-hand side of (A.10) gives

$$\left|\widetilde{\psi}(iy) - 1 - h(y)\right| \le \varepsilon h(1)y^{\nu} + O(y). \tag{A.13}$$

Since ε is arbitrary and $h(y) = y^{\nu}h(1)$, this gives (A.6) with $b2^{\nu} = h(1) \stackrel{\text{(A.8)}}{=} \frac{1}{\pi} \int_{-\infty}^{\infty} \frac{\chi(x)|x|^{\nu}}{1+x^2} dx$. Using the symmetry of $\chi(x)$, this becomes

$$b = \frac{1}{\pi} (c + \overline{c}) \int_0^\infty \frac{x^{\nu}}{1 + x^2} dx = \frac{2 \operatorname{Re}(c)}{\pi} \int_0^\infty \frac{x^{\nu}}{1 + x^2} dx.$$

The remaining integral is classical:

$$\int_0^\infty \frac{x^{\nu}}{1+x^2} \, dx = \frac{\pi}{2} \csc\left(\frac{\pi(\nu+1)}{2}\right) = \frac{\pi}{2} \sec\left(\frac{\pi\nu}{2}\right), \qquad 0 < \nu < 1.$$

Therefore

$$b = \operatorname{Re}(c) \sec\left(\frac{\pi\nu}{2}\right),$$

which is real and nonzero since $c \notin i\mathbb{R}$ and $\cos(\frac{\pi\nu}{2}) \neq 0$ for $0 < \nu < 1$.

We now prove the main claim in (6.5).

Lemma A.2. Let ϕ be as in (A.1). Assume that for some $c \in \mathbb{C} \setminus i\mathbb{R}$ and $\nu \in (0,1)$,

$$\phi(e^{it}) = 1 + (c\mathbb{1}_{(t>0)} + \overline{c}\mathbb{1}_{(t<0)})|t|^{\nu} + o(t^{\nu}), \quad as \ t \to 0.$$
(A.14)

Then $\operatorname{Re}(c) < 0$ and setting $a = -\frac{\operatorname{Re}(c)}{\Gamma(1-\nu)} \sec\left(\frac{\pi\nu}{2}\right) > 0$,

$$\mathbb{P}[X > R] = aR^{-\nu} + o(R^{-\nu}), \quad as \ R \to \infty. \tag{A.15}$$

Proof. By a standard Tauberian theorem for the Laplace transform (see, e.g., [Fel71, Example (c), Page 447] or [BGT87, Corollary 8.1.7]), for any constant a > 0, the asymptotics

$$\phi(1-r) = 1 - \Gamma(1-\nu)ar^{\nu} + o(r^{\nu}), \quad (0,1) \ni r \to 0$$
(A.16)

implies (A.15). So, we need to show that (A.14) implies (A.16) with $a = -\frac{\text{Re}(c)}{\Gamma(1-\nu)} \sec\left(\frac{\pi\nu}{2}\right) > 0$. This, in turn, follows from Lemma A.1 applied to the holomorphic function ϕ (note that, since $0 < \nu < 1$, a is positive only if Re(c) < 0).

We now prove the main claim in (6.6).

Lemma A.3. Let ϕ be as in (A.1). Assume that for some $c_1 > 0$, $c_2 \in \mathbb{C} \setminus \mathbb{R}$, and $\nu \in (0,1)$,

$$\phi(e^{it}) = 1 + ic_1 t + (c_2 \mathbb{1}_{(t>0)} + \overline{c}_2 \mathbb{1}_{(t<0)})|t|^{1+\nu} + o(t^{1+\nu}), \quad as \ t \to 0.$$
 (A.17)

Then $\operatorname{Im}(c_2) < 0$ and setting $a = -\frac{\nu}{\Gamma(1-\nu)} \sec(\frac{\pi\nu}{2}) \operatorname{Im}(c_2) > 0$,

$$\mathbb{P}[X > R] = aR^{-\nu - 1} + o(R^{-\nu - 1}), \quad as \ R \to \infty.$$
 (A.18)

Proof. By a standard Tauberian theorem for the Laplace transform (see, e.g., [BGT87, Theorem 8.1.6] with n = 1), for any $b \in \mathbb{R} \setminus \{0\}$, the asymptotics

$$\phi(1-r) = 1 - c_1 r + br^{1+\nu} + o(r^{1+\nu}), \quad (0,1) \ni r \to 0$$
(A.19)

implies (A.18) with $a = \frac{b\nu}{\Gamma(1-\nu)}$, which is necessarily positive, since $b \neq 0$ and probabilities are non-negative. So, we need to show that (A.17) implies (A.19) with the constant $b = -\operatorname{Im}(c_2)\sec(\frac{\pi\nu}{2})$. Then the fact that $\operatorname{Im}(c_2) < 0$ immediately follows from the fact that a > 0.

The asymptotics (A.17) implies that $\frac{d}{dt}\phi(e^{it})$ exists and equals ic_1 . By the main theorem of [Pit56], this implies that $\lim_{T\to\infty} \mathbb{E}[X\mathbb{1}_{\{|X|\leq T\}}] = c_1$. Since X is non-negative, this implies that $\lim_{T\to\infty} \mathbb{E}[X\mathbb{1}_{(X\leq T)}] = c_1$. By the monotone convergence theorem, this implies that $\mathbb{E}[X] = c_1$. This, in turn, implies that the complex derivative

$$\phi'(z) = \lim_{\overline{\mathbb{D}} \ni z} \frac{\phi(z) - 1}{z - 1}$$

exists and equals c_1 .

Let

$$G(z) := \frac{\phi(z) - 1}{c_1(z - 1)}.$$

The previous paragraph implies that G is continuous on $\overline{\mathbb{D}}$ and holomorphic on \mathbb{D} . By (A.17) and since $e^{it} = 1 + it + O(t^2)$ as $t \to 0$,

$$G(e^{it}) = 1 + (c_3 \mathbb{1}_{(t>0)} + \overline{c}_3 \mathbb{1}_{(t<0)})|t|^{\nu} + o(t^{\nu}), \text{ as } t \to 0$$

where $c_3 = c_2/(ic_1) \in \mathbb{C} \setminus i\mathbb{R}$. By Lemma A.1 applied to G,

$$G(1-r) = 1 + (\text{Re}(c_3) \sec(\frac{\pi \nu}{2})) r^{\nu} + o(r^{\nu}), \text{ as } r \to 0.$$

Re-arranging this implies (A.19) with $b = -c_1 \operatorname{Re}(c_2/(ic_1)) \operatorname{sec}(\frac{\pi\nu}{2}) = -\operatorname{Im}(c_2) \operatorname{sec}(\frac{\pi\nu}{2})$, where we used that c_1 is real.

Proof of Proposition 6.1. In the case of Assumption 1, the asymptotics (6.5) and the fact that Re(c) < 0 follow from Lemma A.2. The fact that Im(c) > 0 is justified in Lemma A.4 below. The case of Assumption 2 follows directly from Lemma A.3.

A.2 Proof that the imaginary part is positive for small t when $0 < \nu < 1$

Here we restrict to the case where X is a non-negative *integer*-valued random variable with probability mass function f and prove the claims about the positivity of the imaginary part of the constant c appearing in (6.3). Since

$$\operatorname{Im}(\phi(e^{it})) = \sum_{k \ge 0} f(k) \operatorname{Im}(e^{itk}) = \sum_{k \ge 0} f(k) \sin(tk),$$

and Assumption 1 guarantees that for some $c \in \mathbb{C} \setminus i\mathbb{R}$ and $\nu \in (0,1)$,

$$\varphi(t) = \phi(e^{it}) = 1 + (c\mathbb{1}_{(t>0)} + \overline{c}\mathbb{1}_{(t<0)})|t|^{\nu} + o(t^{\nu}), \quad \text{as } t \to 0,$$
(A.20)

it is sufficient to establish the following result.

Lemma A.4. Let $f: \mathbb{N}_0 \to [0, \infty)$ and set $S(k) := \sum_{y \geq k} f(y)$. Assume that for some c' > 0 and $0 < \nu < 1$,

$$S(k) = c' k^{-\nu} + o(k^{-\nu}), \quad as \ k \to \infty.$$
 (A.21)

Then there exists $t_0 > 0$ such that

$$\sum_{k\geq 0} f(k) \sin(tk) > 0 \qquad \text{for all } t \in (0, t_0].$$

We first prove two preliminary lemmas.

Lemma A.5. For every t > 0,

$$\sum_{k\geq 0} f(k)\sin(tk) = \sum_{k\geq 0} S(k+1)(\sin((k+1)t) - \sin(kt)). \tag{A.22}$$

Equivalently,

$$\sum_{k>0} f(k)\sin(tk) = \int_0^\infty S(\lfloor u/t \rfloor + 1)\cos u \, du. \tag{A.23}$$

Proof. For $N \geq 1$, by telescoping,

$$\sum_{k=0}^{N} f(k)\sin(tk) = \sum_{k=0}^{N-1} S(k+1) \left(\sin((k+1)t) - \sin(kt)\right) - S(N+1)\sin(Nt),$$

because f(k) = S(k) - S(k+1). Letting $N \to \infty$, since $S(N+1) = O(N^{-\nu})$ and $\nu > 0$, we get that the boundary term vanishes and (A.22) follows. Using $\sin((k+1)t) - \sin(kt) = \int_{kt}^{(k+1)t} \cos u \, du$ yields (A.23).

Lemma A.6. Let

$$I_{\nu}(t) := \int_{0}^{\infty} \left(\lfloor u/t \rfloor + 1 \right)^{-\nu} \cos u \, du.$$

If $0 < \nu < 1$, then as $t \downarrow 0$,

$$I_{\nu}(t) = t^{\nu} \int_{0}^{\infty} u^{-\nu} \cos u \, du + O(t) = \Gamma(1 - \nu) \sin \frac{\pi \nu}{2} t^{\nu} + o(t^{\nu}). \tag{A.24}$$

Proof. For each $\nu > 0$,

$$I_{\nu}(t) - t^{\nu} \int_{0}^{\infty} u^{-\nu} \cos u \, du = \int_{0}^{\infty} \left[\left(\lfloor u/t \rfloor + 1 \right)^{-\nu} - (u/t)^{-\nu} \right] \cos u \, du.$$

Split the integral at u = t:

$$\left| I_{\nu}(t) - t^{\nu} \int_{0}^{\infty} u^{-\nu} \cos u \, du \right| \le t^{\nu} \int_{0}^{t} u^{-\nu} \, du + \int_{t}^{\infty} \left| \left(\lfloor u/t \rfloor + 1 \right)^{-\nu} - (u/t)^{-\nu} \right| du.$$

The first term is

$$t^{\nu} \int_0^t u^{-\nu} \, du = \frac{t}{1 - \nu}.$$

For the second term, set $x = u/t \ge 1$. By the mean value theorem for $x \mapsto x^{-\nu}$, there is a constant $C = C(\nu)$ such that for $x \ge 1$,

$$|(\lfloor x \rfloor + 1)^{-\nu} - x^{-\nu}| \le C x^{-\nu - 1}.$$

Hence

$$\int_{t}^{\infty} \left| \left(\lfloor u/t \rfloor + 1 \right)^{-\nu} - (u/t)^{-\nu} \right| du \le C \int_{t}^{\infty} (u/t)^{-\nu - 1} du = Ct.$$

Combining the two bounds gives

$$I_{\nu}(t) = t^{\nu} \int_{0}^{\infty} u^{-\nu} \cos u \, du + O(t).$$

Since $0 < \nu < 1$, we have $t = o(t^{\nu})$, so the remainder is $o(t^{\nu})$. Finally, using the classical identity (valid for $0 < \nu < 1$)

$$\int_0^\infty u^{-\nu}\cos u \, du = \Gamma(1-\nu)\sin\frac{\pi\nu}{2},$$

we obtain (A.24).

Proof of Lemma A.4. Write $F(t) := \sum_{k \geq 0} f(k) \sin(tk)$. By Lemma A.5,

$$F(t) = \int_0^\infty S(\lfloor u/t \rfloor + 1) \cos u \, du.$$

Decompose $S(n) = c'n^{-\nu} + r(n)$ with $r(n) = o(n^{-\nu})$, and set

$$I_{\nu}(t) := \int_0^{\infty} \left(\lfloor u/t \rfloor + 1 \right)^{-\nu} \cos u \, du, \qquad R(t) := \int_0^{\infty} r(\lfloor u/t \rfloor + 1) \cos u \, du.$$

Then $F(t) = c'I_{\nu}(t) + R(t)$. By Lemma A.6,

$$c'I_{\nu}(t) = c' \Gamma(1-\nu) \sin\left(\frac{\pi\nu}{2}\right) t^{\nu} + o(t^{\nu}).$$

Since $\Gamma(1-\nu)\sin\left(\frac{\pi\nu}{2}\right) > 0$, it remains to show $R(t) = o(t^{\nu})$. Fix $\varepsilon > 0$ and choose K_0 large enough so that $|r(n)| \le \varepsilon n^{-\nu}$ for all $n \ge K_0$. Write

$$R(t) = \sum_{k>0} r(k+1) \int_{kt}^{(k+1)t} \cos u \, du =: R_{$$

where $K := \max\{K_0, \lceil 1/t \rceil\}$, and the sums defining $R_{\leq K}$ and $R_{\geq K}$ run over k < K and $k \geq K$, respectively.

respectively. Since $\left| \int_{kt}^{(k+1)t} \cos u \, du \right| \le t$, we have

$$|R_{< K}(t)| \le t \sum_{k < K} |r(k+1)|.$$

Given $\delta > 0$, pick N such that $|r(n)| \leq \delta n^{-\nu}$ for $n \geq N$. Split the sum at N:

$$t \sum_{k < K} |r(k+1)| \leq t \sum_{k < N} |r(k+1)| + \delta \, t \sum_{N \leq k < K} (k+1)^{-\nu} = O(t + \delta \, t \, K^{1-\nu}).$$

Since $K \approx 1/t$, this yields $|R_{\leq K}(t)| = O(t + \delta t^{\nu}) = o(t^{\nu})$ because $t = o(t^{\nu})$ when $0 < \nu < 1$, and $\delta > 0$ is arbitrary.

Now we look at $R_{\geq K}(t)$. Let $b_k(t) := \int_{kt}^{(k+1)t} \cos u \, du = \sin((k+1)t) - \sin(kt)$. Then $|b_k(t)| \leq 2|\sin(t/2)| \leq t$. By Cauchy–Schwarz,

$$|R_{\geq K}(t)| \le \left(\sum_{k>K} (k+1)^2 r(k+1)^2\right)^{1/2} \left(\sum_{k>K} (k+1)^{-2} b_k(t)^2\right)^{1/2}.$$

For $k \geq K \geq K_0$, we have $|r(k+1)| \leq \varepsilon (k+1)^{-\nu}$, hence

$$\sum_{k \ge K} (k+1)^2 r(k+1)^2 \le \varepsilon^2 \sum_{k \ge K} (k+1)^{2-2\nu} = O(\varepsilon^2 K^{3-2\nu}).$$

Also,

$$\sum_{k>K} (k+1)^{-2} b_k(t)^2 \le t^2 \sum_{k>K} (k+1)^{-2} = O(t^2 K^{-1}).$$

Therefore $|R_{>K}(t)| = O(\varepsilon t K^{1-\nu})$. With $K \simeq 1/t$ this gives $|R_{>K}(t)| = O(\varepsilon t^{\nu})$.

Combining the two bounds and letting $\varepsilon \to 0$ shows $R(t) = o(t^{\nu})$ which completes the proof. \square

References

- [AB25] M. Albenque and J. Bouttier. The slice decomposition of planar hypermaps. ArXiv e-prints, September 2025, 2509.06850.
- [ABB⁺25] A. Adhikari, J. Borga, T. Budzinski, W. Da Silva, and D. Sénizergues. The longest increasing subsequence of Brownian separable permutons. *ArXiv e-prints*, June 2025, 2506.19123.
- [ADH17] A. Auffinger, M. Damron, and J. Hanson. 50 years of first-passage percolation, volume 68 of University Lecture Series. American Mathematical Society, Providence, RI, 2017, 1511.03262. MR3729447
- [AG21] M. Ang and E. Gwynne. Liouville quantum gravity surfaces with boundary as matings of trees. Ann. Inst. Henri Poincaré Probab. Stat., 57(1):1–53, 2021, 1903.09120.

 MR4255166
- [AHPS23] J. Aru, N. Holden, E. Powell, and X. Sun. Brownian half-plane excursion and critical Liouville quantum gravity. J. Lond. Math. Soc. (2), 107(1):441–509, 2023, 2109.00275. MR4535017
- [Ang03] O. Angel. Growth and percolation on the uniform infinite planar triangulation. Geom. Funct. Anal., 13(5):935–974, 2003, 0208123. MR2024412
- [ASY25] M. Ang, X. Sun, and P. Yu. The p- θ relation in mating of trees. ArXiv e-prints, October 2025, 2510.13683.
- [BBF⁺18] F. Bassino, M. Bouvel, V. Féray, L. Gerin, and A. Pierrot. The Brownian limit of separable permutations. *Ann. Probab.*, 46(4):2134–2189, 2018, 1602.04960. MR3813988
- [BBMF11] N. Bonichon, M. Bousquet-Mélou, and E. Fusy. Baxter permutations and plane bipolar orientations. Sém. Lothar. Combin., 61A:Art. B61Ah, 29, 2009/11, 0805.4180. MR2734180
- [BCS06] M. Balázs, E. Cator, and T. Seppäläinen. Cube root fluctuations for the corner growth model associated to the exclusion process. *Electron. J. Probab.*, 11:no. 42, 1094–1132, 2006, math/0603306. MR2268539
- [BD94] J. Bertoin and R. A. Doney. On conditioning a random walk to stay nonnegative. $Ann.\ Probab.,\ 22(4):2152-2167,\ 1994.\ MR1331218$
- [BDG25] J. Borga, S. Das, and E. Gwynne. Longest increasing subsequences in skew Brownian permutons and directed paths in Liouville quantum gravity. In preparation, 2025.
- [Ber07] O. Bernardi. Bijective counting of tree-rooted maps and shuffles of parenthesis systems. Electron. J. Combin., 14(1):Research Paper 9, 36 pp. (electronic), 2007, math/0601684. MR2285813 (2007m:05125)
- [BFL25] O. Bernardi, É. Fusy, and S. Liang. Grand-Schnyder Woods. *Annals of combinatorics*, 29(2):273–373, 2025, arXiv:2303.15630.
- [BGM24] J. Bouttier, E. Guitter, and G. Miermont. On quasi-polynomials counting planar tight maps. Comb. Theory, 4(1):Paper No. 12, 70, 2024, 2203.14796. MR4770591

- [BGS22] J. Borga, E. Gwynne, and X. Sun. Permutons, meanders, and SLE-decorated Liouville quantum gravity. *Journal of the European Mathematical Society*, to appear, 2022, 2207.02319.
- [BGT87] N. H. Bingham, C. M. Goldie, and J. L. Teugels. Regular variation, volume 27 of Encyclopedia of Mathematics and its Applications. Cambridge University Press, Cambridge, 1987. MR898871 (88i:26004)
- [Bor22] J. Borga. The permuton limit of strong-Baxter and semi-Baxter permutations is the skew Brownian permuton. *Electron. J. Probab.*, 27:53, 2022, 2112.00159. Id/No 158.
- [Bor23] J. Borga. The skew Brownian permuton: A new universality class for random constrained permutations. *Proc. Lond. Math. Soc.* (3), 126(6):1842–1883, 2023, 2112.00156.
- [BP24] N. Berestycki and E. Powell. Gaussian free field and Liouville quantum gravity. Cambridge University Press, 2024, 2404.16642. To appear.
- [BS01] I. Benjamini and O. Schramm. Recurrence of distributional limits of finite planar graphs. *Electron. J. Probab.*, 6:no. 23, 13 pp. (electronic), 2001, 0011019. MR1873300 (2002m:82025)
- [BSS24] O. Busani, T. Seppäläinen, and E. Sorensen. The stationary horizon and semi-infinite geodesics in the directed landscape. *Ann. Probab.*, 52(1):1–66, 2024. MR4698024
- [Bus55] H. Busemann. The geometry of geodesics. Academic Press, Inc., New York, 1955. MR75623
- [Bus24] O. Busani. Diffusive scaling limit of the Busemann process in last passage percolation. Ann. Probab., 52(5):1650–1712, 2024, 2110.03808. MR4791418
- [CL15] N. Curien and J.-F. Le Gall. First-passage percolation and local modifications of distances in random triangulations. *ArXiv e-prints*, November 2015, 1511.04264.
- [CV81] R. Cori and B. Vauquelin. Planar maps are well labeled trees. Canadian J. Math., 33(5):1023–1042, 1981. MR638363
- [DBT88] G. Di Battista and R. Tamassia. Algorithms for plane representations of acyclic digraphs. *Theoretical Computer Science*, 61(2-3):175–198, 1988.
- [DDDF20] J. Ding, J. Dubédat, A. Dunlap, and H. Falconet. Tightness of Liouville first passage percolation for $\gamma \in (0,2)$. Publ. Math. Inst. Hautes Études Sci., 132:353–403, 2020, 1904.08021. MR4179836
- [DDG23] J. Ding, J. Dubédat, and E. Gwynne. Introduction to the Liouville quantum gravity metric. In *ICM—International Congress of Mathematicians. Vol. 6. Sections* 12–14, pages 4212–4244. EMS Press, Berlin, [2023] ©2023, 2109.01252. MR4680401
- [DFdMR95] H. De Fraysseix, P. O. de Mendez, and P. Rosenstiehl. Bipolar orientations revisited. Discrete Applied Mathematics, 56(2-3):157–179, 1995.
- [DG20] J. Ding and E. Gwynne. The fractal dimension of Liouville quantum gravity: universality, monotonicity, and bounds. *Communications in Mathematical Physics*, 374:1877–1934, 2020, 1807.01072.

- [DMS21] B. Duplantier, J. Miller, and S. Sheffield. Liouville quantum gravity as a mating of trees. *Astérisque*, (427):viii+257, 2021, 1409.7055. MR4340069
- [DOV22] D. Dauvergne, J. Ortmann, and B. Virág. The directed landscape. *Acta Math.*, 229(2):201–285, 2022, 1812.00309. MR4554223
- [DS11] B. Duplantier and S. Sheffield. Liouville quantum gravity and KPZ. *Invent. Math.*, 185(2):333–393, 2011, 1206.0212. MR2819163 (2012f:81251)
- [DV21] D. Dauvergne and B. Virág. The scaling limit of the longest increasing subsequence. $ArXiv\ e\text{-}prints,\ April\ 2021,\ 2104.08210.$
- [DW15a] D. Denisov and V. Wachtel. Random walks in cones. *Ann. Probab.*, 43(3):992–1044, 2015, 1110.1254. MR3342657
- [DW15b] J. Duraj and V. Wachtel. Invariance principles for random walks in cones. *ArXiv* e-prints, August 2015, 1508.07966.
- [DZ10] A. Dembo and O. Zeitouni. Large deviations techniques and applications, volume 38 of Stochastic Modelling and Applied Probability. Springer-Verlag, Berlin, 2010. Corrected reprint of the second (1998) edition. MR2571413 (2011b:60094)
- [Fel71] W. Feller. An introduction to probability theory and its applications. Vol. II. John Wiley & Sons, Inc., New York-London-Sydney, second edition, 1971. MR270403
- [Fel04] S. Felsner. Lattice structures from planar graphs. The electronic journal of combinatorics, pages R15–R15, 2004.
- [FFNO11] S. Felsner, E. Fusy, M. Noy, and D. Orden. Bijections for Baxter families and related objects. J. Combin. Theory Ser. A, 118(3):993–1020, 2011, 0803.1546. MR2763051
- [FP05] P. A. Ferrari and L. P. R. Pimentel. Competition interfaces and second class particles. Ann. Probab., 33(4):1235–1254, 2005, math/0406333. MR2150188
- [FPS09] É. Fusy, D. Poulalhon, and G. Schaeffer. Bijective counting of plane bipolar orientations and Schnyder woods. *European J. Combin.*, 30(7):1646–1658, 2009, arXiv:0803.0400. MR2548656 (2010j:05047)
- [Gan22] S. Ganguly. Random metric geometries on the plane and Kardar-Parisi-Zhang universality. *Notices Amer. Math. Soc.*, 69(1):26–35, 2022, 2110.11287. MR4353350
- [GH24] S. Ganguly and M. Hegde. Fractal structure in the directed landscape. In *Probability* and stochastic processes—a volume in honour of Rajeeva L. Karandikar, Indian Stat. Inst. Ser., pages 129–147. Springer, Singapore, [2024] ©2024. MR4824376
- [GHS16] E. Gwynne, N. Holden, and X. Sun. Joint scaling limit of a bipolar-oriented triangulation and its dual in the peanosphere sense. *Acta Mathematica Sinica, English Series*, to appear, 2016, 1603.01194.
- [GHS20] E. Gwynne, N. Holden, and X. Sun. A mating-of-trees approach for graph distances in random planar maps. *Probab. Theory Related Fields*, 177(3-4):1043–1102, 2020, 1711.00723. MR4126936

- [GHS23] E. Gwynne, N. Holden, and X. Sun. Mating of trees for random planar maps and Liouville quantum gravity: a survey. In *Topics in statistical mechanics*, volume 59 of *Panor. Synthèses*, pages 41–120. Soc. Math. France, Paris, 2023, 1910.04713. MR4619311
- [GM21] E. Gwynne and J. Miller. Existence and uniqueness of the Liouville quantum gravity metric for $\gamma \in (0, 2)$. *Invent. Math.*, 223(1):213–333, 2021, 1905.00383. MR4199443
- [GP19] E. Gwynne and J. Pfeffer. Bounds for distances and geodesic dimension in Liouville first passage percolation. *Electronic Communications in Probability*, 24:no. 56, 12, 2019, 1903.09561.
- [GP22] E. Gwynne and J. Pfeffer. KPZ formulas for the Liouville quantum gravity metric. *Trans. Amer. Math. Soc.*, 375(12):8297–8324, 2022, 1905.11790. MR4504639
- [Gwy20] E. Gwynne. Random surfaces and Liouville quantum gravity. *Notices Amer. Math. Soc.*, 67(4):484–491, 2020, 1908.05573. MR4186266
- [GZ22] S. Ganguly and L. Zhang. Fractal geometry of the space-time difference profile in the directed landscape via construction of geodesic local times. *ArXiv e-prints*, April 2022, 2204.01674.
- [Joh00] K. Johansson. Shape fluctuations and random matrices. Comm. Math. Phys., 209(2):437–476, 2000. MR1737991
- [JS03] J. Jacod and A. N. Shiryaev. Limit theorems for stochastic processes, volume 288 of Grundlehren der Mathematischen Wissenschaften [Fundamental Principles of Mathematical Sciences]. Springer-Verlag, Berlin, second edition, 2003. MR1943877
- [KMSW19] R. Kenyon, J. Miller, S. Sheffield, and D. B. Wilson. Bipolar orientations on planar maps and SLE_{12} . Ann. Probab., 47(3):1240-1269, 2019, 1511.04068. MR3945746
- [KMT76] J. Komlós, P. Major, and G. Tusnády. An approximation of partial sums of independent RV's, and the sample DF. II. Z. Wahrscheinlichkeitstheorie und Verw. Gebiete, 34(1):33–58, 1976. MR0402883
- [KPZ86] M. Kardar, G. Parisi, and Y.-C. Zhang. Dynamic scaling of growing interfaces. *Phys. Rev. Lett.*, 56:889–892, March 1986.
- [Le 13] J.-F. Le Gall. Uniqueness and universality of the Brownian map. Ann. Probab., 41(4):2880–2960, 2013, 1105.4842. MR3112934
- [Le 19] J.-F. Le Gall. Brownian geometry. Jpn.~J.~Math.,~14(2):135-174,~2019,~1810.02664. MR4007665
- [Lem67] A. Lempel. An algorithm for planarity testing of graphs. In *Theory of Graphs: International Symposium.*, pages 215–232. Gorden and Breach, 1967.
- [Lig70] T. M. Liggett. Weak convergence of conditioned sums of independent random vectors. Trans. Amer. Math. Soc., 152:195–213, 1970. MR268940
- [LSW24] Y. Li, X. Sun, and S. S. Watson. Schnyder woods, SLE₁₆, and Liouville quantum gravity. *Trans. Am. Math. Soc.*, 377(4):2439–2493, 2024, 1705.03573.

- [Mie13] G. Miermont. The Brownian map is the scaling limit of uniform random plane quadrangulations. *Acta Math.*, 210(2):319–401, 2013, 1104.1606. MR3070569
- [Mie21] G. Miermont. Compact Brownian surfaces. In Stochastic analysis, random fields and integrable probability—Fukuoka 2019, volume 87 of Adv. Stud. Pure Math., pages 173—198. Math. Soc. Japan, Tokyo, [2021] ©2021. MR4397422
- [MS17] J. Miller and S. Sheffield. Imaginary geometry IV: interior rays, whole-plane reversibility, and space-filling trees. *Probab. Theory Related Fields*, 169(3-4):729–869, 2017, 1302.4738. MR3719057
- [MS20] J. Miller and S. Sheffield. Liouville quantum gravity and the Brownian map I: the QLE(8/3,0) metric. Invent. Math., 219(1):75–152, 2020, 1507.00719. MR4050102
- [MS21] J. Miller and S. Sheffield. Liouville quantum gravity and the Brownian map II: Geodesics and continuity of the embedding. *Ann. Probab.*, 49(6):2732–2829, 2021, 1605.03563. MR4348679
- [Mul67] R. C. Mullin. On the enumeration of tree-rooted maps. Canad. J. Math., 19:174–183, 1967. MR0205882 (34 #5708)
- [Pit56] E. J. G. Pitman. On the derivatives of a characteristic function at the origin. *Ann. Math. Statist.*, 27:1156–1160, 1956. MR84947
- [Pro02] J. Propp. Lattice structure for orientations of graphs. arXiv preprint math/0209005, 2002, arXiv:math/0209005.
- [RV25] M. Rahman and B. Virág. Infinite geodesics, competition interfaces and the second class particle in the scaling limit. Ann. Inst. Henri Poincaré Probab. Stat., 61(2):1075– 1126, 2025, 2112.06849. MR4901636
- [Sch97] G. Schaeffer. Bijective census and random generation of Eulerian planar maps with prescribed vertex degrees. *Electron. J. Combin.*, 4(1):Research Paper 20, 14 pp. (electronic), 1997. MR1465581 (98g:05074)
- [Sep17] T. Seppäläinen. Variational formulas, Busemann functions, and fluctuation exponents for the corner growth model with exponential weights. *ArXiv e-prints*, September 2017, 1709.05771.
- [She16] S. Sheffield. Quantum gravity and inventory accumulation. *Ann. Probab.*, 44(6):3804–3848, 2016, 1108.2241. MR3572324
- [She23] S. Sheffield. What is a random surface? In *ICM—International Congress of Mathematicians*. Vol. 2. Plenary lectures, pages 1202–1258. EMS Press, Berlin, [2023] ©2023, 2203.02470. MR4680280
- [Spi76] F. Spitzer. *Principles of random walk*. Springer-Verlag, New York-Heidelberg, second edition, 1976. Graduate Texts in Mathematics, Vol. 34. MR0388547 (52 #9383)
- [Tam13] R. Tamassia. Handbook of graph drawing and visualization. CRC press, 2013.
- [Zai98] A. Y. Zaitsev. Multidimensional version of the results of Komlós, Major and Tusnády for vectors with finite exponential moments. *ESAIM Probab. Statist.*, 2:41–108, 1998. MR1616527